

# Asymmetric Intramolecular C–H Aminations with Chiral-at-Ruthenium Complexes

A DISSERTATION

In

Chemistry

Presented to the Faculties of Philipps-Universität Marburg in Partial Fulfillment  
of the Requirements for the Degree of Doctor of Science

(Dr. rer. nat.)

**Zijun Zhou**

Anhui, P. R. China

Marburg/Lahn 2020



Die vorliegende Dissertation entstand in der Zeit von Aug 2017 bis Oct 2020 am Fachbereich Chemie der Philipps-Universität Marburg unter der Betreuung von Herrn Prof. Dr. Eric Meggers.

Vom Fachbereich Chemie der Philipps-Universität Marburg (Hochschulkenziffer: 1180) als Dissertation am \_\_\_\_\_ angenommen.

Erstgutachter: Prof. Dr. Eric Meggers

Zweitgutachter: Prof. Dr. Armin Geyer

weitere Mitglieder Prüfungskommission: Prof. Dr. Jörg Sundermeyer

Tag der mündlichen Prüfung: \_\_\_\_\_



# **Acknowledgements**

It's really a wonderful life experience to study and get my Ph.D degree in the Meggers group at Philipps-Universität Marburg. I would like to thank everybody who has helped and supported me over the past few years.

I would like to firstly thank my dear supervisor Prof. Dr. Meggers, for his kind help, teachment, and supervision over both my M.Sc. and Ph.D. studies. It's not only the scientific attitudes from him deeply impressed me but also his patience, warm heart and wisdom. During the past few years, he has teached me a lot of the scientific skills and supervised me for solving a lot of problems occurred during my research progress.

Next, I am grateful to Prof. Armin Geyer and Prof. Jörg Sundermeyer for referring this thesis and participating in the defense committee.

Thanks a lot to Dr. Shuming Chen and Prof. K. N. Houk for the computational support. Thanks a lot to Dr. Klaus Harms, Radostan Riedel and Sergei Ivlev for the measurement and analysis of all single crystals. Thanks a lot to Dr. Xiulan Xie for the analysis of NMR spectras.

I would like to thank all of my collogues in the Meggers group as well as the collaborators from the department and other institutes. Thanks a lot to Dr. Lilu Zhang, Ina Pinnschmidt, Marcel Hemming for their kind help. Thanks a lot to Liangan Chen, Xiao Zhang, Shipeng Luo, Jiajia Ma, Yuzheng, Xiaoqiang Huang, Jie Qin, Ying Hu, Yuqi Tan, Chenhao Zhang, Erik Winterling, Yvonne Grell, Philipp Steinlandt, Xiang Shen, Tianjiao Cui, Feng Han, Xingwen Zheng, Xin Nie, for their helpful suggestions and cooperation for my research progress. I want to thank my dear mates Xiang Shen and Chenhao Zhang independently for their endless support and encouragement for me when I felt very sad, without you guys I would be lost and couldn't survive and fight against my sadness! Thanks a lot to my friend Marcel Hemming, you are the source of everyday's happyness, I like you so much! Thanks a lot to Philipp Steinlandt for translating the abstract into german version and his humor everyday! Thanks a lot for our lab's angel Yvonne Grell! Thanks a lot for Erik's talented brain and helpful discussions! Thanks a lot to all of the group members! Besides, I really appreciate for the help and company from the other current group members, Xin, Tianjiao, Feng!

At last, I would like to appreciate my beloved families for their constant support and endless encouragement! Best wishes for all of my beloved families, friends and my future life!



# Publications and Poster Presentations

## Publications:

1. **Zijun Zhou**, Yuqi Tan, Xiang Shen, Sergei Ivlev, Eric Meggers, Catalytic Enantioselective Synthesis of  $\beta$ -Amino Alcohols via Nitrene Insertion. *Manuscript submitted*.
2. **Zijun Zhou**, Yuqi Tan, Tatsuya Yamahira, Sergei Ivlev, Xiulan Xie, Radostan Riedel, Marcel Hemming, Masanari Kimura, Eric Meggers, Catalytic Enantioselective Ring-Closing C(sp<sup>3</sup>)-H Amination of Urea Derivatives. *Chem* **2020**, *6*, 2024. (“Free-featured Article”) (“Most Read”) (Highlighted by Bas de Bruin et al. *Chem* **2020**, *6*, 1847.)
3. **Zijun Zhou**, Shuming Chen, Yubiao Hong, Erik Winterling, Yuqi Tan, Klaus Harms, K. N. Houk, Eric Meggers, Non-C<sub>2</sub>-Symmetric Chiral-at-Ruthenium Catalyst for Highly Efficient Enantioselective Intramolecular C(sp<sup>3</sup>)-H Amidation. *J. Am. Chem. Soc.* **2019**, *141*, 19048.
4. **Zijun Zhou**, Shuming Chen, Jie Qin, Xin Nie, Xingwen Zheng, Klaus Harms, Radostan Riedel, K. N. Houk, Eric Meggers, Catalytic Enantioselective Intramolecular C(sp<sup>3</sup>)-H Amination of 2-Azidoacetamides. *Angew. Chem. Int. Ed.* **2019**, *58*, 1088. (“Hot Paper”)
5. **Zijun Zhou**, Xin Nie, Klaus Harms, Radostan Riedel, Lilu Zhang, Eric Meggers, Enantioconvergent Photoredox Radical-Radical Coupling Catalyzed by a Chiral-at-Rhodium Complex. *Sci. China Chem.* **2019**, *62*, 1512. (“Invited Submission”)
6. Jie Qin, **Zijun Zhou**, Tianjiao Cui, Marcel Hemming, Eric Meggers, Enantioselective Intramolecular C-H Amination of Aliphatic Azides by Dual Ruthenium and Phosphine Catalysis. *Chem. Sci.* **2019**, *10*, 3202.
7. Guanghui Wang, **Zijun Zhou**, Xiang Shen, Sergei Ivlev, Eric Meggers, Asymmetric Catalysis with a Chiral-at-Osmium Complex. *Chem. Commun.* **2020**, *56*, 7714.

## Poster Presentation:

“ORCHEM 2018”, Poster: Catalytic Enantioselective Intramolecular C(sp<sup>3</sup>)-H Amination of 2-Azidoacetamides, 10-12 September **2018**, Berlin, Germany.





## **Abstract**

Chiral transition-metal catalysts in which the chirality only originates from a stereogenic metal center have attracted much attention in the past few years as their excellent catalytic performance has been illustrated through diverse applications in catalytic asymmetric reactions, especially enantioselective intramolecular C–H amination reactions. This thesis reports the synthesis of a series of newly modified chiral-at-metal ruthenium catalysts and their applications in challenging enantioselective intramolecular C–H amination reactions.

1) Synthesis of diverse ruthenium-based chiral catalysts with exclusive metal-centered chirality as a catalyst tool box was accomplished. Through modifications of the chelating carbene ligand, the catalyst's property were changed, thus, behaved differently in catalytic asymmetric transformations. The newly modified ruthenium catalysts were used in different catalytic asymmetric intramolecular C–H amination reactions which are reported on chapter 2.1-2.4 of this thesis.

2) An catalytic enantioselective ring-closing C–H amination of 2-azidoacetamides was developed. A chiral-at-metal ruthenium complex served as the catalyst and provided chiral imidazolidin-4-ones in 31-95% yields, with enantioselectivities up to 95% ee, and catalyst loadings down to 0.1 mol% (740 TON). Mechanistic experiments reveal the importance of the amide group presumably by enabling an initial bidentate coordination of the 2-azidoacetamides to the catalyst (Chapter 2.1).

3) An application of a new class of chiral-at-metal ruthenium catalysts for enantioselective C–H amidations was developed. In the catalyst scaffold, ruthenium is cyclometalated by two 7-methyl-1,7-phenanthroline heterocycles, resulting in chelating pyridylidene remote *N*-heterocyclic carbene ligands (rNHCs). The non- $C_2$ -symmetric chiral-at-ruthenium complexes displayed unprecedented catalytic activity for the intramolecular C–H amidation of 1,4,2-dioxazol-5-ones and provided chiral  $\gamma$ -lactams with up to 98% ee and catalyst loadings down to 0.005 mol% (up to 11200 TON), while the  $C_2$ -symmetric diastereomer favored an undesired Curtius-type rearrangement. DFT calculations elucidated the origins of the superior C–H amidation reactivity displayed by the non- $C_2$ -symmetric catalysts compared to related  $C_2$ -symmetric counterparts (Chapter 2.2).

4) An enantioselective intramolecular C–H amination of *N*-benzoyloxyureas using a chiral-at-metal ruthenium catalyst was reported, providing chiral 2-imidazolidinones in yields of up to

99% and with up to 99% ee. Catalyst loadings down to 0.05 mol% were feasible. Control experiments were performed which support a stepwise nitrene insertion mechanism through hydrogen atom transfer of a ruthenium nitrenoid intermediate followed by a radical recombination. Chiral imidazolidines are prevalent in bioactive compounds and can be converted to chiral vicinal diamines in a single step. The synthetic value of the new method was demonstrated for the synthesis of intermediates of the drugs levamisole and dexamisole, the bisindole alkaloids topsentine D and spongotine A, and a chiral organocatalyst. (Chapter 2.3).

5) Chiral  $\beta$ -amino alcohols are important building blocks for the synthesis of drugs, natural products, chiral auxiliaries, chiral ligands and chiral organocatalysts. The catalytic asymmetric  $\beta$ -amination of alcohols offers a direct strategy to access this class of synthetic intermediates. In this part, we report a general intramolecular C–H nitrene insertion method for the synthesis of chiral oxazolidin-2-ones as precursors of chiral  $\beta$ -amino alcohols was developed. Specifically, the ring-closing C–H amination of *N*-benzoyloxycarbamates with just 2 mol% of a chiral ruthenium catalyst provided cyclic carbamates in up to 99% yield and with up to 99% ee. The method is applicable to benzylic, allylic, and propargylic C–H bonds and can even be applied to completely non-activated C–H bonds, although with somewhat reduced yields and stereoselectivities. The obtained cyclic carbamates can subsequently be hydrolyzed to obtain chiral  $\beta$ -amino alcohols. The method is highly practical as the catalyst can be easily synthesized in a gram scale and can be recycled after the reaction for further use. The synthetic value of the new method was demonstrated with the asymmetric synthesis of chiral oxazolidin-2-one as intermediate for the synthesis of the natural product (-)-aurantiolavine and chiral  $\beta$ -amino alcohols that are intermediates for the synthesis of chiral Box-ligand and the natural products hamacanthin A and dragmacidin A (Chapter 2.4).

# Zusammenfassung

Chirale Übergangsmetall-Katalysatoren, deren Chiralität exklusiv auf einem stereogenen Metallzentrum basiert, haben in den letzten Jahren viel Aufmerksamkeit bekommen, da ihre hervorragenden katalytischen Eigenschaften durch verschiedene Anwendungen in asymmetrischen Reaktionen, insbesondere enantioselektiven, intramolekularen C–H Aminierungen, gezeigt wurden. Diese Arbeit berichtet über die Synthese einer Reihe neuer *chiral-at-metal* Ruthenium-Katalysatoren sowie deren Anwendung bei herausfordernden, enantioselektiven, intramolekularen C–H Aminierungen.

1) Synthese verschiedener chiraler Ruthenium-Katalysatoren mit exklusiv metallzentrierter Chiralität, die entweder eine  $\Lambda$ - (linkshändiger Propeller) oder  $\Delta$ - (rechtshändiger Propeller) Konfiguration aufweisen. Durch Modifikationen des chelatisierenden Carbenliganden wurden die elektronischen Eigenschaften des Katalysators verändert und deren Einfluss in asymmetrischen Transformationen untersucht. Die neu modifizierten Ruthenium-Katalysatoren wurden in verschiedenen katalytischen, intramolekularen C–H-Aminierungen verwendet, über die in Kapitel 2.1-2.4 berichtet wurde.

2) Eine enantioselektive, ringschließende C–H-Aminierung von 2-Azidoacetamiden wird durch einen *chiral-at-metal* Rutheniumkomplex katalysiert und liefert chirale Imidazolidin-4-one in 31 bis 95% Ausbeute mit Enantioselektivitäten von bis zu 95% *ee* und Katalysatorbeladungen von bis zu 0.1 mol% (740 TON). Mechanistische Experimente zeigen die Bedeutung der Amid-Gruppe, die vermutlich eine anfängliche bidentate Koordination der 2-Azidoacetamide an den Katalysator ermöglicht (Kapitel 2.1).

3) Eine neue Klasse von chiralen Ruthenium-Katalysatoren wird vorgestellt, bei der Ruthenium durch zwei 7-Methyl-1,7-phenanthrolinium-Heterocyclen cyclometalliert wird, was zu chelatisierenden Pyridyliden-Liganden (entfernte N-Heterocyclische Carben-Liganden (rNHCs)) führt. Diese Arbeit befasst sich mit der Bedeutung der relativen metallzentrierten Stereochemie. Nur die nicht  $C_2$ -symmetrischen chiralen Rutheniumkomplexe zeigen eine beispiellose katalytische Aktivität für die intramolekulare C–H-Amidierung von 1,4,2-Dioxazol-5-onen, um chirale  $\gamma$ -Lactame mit einem Enantiomerenverhältnis von bis zu 98% *ee* bei einer Katalysatorbeladung von bis zu 0.005 mol% (bis-

zu 11200 TON) zu erhalten. Das  $C_2$ -symmetrische Diastereomer führt dagegen zu einer unerwünschten Umlagerung vom CURTIUS-Typ. Für diesen Teil wurden zudem DFT-Berechnungen durchgeführt, die eine Erklärung für das überlegene Reaktionsverhalten des nicht  $C_2$ -symmetrischen Katalysators gegenüber den verwandten  $C_2$ -symmetrischen Komplexen in der C–H-Amidierung liefern sollen (Kapitel 2.2).

4) Eine enantioselektive intramolekulare C–H-Aminierung von *N*-Benzoyloxyharnstoff unter Verwendung eines *chiral-at-metal* Ruthenium-Katalysators wird berichtet, die chirale 2-Imidazolidinone in Ausbeuten von bis zu 99% und mit bis zu 99% *ee* liefert. Katalysatorbeladungen bis zu 0.05 mol% sind möglich. Kontrollexperimente unterstützen einen schrittweisen Nitren-Insertionsmechanismus durch Wasserstoffatomtransfer eines Rutheniumnitrenoid-Intermediats gefolgt von einer radikalischen Rekombination. Chirale Imidazolidine sind in bioaktiven Verbindungen weit verbreitet und können in einem einzigen Schritt in chirale, vicinale Diamine umgesetzt werden. Die synthetische Bedeutung dieser neuen Methode wird für die Darstellung von Zwischenprodukten der Wirkstoffe Levamisol und Dexamisol, der Bisindolalkaloide Topsentin D und Spongotin A sowie eines chiralen Organokatalysators demonstriert (Kapitel 2.3).

5) Chirale  $\beta$ -Aminoalkohole sind wichtige Bausteine für die Synthese von Arzneimitteln, Naturstoffen, chiralen Auxiliaren, chiralen Liganden und chiralen Organokatalysatoren. Die katalytische, asymmetrische  $\beta$ -Aminierung von Alkoholen bietet eine direkte Strategie für den Zugang zu dieser Klasse synthetischer Zwischenprodukte. In diesem Teil berichten wir über eine allgemeine intramolekulare C–H-Nitren-Insertionsmethode zur Synthese von chiralen Oxazolidin-2-onen als Vorläufer von chiralen  $\beta$ -Aminoalkoholen. Insbesondere liefert die ringschließende  $C(sp^3)$ -H-Aminierung von *N*-Benzoyloxy-carbamat mit nur 2 mol% eines chiralen Ruthenium-Katalysators cyclische Carbamate mit bis zu 99% Ausbeute und 99% *ee*. Das Verfahren ist auf benzyliche, allyliche und propargyliche C–H-Bindungen anwendbar und kann sogar bei vollständig unaktivierten C–H-Bindungen verwendet werden, wenn auch mit verringerten Ausbeuten und Stereoselektivitäten. Die erhaltenen cyclischen Carbamate können anschließend hydrolysiert werden, um chirale  $\beta$ -Aminoalkohole zu erhalten. Das Verfahren ist sehr praktisch, da der Katalysator ohne Probleme im Gramm-Maßstab synthetisiert und nach der Reaktion zur weiteren Verwendung wiedergewonnen werden kann. Der synthetische Wert der neuen Methode wird anhand der asymmetrischen Darstellung von chiraalem Oxazolidin-2-on als Intermediat für die Synthese des

Naturstoffs (-)-Aurantiolavin und chiraler  $\beta$ -Aminoalkohole demonstriert, die Zwischenprodukte für die Synthese von chiralen Box-Liganden und den Naturstoffen Hamacanthin A und Dragmacidin A sind (Kapitel 2.4).



# **Table of Contents**

<b>Acknowledgements</b> .....	<b>V</b>
<b>Publications and Poster Presentations</b> .....	<b>VII</b>
<b>Abstract</b> .....	<b>IX</b>
<b>Zusammenfassung</b> .....	<b>X</b>
<b>Table of Contents</b> .....	<b>XI</b>
<b>Chapter 1: Theoretical Part</b> .....	<b>18</b>
<b>1.1 Introduction</b> .....	<b>1</b>
<b>1.2 Asymmetric Intramolecular C–H Aminations</b> .....	<b>1</b>
1.2.1 Synthesis of Cyclic Sulfamidates .....	2
1.2.2 Synthesis of Cyclic Sulfamides .....	4
1.2.3 Synthesis of Cyclic Sulfonamides .....	8
1.2.4 Synthesis of Cyclic Carbamates .....	8
1.2.5 Synthesis of Lactams .....	9
1.2.6 Synthesis of Cyclic Ureas.....	10
1.2.7 Synthesis of Boc-Protected Cyclic Amines .....	11
<b>1.3 Asymmetric Intermolecular C–H Aminations</b> .....	<b>12</b>
1.3.1 Rhodium Catalyst Systems.....	13
1.3.2 Ruthenium Catalyst Systems.....	16
1.3.3 Silver, Manganese, and Iron Catalyst Systems.....	17
<b>1.4 Aim of the Thesis</b> .....	<b>18</b>
<b>Chapter 2: Results and Discussion</b> .....	<b>22</b>
<b>2.1 Catalytic Enantioselective Intramolecular C–H Amination of 2-Azidoacetamides</b> .....	<b>22</b>
2.1.1 Research Background and Reaction Design.....	22
2.1.2 Synthesis of Modified Chiral-at-Ruthenium Catalysts.....	23
2.1.3 Initial Experiments and Reaction Development.....	24
2.1.4 Substrate Scope .....	26
2.1.5 Mechanistic Study .....	27
2.1.6 Conclusions .....	31
<b>2.2 Enantioselective Synthesis of <math>\gamma</math>-Lactams by Intramolecular C–H Amidation</b> .....	<b>33</b>
2.2.1 Research Background and Reaction Design.....	33
2.2.2 Synthesis of Chiral-at-ruthenium Catalysts .....	35
2.2.3 Initial Experiments and Reaction Development.....	38
2.2.4 Substrate Scope .....	39
2.2.5 Synthetic Applications.....	41
2.2.6 Mechanistic Study .....	42
2.2.7 Conclusions .....	47

<b>2.3 Enantioselective Synthesis of 2-Imidazolidinones by Intramolecular C–H Amidation...</b>	<b>49</b>
2.3.1 Research Background and Reaction Design.....	49
2.3.2 Initial Experiments and Reaction Development.....	50
2.3.3 Substrate Scope .....	52
2.3.4 Mechanistic Study .....	53
2.3.5 Synthetic Applications.....	56
2.3.6 Conclusions .....	57
<b>2.4 Enantioselective Synthesis of Cyclic Carbamates by Intramolecular C–H Amidation...</b>	<b>60</b>
2.4.1 Research Background and Reaction Design.....	60
2.4.2 Synthesis of New Chiral-at-ruthenium Catalyst.....	62
2.4.3 Initial Experiments and Reaction Development.....	63
2.4.4 Substrate Scope .....	64
2.4.5 Synthetic Applications.....	67
2.4.6 Conclusions .....	69
<b>Chapter 3: Summary and Outlook .....</b>	<b>71</b>
<b>3.1 Summary .....</b>	<b>71</b>
<b>3.2 Outlook .....</b>	<b>74</b>
<b>Chapter 4: Experimental Part.....</b>	<b>76</b>
<b>4.1 Materials and Methods.....</b>	<b>76</b>
<b>4.2 Catalytic Enantioselective Intramolecular C–H Amination of 2-Azidoacetamides.....</b>	<b>79</b>
4.2.1 Synthesis of the Ruthenium Catalysts .....	79
4.2.2 Synthesis of the Substrates .....	85
4.2.3 Catalytic Asymmetric Intramolecular C–H Aminations.....	94
4.2.4 Mechanistic Studies.....	106
4.2.5 Single Crystal X-Ray Diffraction Studies .....	112
<b>4.3 Enantioselective Synthesis of <math>\gamma</math>-Lactams by Intramolecular C–H Amidation.....</b>	<b>119</b>
4.3.1 Synthesis of the Ruthenium Catalysts .....	119
4.3.2 Synthesis of the Substrates .....	123
4.3.3 Ruthenium Catalyzed Enantioselective Intramolecular C–H Amidations.....	128
4.3.4 Gram-Scale Reactions and Mechanistic Study.....	138
4.3.5 Single Crystal X-Ray Diffraction Studies .....	146
<b>4.4 Enantioselective Synthesis of 2-Imidazolidinones by Intramolecular C–H Amidation. 150</b>	<b>150</b>
4.4.1 Synthesis of the Substrates .....	150
4.4.2 Ruthenium Catalyzed Intramolecular C–H Amidations .....	160
4.4.3 Mechanistic Experiments .....	173
4.4.4 Synthetic applications.....	176
4.4.5 Single Crystal X-Ray Diffraction Studies .....	180
<b>4.5 Enantioselective Synthesis of Cyclic Carbamates by Intramolecular C–H Amidation. 184</b>	<b>184</b>
4.5.1 Synthesis of the Ruthenium Catalyst.....	184
4.5.2 Synthesis of the Substrates .....	185



4.5.3 Ruthenium Catalyzed Asymmetric Intramolecular C–H Amidation .....	197
4.5.4 Mechanistic Experiments .....	213
4.5.5 Synthetic Applications.....	215
4.5.6 Single Crystal X-Ray Diffraction Studies .....	218
<b>Chapter 5: Appendices .....</b>	<b>221</b>
<b>5.1 List of Abbreviations .....</b>	<b>221</b>
<b>5.2 List of Figures.....</b>	<b>224</b>
<b>5.3 List of Tables .....</b>	<b>229</b>
<b>5.4 List of New Transition Metal Complexes.....</b>	<b>230</b>
<b>5.4 List of New Organic Compounds .....</b>	<b>231</b>
<b>Statement.....</b>	<b>237</b>
<b>Curriculum Vitae.....</b>	<b>238</b>



# Chapter 1: Theoretical Part

## 1.1 Introduction

The prevalence of chiral amines in pharmaceuticals, natural products, fine chemicals, agrochemicals, and as reagents or chiral ligands of asymmetric catalysts in organic synthesis has motivated the organic chemist for developing mild, efficient and convenient methodology for the construction of chiral C-N bonds. The typical conventional synthetic methods rely on functional group conversions, such as the cross-coupling reaction of aryl- or alkenyl (pseudo)halides with amines under optimal catalytic systems (**Figure 1a**).<sup>1</sup> Recently, the construction of C-N bonds by direct C-H amination, without the preinstallation of any reactive functional group, has attracted much attention. Among them, C-H amination via nitrene insertion is one of the most efficient method for building a chiral C-N bond (**Figure 1b**). With high motivation for making progress in this field, recently, different linear and cyclic chiral amines and amides have been synthesized through this methodology.<sup>2</sup>

Catalytic asymmetric amination via nitrene insertion:

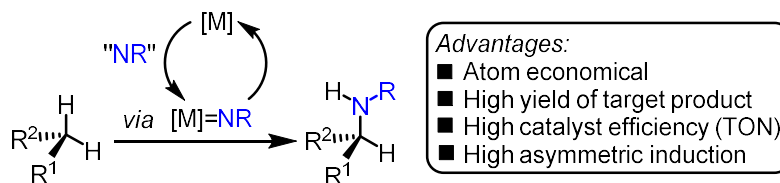


**Figure 1.** General concept of asymmetric amination via nitrene insertion.

## 1.2 Asymmetric Intramolecular C-H Aminations

The transition-metal catalyzed ring-closing C-H amination via nitrenoid intermediate is one of the most powerful tool for the synthesis of chiral nitrogen-containing heterocycles. In one mechanistic manifold, intermediate transition metal nitrenoid insert a nitrogen atom between C-H bonds to build a C-N bond in either a stepwise or concerted fashion. As shown in **Figure 2**, nitrene precursor undergo the activation of transition-metal catalyst and generate either singlet or triplet metal-nitrenoid intermediate. Singlet nitrenes undergo a concerted C-H insertion and triplet nitrenes undergo hydrogen atom transfer (HAT) followed by fast radical recombination, which leads to the formation of catalyst bound product. Product release and new substrate participation finishes the whole catalytic cycle. Different functional groups served as nitrene precursors have been developed in the past few decades<sup>1</sup> and the intramolecular version of the reaction renders directing groups obsolete, while exerting high control over the regioselectivity. This methodology has been applied to the catalytic

asymmetric synthesis of cyclic sulfamidates, sulfamides, sulfonamides, carbamates, lactams, ureas, Boc-protected pyrrolidines, and related Boc-protected heterocycles. The following section will briefly review the asymmetric intramolecular ring-closing C–H amination reactions.

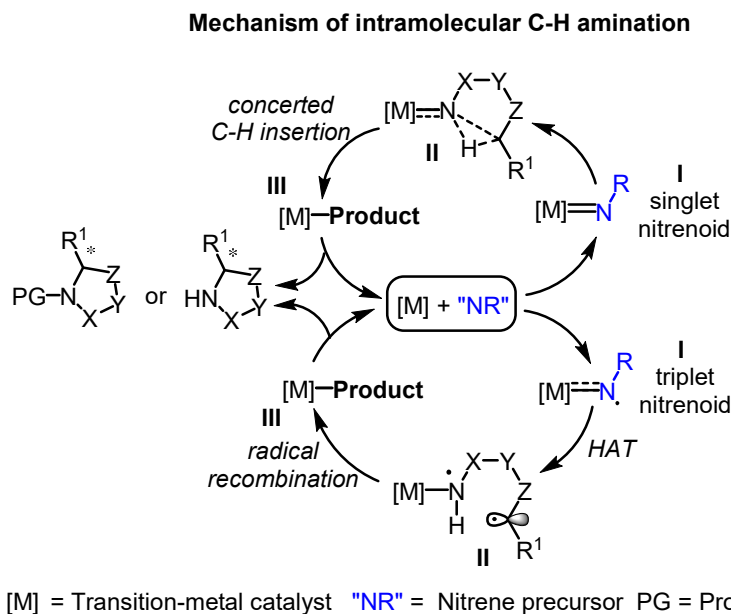


**Figure 1.** Mechanism of intramolecular C–H amination via metal-nitrenoid intermediate.

### 1.2.1 Synthesis of Cyclic Sulfamidates

Chiral cyclic sulfamidates are very useful organic small molecules as it can be used for further one step ring-open to the corresponding  $\beta$ - or  $\gamma$ -amino alcohols which are widely used as intermediates for the synthesis of drugs, natural products and as chiral ligands used in asymmetric catalysis.<sup>3</sup>

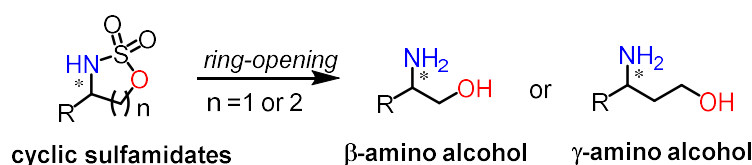


**Figure 3.** Ring-opening of chiral cyclic sulfamidates.

In 2002, Chi-Ming Che and co-workers demonstrated for the first time about highly enantioselective intramolecular ring-closing C–H aminations by detailed investigation of the ruthenium porphyrin catalyzed asymmetric synthesis of chiral cyclic sulfamidates (**Figure 4**).<sup>3</sup> The ring-closing C–H aminations were of high diastereoselectivity and enantioselectivity which provided 5- or 6-membered chiral cyclic sulfamidates in up to 77% yield and 87% ee. Different functional groups on the phenyl moiety were well tolerated. Although the yields were only modest, the overall results were quite impressive.

Chiming Che (2002)

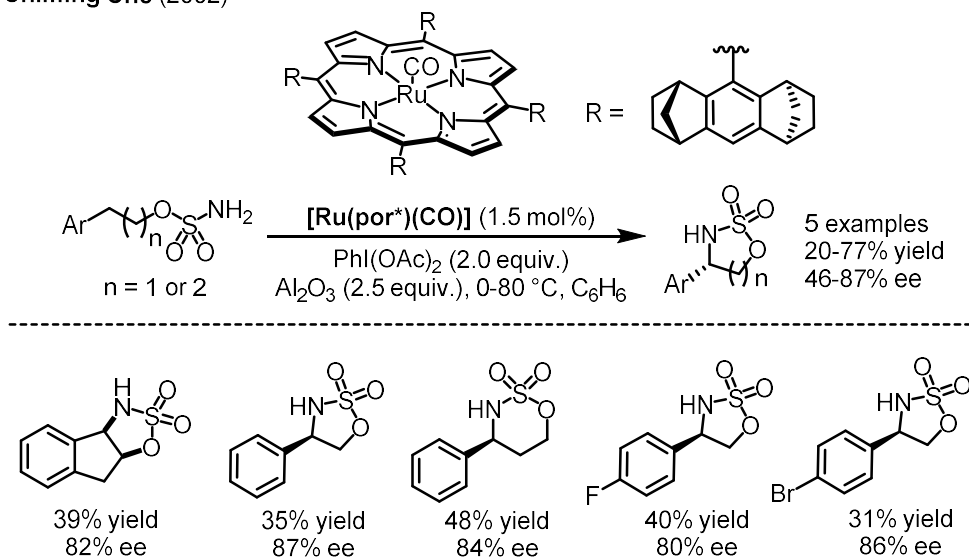


**Figure 4.** Research from the Chi-Ming Che group on the synthesis of chiral cyclic sulfamidates.

In 2008, the Blakey group subsequently reported a simplified ruthenium catalyst system for this reaction. Such ruthenium(II)–pybox complexes were readily prepared by using a method developed by Nishiyama’s group.<sup>4</sup> For the same transformations of linear sulfamidates to cyclic sulfamidates, this catalyst system provided much better results with up to 93% yield and 92% ee and in some cases with excellent diastereoselectivity for the formation of 6-membered cyclic sulfamidates as benzylic C–H bonds are more active than aliphatic C–H bonds at the stage of C–H insertion (**Figure 5**).

Simon Blakey (2008)

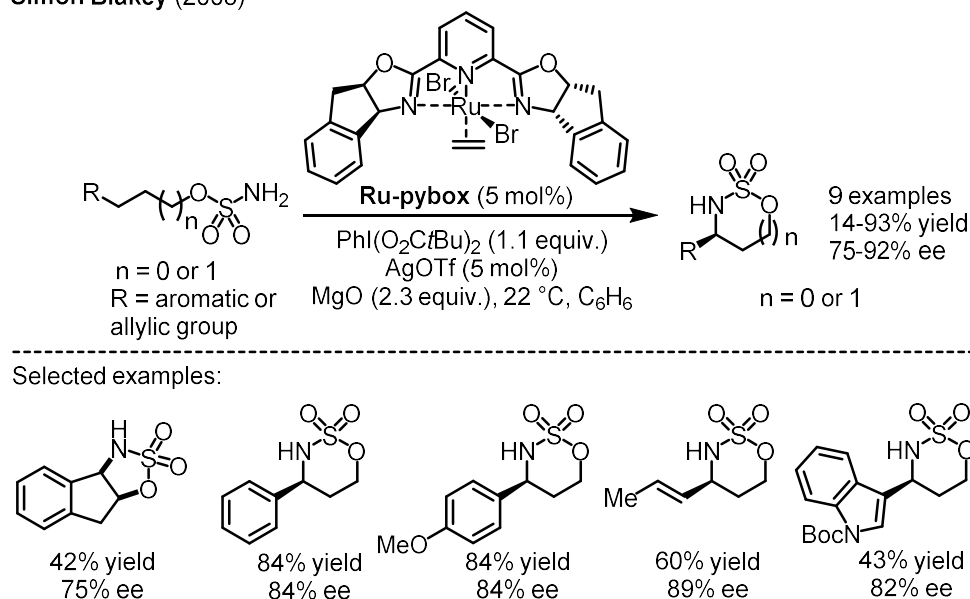


**Figure 5.** Research from the Simon Blakey group on the synthesis of chiral cyclic sulfamidates.

Almost at the same time, the Du Bois group reported a chiral rhodium carboxamidate catalyzed

enantioselective ring-closing C–H amination of sulfamidates.<sup>5</sup> The newly designed dirhodium catalyst contains a strongly donating carboxamidate ligand instead of carboxylate which increases the capacity of the dirhodium centers for backbonding to the  $\pi$ -acidic nitrene ligand, thus affording a more stable and potentially more discriminating oxidant. As shown in **Figure 6**,  $\text{Rh}_2(\text{S-nap})_4$  displays unprecedented catalytic performance for the enantioselective intramolecular amination of benzylic C–H bonds with up to 98% yield and 99% ee. The design and development of this unique dirhodium complex further advance methods on enantioselective intramolecular C–H amination for the synthesis of chiral cyclic sulfamidates.

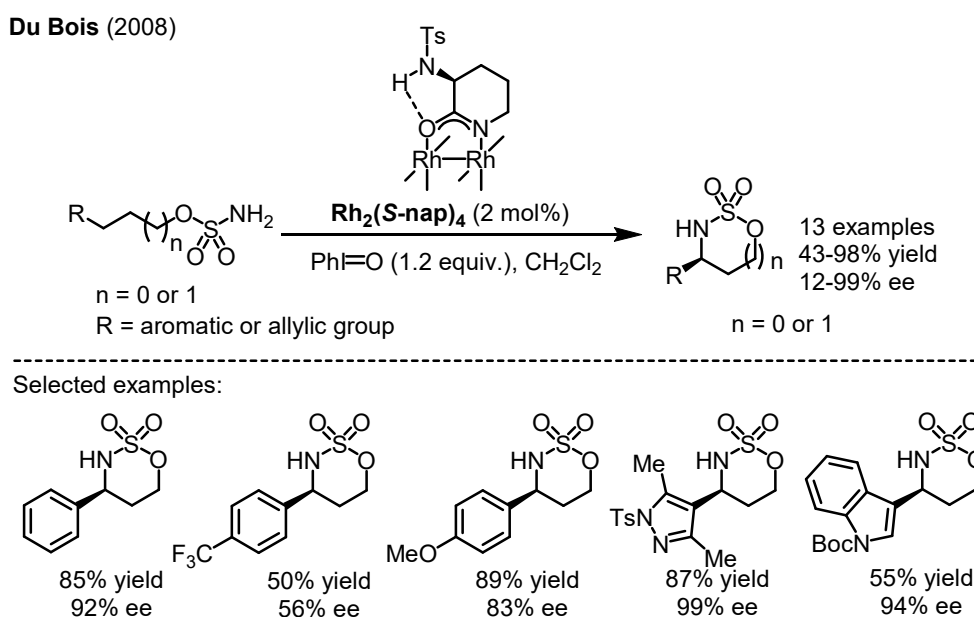


**Figure 6.** Research from the Du Bois group on the synthesis of chiral cyclic sulfamidates.

### 1.2.2 Synthesis of Cyclic Sulfamides

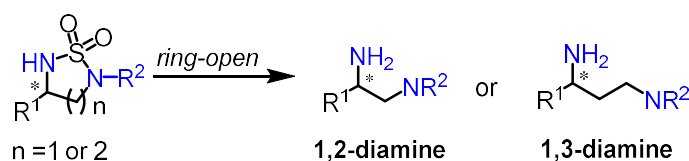


**Figure 7.** Ring-open of chiral cyclic sulfamides.

Although the structure of sulfamides are similar with sulfamidates which contain a nitrogen instead of the oxygen atom, they are different types of useful scaffolds as it can be manipulated for further one step ring-opening to the corresponding 1,2- or 1,3-diamines which are well-known synthetic intermediates for drugs, natural products and as chiral ligands used in asymmetric catalysis (**Figure 7**).<sup>6-8</sup>

In 2011, the Katsuki group firstly reported the synthesis of chiral cyclic sulfamides by efficient

intramolecular nitrene C–H insertion using sulfonyl azide substrates together with their newly invented **Ir-salen** catalyst (**Figure 8**).<sup>6</sup> The C–H aminations proceeded smoothly and provided target 5-membered sulfamides in 49% yield and 74% ee for a phenyl substituent and 65% yield with 75% ee for the *para*-methoxy substituent. Although they only showed two examples, this pioneering work showcased that chiral cyclic sulfamides can be synthesized through efficient nitrene C–H insertion methodology.

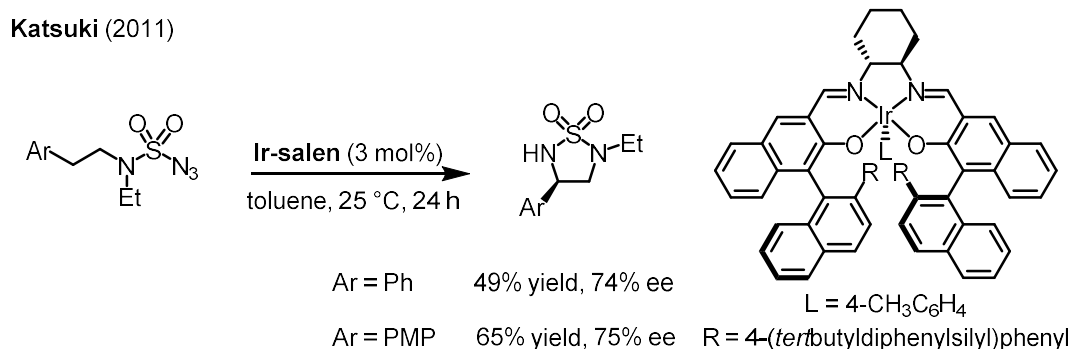


**Figure 8.** Research from the Katsuki group on the synthesis of chiral cyclic sulfamides.

In 2018, the Peter Zhang group explored the synthesis of 6-membered cyclic chiral sulfamides by using their unique chiral cobalt porphyrin catalysts (**Figure 9**).<sup>7a</sup> The ring-closing C–H aminations were of high diastereoselectivity as the major products were always forming in 6-membered rings. This methodology was broadly applicable as they showed it can be applied to efficient benzylic, propargylic, allylic, electron-deficient and even non-activated aliphatic C–H aminations with 25 examples in up to 95% yield and 98% ee.

After systematic research work on modifications of their chiral porphyrin catalysts, they successfully invented a novel *D*<sub>2</sub>-symmetric chiral amidoporphyrin with alkylbridges across two chiral amide units on both sides of the porphyrin plane which is constructed in a modular fashion to permit variation of the bridge length. As showcased with enantioselective intramolecular C–H amination of sulfamoyl azides, the asymmetric 1,5-C–H amination is not easy for enantiocontrol (as shown in **Figure 8** with two examples in up to 75% ee).

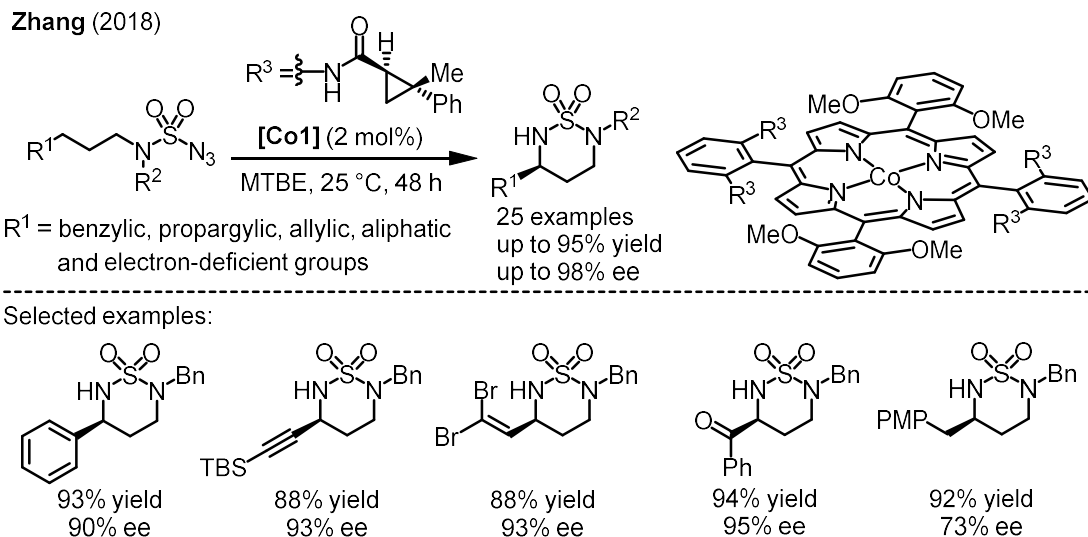


**Figure 9.** Research from the Peter Zhang group on the synthesis of 6-membered chiral cyclic sulfamides.

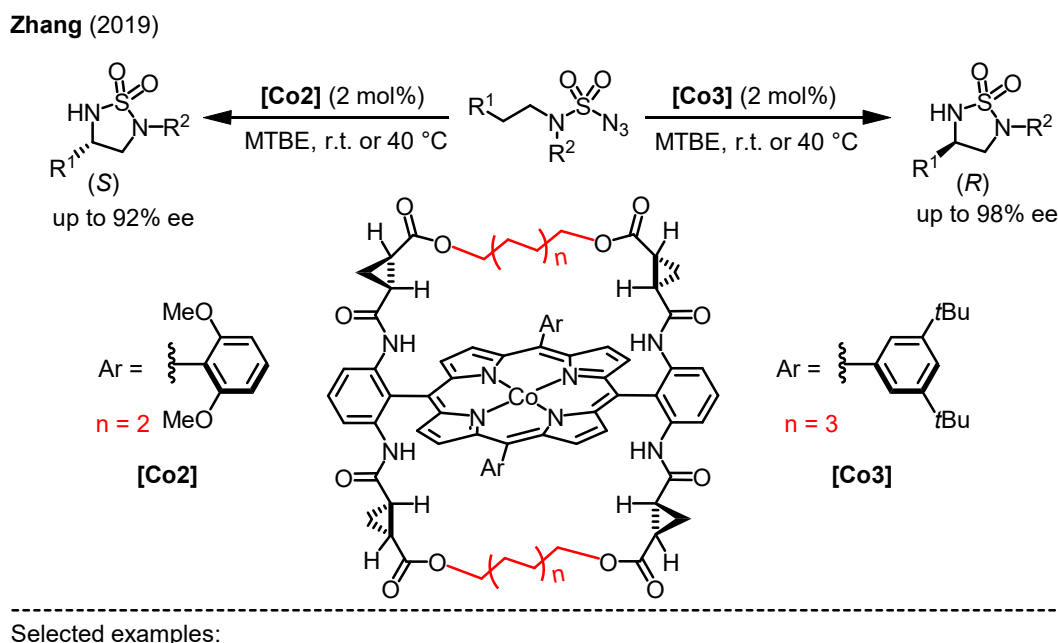


**Figure 10.** Research from the Peter Zhang group on the synthesis of 5-membered chiral cyclic sulfamides.

With the support of new catalysts, the Zhang group found that ring-closing C–H amination reactions could also be applied to the highly enantioselective synthesis of 5-membered chiral cyclic sulfamides. Interestingly, by changing the substituents of the chiral porphyrin ligand, the desired cyclic sulfamide products were formed with switched absolute configurations between (*R*) and (*S*) (**Figure**



10). As shown by the authors, the C–H aminations proceeded effectively at benzylic, propargylic, allylic and also aliphatic C–H bonds with up to 98% yield and 98% ee.<sup>7b</sup>

Subsequently, the Arnold's group invented an enzymatic platform for the asymmetric amination of primary, secondary and tertiary C–H bonds which lead to the formation of corresponding 5- and 6-membered chiral cyclic sulfamides in up to 51400 TTN and 99% ee (**Figure 11**)<sup>8</sup>. The concept “TTN” is a dimensionless number, defined as the ratio of moles of product generated divided by the moles of biocatalyst used in a reaction.

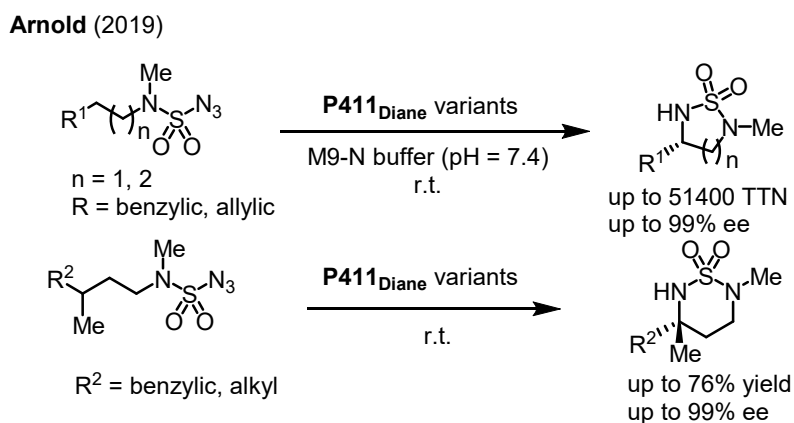
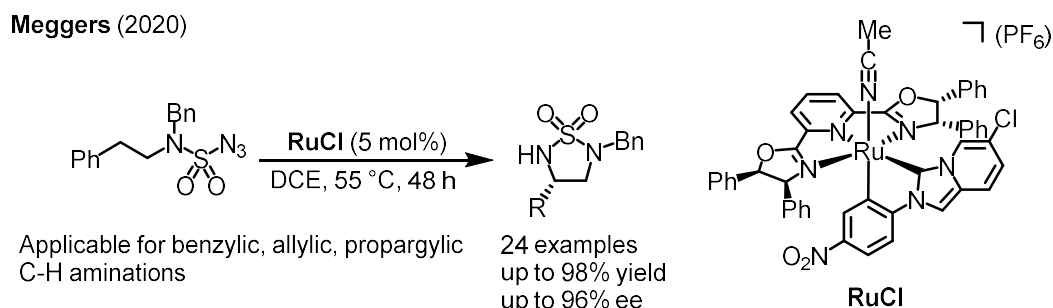


**Figure 11.** Research from the Arnold group on the synthesis of 5- and 6-membered chiral cyclic sulfamides.



Selected examples:

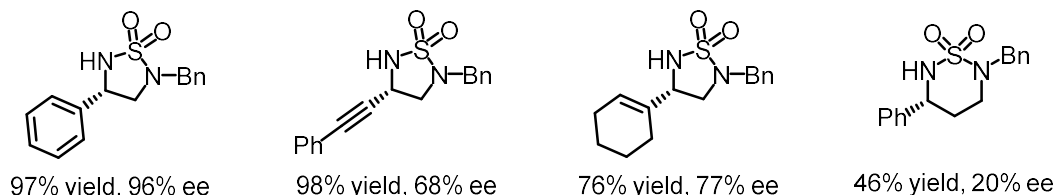


**Figure 12.** Research from the Meggers group on the synthesis of 5- and 6-membered chiral cyclic sulfamides.

In 2020, our group introduced a strategy to increase the utility of chiral pybox metal complexes for asymmetric catalysis by complementing the pybox ligand with an additional bidentate ligand. Such chiral ruthenium catalysts could be successfully applied in asymmetric C–H aminations of sulfamoyl

azides. The C–H aminations could happen at benzylic, propargylic and allylic positions to provide cyclic sulfamides in up to 98% yield and 96% ee (**Figure 12**).<sup>9</sup>

### 1.2.3 Synthesis of Cyclic Sulfonamides

Since 2011, several groups have reported the enantioselective intramolecular C–H amination of sulfamoyl azides to chiral cyclic sulfonamides which is an important structure core in several biological active organic small molecules (**Figure 13**). The Katsuki group firstly invented this kind of transformation by using their chiral **Ir-salen** catalyst in the presence of sulfamoyl azide substrates providing desired 5-membered ring product in 77% yield and 92% ee which is quite impressive.<sup>6</sup> Later, the Arnold group used their unique enzymatic catalyst system for a similar transformation which achieved up to 89% ee.<sup>10</sup> The Fasan group used the same catalyst as Arnold but with some modification of the reaction conditions and the substrate's structure finally improved the results to up to 310 TTN and 91% ee.<sup>11</sup> Further progress was reported by the Hartwig group, they used an **Ir(Me)-PIX CYP<sub>119</sub>** catalyst system, which is a cytochrome P450 enzyme derived from a thermophilic organism and containing an iridium porphyrin cofactor (**Ir(Me)-PIX**) in place of the heme to improve the results to up to 98% yield and 90% ee.<sup>12</sup>

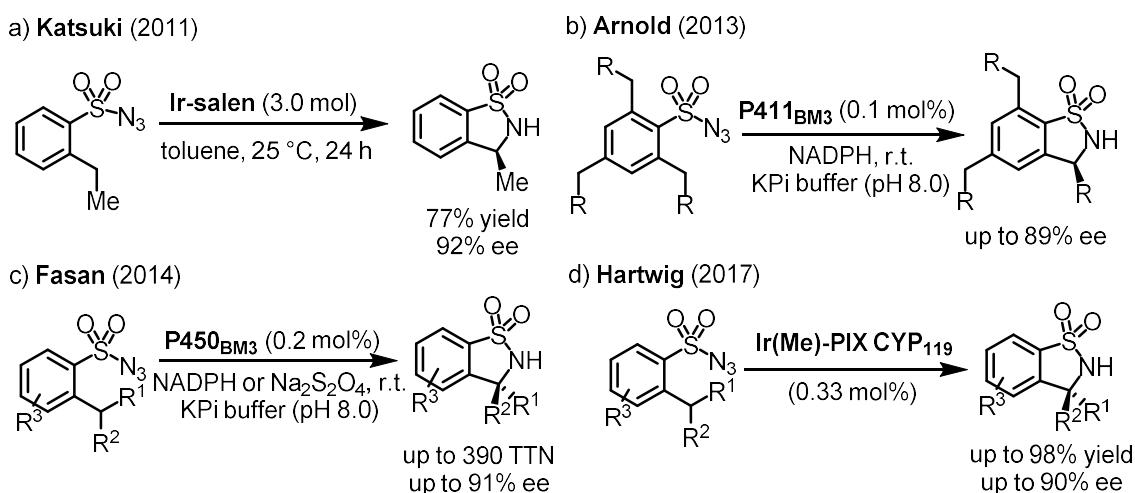


**Figure 13.** Synthesis of chiral sulfonamides via nitrene insertion.

### 1.2.4 Synthesis of Cyclic Carbamates

Compared with chiral sulfamidates, carbamates have the advantage of a more facile ring-opening which can proceed smoothly under mild reaction conditions. Besides, the catalytic intramolecular C–H amination of sulfamidates often lead to the formation of 6-membered cyclic sulfamidates which is not suitable for synthesizing chiral  $\beta$ -amino alcohols. Thus, it makes more sense to put efforts in finding a

suitable catalyst system for the synthesis of chiral cyclic carbamates via nitrene insertion.

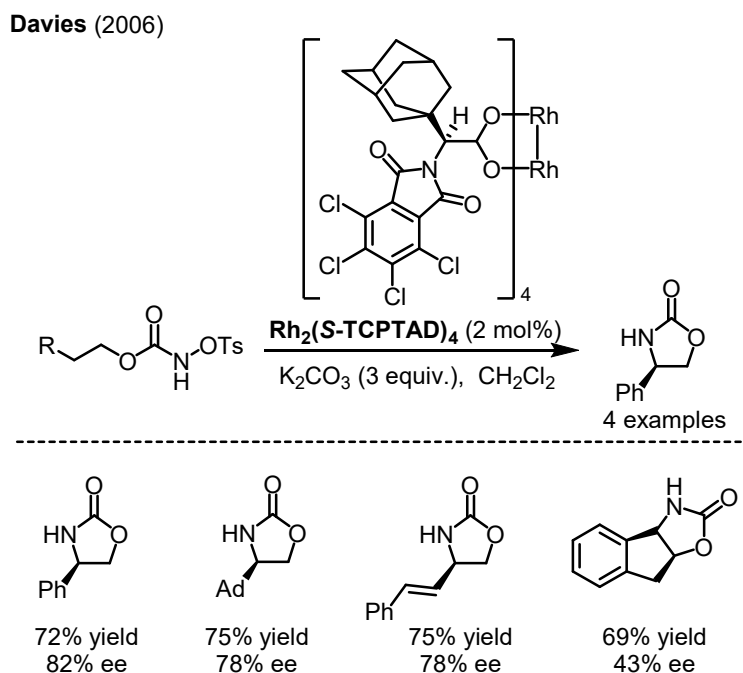


**Figure 14.** Research from the Davies group on the synthesis of chiral cyclic carbamates.

In 2008, the Davies group reported preliminary results on enantioselective intramolecular C–H amination for the synthesis of chiral cyclic carbamates.<sup>13</sup> In their report, they provided only four examples using *N*-tosyloxycarbamates as nitrene precursor under chiral dirhodium catalysis. Unfortunately, yields (62–75%) and enantioselectivities (43–82% ee) were only very modest and not of practical value (**Figure 14**).

### 1.2.5 Synthesis of Lactams

Different with the acylnitrenoid intermediate involved in the synthesis of cyclic carbamates, intramolecular insertion of metal nitrenes into C–H bonds to form  $\gamma$ -lactams has traditionally been hindered by competing isocyanate formation (Curtius rearrangement).<sup>14</sup> In 2018, the Chang's group solved this problem by optimizing a class of pentamethylcyclopentadienyl iridium(III) catalysts for suppression of the competing Curtius decomposition pathway. Modulation of the stereoelectronic properties of the bidentate ligands to be more electron-donating was suggested by density functional theory calculations to lower the C–H insertion barrier favoring the desired C–H amination.<sup>14</sup>

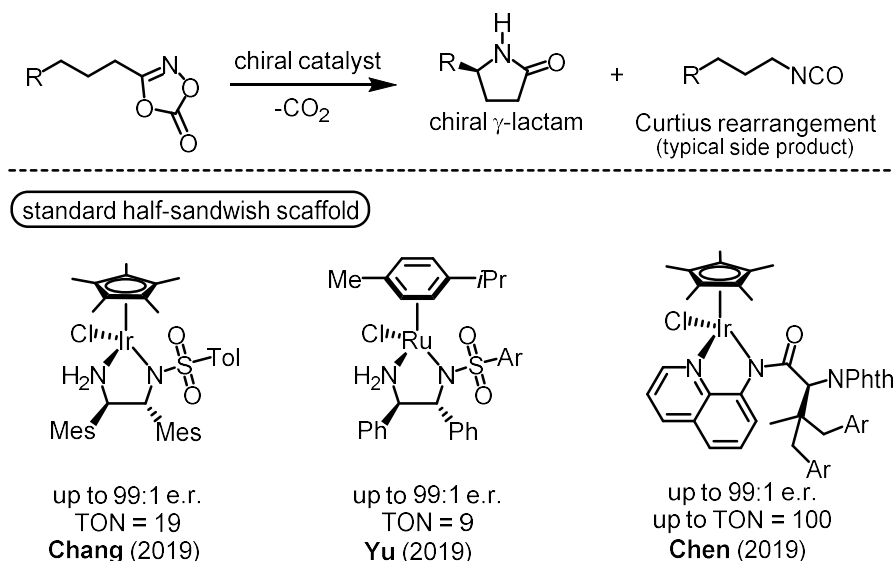


**Figure 15.** Synthesis of chiral lactams via nitrene insertion.

Subsequent research progress of this reaction was reported by the same group as an asymmetric version.<sup>15</sup> By introducing a chiral bidentate ligand, the desired chiral lactam products were formed in up to 99% yield and 99:1 e.r., despite the TON of this transformation was quite low as only 19. Further progresses of this transformation were reported by the Yu group and Chen group,<sup>16,17</sup> the results were further improved to 100 TON. Both of these three reports, the catalysts were similar half-sandwich structures (**Figure 15**).

### 1.2.6 Synthesis of Cyclic Ureas

The asymmetric intramolecular C–H aminations were already reported for several times and have been illustrated as a powerful tool for the synthesis of chiral nitrogen-containing heterocycles. This methodology has been applied to the catalytic asymmetric synthesis of cyclic sulfamidates, sulfamides, sulfonamides, carbamates, and lactams. However, interestingly, urea derivatives as nitrene precursors leading to the catalytic enantioselective formation of chiral cyclic ureas, specifically 2-imidazolidinones, were not reported yet when the work for this thesis was initiated. The only reports were from Du Bois on racemic rhodium-catalyzed ring-closing amination of urea derivatives using  $\text{PhI}(\text{OAc})_2$  as the oxidant.<sup>18</sup> The absence of catalytic enantioselective versions to obtain chiral imidazolidin-2-ones is unfortunate considering the prevalence of this motif in bioactive compounds and their use as chiral auxiliaries.

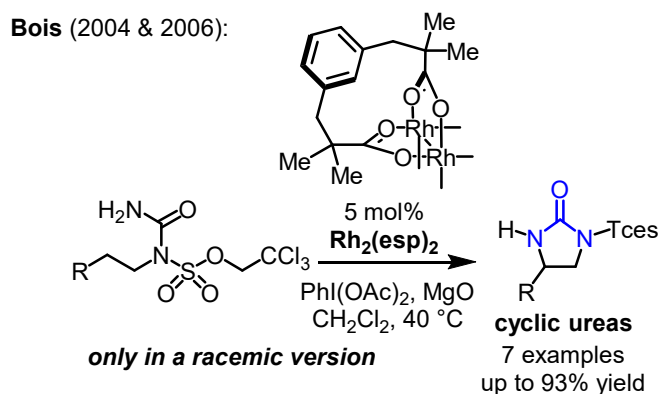


**Figure 16.** Synthesis of cyclic ureas in a racemic version from the Bois group.

Furthermore, chiral 2-imidazolidinones can be converted in a single step to chiral vicinal diamines which are valuable building blocks for the synthesis of medicinal agents, natural products, chiral ligands, and chiral catalysts.

### 1.2.7 Synthesis of Boc-Protected Cyclic Amines

#### Nitrenes with different substituents

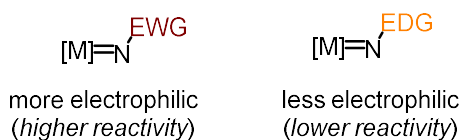


**Figure 17.** Nitrenes with different substituents.

Because of metal-nitrenoid intermediate's electrophilic nature, such kind of nitrenoid intermediates with electron withdrawing groups lead to the formation of more electrophilic nitrenes which exhibit higher reactivity for the C–H amination reactions (**Figure 17**). In contrast, electron donating groups as substituents decrease the reactivity of corresponding nitrene intermediates, thus, the related C–H amination reactions become more difficult.

In 2013, the Betley group firstly reported an iron-catalyzed intramolecular C–H amination of aliphatic organic azide for the synthesis of Boc-protected cyclic amines namely pyrrolidines and the de Bruin group introduced a chiral cobalt porphyrin catalyst system which could get a preliminary result in an enantioselective version as showcased with only one example with 22% yield and 46% ee (**Figure 18**).<sup>19</sup>

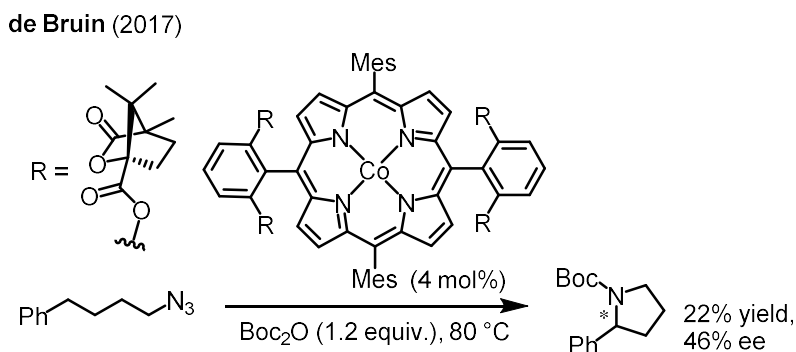


**Figure 18.** Research progress on the synthesis of the chiral Boc-protected pyrrolidine.

### 1.3 Asymmetric Intermolecular C–H Aminations

As compared with intramolecular C–H aminations, the intermolecular version has its particular advantages for the synthesis of chiral amines. As discussed in the above chapter 1.2, intramolecular C–H aminations are more efficient, with high asymmetric induction, but they often need several steps of additional transformations to achieve the synthesis of final chiral amines. Due to this further ring-opening step, some functional groups are not well tolerated (**Figure 19a**). The asymmetric intermolecular C–H amination via nitrene insertion to the C–H bonds can build a chiral C–N bond directly, which is much more convenient than the corresponding intramolecular version. The intermolecular C–H amination reactions also face several challenges, such as low efficiency and site-selectivity in outer-sphere C–H aminations and the enantioselectivity of the desired amination products are not as good as related intramolecular C–H aminations (**Figure 19b**).

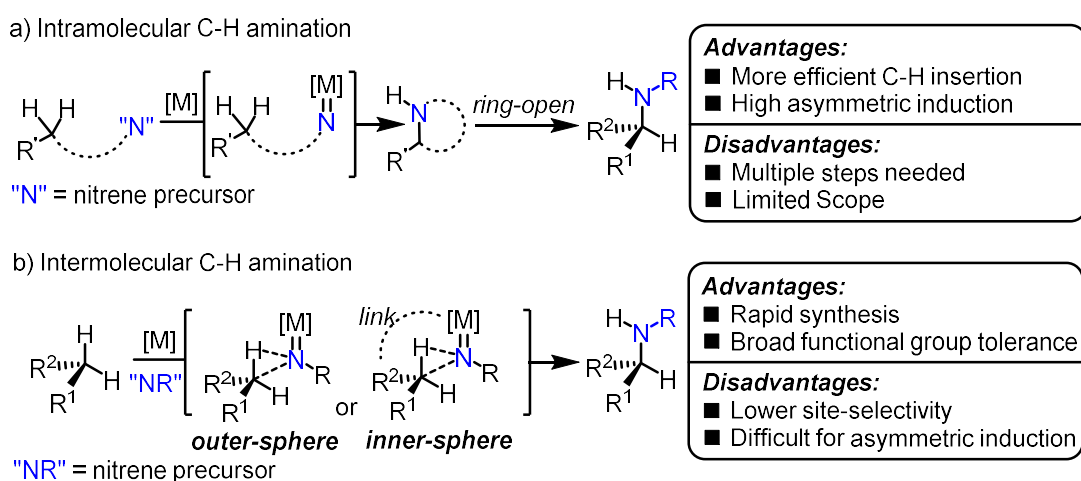


**Figure 19.** Comparison of intra- and intermolecular C–H amination for the synthesis of chiral amines.

Although, the asymmetric intermolecular C–H amination reactions are very challenging, several successful examples have already been reported in the past few decades. The following section will

briefly review the asymmetric intermolecular C–H amination reactions and category them by different transition-metal catalyst systems.

### 1.3.1 Rhodium Catalyst Systems

Among the reported examples of asymmetric intermolecular C–H aminations, rhodium-centered catalysts were the most frequently used transition metal catalysts. Such as dirhodium paddlewheel complexes, which feature significant structural rigidity, ease of ligand exchange, facile diaxial coordination sites, and relatively low oxidation potential, are widely utilized in asymmetric C–H aminations. Pioneering work by the Müller group for direct C–H amination of an indane substrate with dirhodium catalyst provided the desired C–H amination product in 71% yield and 30% ee as a groundbreaking result.<sup>20</sup> The result has been further improved by the Hashimoto group to 82% yield and 70% ee by modification of the dirhodium catalyst's bidentate chiral ligand (**Figure 20**).<sup>21</sup>

In 2006, the Davies group disclosed an intermolecular benzylic C–H amination system using a dirhodium(II) complex as the catalyst, which led to the formation of desired intermolecular C–H amination products in up to 95% yield and 94% ee (**Figure 21**).<sup>13</sup>

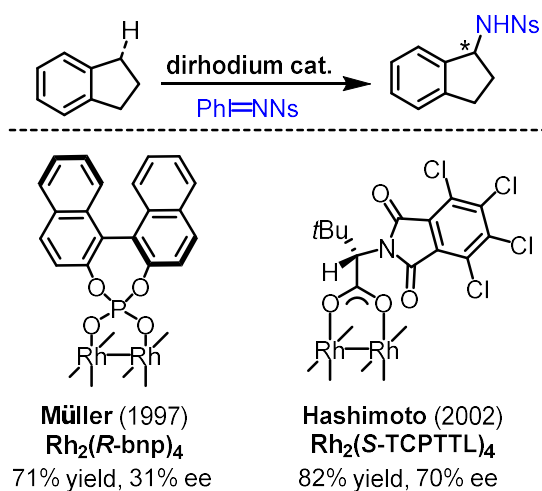


**Figure 20.** Pioneering work on intermolecular C–H amination of indane substrate.

Davies (2006)

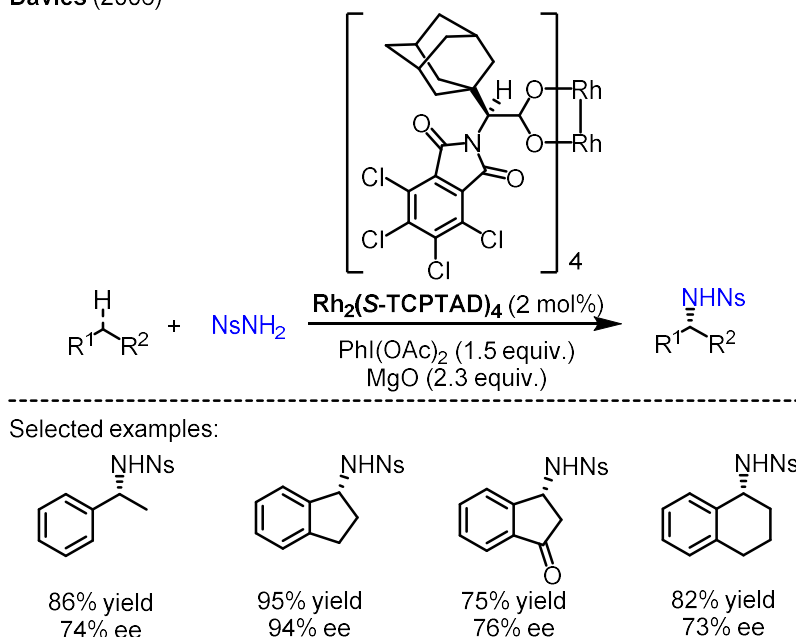


**Figure 21.** Intermolecular C–H amination work from the Davies group.

In 2019, the Dauban group made further modifications of the dirhodium catalysts, combining the pentafluorobenzyl sulfamate with the chiral rhodium complex **Rh<sub>2</sub>(S-tfptad)<sub>4</sub>** which has led to the development of a catalytic asymmetric intermolecular C–H amination reaction with a broad scope in excellent yields and enantioselectivities. The reaction could scale up to gram-scale with equal efficiency (**Figure 22**).<sup>22</sup>

Dauban (2019)

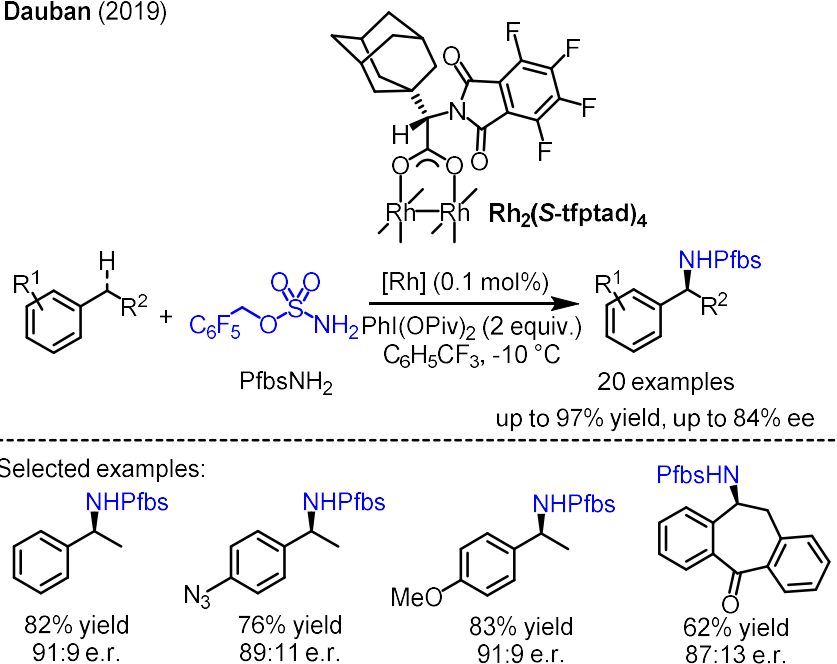


**Figure 22.** Intermolecular C–H amination work from the Dauban group.



In 2013, the Bach group developed a dual catalysis system, in which the rhodium center is responsible for activating PftbsNH<sub>2</sub> substrate to generate rhodium-nitrenoid intermediate, and the ligand contains a chiral amide functional group which can form hydrogen bond activation with another substrate, thus, providing high asymmetric induction with up to 74% ee (**Figure 23**).<sup>23</sup>

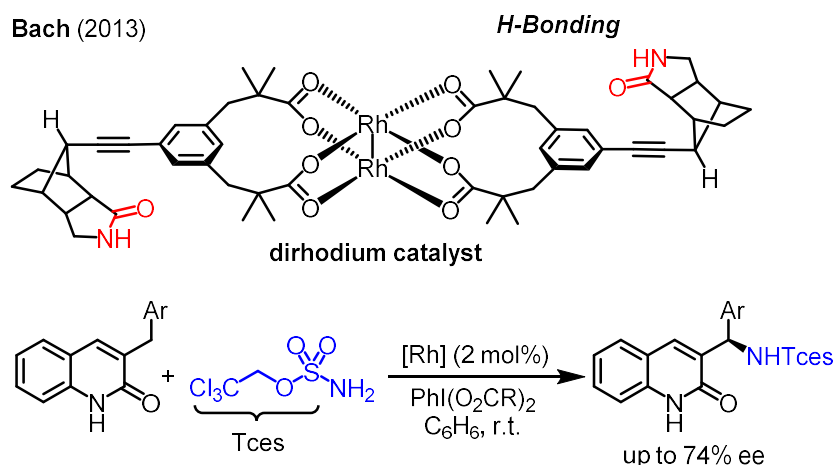


**Figure 23.** Intermolecular C–H amination work from the Bach group.

Besides, chiral rhodium cyclopentadiene complexes have been reported as efficient catalysts used in asymmetric C–H functionalization reactions. In 2019, the Matsunaga group reported a chiral carboxylic acid assisted enantioselective intermolecular benzylic C–H amination with 46-99% yield and up to 88% ee. From their proposed mechanism, the binaphthyl-based chiral carboxylic acid assisted the enantioselective cleavage of methylene C–H bonds in building a chiral C–N bond (**Figure 24**).<sup>24</sup>

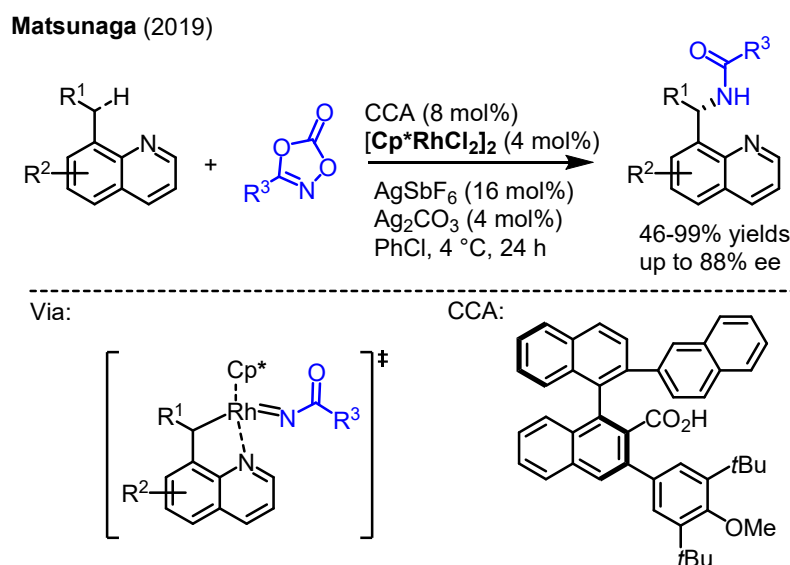


**Figure 24.** Intermolecular C–H amination work from the Matsunaga group.

Recently, the Blakey group reported an asymmetric inner-sphere C–H amination reaction (**Figure 25**). They developed a new planar chiral rhodium indenyl complex for regio- and enantioselective amination of allylic C–H bonds. The reaction exhibited broad functional group compatibility, provided an array of enantioenriched allylic amide products from readily available alkene starting materials. Crystallographic experiments supported the electronic transmission of asymmetry from the planar chiral indenyl ligand to the  $\pi$ -allyl ligand as a critical intermediate in the catalytic cycle. The overall results are quite impressive as 24 examples in up to 90% yield and 99:1 e.r.<sup>25</sup>

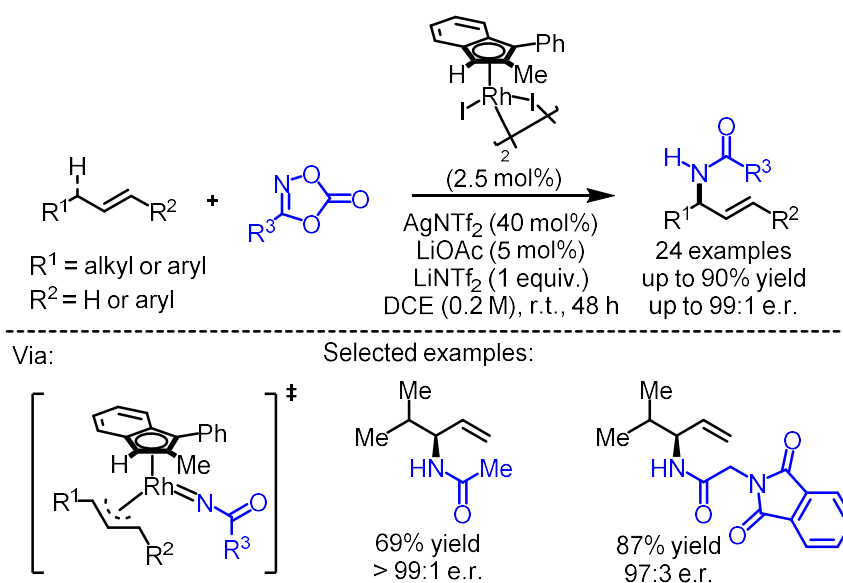


**Figure 25.** Intermolecular C–H amination work from the Blakey group.

### 1.3.2 Ruthenium Catalyst Systems

In 1999, the Chi-Ming Che group reported the first example of a ruthenium-centered chiral catalyst for asymmetric intermolecular C–H aminations (**Figure 26**). The enantioselective intermolecular amination at benzylic C–H bonds provided target chiral sulfonylamides in up to 58% yield as preliminary results.<sup>26</sup>

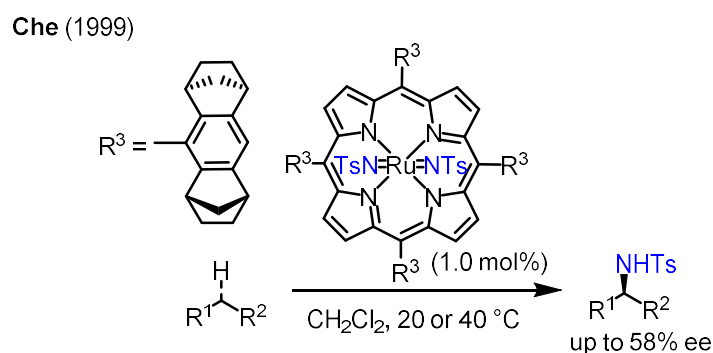


**Figure 26.** Intermolecular C–H amination work from the Chi-Ming Che group.

In 2003, the Katsuki group invented the **Ru(salen)(CO)** catalyst and successfully applied it in the asymmetric intermolecular C–H amination of allylic C–H bonds in up to 80% ee. The yield of the desired product was relatively low. The same group reported an improved result in 2011. They used the modified substrate **SESN<sub>3</sub>** and catalyst. Finally, the results were improved to 99% ee with broad substrate scope as shown for 22 examples (**Figure 27**).<sup>27</sup>

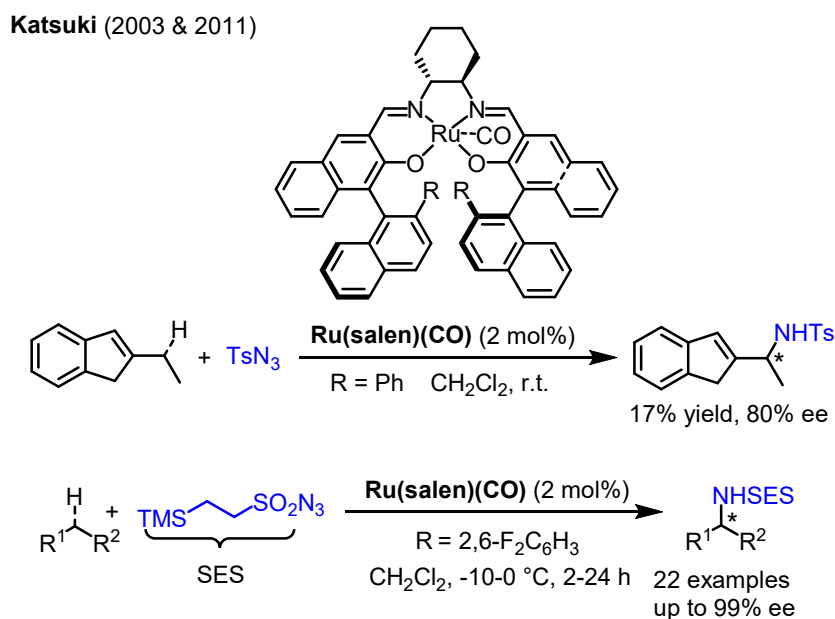


**Figure 27.** Intermolecular C–H amination work from the Katsuki group.

### 1.3.3 Silver, Manganese, and Iron Catalyst Systems

Transition metals such as silver, manganese, and iron were also reported to be used as catalysts in this kind of transformations. In 2001, the Katsuki group reported a chiral manganese salen complex catalyzed intermolecular C–H aminations of benzylic C–H bonds in up to 71% yield and 89% ee (**Figure 28a**).<sup>28</sup> Later, in 2017, the Arnold group successfully applied their chiral iron-porphyrin based enzymatic catalyst system in asymmetric intermolecular C–H amination of benzylic C–H bonds. The desired chiral amides were obtained in up to >99% ee and up to 1300 TON (**Figure 28b**).<sup>29</sup> Subsequently, in 2020, the same group reported the asymmetric primary C–H aminations at both benzylic and allylic C–H bonds provided desired chiral amines in up to 3930 TTN and 96% ee (**Figure 28c**).<sup>30</sup> Recently, the Bach group reported a dual catalytic system in which the chiral ligand forming hydrogen bonds with substrates and led to high asymmetric induction for the synthesis of desired amination products in up to 88% yield and 97% ee (**Figure 28d**).<sup>31</sup>

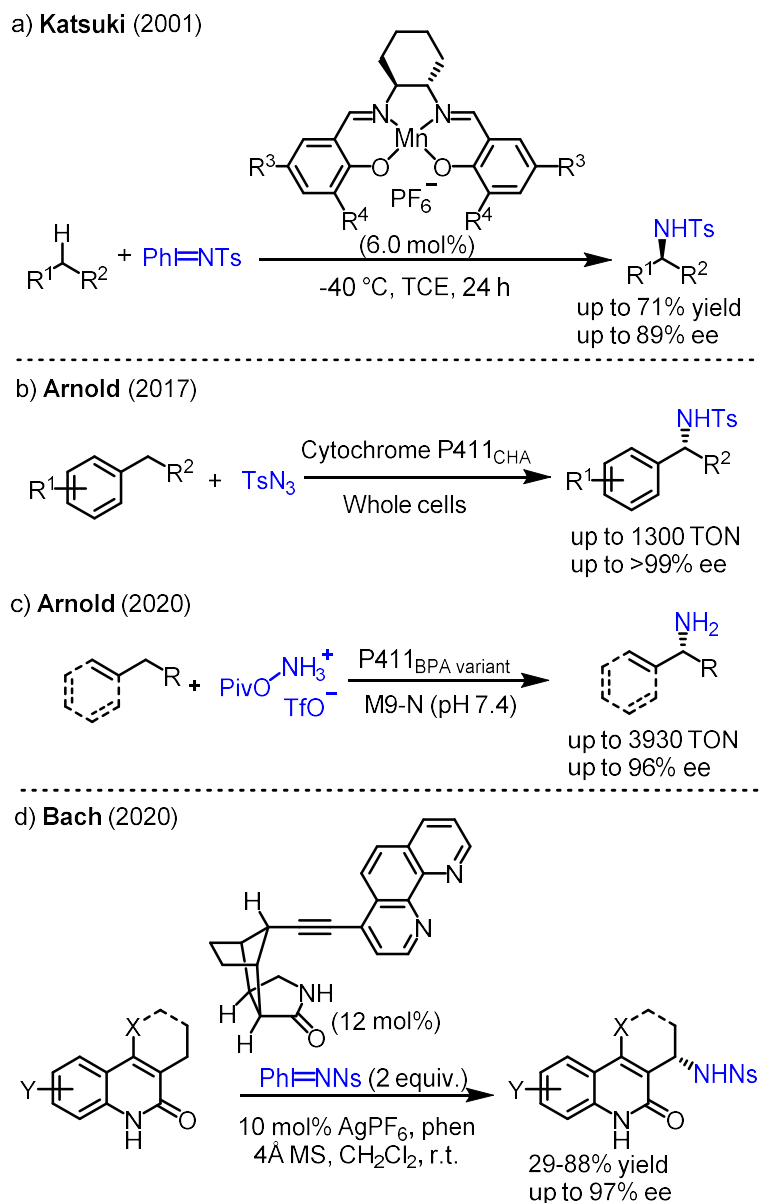


**Figure 28.** Other transition-metals catalyzed asymmetric intermolecular C–H aminations.

#### 1.4 Aim of the Thesis

Chiral-at-metal ruthenium complexes developed in our group are powerful catalysts and can be applied in efficient asymmetric catalysis as demonstrated for enantioselective alkynylations of trifluoromethyl ketones.<sup>32</sup> Since ruthenium-centered transition-metal complexes were already reported as effective catalysts for asymmetric C–H amination reactions, we envisioned that our chiral-at-ruthenium complexes could also catalyze asymmetric C–H amination reactions.

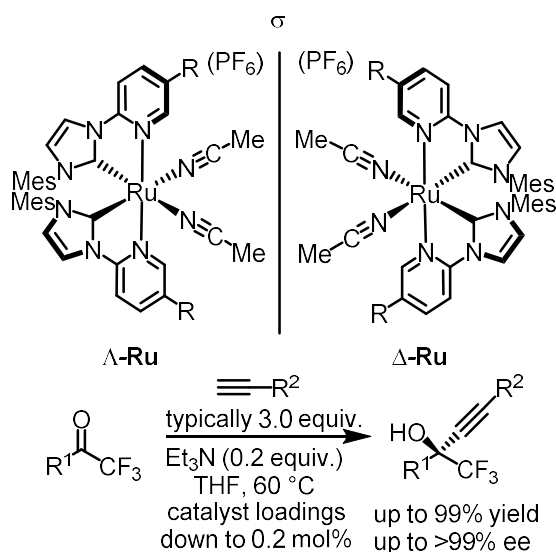


**Figure 29.** Chiral-at-metal ruthenium catalysts for asymmetric alkylation reactions.

### 1) Building a chiral-at-ruthenium catalyst toolbox

In previous investigations on the catalytic asymmetric alkylation of trifluoromethyl ketones, only two different chiral-at-metal ruthenium complexes were investigated. In this thesis, we aimed to make further modifications of such chiral-at-metal ruthenium complexes to build a chiral catalyst toolbox for detailed investigations of asymmetric intramolecular C–H amination reactions.

### 2) Apply chiral-at-ruthenium catalysts in asymmetric intramolecular C–H aminations

Transition-metal catalyzed asymmetric C–H aminations are a very attractive topic in current organic synthesis. Despite much efforts were already being put into this area, the intramolecular C–H amination remained some unsolved problems. To find an efficient asymmetric catalyst system is always an appealing project in this area. In this thesis, we aimed at achieving efficient asymmetric intramolecular C–H aminations with judiciously modified chiral-at-ruthenium catalysts and suitable substrates.

## References

1. Y. Park, Y. Kim, S. Chang, *Chem. Rev.* **2017**, *117*, 9247.
2. H. Hayashi, T. Uchida, *Eur. J. Org. Chem.* **2020**, *8*, 909.
3. J.-L. Liang, S.-X. Yuan, J.-S. Huang, W.-Y. Yu, C.-M. Che, *Angew. Chem. Int. Ed.* **2002**, *41*, 3465.
4. E. Milczek, N. Boudet, S. Blakey, *Angew. Chem. Int. Ed.* **2008**, *47*, 6825.
5. D. N. Zalatan, J. Du Bois, *J. Am. Chem. Soc.* **2008**, *130*, 9220.

6. M. Ichinose, H. Suematsu, Y. Yasutomi, Y. Nishioka, T. Uchida, T. Katsuki, *Angew. Chem. Int. Ed.* **2011**, *50*, 9884.
7. (a) C. Li, K. Lang, H. Lu, Y. Hu, X. Cui, L. Wojtas, X. P. Zhang, *Angew. Chem. Int. Ed.* **2018**, *57*, 16837. (b) K. Lang, S. Torker, L. Wojtas, X. P. Zhang, *J. Am. Chem. Soc.* **2019**, *141*, 12388.
8. Y. Yang, I. Cho, X. Qi, P. Liu, F. H. Arnold, *Nat. Chem.* **2019**, *11*, 987.
9. X. Nie, Z. H. Yan, S. Ivlev, E. Meggers, *J. Org. Chem.* **2020**, manuscript to be submitted.
10. J. A. McIntosh, P. S. Coelho, C. C. Farwell, Z. J. Wang, J. C. Lewis, T. R. Brown, F. H. Arnold, *Angew. Chem. Int. Ed.* **2013**, *52*, 9309.
11. R. Singh, M. Bordeaux, R. Fasan, *ACS Catal.* **2014**, *4*, 546.
12. P. Dydio, H. M. Key, H. Hayashi, D. S. Clark, J. F. Hartwig, *J. Am. Chem. Soc.* **2017**, *139*, 1750.
13. R. P. Reddy, H. M. L. Davies, *Org. Lett.* **2006**, *8*, 5013.
14. S. Y. Hong, Y. Park, Y. Hwang, Y. B. Kim, M. Baik, S. Chang, *Science* **2018**, *359*, 1016.
15. Y. Park, S. Chang, *Nat. Catal.* **2019**, *9*, 3360.
16. Q. Xing, C.-M. Chan, Y.-W. Yeung, W.-Y. Yu, *J. Am. Chem. Soc.* **2019**, *141*, 3849.
17. H. Wang, Y. Park, Z. Bai, S. Chang, G. He, G. Chen, *J. Am. Chem. Soc.* **2019**, *141*, 7194.
18. M. Kim, J. V. Mulcahy, C. G. Espino, J. Du Bois, *Org. Lett.* **2006**, *8*, 1073.
19. P. F. Kuijpers, M. J. Tiekink, W. B. Breukelaar, D. L. J. Broere, N. P. van Leest, J. I. van der Vlugt, J. N. H. Reek, B. de Bruin, *Chem. Eur. J.* **2017**, *23*, 7945.
20. P. Müller, C. Baud, Y. Jacquier, M. Moran, A. Ngeli, *J. Phys. Org. Chem.* **1996**, *9*, 341.
21. M. Yamawaki, H. Tsutsui, S. Kitagaki, M. Anada, M. Tanaka, N. Shimada, H. Nambu, M. Yamawaki, S. Hashimoto, *Tetrahedron Lett.* **2002**, *43*, 9561.
22. A. Nasrallah, V. Boquet, A. Hecker, P. Retailleau, B. Darses, P. Dauban, *Angew. Chem. Int. Ed.* **2019**, *58*, 8192.
23. T. Höke, E. Herdtweck, T. Bach, *Chem. Commun.* **2013**, *49*, 8009.
24. S. Fukagawa, Y. Kato, R. Tanaka, M. Kojima, T. Yoshino, S. Matsunaga, *Angew. Chem. Int. Ed.* **2019**, *58*, 18154.
25. C. M. B. Farr, A. M. Carzerouni, B. Park, C. D. Poff, J. Won, K. R. Sharp, M. Baik, S. B. Blakey, *J. Am. Chem. Soc.* **2020**, *142*, 13996.
26. X. Zhou, X. Yu, J. Huang, C.-M. Che, *Chem. Commun.* **1999**, 2377.
27. Y. Nishioka, T. Uchida, T. Katsuki, *Angew. Chem. Int. Ed.* **2013**, *52*, 1739.

28. Y. Kohmura, T. Katsuki, *Tetrahedron Lett.* **2001**, *42*, 3339.
29. C. K. Prier, R. K. Zhang, A. R. Buller, S. Brinkmann-Chen, F. H. Arnold, *Nat. Chem.* **2017**, *9*, 629.
30. Z. J. Jia, S. Gao, F. H. Arnold, *J. Am. Chem. Soc.* **2020**, *142*, 10279.
31. R. R. Annapureddy, C. Jandl, T. Bach, *J. Am. Chem. Soc.* **2020**, *142*, 7374.
32. Y. Zheng, Y. Tan, K. Harms, M. Marsch, R. Riedel, L. Zhang, E. Meggers, *J. Am. Chem. Soc.* **2017**, *139*, 4322.

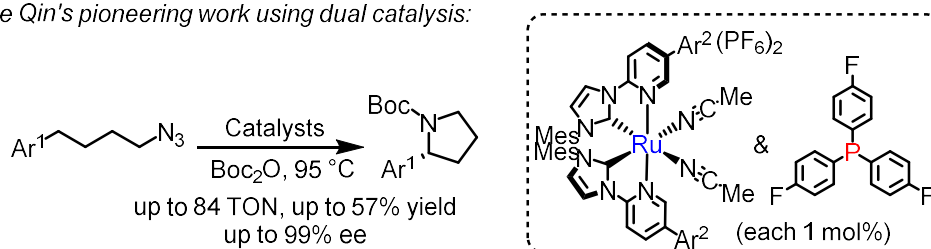
## Chapter 2. Results and Discussion

### 2.1 Catalytic Enantioselective Intramolecular C–H Amination of 2-Azidoacetamides

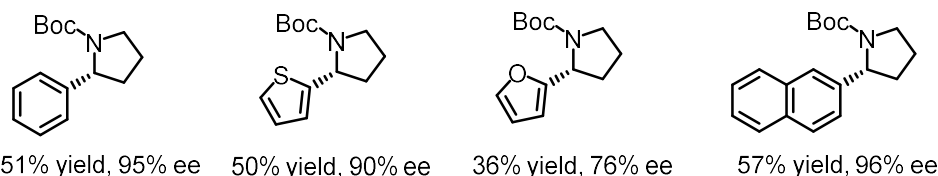
#### 2.1.1 Research Background and Reaction Design

Ruthenium catalyzed enantioselective intramolecular C–H amination using aliphatic organic azides<sup>1</sup> as nitrene precursors led to the formation of target cyclic Boc-protected pyrrolidine products as initial ground-breaking results obtained by Jie Qin, who is a former member of the Meggers group (**Figure 30a**). The same transformations were reported for several times as racemic versions<sup>2,3</sup>. Thus, the highly enantioselective intramolecular C–H aminations using aliphatic organic azides as nitrene precursors is an unsolved problem. The author of this thesis started to pursue his doctoral degree in the Meggers group when Jie Qin needed a partner to help him work together to improve the initial results.

a) *Jie Qin's pioneering work using dual catalysis:*



Selected examples: **only in moderate yields** (around 50%)



b) *My new designment:*

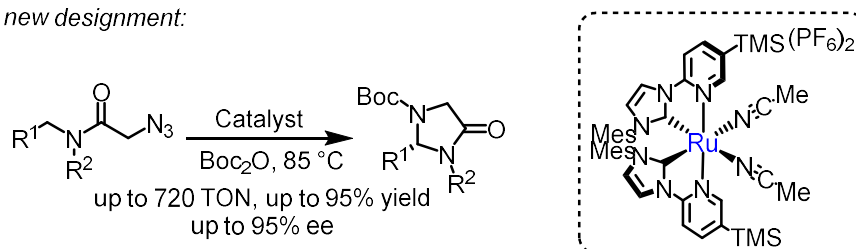


**Figure 30.** a) Pioneering work on ruthenium catalyzed intramolecular C–H aminations using aliphatic organic azides as nitrene precursors by the former group member Jie Qin. b) My new reaction designment.

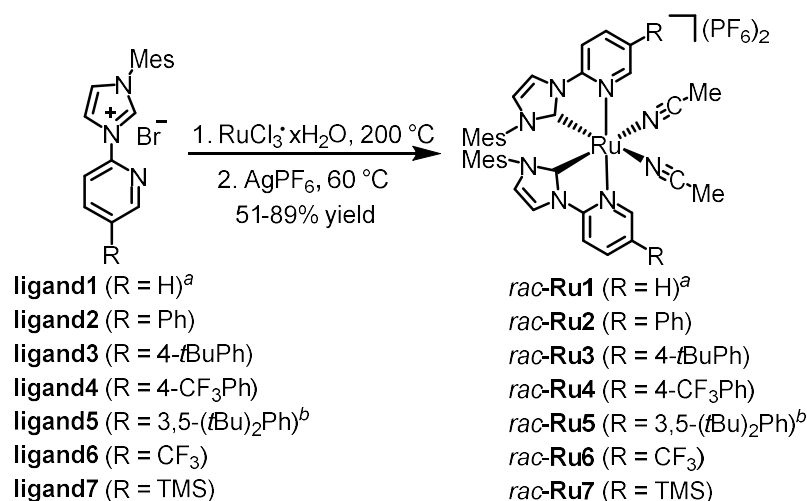
The author of this thesis helped Jie Qin to improve the results by synthesizing a series of newly modified chiral ruthenium catalysts and improved the results to 95% ee. As shown in the above figure, the target chiral pyrrolidine products were always forming in only modest yields of around 50%,<sup>5</sup> thus, the author of this thesis decided to explore a new class of aliphatic organic azides as nitrene precursors for intramolecular C–H aminations with the purpose of achieving higher yields of the target



ring-closing C–H amination products in combination with modified chiral-at-ruthenium catalysts (**Figure 30b**).<sup>6</sup>

### 2.1.2 Synthesis of Modified Chiral-at-Ruthenium Catalysts

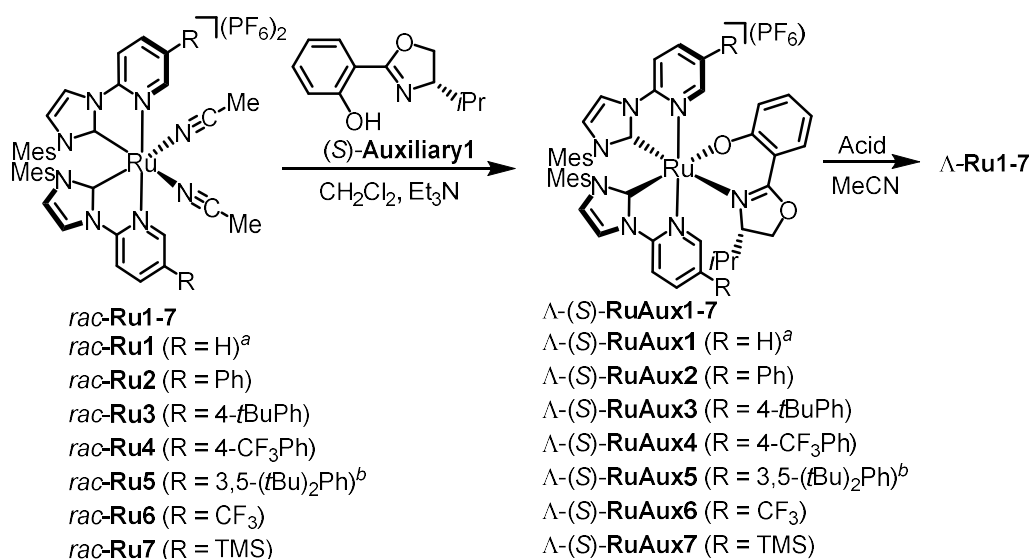
The general synthetic route of chiral-at-ruthenium catalysts was established by our previous group member Yu Zheng. I directly followed his method for the attempts on the synthesis of different racemic ruthenium catalysts. To our delight, the methodology was generally applicable for modifications of various substituents on the pyridine moiety (**Figure 31**). The desired racemic ruthenium catalysts were obtained in 51-89% yield. It's noteworthy that the TMS-substituted ruthenium catalyst was obtained in a low yield of 51% under standard complexation conditions. Further optimization of the reaction conditions by reducing the temperature from 200 °C to 185 °C successfully improved the yield to above 70%.



**Figure 21.** Attempts on the synthesis of different racemic ruthenium catalysts based on modifications of the pyridine moiety. [a] Yu Zheng's reported results. [b] Jie Qin's reported results.

With isolated analytical pure racemic ruthenium catalysts in hand, next, we performed the chiral-auxiliary-mediated synthesis of enantiomerically pure  $\Lambda$ -RuAux1-7 via Yu Zheng's established synthetic method. Under the standard 2-steps procedure, the desired enantiomerically pure  $\Lambda$ -RuAux1-7 were obtained (**Figure 32**).

The absolute configuration of standard ruthenium *bis*-NHC catalyst  $\Lambda$ -Ru1 was confirmed via single crystal diffraction. As similar structures, we identified the absolute configurations of newly modified ruthenium catalysts by comparing their CD spectra. As shown in **Figure 33**, the CD spectra of the representative ruthenium catalyst  $\Lambda$ -Ru7 contains a similar trend with the reported  $\Lambda$ -Ru1.

Synthetic route of  $\Lambda$ -Ru1-7:

**Figure 3.** Chiral-auxiliary-mediated synthesis of enantiomerically pure  $\Lambda$ -RuAux1-7. [a] Yu Zheng's reported results. [b] Jie Qin's reported results.

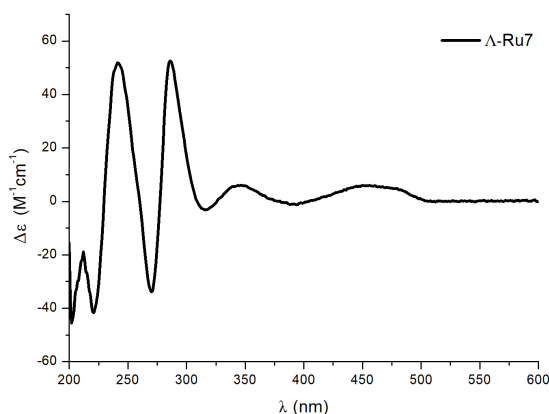


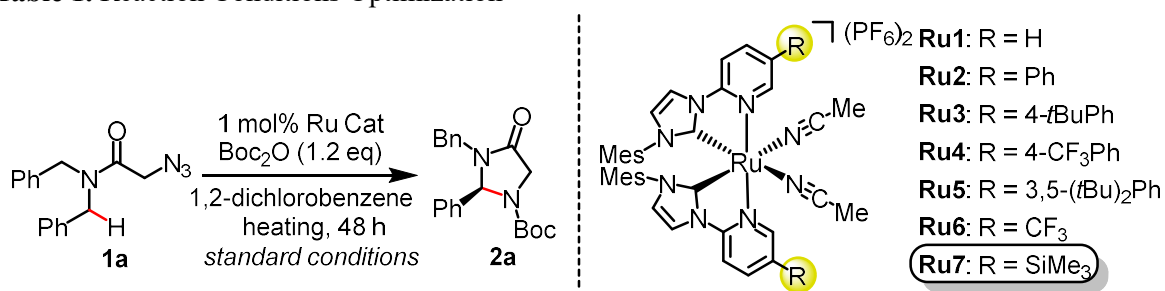
**Figure 33.** CD spectra of  $\Lambda$ -Ru7 recorded in CH<sub>3</sub>OH (0.2 mM).

### 2.1.3 Initial Experiments and Reaction Development

During an initial screening of suitable substrates for a ring-closing C–H amination, I followed exactly the same conditions which Jie Qin used in his system (without phosphine additive instead) and found that 2-azido-*N,N*-dibenzylacetamide (**1a**) was converted to Boc-protected 3-benzyl-2-phenylimidazolidin-4-one (*S*)-**2a** in 28% NMR yield and 52% ee using ruthenium catalyst  $\Lambda$ -Ru1 (1 mol%) in the presence of Boc<sub>2</sub>O (1.2 equiv) in 1,2-dichlorobenzene (1 M) at 95 °C (Table 1, entry 1). This kind of product is a new structure motif in ring-closing C–H amination area, nobody have achieved it through nitrene<sub>2</sub> insertion. Thus, it was promising to further optimize the reaction conditions to improve the preliminary result we obtained. Since I already had a series of newly

modified ruthenium catalysts in the fridge, I just tested all of them and hoped to get better results.

**Table 1.** Reaction Conditions Optimization<sup>a</sup>



Entry	Catalyst	Conditions <sup>b</sup>	T (°C)	NMR yield (%) <sup>c</sup>	ee (%) <sup>d</sup>
1	$\Lambda$ - <b>Ru1</b>	standard	95	28	52 ( <i>S</i> )
2	$\Lambda$ - <b>Ru2</b>	standard	85	68	60 ( <i>S</i> )
3	$\Lambda$ - <b>Ru3</b>	standard	85	72	73 ( <i>S</i> )
4	$\Lambda$ - <b>Ru4</b>	standard	85	59	76 ( <i>S</i> )
5	$\Lambda$ - <b>Ru5</b>	standard	85	83	56 ( <i>S</i> )
6	$\Lambda$ - <b>Ru6</b>	standard	85	37	86 ( <i>S</i> )
7	$\Lambda$ - <b>Ru7</b>	standard	85	84 (80) <sup>e</sup>	91 ( <i>S</i> )
8	$\Delta$ - <b>Ru7</b>	standard	85	83	91 ( <i>R</i> )
9	$\Lambda$ - <b>Ru7</b>	0.2 mol% cat <sup>f</sup>	90	71 <sup>g</sup>	91 ( <i>S</i> )
10	$\Lambda$ - <b>Ru7</b>	0.1 mol% cat <sup>f</sup>	95	74 <sup>h</sup>	90 ( <i>S</i> )
11	$\Lambda$ - <b>Ru7</b>	under air	85	58	90 ( <i>S</i> )
12	$\Lambda$ - <b>Ru7</b>	no Boc <sub>2</sub> O	85	<1 <sup>i</sup>	-
13	$\Lambda$ - <b>IrS</b>	standard	85	9	n.d. <sup>j</sup>
14	$\Lambda$ - <b>RhS</b>	standard	85	<1	-

[a] Standard conditions: **1a** (0.2 mmol), Boc<sub>2</sub>O (0.24 mmol), Ru catalyst (0.002 mmol) in 1,2-dichlorobenzene (0.2 mL) stirred at the indicated temperature for 48 h under N<sub>2</sub> unless noted otherwise. [b] Deviations from standard conditions are shown. [c] Determined by <sup>1</sup>H NMR of the crude products using Cl<sub>2</sub>CHCHCl<sub>2</sub> as internal standard. [d] Enantiomeric excess determined by HPLC analysis of the crude main product on a chiral stationary phase. [e] Isolated yield in brackets. [f] Reaction time increased to 96 h. [g] 19% starting material left. [h] 14% starting material left. [i] Product refers to the unprotected amine. [j] Not determined.

As expected, the ruthenium catalyst played an important role in getting different results. A phenyl-modified catalyst  $\Lambda$ -**Ru2** provided an improved yield of 68% at 85 °C but only 60% ee (entry 2). Different substituents within the phenyl moiety ( $\Lambda$ -**Ru3-Ru5**) did not provide satisfactory enantioselectivities (entries 3–5). Interestingly, the CF<sub>3</sub>-functionalized catalyst  $\Lambda$ -**Ru6** afforded 86% ee but only 37% yield (entry 6). The best results were obtained with the bulky trimethylsilyl (TMS)-functionalized ruthenium complex  $\Lambda$ -**Ru7** which provided 84% NMR yield (80% isolated yield) and 91% ee (entry 7). In addition, the catalyst  $\Delta$ -**Ru7** featuring a metal-centered  $\Delta$ -configuration provided the product **2a** in the same yield and enantioselectivity, but with opposite absolute configuration (entry 8). The catalyst loading can be reduced to 0.2 mol% (entry 9) and even 0.1 mol%

(entry 10) without affecting the enantioselectivity. The reduced reaction rate needs to be compensated by increasing the reaction temperature and time. Importantly, air atmosphere reduces the yield significantly (entry 10) while Boc<sub>2</sub>O is required for this conversion (entry 12). Finally, it is noteworthy that our previously reported bis-cyclometalated chiral-at-metal catalysts  $\Lambda$ -**IrS** and  $\Lambda$ -**RhS** are almost or completely inactive for this transformation (entries 13-14).

#### 2.1.4 Substrate Scope

With the optimized catalyst and reaction conditions in hand, we started to investigate the substrate scope with respect of 2-azido-*N,N*-dibenzylacetamides (**Figure 34**). Methyl groups in *para*- or *meta*-position of the phenyl moiety were well tolerated (imidazolidinones **2b** and **2c**), but the sterically hindering *ortho*-methyl group (**2d**) led to a reduced yield of 52% and 87% ee. Electron-donating groups appeared to be beneficial cause transition-metal nitrenoid intermediate prefers electron-rich C–H bonds. For example, a *para*-methoxy group provided the Boc-protected imidazolidinone **2e** with a higher yield of 95% and 90% ee. Chlorines on the phenyl moiety (**2f**, **2g**) did not affect the outcome of the reaction whereas strongly electron withdrawing CF<sub>3</sub> and fluorine substituents provided lower yields. Substrates with the heteroaromatic furan (**2j**) and thiophene (**2k**) moieties afforded slightly reduced yields and enantioselectivities. Replacing the aryl moiety with an ester group provided the desired cyclic product (**2l**) with 32% ee. We were not satisfied with the result of only 32% ee and luckily found that it can be improved to 70% ee by using  $\Lambda$ -**Ru5** catalyst instead. Finally, 2-azidoacetamides with two different substituents could also be employed and provided the imidazolidinones (**2m-2o**). However, a bulky *tert*-butyl group at the amide nitrogen lead to a vastly diminished enantioselectivity of just 23% ee (**2o**). No desired product was obtained for 2-azido-*N,N*-di(phenethyl)acetamide or 2-azido-*N,N*-di(allyl)acetamide as the substrates.

Next, we investigated azidoacetamides derived from isoindolines. We were delighted to find isoindolyl-*N*-(2-azidoacetamide) provided the desired tricyclic ring-closing C–H amination product **2p** smoothly in 74% yield and with 94% ee. An extended aromatic system (**2q**), electron withdrawing (**2r**), and electron donating (**2s**) moieties were well tolerated. Furthermore, azidoacetamides derived from 1,2,3,4-tetrahydroisoquinoline and 1,2,3,4-tetrahydro- $\beta$ -carboline provided the desired cyclization products **2t** and **2u**, respectively, upon increasing the reaction temperature and reaction time, albeit with reduced yields (**Figure 35**).

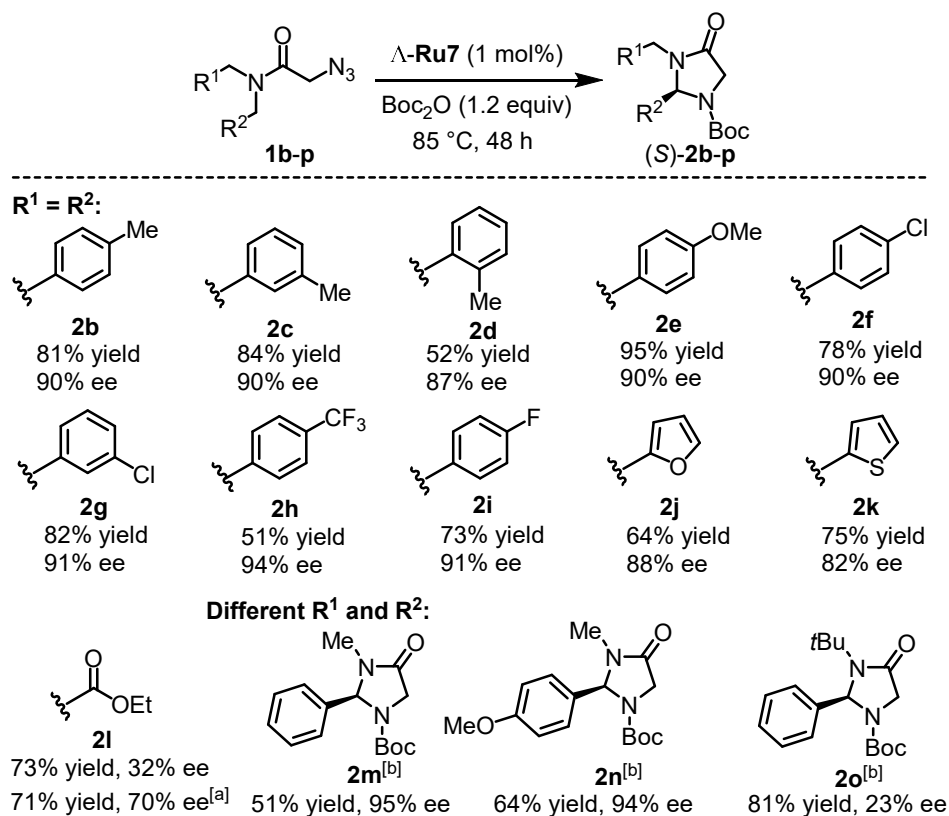


**Figure 34.** Substrate scope. <sup>[a]</sup> $\Delta$ -Ru5 as the catalyst instead. <sup>[b]</sup>Reaction temperature of 95 °C instead.

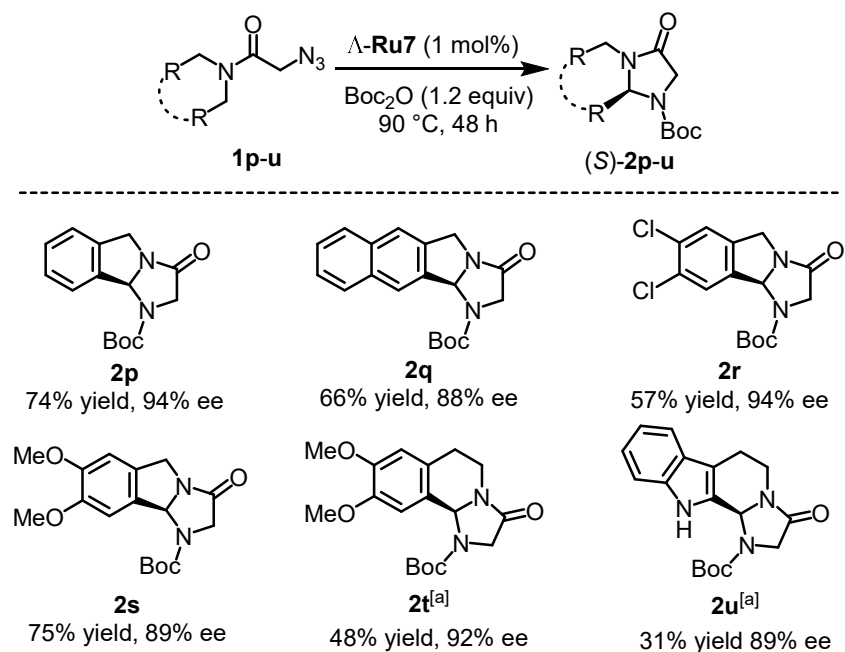


**Figure 35.** Synthesis of tri- and tetracyclic structures. <sup>[a]</sup>Reaction temperature of 105 °C for 60 h instead.

### 2.1.5 Mechanistic Study

The proposed mechanism is shown on **Figure 36**. The reaction is initiated by ruthenium coordination to the 2-azidoacetamide in a bidentate fashion through the amide carbonyl group and the  $\alpha$ -nitrogen of the azide (intermediate **I**). Such coordination modes of organic azides have been

reported.<sup>7</sup> A subsequent release of N<sub>2</sub> generates the chelated ruthenium-imido intermediate **II**, followed by dissociation of the amide (**III**), and a subsequent stereocontrolled insertion of the nitrene moiety into the C–H bond to provide a ruthenium-coordinated imidazolidinone (**IV**). Finally, the released imidazolidinone product is Boc-protected to suppress product inhibition. The Houk group coordinated to our research by performing Density Functional Theory (DFT) calculations to probe the validity of this mechanistic proposal. The maximum free energy barrier of this proposed reaction pathway was calculated to be 22.0 kcal/mol for the major enantiomer (*vide infra*), with irreversible C–H insertion and overall highly exergonic formation of the aminated product.

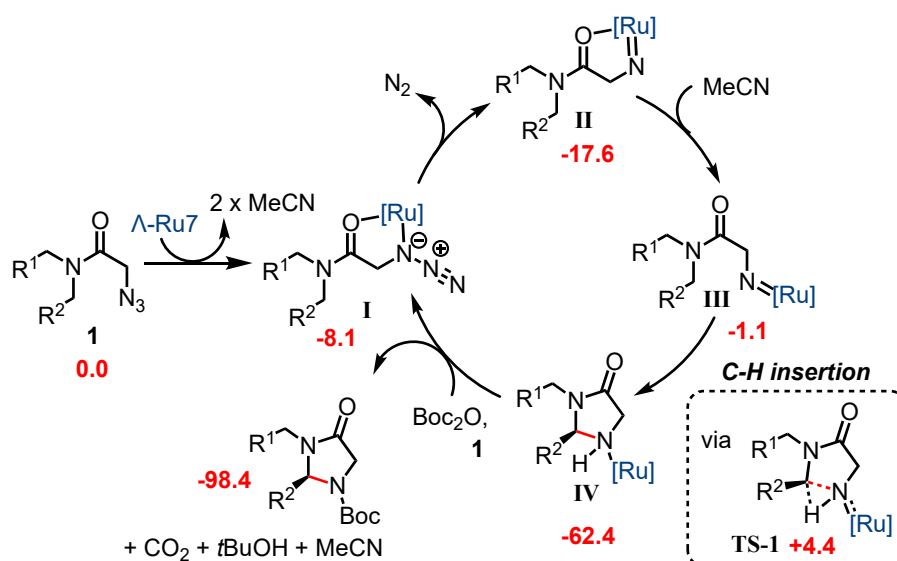


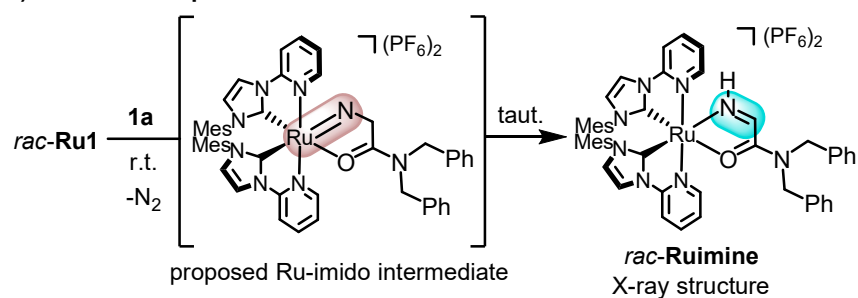
**Figure 36.** Proposed mechanism and DFT free energies (in kcal/mol) calculated with R<sup>1</sup> = R<sup>2</sup> = Ph at the M06-D3/6-311++G(d,p)-SDD, SMD (1,2-dichlorobenzene)//B3LYP-D3/6-31G(d)-LANL2DZ level of theory. These DFT calculations were performed by Dr. Shuming Chen (Houk group, UCLA).

Our mechanistic experiments support the proposed mechanism. Reaction of the 2-azidoacetamide **1a** with equimolar amounts of a racemic ruthenium catalyst (*rac*-**Ru1**) at room temperature provided quantitatively the chelated imine complex *rac*-**Ruimine** which was characterized by X-ray crystallography (**Figure 37a**).

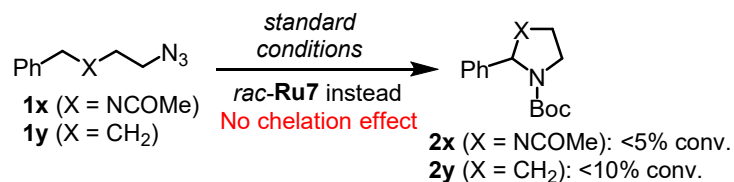
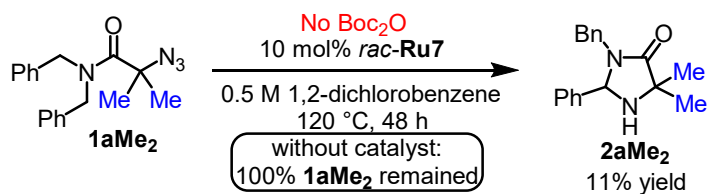
The generation of *rac*-**Ruimine** is a strong indication of the intermediate formation of the proposed chelated azide (**I**) and subsequent ruthenium-imido complex **II** (**Figure 36**), which tautomerizes to its corresponding imine upon 1,2–H shift. Such tautomerizations of ruthenium-imido complexes to their imines are well established.<sup>8</sup> DFT calculations revealed that in this system the tautomerization is strongly exergonic, with a free energy change of -46.2 kcal/mol. However, at high temperatures the 1,2–H shift apparently cannot compete with the C–H amination step.

Changing the position of the amide functionality (**1x**) or removing it altogether (**1y**) suppresses the reaction or leads to very low conversions, respectively, further supporting the important role of the amide group in the ring-closing C–H amination of 2-azidoacetamides (**Figure 37b**). In another important mechanistic control experiment, we found that the bulky substrate **1aMe<sub>2</sub>**, bearing two additional methyl groups in  $\alpha$ -position to the azido group, furnished the ring-closing C–H amination product **2aMe<sub>2</sub>** in 11% yield in the absence of Boc<sub>2</sub>O (**Figure 37c**). From this we conclude that Boc<sub>2</sub>O is not required for the C–H amination step but important for protecting the secondary amine and preventing its coordination to the catalyst. In **2aMe<sub>2</sub>**, the steric hindrance of the two methyl groups makes this protection unnecessary. The observed kinetic isotope effects (KIE) are low and indicate singlet nitrene insertion with concerted N–C and N–H formation rather than stepwise radical reaction through a triplet nitrene (**Figure 37d**) as compared with reported literatures.<sup>9</sup> An internal competition experiment with a 2-azido-*N,N*-dibenzylacetamide (**1z**) which contains one electron-rich and one electron-deficient benzyl group reveals a preference for electron rich C–H groups and suggests an electrophilic character of the ruthenium nitrene intermediate (**Figure 37e**). To elucidate the origins of the asymmetric induction in this reaction, DFT calculations were used to locate the C–H insertion transition states (**Figure 38**). **TS-1-major**, which leads to the observed major enantiomer of the product, is favored by 2.0 kcal/mol, in excellent agreement with the experimental value of 1.7–1.8 kcal/mol. A variety of functionals were tested, and all gave similar results to those reported in the text. In **TS-1-major**, a favorable  $\pi$ - $\pi$ stacking interaction is observed between the upright Ph ring on the substrate and the PyNHC ligand. This stabilizing interaction is absent in **TS-1-minor**. In addition, a steric clash exists in **TS-1-minor** between the C–H bond undergoing insertion and the *N*-Mes group on the ligand, with a H...H distance of 2.23 Å. The steric pocket created by the ligand framework has a sterically congested bottom half due to the presence of TMS and *N*-Mes groups. As a result, the longer and more flexible *N*-Bn moiety is better accommodated in this part of the steric pocket (**TS-1-major**) than the shorter and more rigid Ph moiety (**TS-1-minor**). The substrate and the catalyst framework are calculated to be 1.0 and 0.7 kcal/mol less distorted in **TS-1-major** than in **TS-1-minor**, respectively, which also indicates a superior steric fit between the substrate and the catalyst framework in **TS-1-major**.

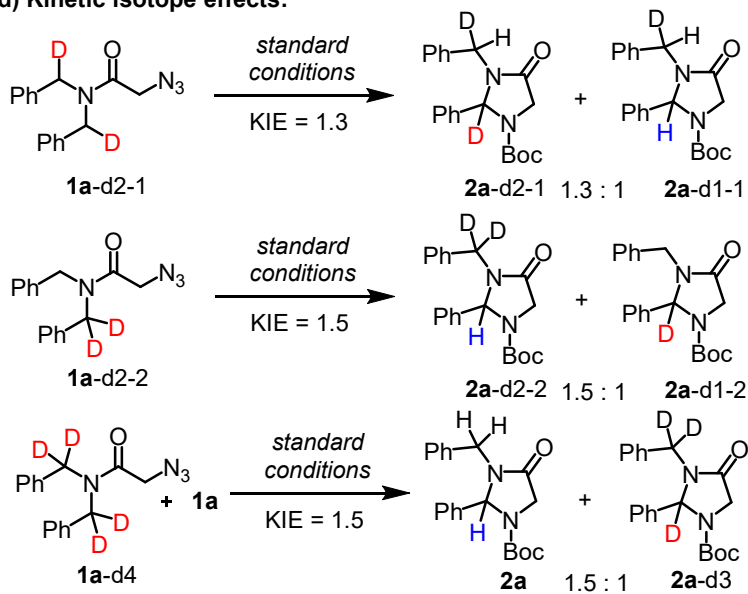
## a) Ru imine complex formation under mild conditions:



## b) Probing presence and position of amide group:


 c) Isolated C-H amination product without Boc<sub>2</sub>O:


## d) Kinetic isotope effects:



## e) Competition experiment:

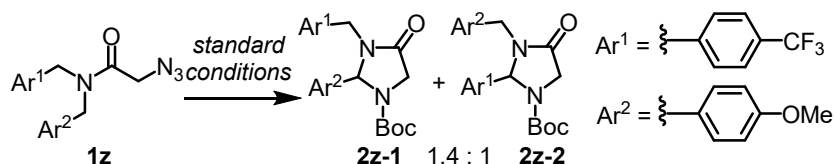
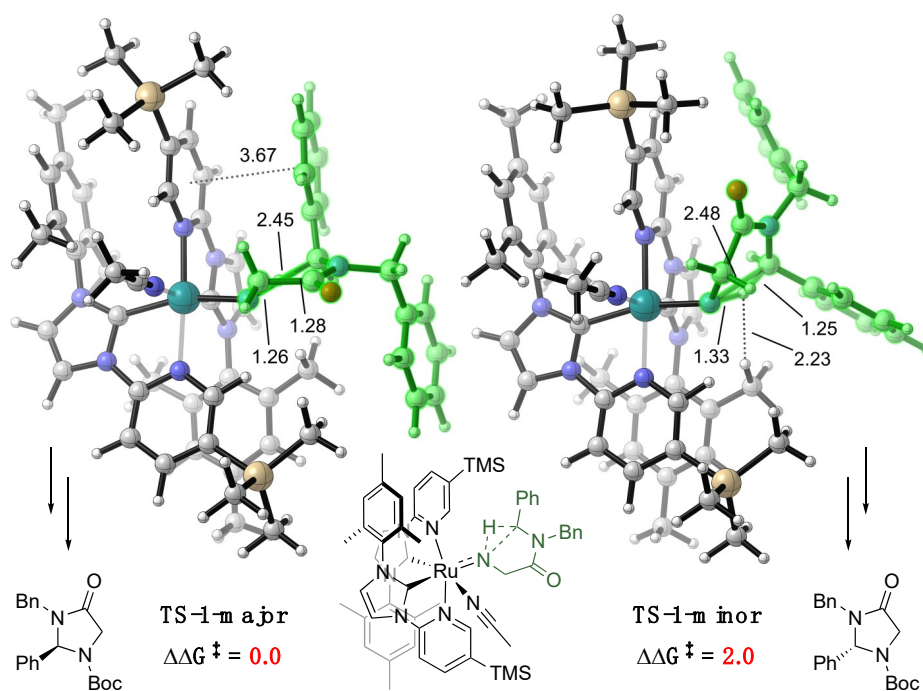


Figure 37. Mechanistic experiments.





**Figure 38.** Calculated transition state structures for the C–H insertion step at the M06-D3/6-311++G(d,p)-SDD, SMD (1,2-dichlorobenzene)//B3LYP-D3/6-31G(d)-LANL2DZ level of theory. Energies are shown in kcal/mol. Interatomic distances are denoted in Ångströms. Calculations performed by Dr. Shuming Chen (Houk group, UCLA).

### 2.1.6 Conclusions

In conclusion, we here presented a ruthenium-catalyzed enantioselective ring-closing C–H amination of 2-azidoacetamides giving rise to chiral imidazolidin-4-ones, which find applications as auxiliaries for the synthesis of unnatural amino acids,<sup>10</sup> as building blocks for the synthesis of natural products,<sup>11</sup> and as asymmetric organocatalysts<sup>12</sup>. This work demonstrates the capability of chiral-at-metal bis(pyridyl-NHC) ruthenium complexes for highly efficient asymmetric intramolecular C–H aminations.

### References

1. E. T. Hennessy, T. A. Betley, *Science*, **2013**, *340*, 591.
2. D. L. J. Broere, B. de Bruin, J. N. H. Reek, M. Lutz, S. Dechert, J. I. vander vlugt, *J. Am. Chem. Soc.* **2014**, *136*, 11574.
3. B. Bagh, D. L. J. Broere, V. Sinha, P. F. Kujpers, N. P. Vanleest, B. de Bruin, S. Demeshko, M. A. Siegler, J. I. vander vlugt, *J. Am. Chem. Soc.* **2017**, *139*, 5117.

4. P. F. Kuijpers, M. J. Tiekink, W. B. Breukelaar, D. L. J. Broere, N. P. van Leest, J. I. van der Vlugt, J. N. H. Reek, B. de Bruin, *Chem. Eur. J.* **2017**, *23*, 7945.
5. J. Qin, Z. Zhou, T. Cui, M. Hemming, E. Meggers, *Chem. Sci.* **2019**, *10*, 3202.
6. Z. Zhou, S. Chen, J. Qin, X. Nie, X. Zheng, K. Harms, R. Riedel, K. N. Houk, E. Meggers, *Angew. Chem. Int. Ed.* **2019**, *58*, 1088.
7. H. Takeuchi, S.-i. Yanagida, T. Ozaki, S. Hagiwara, S. Eguchi, *J. Org. Chem.* **1989**, *54*, 431.
8. (a) G. Albertin, S. Antoniutti, J. Castro, *J. Organomet. Chem.* **2010**, *695*, 574. (b) J. H. Lee, S. Gupta, W. Jeong, Y. H. Rhee, J. Park, *Angew. Chem. Int. Ed.* **2012**, *51*, 10851. (c) Y. Kim, H. Pak, Y. Rhee, J. Park, *Chem. Commun.* **2016**, *52*, 6549.
9. (a) F. Collet, C. Lescot, C. Liang, P. Dauban, *Dalton Trans.* **2010**, *39*, 10401. (b) K. W. Fiori, C. G. Espino, B. H. Brodsky, J. Du Bois, *Tetrahedron* **2009**, *65*, 3042. (c) M. E. Harvey, D. G. Musaev, J. Du Bois, *J. Am. Chem. Soc.* **2011**, *133*, 17207. (d) H. Lu, Y. Hu, H. Jiang, L. Wojtas, X. P. Zhang, *Org. Lett.* **2012**, *14*, 5158. (e) J. M. Alderson, A. M. Phelps, R. J. Scamp, N. S. Dolan, J. M. Schomaker, *J. Am. Chem. Soc.* **2014**, *136*, 16720. (f) J. R. Clark, K. Feng, A. Sookezian, M. C. White, *Nat. Chem.* **2018**, *10*, 583. For a representative concerted C-H insertion, see: (g) S. Y. Hong, Y. Park, Y. Hwang, Y. B. Kim, M.-H. Baik, S. Chang, *Science* **2018**, *359*, 1016.
10. (a) R. Polt, D. Seebach, *J. Am. Chem. Soc.* **1989**, *111*, 2622. (b) S. W. Baldwin, A. Long, *Org. Lett.* **2004**, *6*, 1653.
11. (a) C. C. Hughes, D. Trauner, *Angew. Chem. Int. Ed.* **2002**, *41*, 4556. As core structural motif in natural products and pharmaceuticals, see: (b) G. Schneider, U. Fechner, *Nat. Rev. Drug Discovery* **2005**, *4*, 649; (c) S. B. Mhaske, N. P. Argade, *Tetrahedron* **2006**, *62*, 9787.
12. S. G. Quellet, J. B. Tuttle, D. W. C. MacMillan, *J. Am. Chem. Soc.* **2005**, *127*, 32.

## 2.2 Enantioselective Synthesis of $\gamma$ -Lactams by Intramolecular C–H Amidation

### 2.2.1 Research Background and Reaction Design

The group member Yubiao Hong firstly explored the synthetic route of the new ruthenium complexes  $\Lambda$ -**Ru8** and  $\Lambda$ -**Ru9** starting from heterocyclic 7-methyl-3-phenyl-1,7-phenanthroline hexafluorophosphate as the ligand of choice (**Figure 39**). It's no doubt that his pioneering exploration provided us the initial inspiration. But there were several specific issues that remained unsolved, which were very important for making further progress. The synthetic route needed some further modifications for getting higher yields, and the enantioselectivity of the final catalyst was not sufficient for using it in asymmetric catalysis. During that time, Yubiao Hong was busy making progress on his very promising chiral-at-iron catalyst project and decided not to pursue this catalyst anymore. Therefore, the author of this thesis decided to investigate further this new class of chiral-at-ruthenium complexes and apply them to new enantioselective C-H amination reactions.

Yubiao Hong's initial pioneering exploration of new ruthenium catalysts

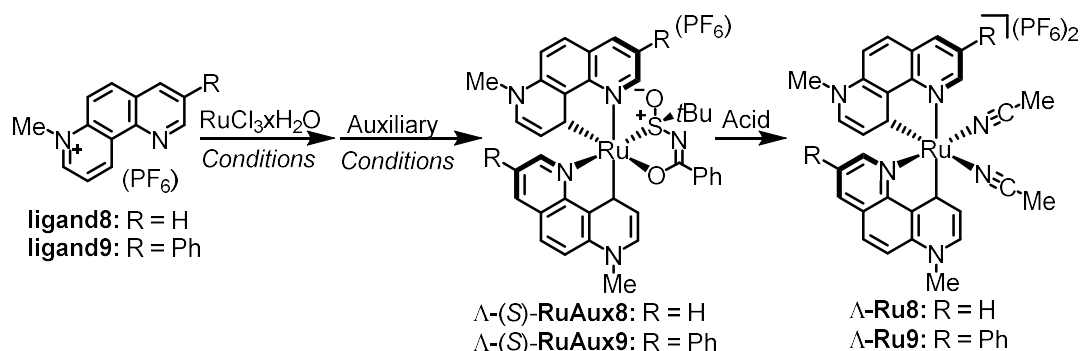


**Figure 39.** Yubiao Hong's pioneering exploration of new ruthenium complexes.

As shown in **Figure 39**, the main difference between the previous ruthenium scaffold and the new one are the different NHC ligands. The previous ruthenium scaffold contains normal NHC ligands, which are less electron-donating compared with the new scaffold, which contains remote NHC ligands.<sup>1</sup> Thus, the ruthenium center of the new platform is more electron-rich than the previous ruthenium scaffold. After understanding the most significant differences between these ruthenium catalysts, the author of this thesis had a feeling that we should explore reactions which need an especially electron-rich ruthenium metal center for catalysis.

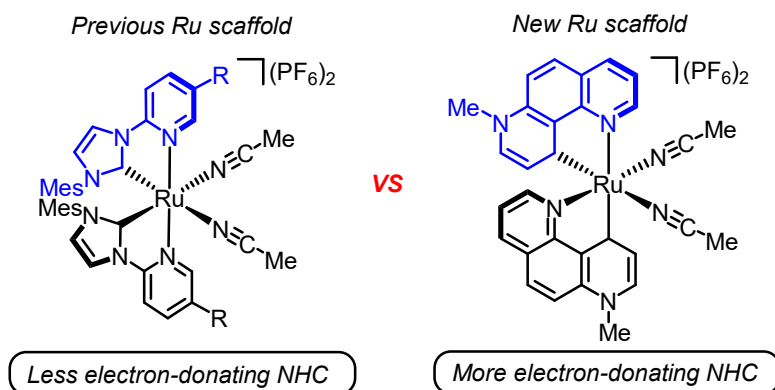


**Figure 39.** Main difference between previous ruthenium scaffold and the new one.

In 2018, the Chang group reported a streamlined synthetic methodology for  $\gamma$ -lactams via nitrene insertion catalyzed by electron-rich iridium catalysts (**Figure 40**). Modulation of the stereoelectronic properties of the auxiliary bidentate ligands to be more electron-donating was suggested by density functional theory calculations to lower the C–H insertion barrier favoring the desired reaction.<sup>2</sup>

**Chang (2018):** Electron rich iridium complex catalyzed intramolecular C–H amidation

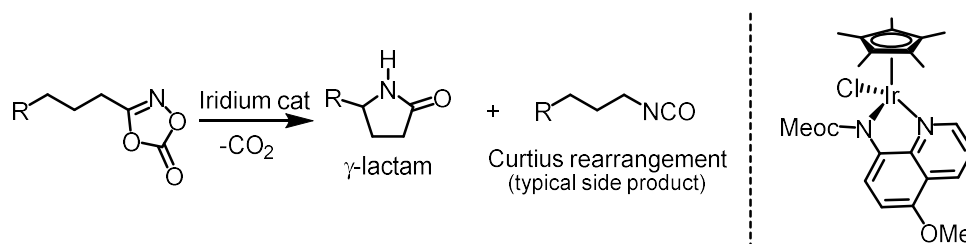


**Figure 40.** Intramolecular C–H amidation catalyzed by electron rich iridium complex from Chang's group.

After checking their supplementary files, the author of this thesis found that some ruthenium complexes (such as ruthenium porphyrin catalysts) could also catalyze this transformation and provide Curtius rearrangement products as major products. Thus, the author of this thesis thought the chiral-at-ruthenium catalysts could also catalyze the same transformation to afford the desired C–H insertion products (**Figure 41**).

**Idea of trying intramolecular C–H amidation reactions**

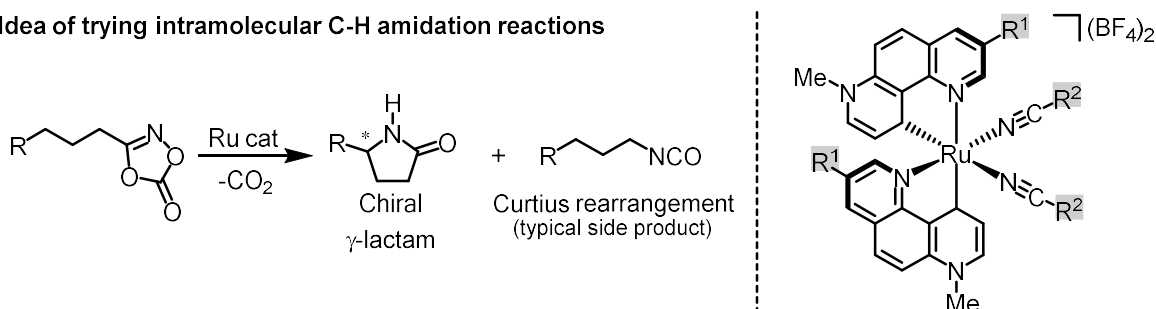


**Figure 41.** Idea of applying our new ruthenium catalyst scaffold in asymmetric intramolecular C–H amidation reactions.

## 2.2.2. Synthesis of Chiral-at-Ruthenium Catalysts

According to Yubiao Hong's synthetic route with slight modifications, we chose the heterocycle 7-methyl-3-phenyl-1,7-phenanthroline hexafluorophosphate (**ligand9**) as our ligand of choice. Reaction of RuCl<sub>3</sub> hydrate with **ligand9** in 2-ethoxyethanol:water (4:1) at 125 °C afforded the racemic chloro-bridged dimer complex *rac*-**Rudimer2** (88% yield). Each ruthenium is cyclometalated by two 1,7-phenanthroline ligands, which are electronically best described as chelating pyridyl pyridylidene ligands. The racemic mixture was next reacted with (*R*)- or (*S*)-*N*-benzoyl-*tert*-butanesulfonamide in the presence of K<sub>2</sub>CO<sub>3</sub> to provide the complexes  $\Lambda$ -(*S*)-**RuAux9** or  $\Delta$ -(*R*)-**RuAux9** as single stereoisomers in 46% and 44% yield, respectively. Interestingly, in the course of the formation of the *N*-sulfinylcarboximidate complexes, an unexpected but important isomerization of the chelating pyridylidene ligands occurred (this step is the crucial step for getting non-*C*<sub>2</sub>-symmetric catalyst's structure, namely, auxiliary induced isomerization). The non-*C*<sub>2</sub>-symmetric structure and corresponding absolute configuration of this ruthenium auxiliary complex are confirmed by the X-ray diffraction study of a simplified auxiliary complex  $\Lambda$ -(*S*)-**RuAux8** conducted by Yubiao Hong.

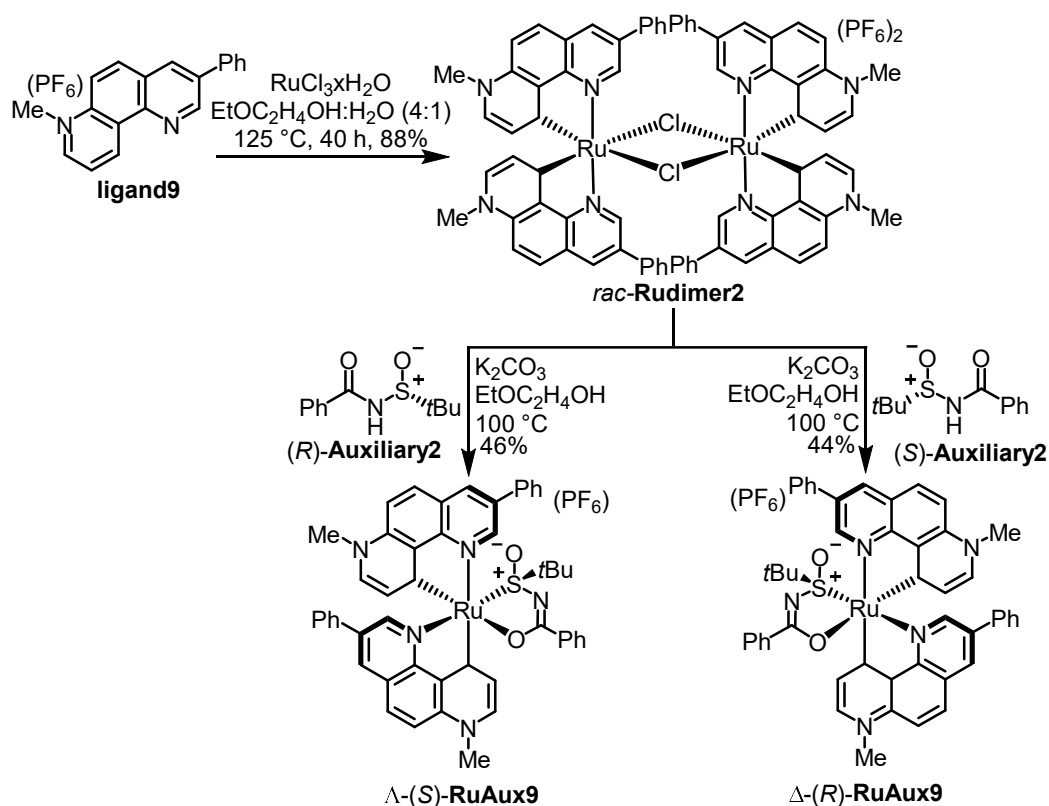


**Figure 42.** My modified synthetic routes of the ruthenium complexes.

After having the auxiliary complexes, we started the investigation of how to remove the chiral

auxiliaries. At the beginning, the author of this thesis directly used Yubiao Hong's standard reaction conditions with overnight as reaction time instead. Accidently, the author of this thesis found the final catalyst completely racemized. To judge the catalyst's enantio-purity, the author of this thesis performed an indirect way as using the result of the intramolecular C-H amidation reaction (it was due to the dicationic complex that couldn't be separated well by HPLC conditions). As shown in **Figure 43**,  $\Lambda$ -(S)-RuAux9 under acid promoted acetonitrile substitution of the bidentate ligand led to the formation of the final ruthenium catalyst. When the author of this thesis used Yubiao Hong's synthesized ruthenium catalyst, we got 45% ee of the target product, but with my newly synthesized one, 0% ee was obtained. It was quite unfortunate to get this result, but it also meant that the removal of auxiliary played an important role in getting highly enantiomeric pure final ruthenium catalysts.

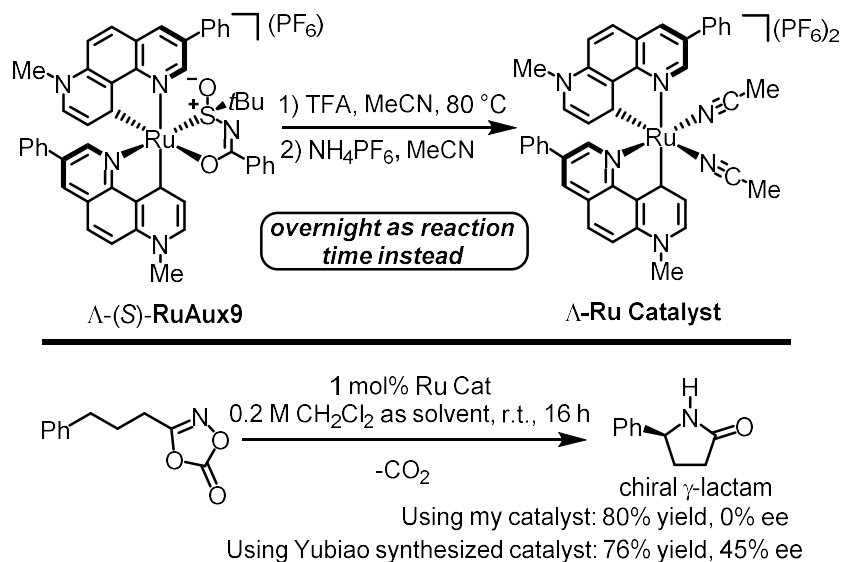
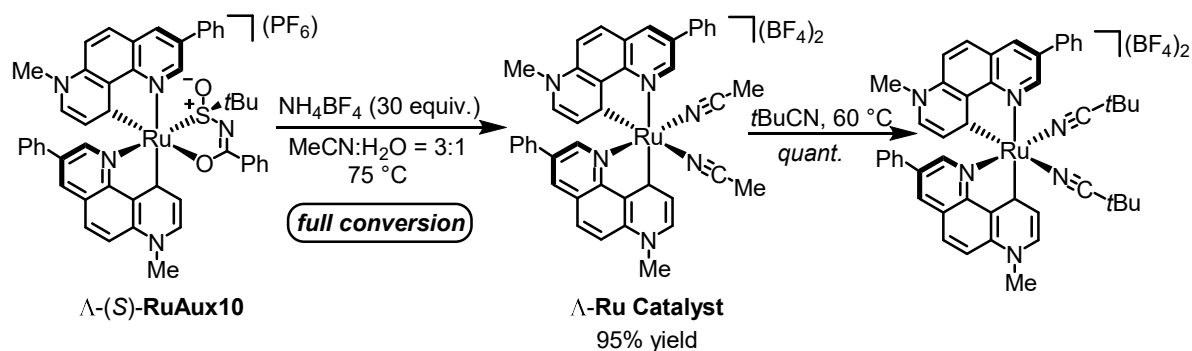


**Figure 43.** Comparison of catalytic results by using different ruthenium catalysts.

The author of this thesis thought maybe TFA is too acidic and led to the racemization of the ruthenium catalyst. The longer the reaction time, the more racemization occurred. So the author of this thesis decided to perform the auxiliary removal step in a shorter time as 30 mins. To our delight, the result further improved to 60% ee. The author of this thesis also tried different reaction solvents and finally found 1,2-dichlorobenzene was the solvent of choice, which led to 66% ee by using the same batch of ruthenium catalysts. Next, using  $\text{NH}_4\text{PF}_6$  instead of TFA for the same transformation was performed in order to get higher ee values. Surprisingly, the result further improved to 84% ee. Due to  $\text{NH}_4\text{PF}_6$  is a weak acid, the reaction needed 100 °C as the reaction temperature (**Figure 44**).



the desired ruthenium catalyst was isolated in 95% yield. By performing further modification of coordinated acetonitrile ligands to isobutylnitrile we got the final catalyst. The absolute configuration of this catalyst was confirmed by the X-ray diffraction study of a simplified ruthenium catalyst as  $\Lambda$ -configuration.

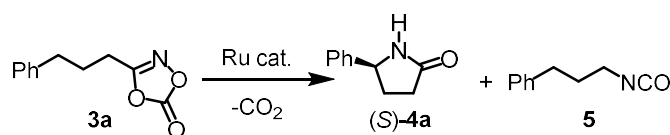
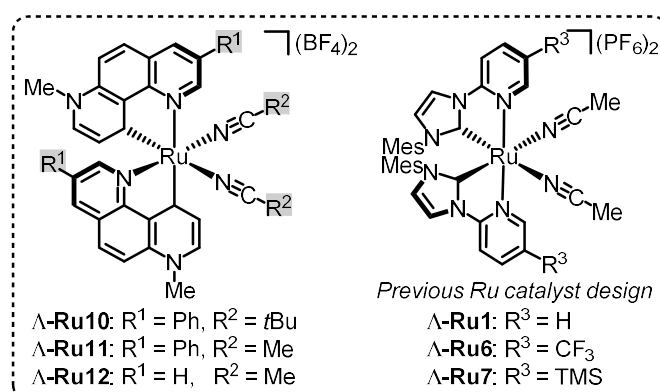


**Figure 46.** New results by performing the reaction using  $\text{NH}_4\text{BF}_4$  as source of acid in different conditions. X =  $\text{PF}_6$  or  $\text{BF}_4$ . water acetonitrile solvent mixture and further modification of catalyst.

### 2.2.3 Initial Experiments and Reaction Development

We firstly investigated the catalytic properties of the new chiral-at-ruthenium complexes and found that  $\Lambda$ -Ru10 displayed excellent catalytic activity for the intramolecular C–H amidation of 1,4,2-dioxazol-5-ones. For example, using just 0.5 mol% of  $\Lambda$ -Ru10 at room temperature catalyzed the conversion of **3a** to the  $\gamma$ -lactam (*S*)-**4a** in 92% yield and with 90% ee (Table 1, entry 1). The related catalysts  $\Lambda$ -Ru11 (acetonitriles instead of pivalonitriles) and  $\Lambda$ -Ru12 (devoid of phenyl groups and acetonitriles instead of pivalonitriles) provided lower yields and enantioselectivities for this conversion and higher yields of side product isocyanate formation (entries 2 and 3). Importantly, as a comparison, our previous chiral-at-ruthenium complexes **Ru1** and **Ru6-7**, which were demonstrated to be very suitable catalysts for enantioselective C–H aminations of aliphatic azides, did not afford any detectable amounts of the C–H amidation product but instead quantitatively provided the isocyanate compound **5** (entries 4-6). Thus,  $\Lambda$ -Ru10 has very distinct catalytic properties. The yield and enantioselectivity of  $\Lambda$ -Ru10-catalyzed conversion **3a**→(*S*)-**4a** could be further improved to 95% yield and 92% ee by performing the reaction at 4 °C. To demonstrate the exceptional catalytic activity of  $\Lambda$ -Ru10, catalyst loading was further reduced (entries 7-9). At a catalyst loading of just 0.05 mol% the intramolecular C–H amidation still occurred with 93% yield and 90% ee.



Table 2. Comparison of different ruthenium catalysts<sup>a</sup>

entry	catalyst	loading (mol %)	T (°C)	yield (%) <sup>b</sup>		ee (%) <sup>c</sup>
				3a	5	
1	$\Lambda$ -Ru10	0.5	r.t.	93 (92) <sup>d</sup>	6	90
2	$\Lambda$ -Ru11	0.5	r.t.	92 (91) <sup>d</sup>	7	89
3	$\Lambda$ -Ru12	0.5	r.t.	84 (82) <sup>d</sup>	15	84
4	$\Lambda$ -Ru1	0.5	r.t.	-	>99	-
5	$\Lambda$ -Ru6	0.5	r.t.	-	>99	-
6	$\Lambda$ -Ru7	0.5	r.t.	-	>99	-
7	$\Lambda$ -Ru10	0.5	4	95 (95) <sup>d</sup>	5	92
8 <sup>e</sup>	$\Lambda$ -Ru10	0.1	4	95 (95) <sup>d</sup>	5	92
9 <sup>f</sup>	$\Lambda$ -Ru10	0.05	4	93 (93) <sup>d</sup>	7	90

<sup>a</sup>Standard conditions: **3a** (0.2 mmol) and Ru catalyst (0.05-0.5 mol%) in 1,2-dichlorobenzene (0.4 mL) stirred at the indicated temperature for 8 h under an atmosphere of nitrogen. <sup>b</sup>Yields based on <sup>1</sup>H NMR analysis. <sup>c</sup>Enantiomeric ratio of the crude product determined by HPLC analysis on a chiral stationary phase. <sup>d</sup>Isolated yields in brackets. <sup>e</sup>Reaction time of 30 h instead. <sup>f</sup>Reaction time of 48 h instead.

## 2.2.4 Substrate Scope

With the optimized catalyst and reaction conditions in hand, we performed a substrate scope (Figure 47). A methyl group in *para*-position of the phenyl moiety was well tolerated and provided 96% yield with 90% ee (**4b**). An electron-donating methoxy group in the *para*-position of the phenyl moiety provided an almost quantitative yield but with a reduced enantioselectivity (**4c**). An electron-withdrawing nitro substituent at the *para*-position of the phenyl moiety gave 84% yield with 90% ee (**4d**). Halogen substituents at the *para*-position of the phenyl moiety were also well tolerated

and provided high yields and good enantioselectivities (**4e**, **4f**). Of note, both the brominated (**4e**) and iodinated (**4f**)  $\gamma$ -lactam products were improved to 98% ee after a single recrystallization in ethyl acetate. Replacing the phenyl moiety with a sterically more demanding naphthyl moiety provided the desired lactam product (**4g**) with 95% yield and 84% ee. A substrate with the heteroaromatic thiophene (**4h**) afforded a lower yield with 88% ee.

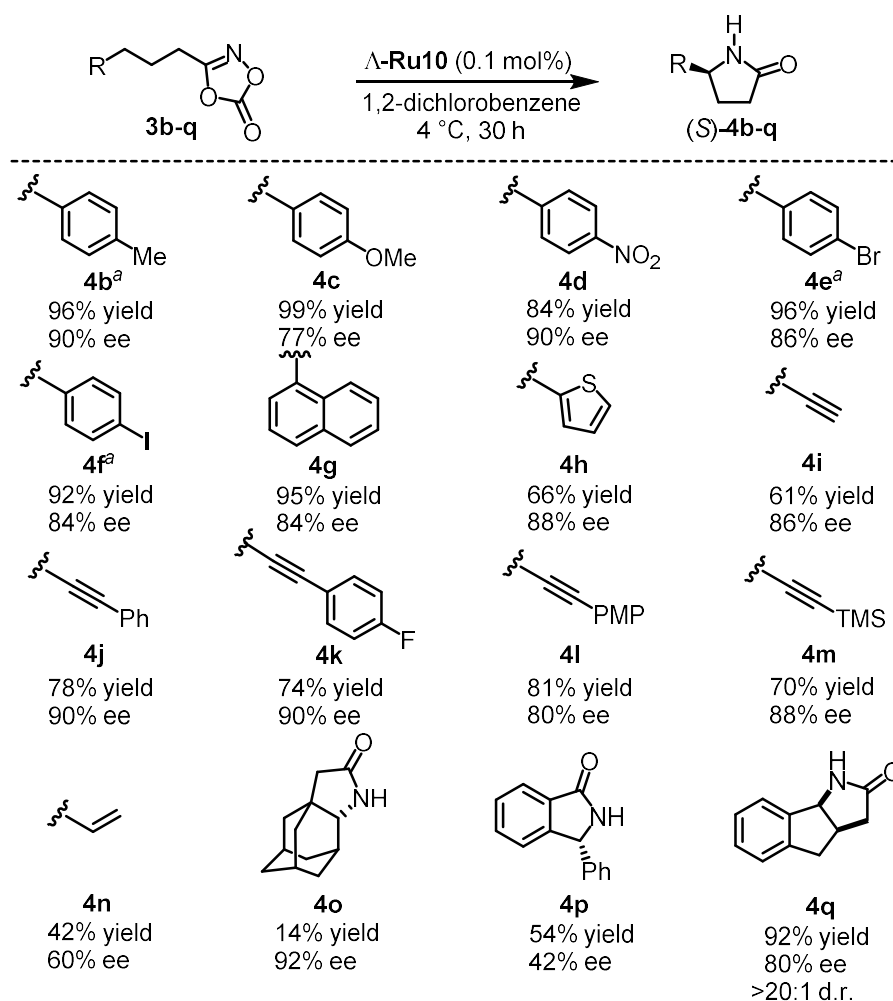


**Figure 4.** Substrate scope.

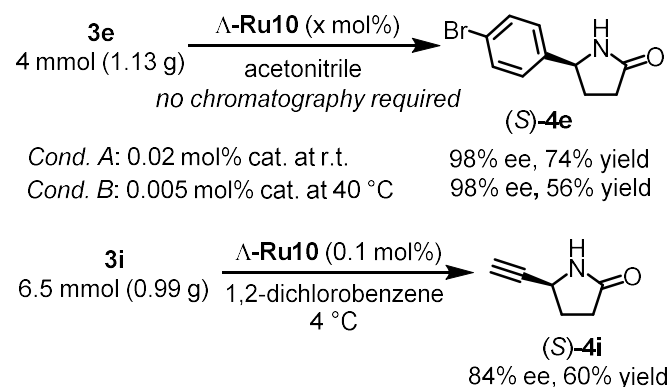
Next, we performed reactions of 1,4,2-dioxazol-5-ones with alkynyl substituents adjacent to the  $\gamma$ -C–H group which afforded chiral  $\gamma$ -alkynyl lactams in 61–81% yield and with up to 90% ee (**4i–m**). It is noteworthy that a terminal alkyne ( $\gamma$ -lactam **4i**) and TMS-functionalized alkyne ( $\gamma$ -lactam **4m**) were not included in previous reports on the direct enantioselective C–H amidation using 1,4,2-dioxazol-5-ones. Finally, with respect to substrate scope, a vinyl group next to the  $\gamma$ -C–H afforded the  $\gamma$ -vinyl lactam **4n** with modest 42% yield and 60% ee. If the  $\gamma$ -C–H is not activated by a  $\pi$ -system, the yields are low as shown for the adamantyl product **4o**. The synthesis of a chiral

isoindolinone (**4p**) and a desymmetrization generating two stereocenters (**4q**) are also shown in the substrate scope.

### 2.2.5 Synthetic Applications

The practical value of our developed C–H amidation catalyst was demonstrated in a gram-scale synthesis of (*S*)-**4e** with a catalyst loading of 0.02 mol% (**Figure 48a**). Interestingly, the isolation of the desired C–H amidation product was performed without column chromatography by only precipitation and crystallization in 74% yield and with 98% ee. It is noteworthy that the catalyst loading can be further reduced to merely 0.005 mol% to provide (*S*)-**4e** with 56% yield and 98% ee (TON number = 11200) at the same reaction scale. We believe this is the highest TON number reported for asymmetric transition-metal complex catalyzed ring-closing C–H nitrogenations. A gram-scale synthesis was also demonstrated for the terminal alkyne-functionalized  $\gamma$ -lactam (*S*)-**4i** and obtained in 60% yield with 84% ee. Chiral  $\gamma$ -lactams are useful intermediates for the synthesis of bioactive molecules such as natural products and drugs. For example, the  $\gamma$ -lactam (*R*)-**4e** has been reported as an intermediate for the synthesis of a compound for the treatment of inflammatory disorders and a hydroxamate-based inhibitor of deacetylases B. Chiral  $\gamma$ -lactam (*S*)-**4i**, containing a terminal alkyne, was reported as a synthetic intermediate used in the total syntheses of the natural products (-)-isoretronecanol, (-)-Heliotridane,<sup>3a</sup> and the GABA aminotransferase and glutamic acid decarboxylase inhibitor (*S*)-(+)-4-amino-5-Hexynoic acid<sup>3b</sup> (**Figure 48b**). (*S*)-**4i** was previously synthesized in multiple steps starting from chiral amino acids or amino ester.

## (a) Gram-scale synthesis of (S)-10e and (S)-10i:



## (b) Product transformations of (S)-10i:

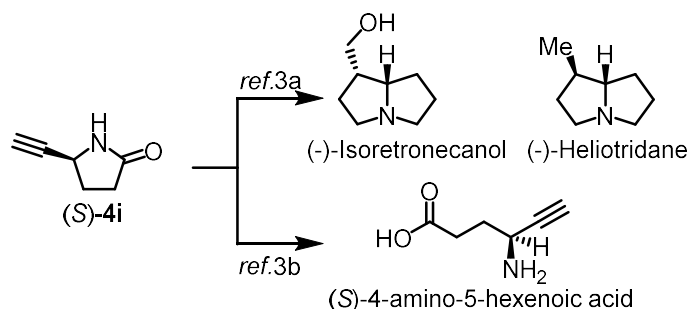


**Figure 48.** Gram-scale reaction with low catalyst loading and further transformations. (a) Gram-scale synthesis of (S)-4e and (S)-4i. (b) Synthetic applications of (S)-4i.

## 2.2.6 Mechanistic Study

The proposed mechanism is shown in **Figure 49**. The reaction is initiated by ruthenium coordination to the 1,4,2-dioxazol-5-one (intermediate **II**). A subsequent fragmentation and release of CO<sub>2</sub> gas generates the ruthenium-imido intermediate **III**, followed by stereocontrolled insertion of the nitrene moiety into the C–H bonds (**IV**) and subsequent release of the lactam product finish the whole catalytic cycle.

We started our mechanistic study by investigating the influence of the relative stereochemistry of the new ruthenium catalyst scaffold on promoting C–H amidation reactivity. The complex **Ru10** features non-C<sub>2</sub>-symmetry, whereas all catalysts previously developed in our group for asymmetric C–H aminations (**Ru1** and **Ru6-7**) display C<sub>2</sub>-symmetry, but only provide the undesired Curtius-type rearrangement products (Table 2, entries 4-6). To evaluate the importance of the relative stereochemistry around the metal center, and the potential electronic role of the rNHC ligands, we synthesized the C<sub>2</sub>-symmetric diastereomer of **Ru10** (C<sub>2</sub>-rNHCRu) and subjected it to standard reaction conditions with dioxazolone **Ru10**. Revealingly, the Curtius-type rearrangement product **11** was formed as the major reaction product in 60% yield with only 38% C–H amidation, demonstrating

that the relative stereochemistry of **Ru10** has a significant effect on the reaction outcome (**Figure 50a**).

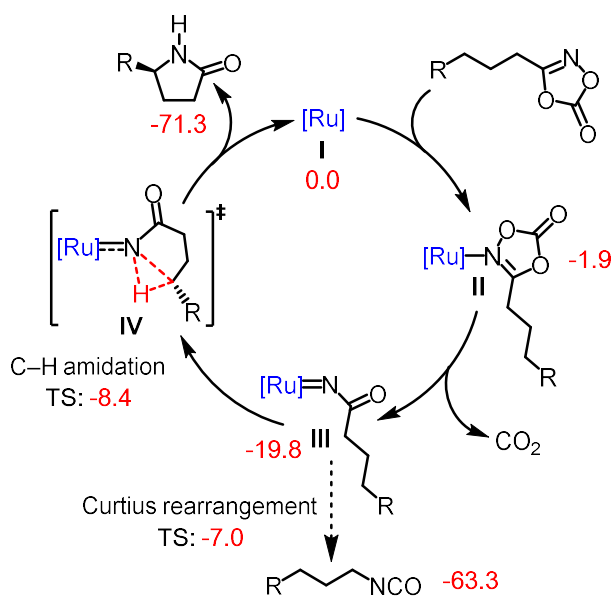


**Figure 5.** Proposed mechanism. Dr. Shuming Chen from the Houk group at UCLA performed the DFT calculations.

An intermolecular KIE value of 1.2 was determined by measuring initial C–H amidation rates of non-deuterated and bis-deuterated substrates (**Figure 50b**). The C–H amidations with substrate bearing a benzylic-CHD stereocenter were tested by using different **Ru10** catalysts. Both  $\Lambda$ - or  $\Delta$ -**Ru10** gave a KIE value of 1.1, while  $C_2$ -rNHCRu, the  $C_2$ -symmetric diastereomer of **Ru10**, afforded a KIE value of 1.3. Low KIE values were also obtained in related work by Chang, Yu, and Chen using dioxazolones as nitrene precursors.<sup>4,5,6</sup> These results indicate a singlet nitrene insertion with a concerted N–C and N–H formation pathway,<sup>7</sup> although a stepwise radical reaction through a triplet nitrene cannot be totally excluded. We also tested the stereochemistry of the reaction by subjecting the non-racemic (98% ee) chiral substrate (*R*)-**3a-Me** to the C–H amidation conditions. As a result, (*S*)-**4a-Me** with retention of configuration at the reacted carbon was obtained as the major product with both  $\Lambda$ - and  $\Delta$ -**Ru10**, but the  $\Lambda$ -catalyst reacts significantly faster with higher yield and affords the  $\gamma$ -lactam with a higher enantiomeric excess, thus revealing a high stereochemical discrimination between the two enantiotopic C–H bonds (**Figure 50c**).

Transition metal nitrenoids have been reported to transfer the nitrene fragment to phosphines to furnish iminophosphoranes.<sup>8-10</sup> To gain experimental evidence for the formation of an intermediate ruthenium nitrenoid in our catalytic system, we performed a trapping experiment with  $PPh_3$  using a dioxazolone substrate (**3t**) that is not capable of undergoing an intramolecular  $\delta$ -C–H insertion (**Figure**

**50d**). As a result, the expected iminophosphorane **4t** was formed in 81% yield under our standard reaction conditions which is consistent with our assumption that the ruthenium-catalyzed reaction proceeds through an intermediate ruthenium nitrenoid.

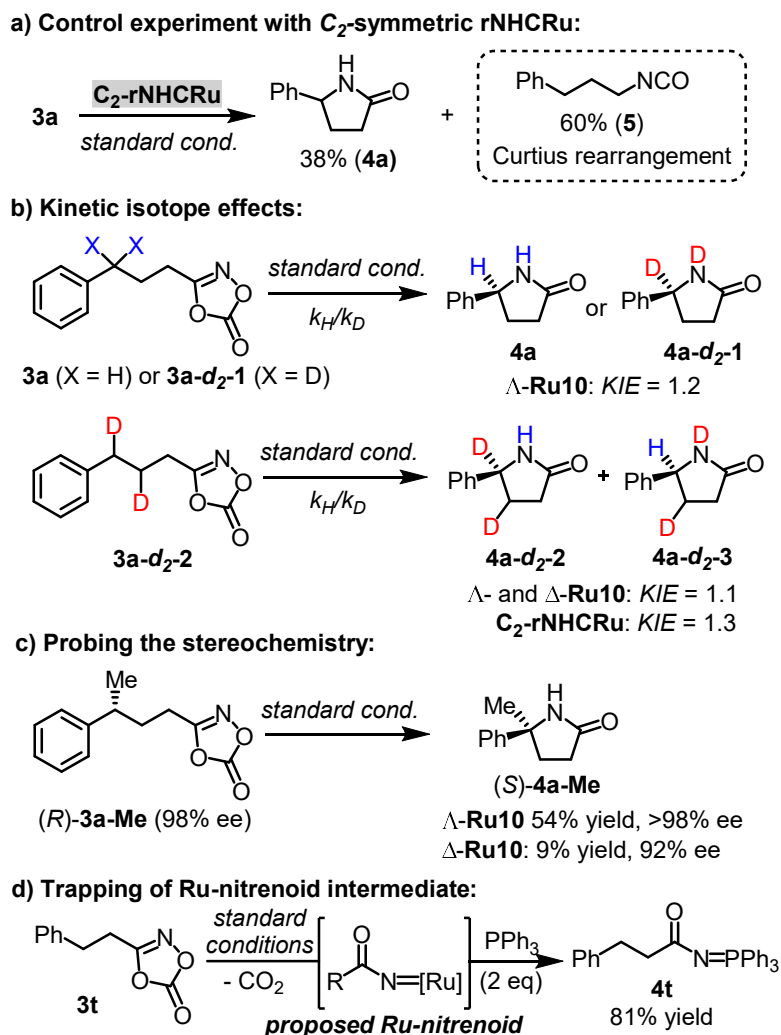


**Figure 50.** Control experiments for elucidating the mechanism.

Calculated structures of ruthenium *N*-acylnitrenes (**a–c**) formed with the three model catalysts **Ru12**, its C<sub>2</sub>-symmetric diastereomer, and **Ru1**, are shown in **Figure 51**. Both **Ru12** and C<sub>2</sub>-**Ru12** bear rNHC ligands, while **Ru1** has normal NHC (nNHC) ligands. Hirshfeld charge analysis shows that rNHC-bearing **a** (from **Ru12**) and **b** (from C<sub>2</sub>-**Ru12**) have more electron-rich nitrene fragments (highlighted in green) than **c**.<sup>11</sup> This is consistent with the expected higher σ-donating ability of rNHC over nNHC ligands.<sup>12</sup> The calculated structures also reveal another factor that influences the electron-richness of the nitrenes, namely NCH...O=C hydrogen bonds between the carbonyl group of the acylnitrene and the polarized C–H bond in 2-position of the closeby pyridyl ligand. This NCH...O=C hydrogen bond is significantly stronger in **b** (2.17 Å) and **c** (2.05 Å), which are both

derived from  $C_2$ -symmetric catalysts, than in **a** (2.30 Å) derived from a non- $C_2$ -symmetric catalyst. In **a**, the metal's coordination bond to one of the pyridine nitrogens is lengthened (2.24 Å, versus 2.15 Å in **b** and **c**) due to being positioned *trans* to the strongly  $\sigma$ -donating rNHC carbene carbon.<sup>13</sup> The longer Ru–N(pyridine) bond leads to a more electron-rich pyridine nitrogen and a less acidic  $\alpha$ -CH bond which consequently weakens the NCH...O=C hydrogen bond in **a** over **b** and **c**. Both Hirshfeld charges and orbital energies (see **Figure 51**) show that the overall nucleophilicity of the nitrene fragment decreases in the order of **a**>**b**>**c**, predicting that rNHC-bearing, non- $C_2$ -symmetric catalysts should be the most selective for C–H amidation, in agreement with the experimental results (**Table 2**, entries 1–3)

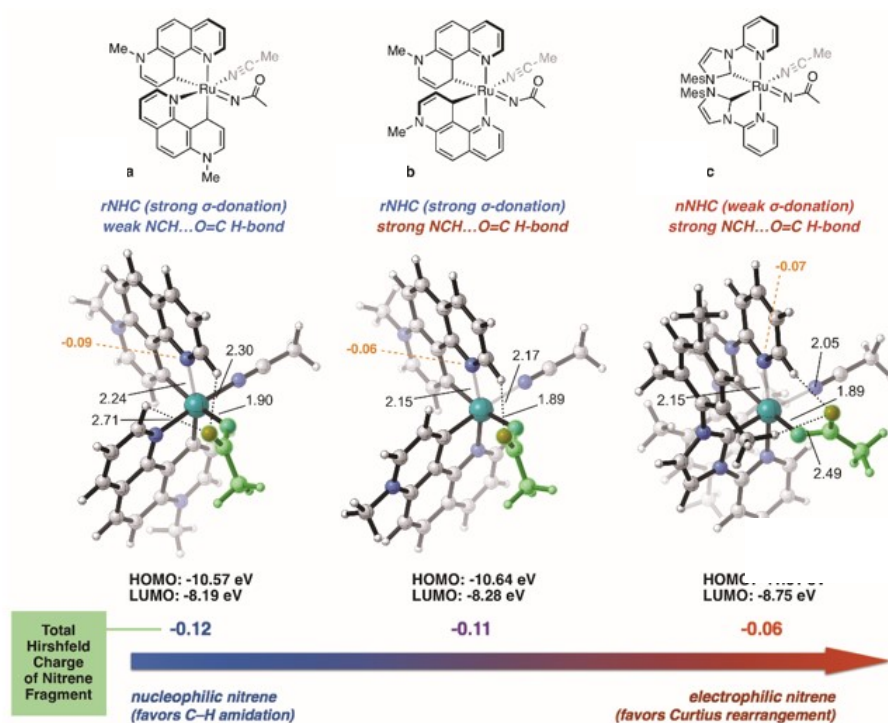


**Figure 51.** Calculated structures of ruthenium nitrene complexes at the B3LYP-D3/6-31G(d)–LANL2DZ (Ru) level of theory. Interatomic distances are in Ångströms (Å). Bolded numbers in orange indicate hirshfeld charges on individual atoms. Calculations performed by Dr. Shuming Chen (Houk group, UCLA).

**Figure 52** shows the calculated transition states for the C–H amidation and Curtius rearrangement with substrate **3a** and the catalysts **Ru11** (non- $C_2$ -symmetry) and **Ru1** ( $C_2$ -symmetry). For **Ru11**, C–H amidation proceeds with a barrier of 11.4 kcal/mol, 1.4 kcal/mol lower than for the Curtius rearrangement pathway. This result is in excellent agreement with the experimentally observed product ratio (**4a**:**5** = 92:7,  $\Delta\Delta G^\ddagger = 1.6$  kcal/mol). For **Ru1**, Curtius rearrangement is more facile with a barrier of 10.5 kcal/mol, while the C–H amidation barrier increases to 15.1 kcal/mol. The large  $\Delta\Delta G^\ddagger$  of 4.6 kcal/mol is consistent with the experimental observation that **Ru1** leads exclusively to the

Curtius rearrangement product.

Aside from higher nitrene electrophilicity, we hypothesized that steric factors may also play a role. In **Ru1** two mesityl groups are in close vicinity to the active site and may disfavor C–H amidation because of the more sterically demanding transition state, in which the nitrene alkyl chain must fold into a particular conformation in order to cyclize.

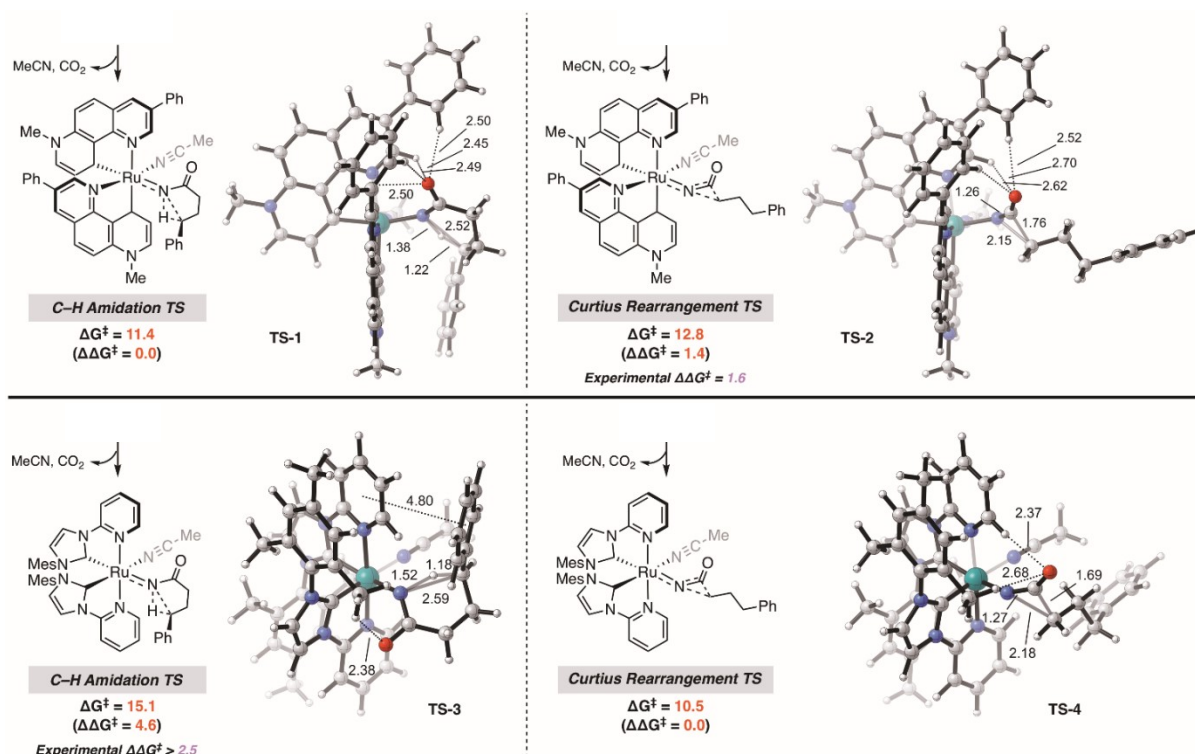


**Figure 52.** Calculated C–H amidation and Curtius rearrangement transition states at the M06-D3/6-311++G(d,p)–SDD (Ru), SMD (1,2-dichlorobenzene) // B3LYP-D3/6-31G(d)–LANL2DZ (Ru) level of theory. Interatomic distances are in ångströms (Å). Energies are in kcal/mol. Activation barriers are calculated with respect to the lowest-energy conformers of Ru nitrene intermediate **III**. Calculations performed by Dr. Shuming Chen (Houk group, UCLA).

Finally, the Houk group helped us for calculating C–H amidation transition states for the reaction **3a**→**4a** catalyzed by  $\Lambda$ -**Ru11**, leading to different enantiomers of the lactam product. **TS-1**, which leads to the major enantiomer (*S*)-**4a**, is favored by 1.9 kcal/mol, in good agreement with the observed e.r. of 94:6 ( $\Delta\Delta G^\ddagger = 1.6$  kcal/mol). A stabilizing  $\pi$ - $\pi$  stacking interaction exists between the nitrene phenyl group and the rNHC ligand. In **TS-1-ent**, the cyclizing nitrene fragment is oriented quite differently, with two weaker  $\pi$ - $\pi$  stacking interactions between the nitrene phenyl group and the phenyl substituents on the rNHC ligands (**Figure 53**).

The calculations also established the energetic feasibility of the proposed catalytic cycle (Figure 3). After coordination of the substrate to the Ru center, extrusion of CO<sub>2</sub> to furnish **III** is exergonic



(-17.9 kcal/mol for **Ru11** and **3a**). Both C–H amidation and Curtius rearrangement pathways have low barriers, consistent with the observation that the reactions generally proceed at room temperature or below.

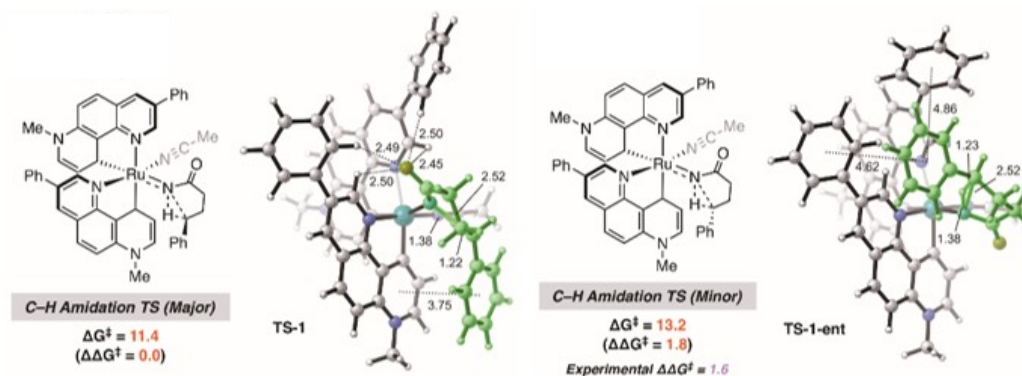


**Figure 53.** Calculated C–H amidation transition states leading to major and minor lactam enantiomers. at the M06-D3/6-311++G(d,p)–SDD (Ru), SMD (1,2-dichlorobenzene) // B3LYP-D3/6-31G(d)–LANL2DZ (Ru) level of theory. Interatomic distances are in ångströms (Å). Energies are in kcal/mol. Activation barriers are calculated with respect to the lowest-energy conformer of Ru nitrene intermediate **III**. Calculations performed by Dr. Shuming Chen (Houk group, UCLA).

### 2.2.7 Conclusions

In conclusion, we explored the applications of a new class of chiral ruthenium catalysts **Ru10**. The new ruthenium catalysts exhibited an exceptional catalytic activity for the enantioselective C–H amidation of 1,4,2-dioxazol-5-ones to chiral  $\gamma$ -lactams, reaching TON of up to 11200 (0.005 mol% catalyst loading). We believe that such a low catalyst loading are unprecedented for enantioselective C–H nitrogenations with non-enzymatic catalysts. Interestingly, the  $C_2$ -symmetric diastereomer of **Ru10**, as well as previously reported  $C_2$ -symmetric ruthenium catalysts suitable for enantioselective C–H aminations, provided instead an undesired Curtius-type rearrangement as the main product. In this catalyst architecture, the relative metal-centered stereochemistry (non- $C_2$  vs.  $C_2$ -symmetry) is therefore crucial for the reactivity and fate of the catalyzed reaction, while the absolute metal-centered stereochemistry ( $\Lambda$  vs.  $\Delta$ ) determines the absolute configuration of the C–H amidation product. Thus, whereas  $C_2$ -symmetric chiral transition metal catalysts are typically desirable for reducing the number of competing processes and transition states, in this catalyst architecture only the diastereomer with lower symmetry provides the desired catalytic activity.

## References

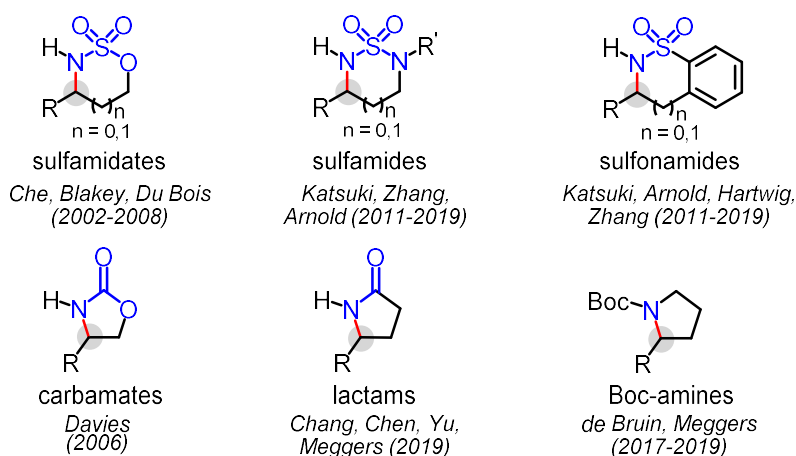
1. (a) H. G. Raubenheimer, S. Cronje, *Dalton Trans.* **2008**, 1265. (b) R. H. Crabtree, *Coord. Chem. Rev.* **2013**, 257, 755. (c) Á. Vivancos, C. Segarra, M. Albrecht, *Chem. Rev.* **2018**, 118, 9493.
2. S. Y. Hong, Y. Park, Y. Hwang, Y. B. Kim, M. Baik, S. Chang, *Science* **2018**, 359, 1016.
3. P.-F. Keusenkothen, M.-B. Smith, *J. Chem. Soc. Perkin Trans.* **1994**, 17, 2485.
4. H. MaAlonan, P. J. Stevenson, *Tetrahedron: Asymmetry* **1995**, 6, 239.
5. Y. Park, S. Chang, *Nat. Catal.* **2019**, 9, 3360.
6. Q. Xing, C.-M. Chan, Y.-W. Yeung, W.-Y. Yu, *J. Am. Chem. Soc.* **2019**, 141, 3849.
7. H. Wang, Y. Park, Z. Bai, S. Chang, G. He, G. Chen, *J. Am. Chem. Soc.* **2019**, 141, 7194.
8. a) E. Milczek, N. Boudét, S. B. Blakey, *Angew. Chem. Int. Ed.* **2008**, 47, 6825. b) K. W. Fiori, C. G. Espino, B. H. Brodsky, J. Du Bois, *Tetrahedron* **2009**, 65, 3042. c) F. Collet, C. Lescot, C. Liang, P. Dauban, *Dalton Trans.* **2010**, 39, 10401. d) M. E. Harvey, D. G. Musaev, J. Du Bois, *J. Am. Chem. Soc.* **2011**, 133, 17207. e) Q. Nguyen, K. Sun, T. G. Driver, *J. Am. Chem. Soc.* **2012**, 134, 7262
9. H. F. Sleiman, S. Mercer, L. McElwee-White, *J. Am. Chem. Soc.* **1989**, 111, 8007.
10. E. W. Harlan, R. H. Holm, *J. Am. Chem. Soc.* **1990**, 112, 186.
11. D. A. Dobbs, R. H. Bergman, *J. Am. Chem. Soc.* **1993**, 115, 3836. d) P. J. Perez, P. S. White, M. Brookhart, J. L. Templeton, *Inorg. Chem.* **1994**, 33, 6050.
12. Determined Ru(II/III) redox potentials for the investigated ruthenium catalysts (**Ru10**: 0.90 V, **Ru11**: 0.90 V, **Ru12**: 0.90 V, **Ru1**: 1.33 V, **Ru6**: 1.33 V, **Ru7**: 1.33 V in MeCN vs. Ag/AgCl) are consistent with a more electron-rich ruthenium center for the complexes bearing rNHC ligands.
13. (a) H. G. Raubenheimer, S. Cronje, *Dalton Trans.* **2008**, 1265. (b) R. H. Crabtree, *Coord. Chem. Rev.* **2013**, 257, 755. (c) Á. Vivancos, C. Segarra, M. Albrecht, *Chem. Rev.* **2018**, 118, 9493.
14. B. J. Coe, S. J. Glenwright, *Coord. Chem. Rev.* **2000**, 203, 5.

## 2.3 Enantioselective Synthesis of 2-Imidazolidinones by Intramolecular C–H Amidations

## 2.3.1 Research Background and Reaction Design

As has been described in the previous chapters, the direct catalytic asymmetric conversion of prochiral  $C(sp^3)$ -H into C-N bonds offers an efficient synthetic route to non-racemic chiral nitrogen-containing molecules. This has been applied to the catalytic asymmetric synthesis of cyclic sulfamidates,<sup>1-3</sup> sulfamides,<sup>4-6</sup> sulfonamides,<sup>7-10</sup> carbamates,<sup>11-12</sup> lactams,<sup>13-16</sup> Boc-protected pyrrolidines,<sup>17,18</sup> and related Boc-protected heterocycles (**Figure 54**).<sup>19</sup> However, interestingly, urea derivatives as nitrene precursors leading to chiral cyclic urea, specifically 2-imidazolidinones, are absent from this list. This is unfortunate considering the prevalence of chiral 2-imidazolidinones in bioactive compounds and their use as chiral auxiliaries.<sup>20,21</sup> Furthermore, chiral 2-imidazolidinones can be converted in a single step to chiral vicinal diamines which are valuable building blocks for the synthesis of medicinal agents, natural products, chiral ligands, and chiral catalysts.<sup>22-23</sup> It was thus the goal to fill this gap and develop an enantioselective intramolecular C-H amination of urea derivatives.

## (a) Chiral azacycles via intramolecular nitrene insertion



## (b) Synthesis of cyclic ureas via intramolecular nitrene insertion

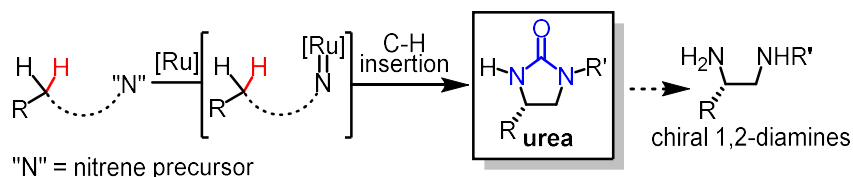
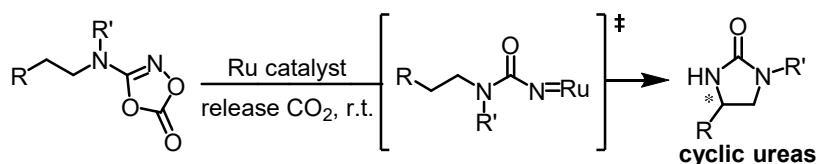


**Figure 54.** Enantioselective intramolecular amination of prochiral  $C(sp^3)$ -H bonds. (a) Chiral heterocycles accessible by this strategy. (b) Reaction design.

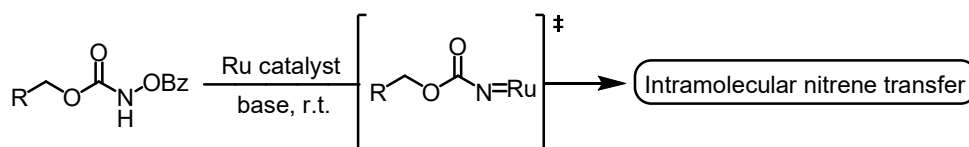
As described in chapter 2.3, our ruthenium complexes were very efficient catalysts for activating 1,4,2-dioxazolone substrates for intramolecular C–H aminations providing chiral cyclic

nitrogen-containing heterocycles. Thus, we envisioned to use similar substrates for the synthesis of cyclic ureas but no synthetic methods are currently available for their synthesis. During that time, the previous group member Yuqi Tan found that the *N*-benzoyloxycarbamates can serve as nitrene precursors together with chiral-at-ruthenium catalysts to afford cyclic carbamates. The author of this thesis therefore decided to investigate related *N*-benzoyloxyureas as nitrene precursors of intramolecular C–H aminations to synthesize chiral cyclic ureas (**Figure 55**).

(a) Initial idea on the synthesis of cyclic ureas via intramolecular nitrene insertion



(b) Yuqi Tan's exploration on using *N*-benzoyloxycarbamate as nitrene precursor



(c) Idea of using *N*-benzoyloxyurea as nitrene precursor for intramolecular amination

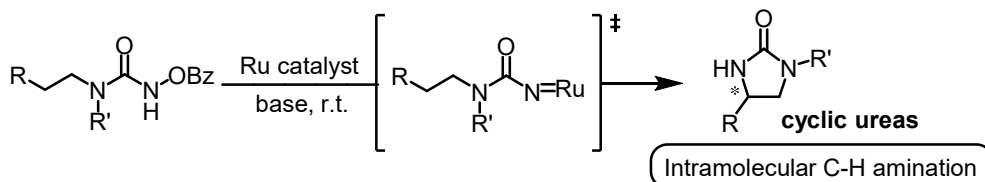


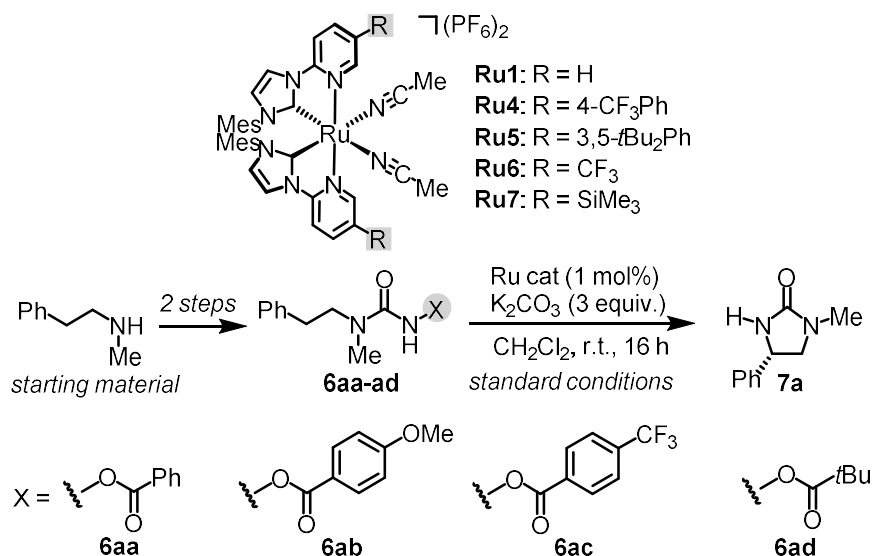
**Figure 55.** (a) Initial idea on the synthesis of cyclic ureas via intramolecular C–H amination. (b) Yuqi Tan's pioneering exploration on using *N*-benzoyloxycarbamates as nitrene precursors for intramolecular nitrene transfer reactions. (c) My idea of reaction design for the synthesis of chiral cyclic ureas.

### 2.3.2 Initial Experiments and Reaction Development

In chapters 2.1 and 2.2 we disclosed enantioselective nitrene insertion chemistry of organic azides and 1,4,2-dioxazol-5-ones using “chiral-at-metal” ruthenium catalysts with exclusive metal-centered chirality (only achiral ligands). We anticipated that this novel class of catalysts would allow us to address the challenge of accessing chiral 2-imidazolidinones by enantioselective C(sp<sup>3</sup>)–H amination from judiciously chosen urea derivatives. We initiated our study with the *N*-benzoyloxyurea **6aa** and envisioned that after release of the benzoate leaving group, an intermediate ruthenium nitrenoid would form and engage in an intramolecular C–H amination. Indeed, in the presence of 1 mol% **Ru1** and K<sub>2</sub>CO<sub>3</sub> (3 equiv.) in CH<sub>2</sub>Cl<sub>2</sub> at room temperature for 16 hours, the 2-imidazolidinone **7a** was formed in

quantitative yield and with 86% ee (Table 3, entry 1).

**Table 3.** Evaluation of the C–H amination reaction<sup>a</sup>



entry	catalysts	X	conditions <sup>b</sup>	yield (%) <sup>c</sup>	ee (%) <sup>d</sup>
1	$\Lambda$ - <b>Ru1</b>	<b>6aa</b>	standard	quant.	86
2	$\Lambda$ - <b>Ru4</b>	<b>6aa</b>	standard	quant.	94
3	$\Lambda$ - <b>Ru5</b>	<b>6aa</b>	standard	quant.	95
4	$\Lambda$ - <b>Ru6</b>	<b>6aa</b>	standard	quant.	94
5	$\Lambda$ - <b>Ru7</b>	<b>6aa</b>	standard	quant. (99) <sup>f</sup>	95
6	$\Lambda$ - <b>Ru7</b>	<b>6ab</b>	standard	quant.	94
7	$\Lambda$ - <b>Ru7</b>	<b>6ac</b>	standard	quant.	94
8	$\Lambda$ - <b>Ru7</b>	<b>6ad</b>	standard	27	91
9	$\Lambda$ - <b>Ru7</b>	<b>6aa</b>	0.5 mol% cat.	quant.	94
10	$\Lambda$ - <b>Ru7</b>	<b>6aa</b>	0.1 mol% cat. <sup>g</sup>	quant.	94
11	$\Lambda$ - <b>Ru7</b>	<b>6aa</b>	0.05 mol% cat. <sup>g</sup>	66	93
12	$\Lambda$ - <b>Ru7</b>	<b>6aa</b>	no base <sup>h</sup>	quant.	94

<sup>a</sup>Standard conditions: Substrate **6aa-6ad** (0.2 mmol), K<sub>2</sub>CO<sub>3</sub> (0.6 mmol), Ru catalyst (0.002 mmol) in CH<sub>2</sub>Cl<sub>2</sub> (2 mL) stirred at the indicated temperature for 16 h under N<sub>2</sub> unless noted otherwise. <sup>b</sup>Deviations from standard conditions are shown. <sup>c</sup>Determined by <sup>1</sup>H NMR of the crude products using Cl<sub>2</sub>CHCHCl<sub>2</sub> as internal standard. <sup>d</sup>Enantiomeric excess determined by HPLC analysis of the crude main product on a chiral stationary phase. <sup>f</sup>Isolated yield in brackets. <sup>g</sup>Reaction executed at 40 °C for 24 h. <sup>h</sup>Increased reaction time of 48 h.

Optimization of the chiral-at-metal ruthenium catalyst (**Ru4-Ru7**, entries 2-5) improved the enantioselectivity to 95% ee using the trimethylsilyl-modified ruthenium catalyst **Ru7**.

Functionalization of the benzoate leaving group with an electron-donating methoxy (**6ab**) (entry 6) or electron-withdrawing CF<sub>3</sub>-group (**6ac**) (entry 7) slightly affected the enantioselectivity. A pivaloate leaving group (**6ad**) only provided the 2-imidazolidinone in 27% yield with 91% ee (entry 8). Interestingly, the catalyst loading can be reduced down to 0.05 mol% upon increasing the reaction time to 24 hours and the temperature to 40 °C. (entries 9-11). The addition of a base is not required but increases the rate of reaction (entry 12).

### 2.3.3 Substrate scope

To explore the scope of this new method, we applied the reaction conditions to a variety of *N*-benzoyloxyurea as shown in **Figure 56**. Benzylic C(sp<sup>3</sup>)-H aminations to chiral 2-imidazolidinones occurred with high yields and high enantioselectivities. For example, a *para*-, *meta*-, and even a sterically very hindering *ortho*-methyl group in the phenyl moiety are well tolerated (products **7d-f**, 92-99% yield, 94-97% ee), as well as an electron-withdrawing fluorine (**7g**) and chlorine substituent (**7h**), and an electron-donating methoxy group (**7i**). A 1-naphthyl group provided the cyclic urea **7j** with 99% yield and 99% ee, while a 2-naphthyl group afforded the cyclic urea **7k** with 97% yield and 90% ee. The smaller 2-thiophene moiety provided the cyclic urea **7l** with 99% yield but a somewhat reduced 88% ee. 2-Imidazolidinone **7m** with stereocenters in the 4- and 5-position was obtained in sluggish 29% yield but 89% ee by desymmetrization of an indane substrate using the ruthenium catalyst  $\Lambda$ -**Ru6** instead of  $\Lambda$ -**Ru7**. However, the desymmetrization of a *N*-benzoyloxyurea derived from 1,3-diphenyl-2-propanamine provided the 4,5-difunctionalized 2-imidazolidinones **7n** with two adjacent stereocenters as a single diastereomer in 93% yield with 94% ee. Besides C(sp<sup>3</sup>)-H aminations at benzylic and allylic positions, ring-closing C(sp<sup>3</sup>)-H amination is also possible at a propargylic position in 89% yield and with 87% ee (**7o**). The ring-closing C(sp<sup>3</sup>)-H amination to 2-imidazolidinones tolerates different *N*-alkyl substituents as shown in **Figure 57**. Ethyl, *n*-butyl, isobutyl, and phenethyl substituents are well tolerated providing the corresponding *N*-alkylated 2-imidazolidinones **7p-s** in 68-99% yield and with 92-95% ee. However, a benzyl substituents results in reduced yields of 37% yield for **7t** (93% ee). Importantly, the ring-closing C(sp<sup>3</sup>)-H amination is applicable to non-alkylated substrates as demonstrated with the product **7u** containing two N-H groups which was afforded in 91% yield and 91% ee. It's worth noting that a substrate bearing a *N*-phenyl substituent (**6v**) only provided the corresponding C(sp<sup>2</sup>)-H amination product (**7v**), which is not desired in this context but by itself a useful transformation.

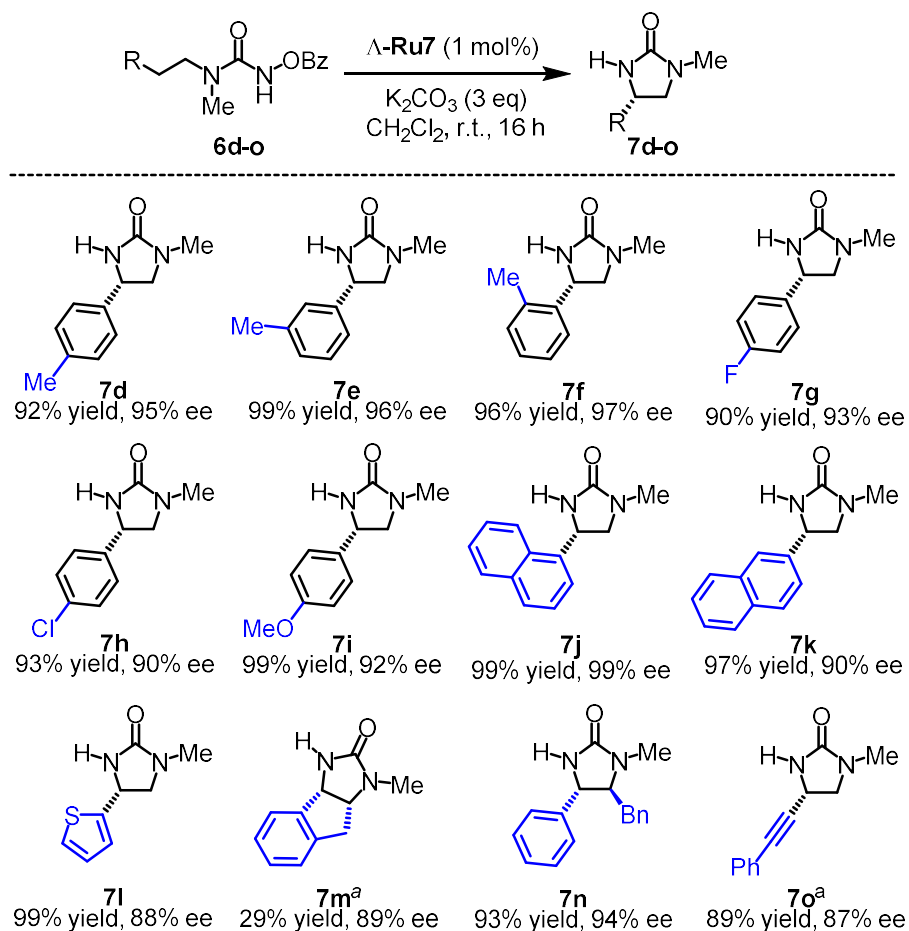


**Figure 56.** Scope with respect to synthesis of *N*-methyl cyclic ureas. <sup>a</sup> $\Delta$ -Ru6 was used as the catalyst instead.

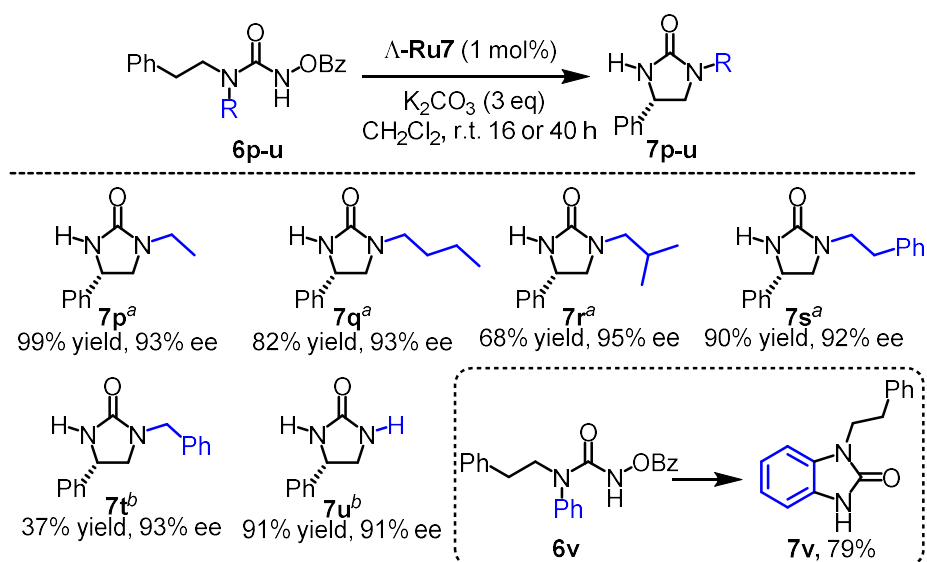


**Figure 57.** Substrate scope. Products **7p-r** formed with regioisomeric ratios of more than 20:1. <sup>a</sup>40 h reaction time. <sup>b</sup>16 hour reaction time.

### 2.3.4 Mechanistic Study

The proposed mechanism is shown in **Figure 58**. Upon release of benzoic acid from the

*N*-benzoyloxyurea, the ruthenium catalyst forms a ruthenium nitrenoid intermediate (**I**). The ruthenium nitrenoid from its triplet state subsequently performs a 1,5-Hydrogen atom transfer (HAT) to provide the radical intermediate **II**. This is followed by C-N bond formation through radical-radical recombination to provide the ruthenium-coordinated product (**III**), which is released to regenerate the active catalyst for a new catalytic cycle.

The radical mechanism is supported by a significant kinetic isotope effect (KIE) of 4.35, which was determined with an intramolecular competition experiment using the deuterated substrate **6aa'** to provide the cyclized products **7a'** and **7a''** with a ratio of 4.35:1 (**Figure 59a**). The high KIE value obtained is a strong indication for the formation of a triplet nitrene intermediate which then engages in radical chemistry. This is in contrast to our previous work on nitrene insertion of 2-azidoacetamides in which a KIE value of 1.5 was determined by an analogous intramolecular competition experiment. That the mechanism proceeds through intermediate radicals is further indicated by an experiment performed with the diastereomeric substrates (*Z*)-**6b** and (*E*)-**6b** (**Figure 59b**). While (*E*)-**6b** formed (*E*)-**7b** under complete retention of the alkene configuration (80% yield, 76% ee), (*Z*)-**6b** (*Z/E* ratio > 20:1) was converted to (*Z/E*)-**7b** with an eroded *Z/E* diastereomeric ratio of just 4.4:1 (73% yield, 91% ee). This can be rationalized with an isomerization from the thermodynamically less stable *Z*-isomer to the preferred *E*-isomer in the course of the C-H amination at the stage of the allyl radical intermediate. However, the radical is apparently short-lived so that no complete isomerization can occur. As expected, the *Z/E*-ratio is temperature dependent with a higher *Z/E*-ratio at lower temperature (5.1:1 at 4 °C) and a lower *Z/E*-ratio at higher temperature (2.9:1 at 40 °C). Finally, a radical mechanism is also supported by the ring-closing C-H amination of the chiral non-racemic substrate (*S*)-**6c** (89% ee) to provide (*S*)-**7c** under retention of configuration for both catalyst enantiomers (**Figure 59c**). However, while the  $\Lambda$ -catalyst provides (*S*)-**7c** with only slightly decreased enantioselectivity (85% ee), the mismatched  $\Delta$ -catalyst leads to a strong erosion of the enantiomeric excess of (*S*)-**7c** (40% ee). This erosion in enantiomeric excess is not consistent with a concerted C-H insertion mechanism but rather indicates a radical pathway in which the  $\Lambda$ -catalyst matches the *S*-configuration of the chiral substrate while the  $\Delta$ -catalyst constitutes a mismatch, thus resulting in a slower radical recombination and subsequent partial racemization.



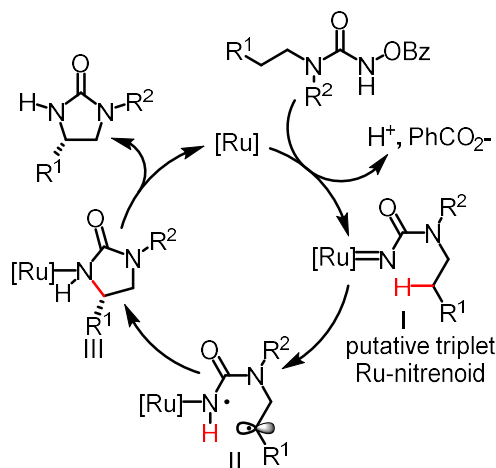
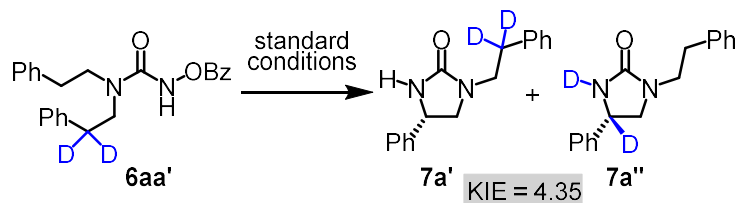
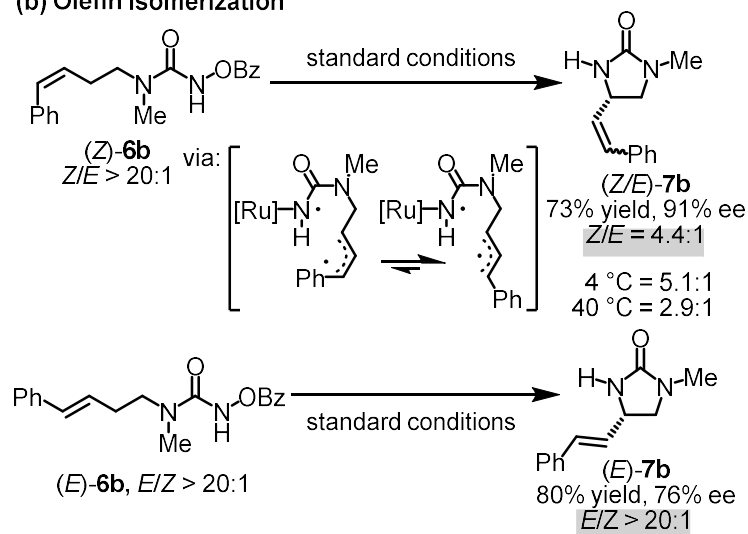


**Figure 58.** Proposed mechanism through an intermediate triplet ruthenium nitrenoid.

**(a) Kinetic isotope experiment**



**(b) Olefin isomerization**



**(c) Stereochemistry**

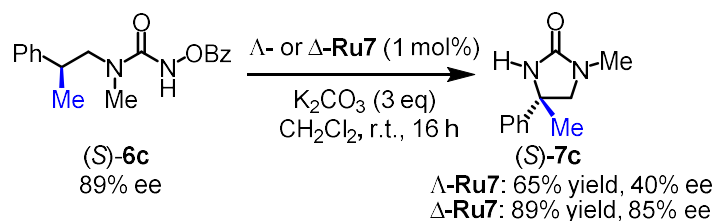


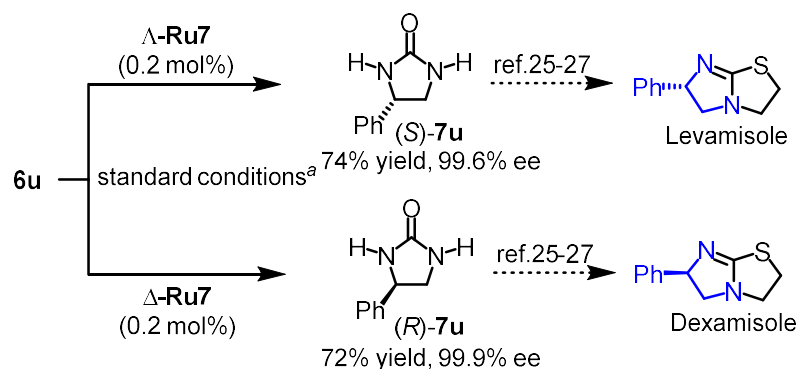
**Figure 59.** Control experiments to probe the proposed radical mechanism.

### 2.3.5 Synthetic Applications

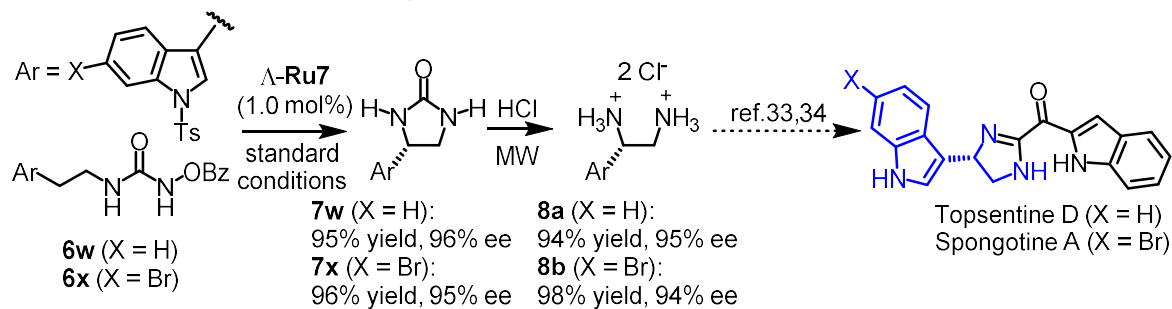
Chiral 2-imidazolidinones are highly valuable building blocks for the synthesis of bioactive compounds such as medicinal agents and natural products. For example, (*S*)-4-phenyl-2-imidazolidinone ((*S*)-**7u**) can be obtained from the *N*-benzoyloxyurea **6u** and just 0.2 mol%  $\Lambda$ -**Ru7** in a yield of 74% with almost perfect enantioselectivity of 99.6% ee after a single recrystallization step (**Figure 60a**). According to reported procedures, this enantiomerically pure 2-imidazolidinone (*S*)-**7u** can be converted to the drug levamisole<sup>24</sup> by first thiation of the urea with Lawesson's reagent<sup>25</sup> followed by cycloalkylation with 1,2-dibromoethane.<sup>26,27</sup> Analogously, the drug dexamisole, which is the enantiomer of levamisole,<sup>28</sup> can be synthesized from (*R*)-**7u** which was obtained from **6u** using  $\Delta$ -**Ru7** instead of  $\Lambda$ -**Ru7**.<sup>29-31</sup>

A second example provides a concise route to the bisindole alkaloids topsentine D and spongotine A (**Figure 60b**). Accordingly, ring-closing C(sp<sup>3</sup>)-H amination of the indole-containing substrates **6w** and **6x** provided under standard conditions the 4-indolyl-2-imidazolidinones **7w** and **7x**, respectively, in high yields and with high ee. These 2-imidazolidinones can be hydrolyzed with concentrated HCl in AcOH at 85 °C under microwave conditions<sup>32</sup> for 10 min to the respective vicinal diamines **8a** and **8b** with almost unchanged enantiomeric excess, and constitute intermediates of the natural products topsentine D<sup>33</sup> and spongotine A,<sup>34</sup> respectively. A third example provides access to the mono-*N*-methylated 1,2-diamine **8c** which was reported as an intermediate for the synthesis of a chiral organocatalyst (**Figure 60c**).<sup>35</sup>

## (a) Application to chiral 2-imidazolidinones



## (b) Application to natural product synthesis



## (c) Application to chiral catalyst synthesis

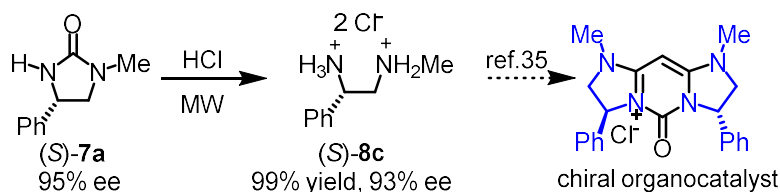


**Figure 60.** Applications to the synthesis of medicinal agents, natural products, and a chiral organocatalyst.  
<sup>a</sup>Standard conditions followed by recrystallization in EtOAc/*n*-Hexane. MW = microwave.

## 2.3.6 Conclusions

To conclude, we here reported the first example of a ring-closing C(sp<sup>3</sup>)-H amination of urea substrates to chiral 2-imidazolidinones in a catalytic enantioselective fashion. Starting from abundant primary or secondary amines, *N*-benzyloxyurea can be synthesized in just 2 steps and enantioselectively cyclized to cyclic urea under mild reaction conditions and using low loadings of a chiral-at-metal ruthenium catalyst. This method will be of significant synthetic interest for future researches since the furnished chiral 2-imidazolidinones and their corresponding chiral 1,2-diamines, obtained through efficient hydrolysis with HCl, are highly valuable chiral building blocks.

## References

1. J.-L. Liang, S.-X. Yuan, J.-S. Huang, W.-Y. Yu, C.-M. Che, *Angew. Chem. Int. Ed.* **2002**, *41*, 3465.
2. E. Milczek, N. Boudet, S. Blakey, *Angew. Chem. Int. Ed.* **2008**, *47*, 6825.
3. D. N. Zalatan, J. Du Bois, *J. Am. Chem. Soc.* **2008**, *130*, 9220.
4. C. Li, K. Lang, H. Lu, Y. Hu, X. Cui, L. Wojtas, X. P. Zhang, *Angew. Chem. Int. Ed.* **2018**, *57*, 16837.
5. K. Lang, S. Torker, L. Wojtas, X. P. Zhang, *J. Am. Chem. Soc.* **2019**, *141*, 12388.
6. Y. Yang, I. Cho, X. Qi, P. Liu, F. H. Arnold, *Nat. Chem.* **2019**, *11*, 987.
7. M. Ichinose, H. Suematsu, Y. Yasutomi, Y. Nishioka, T. Uchida, T. Katsuki, *Angew. Chem. Int. Ed.* **2011**, *50*, 9884.
8. J. A. McIntosh, P. S. Coelho, C. C. Farwell, Z. J. Wang, J. C. Lewis, T. R. Brown, F. H. Arnold, *Angew. Chem. Int. Ed.* **2013**, *52*, 9309.
9. P. Dydio, H. M. Key, H. Hayashi, D. S. Clark, J. F. Hartwig, *J. Am. Chem. Soc.* **2017**, *139*, 1750.
10. Y. Hu, K. Lang, C. Li, J. B. Gill, I. Kim, H. Lu, K. B. Fields, M. Marshall, Q. Cheng, X. Cui, L. Wojtas, X. P. Zhang, *J. Am. Chem. Soc.* **2019**, *141*, 18160.
11. R. P. Reddy, H. M. L. Davies, *Org. Lett.* **2006**, *8*, 5013.
12. H. Lebel, H. Huard, S. Lectard, *J. Am. Chem. Soc.* **2015**, *127*, 14198.
13. Y. Park, S. Chang, *Nat. Catal.* **2019**, *2*, 219.
14. Q. Xing, C.-M. Chan, Y.-W. Yeung, W.-Y. Yu, *J. Am. Chem. Soc.* **2019**, *141*, 3849.
15. H. Wang, Y. Park, Z. Bai, S. Chang, G. He, G. Chen, *J. Am. Chem. Soc.* **2019**, *141*, 7194.
16. Z. Zhou, S. Chen, Y. Hong, E. Winterling, Y. Tan, M. Hemming, K. Harms, K. N. Houk, E. Meggers, *J. Am. Chem. Soc.* **2019**, *141*, 19048.
17. P. F. Kuijpers, M. J. Tiekink, W. B. Breukelaar, D. L. J. Broere, N. P. van Leest, J. I. van der Vlugt, J. N. H. Reek, B. de Bruin, *Chem. Eur. J.* **2017**, *23*, 7945.
18. J. Qin, Z. Zhou, T. Cui, M. Hemming, E. Meggers, *Chem. Sci.* **2019**, *10*, 3202.
19. Z. Zhou, S. Chen, J. Qin, X. Nie, X. Zheng, K. Harms, R. Riedel, K. N. Houk, E. Meggers, *Angew. Chem. Int. Ed.* **2019**, *58*, 1088.
20. S. P. Swain, S. Mohanty, *ChemMedChem* **2019**, *14*, 291.

21. C. Lu, L. Hu, G. Yang, Z. Chen, *Curr. Org. Chem.* **2002**, *16*, 2802.
22. D. Lucet, T. Le Gall, C. Mioskowski, *Angew. Chem. Int. Ed.* **1998**, *37*, 2580.
23. S. R. S. Saibabu Kotti, C. Timmons, G. Li, *Chem. Biol. Drug Des.* **2006**, *67*, 101.
24. W. K. P. Amery, J. P. J. M. Bruynseels, *Int. J. Immunopharmac.* **1992**, *14*, 481.
25. V. K. Sharma, K.-C. Lee, C. Joo, N. Sharma, S.-H. Jung, *Bull. Korean Chem. Soc.* **2011**, *32*, 3009.
26. A. H. M. Raeymaekers, L. F. C. Roevens, P. A. J. Janssen, *Tetrahedron Lett.* **1967**, *8*, 1467.
27. C. Röben, J. A. Souto, Y. González, A. Lishchynskyi, K. Muñiz, *Angew. Chem. Int. Ed.* **2011**, *50*, 9478.
28. S. Keszei, B. Simándi, E. Székely, E. Fogassy, S. János, S. and Kemény, *Tetrahedron: Asymmetry* **1999**, *10*, 1275.
29. V. B. Birman, X. Li, *Org. Lett.* **2006**, *8*, 1351.
30. M. E. Abbasov, R. Alvariño, C. M. Chaheine, E. Alonso, J. A. Sánchez, M. L. Conner, A. Alfonso, M. Jaspars, L. M. Botana, D. Romo, *Nat. Chem.* **2019**, *11*, 342.
31. A. W. Schuppe, Y. Zhao, Y. Liu, T. R. Newhouse, *J. Am. Chem. Soc.* **2019**, *141*, 9191.
32. G. R. Vasanthakumar, V. Bhor, A. Surolia, *Synth. Commun.* **2007**, *37*, 2633.
33. X. Ji, Z. Wang, J. Dong, Y. Liu, A. Lu, Q. Wang, *J. Agric. Food Chem.* **2016**, *64*, 9143.
34. K. Murai, M. Morishita, R. Nakatani, O. Kubo, H. Fujioka, Y. Kita, *J. Org. Chem.* **2007**, *72*, 8947.
35. A. E. Sheshenev, E. V. Boltukhina, A. J. P. White, K. Kuok, *Angew. Chem. Int. Ed.* **2013**, *52*, 6988.

## 2.4 Enantioselective Synthesis of Cyclic Carbamates by Nitrene Insertion

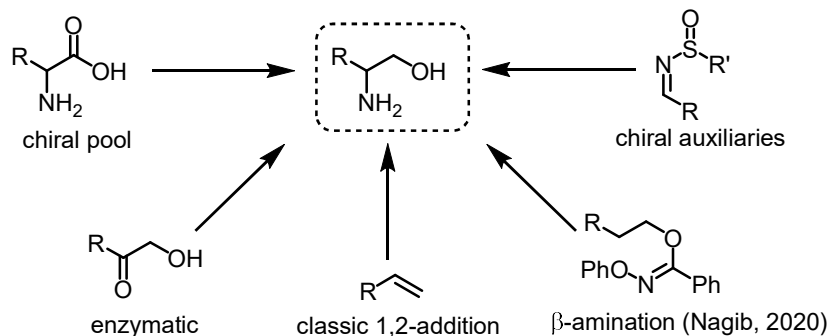
### 2.4.1 Research Background and Reaction Design

Chiral vicinal amino alcohols are indispensable synthetic building blocks. For example, they are frequently used for the synthesis of bioactive compounds<sup>1-3</sup> and are substrates for the synthesis of chiral oxazolines, which represent one of the most frequently used class of chiral ligands in asymmetric transition metal catalysis.<sup>4</sup> Enantiomerically pure chiral  $\beta$ -amino alcohols are typically synthesized by accessing the chiral pool, using chiral auxiliaries, or by applying catalytic asymmetric methods (**Figure 61a**). However, all these standard methods face significant limitations and drawbacks. The reduction of  $\alpha$ -amino acids is only attractive for naturally occurring amino acid side chains and the L-stereochemistry.<sup>5</sup> Chiral auxiliaries, such as Ellman's sulfonamide,<sup>6</sup> have to be employed in uneconomic equimolar amounts, and catalytic asymmetric aminooxygenations of alkenes often lack a high degree of regioselectivity, and entail other drawbacks such as the use of toxic osmium in the case of the Sharpless aminohydroxylation.<sup>7</sup> Biocatalytic approaches have also been reported but rely on substrates and reaction conditions that are compatible with enzymes.<sup>8</sup>

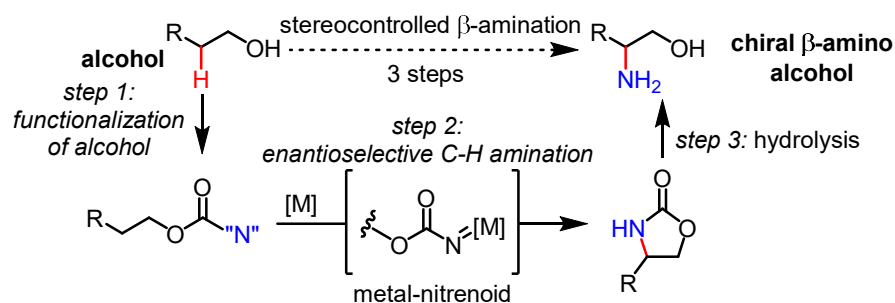
An appealing strategy for the asymmetric synthesis of chiral  $\beta$ -amino alcohols starts from ubiquitous alcohols and builds a  $C(sp^3)$ -N bond including a stereocenter in a single step through regio- and enantioselective ring-closing C-H amination chemistry. The Nagib group recently introduced an impressive method to accomplish this task through a photoredox radical protocol.<sup>9</sup> However, the method requires a complicated cocktail out of iridium photocatalyst and chiral copper catalyst, the use of expensive BARF counterions, in addition to 25 mol% camphoric acid. We envisioned to provide a stereocontrolled and regioselective  $\beta$ - $C(sp^3)$ -H amination of alcohols by exploiting catalytic asymmetric nitrene insertion (**Figure 61b**). Great progress has been made for the catalytic asymmetric synthesis of chiral amines using transition metal nitrenoid chemistry under typically very mild reaction conditions.<sup>10-15</sup> However, a general access to chiral  $\beta$ -amino alcohols in high yields and with high enantioselectivity through enantioselective nitrene insertion remains an unsolved problem. Sulfamate esters have been demonstrated to undergo intramolecular ring closing C-H aminations in the presence of hypervalent iodine reagents to provide cyclic sulfamidates,<sup>16-18</sup> but are difficult to hydrolyze and would preferably provide  $\gamma$ -amino alcohols. The formation of cyclic carbamates through ring-closing  $C(sp^3)$ -H amination would be advantageous. Davies provided four examples using *N*-tosyloxycarbamates under chiral dirhodium catalysis.<sup>19</sup> Unfortunately, yields (62-75%) and

enantioselectivities (43-82% ee) were only very modest and not of practical value.

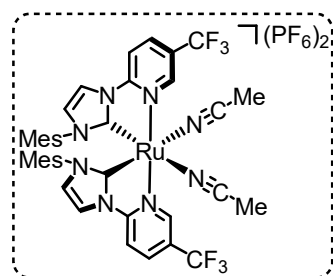
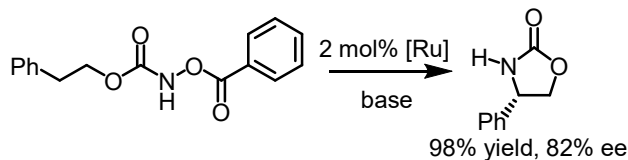
**a) Overview of representative methods for the synthesis of chiral  $\beta$ -amino alcohols**



**b) Strategy to chiral  $\beta$ -amino alcohols via transition-metal nitrenoid intermediates**



**c) Yuqi Tan's result:**



**d) My improved results:**

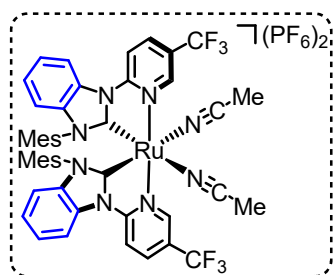
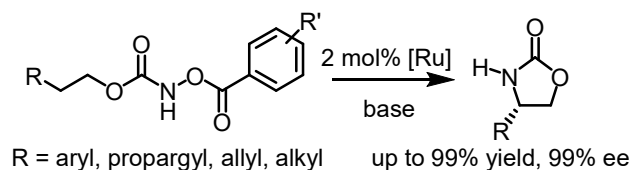


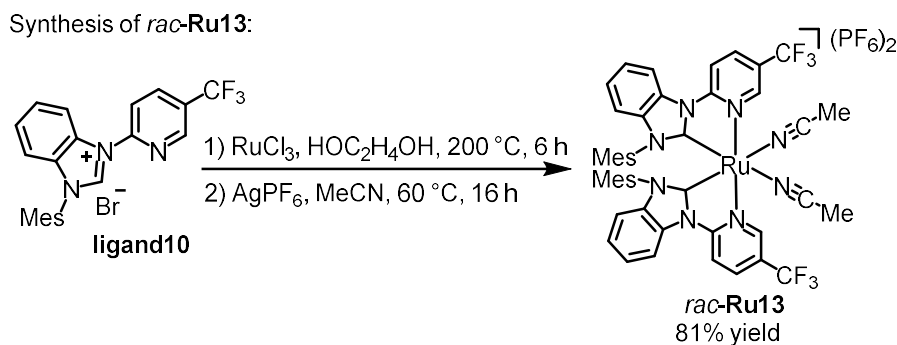
**Figure 61.** (a) Overview of representative methods for the synthesis of chiral  $\beta$ -amino alcohol. (b) Strategy to chiral  $\beta$ -amino alcohols via transition-metal nitrenoid intermediates. (c) Preliminary results obtained by the previous group member Y. Tan. (d) My improved results.

The previous group member Yuqi Tan obtained the preliminary result of the ring-closing C-H amination reaction, which lead to the formation of carbamate product in 98% yield and 82% ee using our standard chiral-at-Ru catalyst (**Figure 61c**). We were not satisfied with the obtained enantioselectivity. The author of this thesis thought if we modified the catalyst and also the leaving group of the substrate, maybe we could improve the enantioselectivity to above 90% ee (**Figure 61d**).

Although, the reaction has been reported with preliminary results, the synthetic utility of this reaction has not been illustrated. There is still no report for using ring-closing C–H amination methodology to synthesize chiral 1,2-amino alcohol via nitrene insertion.

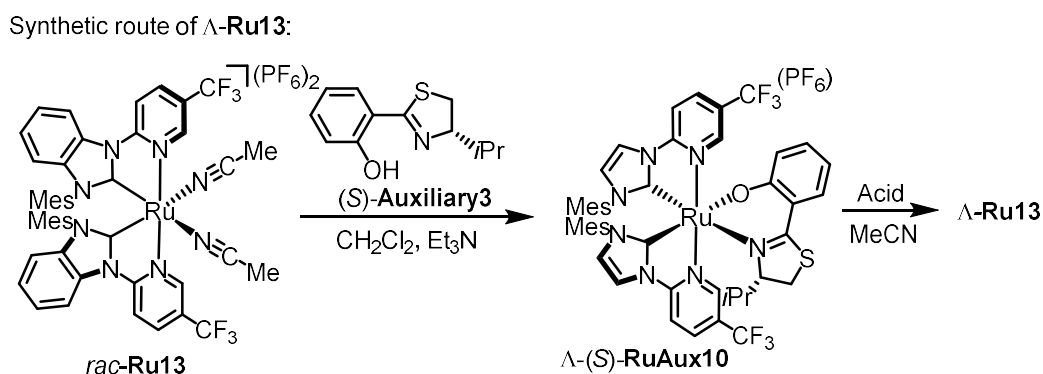
#### 2.4.2 Synthesis of New Chiral-at-Ruthenium Catalyst

As the previous group member Yuqi Tan already screened different reaction conditions in the purpose of getting above 90% ee of the desired carbamate product but often failed. The author of this thesis decided to start to modify the ruthenium catalyst's structure. As shown in **Figure 62**, starting from **ligand10** under standard complexation conditions, the desired *rac*-**Ru13** was obtained in 81% yield (**Figure 62**). The catalyst structure of the newly modified *rac*-**Ru13** has been proved by the single crystal X-ray diffraction study.



**Figure 62.** Attempts on the synthesis of *rac*-**Ru13** based on modification of the NHC moiety.

$\Lambda$ -**RuAux10** was obtained through the chiral-auxiliary-mediated synthesis. It's noteworthy that  $\Lambda$ -**RuAux10** couldn't be synthesized through the standard auxiliary-mediated synthetic route (the intermediate auxiliary complexes couldn't be isolated well by flash column as the two diastereomers were of the same  $R_f$  value), thus, we explored a slightly modified synthetic route which used a new (*S*)-**Auxiliary3** instead of the old one for getting enantiomerically pure  $\Lambda$ -**Ru13** (**Figure 63**).

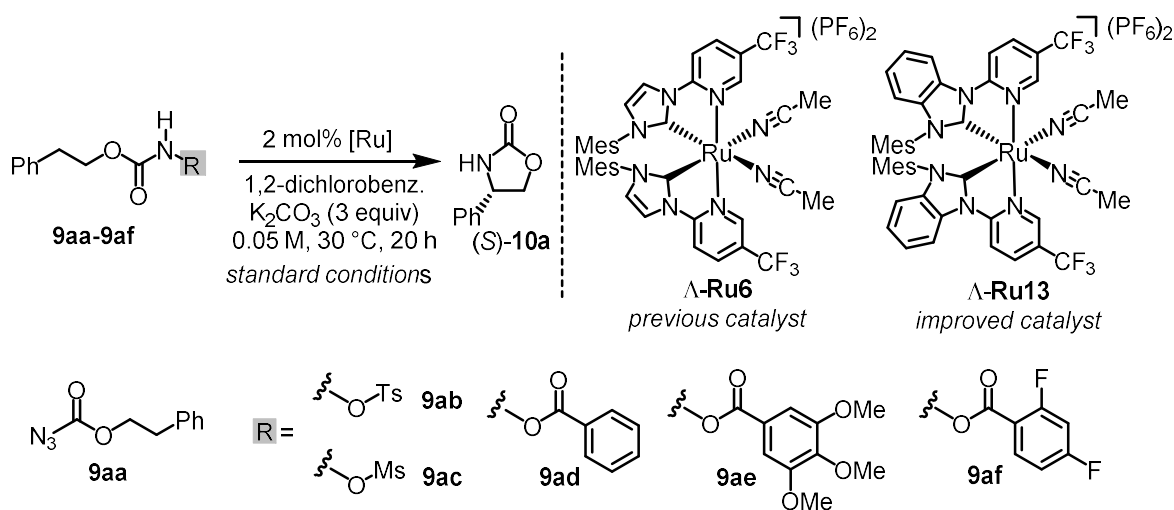


**Figure 63.** Chiral-auxiliary-mediated synthesis of enantiomerically pure  $\Lambda$ -**Ru13**.



### 2.4.3 Initial Experiments and Reaction Development

Azidoformates are well-established precursors of alkoxy carbonylnitrenes upon release of dinitrogen. However, no reaction occurred with phenethyl azidoformate **9aa** at room temperature in the presence of chiral-at-Ru catalyst  $\Lambda$ -**Ru6** (2.0 mol%) (entry 1). Likewise, sulfonyloxycarbamates did not provide satisfactory results. For example, the *N*-toluenesulfonyloxycarbamate **9ab** afforded (*S*)-**10ya** in 69% NMR yield with just 68% ee (entry 2). The related *N*-methylsulfonyloxycarbamate **9ac** afforded (*S*)-**10a** in a higher NMR yield of 94% but with a reduced enantioselectivity of just 62% ee (entry 3). We next turned our attention to *N*-benzoyloxycarbamates. Previous work from our laboratory on intramolecular C–H oxygenations and amino-oxygenations revealed that our chiral-at-Ru catalysts efficiently generate ruthenium nitrenoid intermediates from *N*-benzoyloxycarbamates. In fact, in recent preliminary results we were able to convert the *N*-benzoyloxycarbamate **9ad** to (*S*)-**10a** in 88% yield and with 78% ee (entry 4). Using carbamate **9ad** we next screened solvents and found that 1,2-dichlorobenzene is the solvent of choice and provided almost quantitative NMR yields (98%) with improved 82% ee (entry 5). Since we were not able to further improve the enantioselectivity by modifying the reaction conditions we turned our attention to use modified ruthenium catalyst and discovered that the newly modified ruthenium catalyst (**Ru13**) provided an improved enantiomeric excess of 86% ee under otherwise identical reaction conditions (entry 6). Final improvements were accomplished by functionalizing the benzoate leaving group. Best results were obtained with 3,4,5-trimethoxybenzoate (**9ae**) (entry 7) and 2,4-difluorobenzoate (**9af**) (entry 8) which both afforded the cyclic carbamate (*S*)-**10a** with 90% ee. The 2,4-difluorobenzoyloxycarbamate appears slightly more suitable due to a somewhat higher reactivity. Finally, without base the reaction proceeded very sluggish (entry 9) or performing the reaction under air resulted in a slightly reduced yield (entry 10).

**Table 4.** Initial experiments and optimization.<sup>a</sup>

Entry	Substrate	Catalyst	Conditions <sup>b</sup>	NMR yield (%) <sup>d</sup>	ee (%) <sup>e</sup>
1	<b>9aa</b>	$\Delta$ - <b>Ru6</b>	CH <sub>2</sub> Cl <sub>2</sub> at 25 °C without base	0	n.d.
2	<b>9ab</b>	$\Delta$ - <b>Ru6</b>	CH <sub>2</sub> Cl <sub>2</sub> at 25 °C	69	68
3	<b>9ac</b>	$\Delta$ - <b>Ru6</b>	CH <sub>2</sub> Cl <sub>2</sub> at 25 °C	94	62
4 <sup>f</sup>	<b>9ad</b>	$\Delta$ - <b>Ru6</b>	CHCl <sub>3</sub> at 25 °C	88	78
5	<b>9ad</b>	$\Delta$ - <b>Ru6</b>	standard	98	82
6	<b>9ad</b>	$\Delta$ - <b>Ru13</b>	standard	95	86
7	<b>9ae</b>	$\Delta$ - <b>Ru13</b>	40 °C instead	97	90
8	<b>9af</b>	$\Delta$ - <b>Ru13</b>	standard	quant. (99) <sup>g</sup>	90
9	<b>9af</b>	$\Delta$ - <b>Ru13</b>	no base	< 5	n.d.
10	<b>9af</b>	$\Delta$ - <b>Ru13</b>	under air	92	90

<sup>a</sup>Standard conditions: **9aa** (0.2 mmol), K<sub>2</sub>CO<sub>3</sub> (0.6 mmol), Ru catalyst (0.002 mmol) in 1,2-dichlorobenzene (4 mL) stirred at the 30 °C for 20 h under N<sub>2</sub> unless noted otherwise. <sup>b</sup>Deviations from standard conditions are shown. <sup>c</sup>Conversion. <sup>d</sup>Determined by <sup>1</sup>H NMR of the crude products using Cl<sub>2</sub>CHCHCl<sub>2</sub> as internal standard. <sup>e</sup>Enantiomeric excess determined by HPLC analysis of the crude main product on a chiral stationary phase. <sup>f</sup>Taken from ref. 27. <sup>g</sup>Isolated yield in brackets.

#### 2.4.4 Substrate Scope

With the optimized reaction conditions in hand we investigated the substrate scope. *N*-Benzoyloxycarbamates bearing different aryl substituents at the  $\beta$ -position were tested first. As shown in **Figure 64**, oxazolidin-2-ones with electron donating methoxy substituents in *para*- (**10b**), *meta*- (**10c**) or *ortho*- (**10d**) positions of the phenyl moiety were obtained in almost quantitative yields and with excellent enantioselectivities (90-92% ee). A substrate bearing a sterically very hindering *ortho*-methyl substituent (**10e**) was also well tolerated and provided 99% yield and 92% ee. A 4-phenyl substituent on the phenyl moiety (**10f**) provided almost quantitative yield together with an excellent enantioselectivity of 98% ee. Different electron-withdrawing groups are also accommodated

in *para*-position as demonstrated for an electron-withdrawing fluorine (**10g**, 99% yield, 91% ee), chlorine (**10h**, 92% yield, 88% ee), or bromine (**10i**, 99% yield, 90% ee). A 1-naphthyl group provided the cyclic carbamate **10j** with 99% yield and 93% ee, while a 2-naphthyl group afforded the cyclic carbamate **10k** with 97% yield and 92% ee. A tryptophol-derived substrate provided oxazolidin-2-one in 66% yield and 85% ee (**10l**). The smaller 3-thiophene moiety provided the cyclic carbamate **10m** with 77% yield and 93% ee. Oxazolidin-2-one **10n** with stereocenters in the 4- and 5-positions was obtained in 99% yield and 95% ee by desymmetrization of an indane substrate. A *N*-benzyloxycarbamate derived from 1,3-diphenyl-2-propanol provided the 4,5-difunctionalized oxazolidin-2-one **10o** with two adjacent stereocenters as a 1.8:1 *trans/cis* mixture with respective 92% and 97% ee in overall 83% yield.

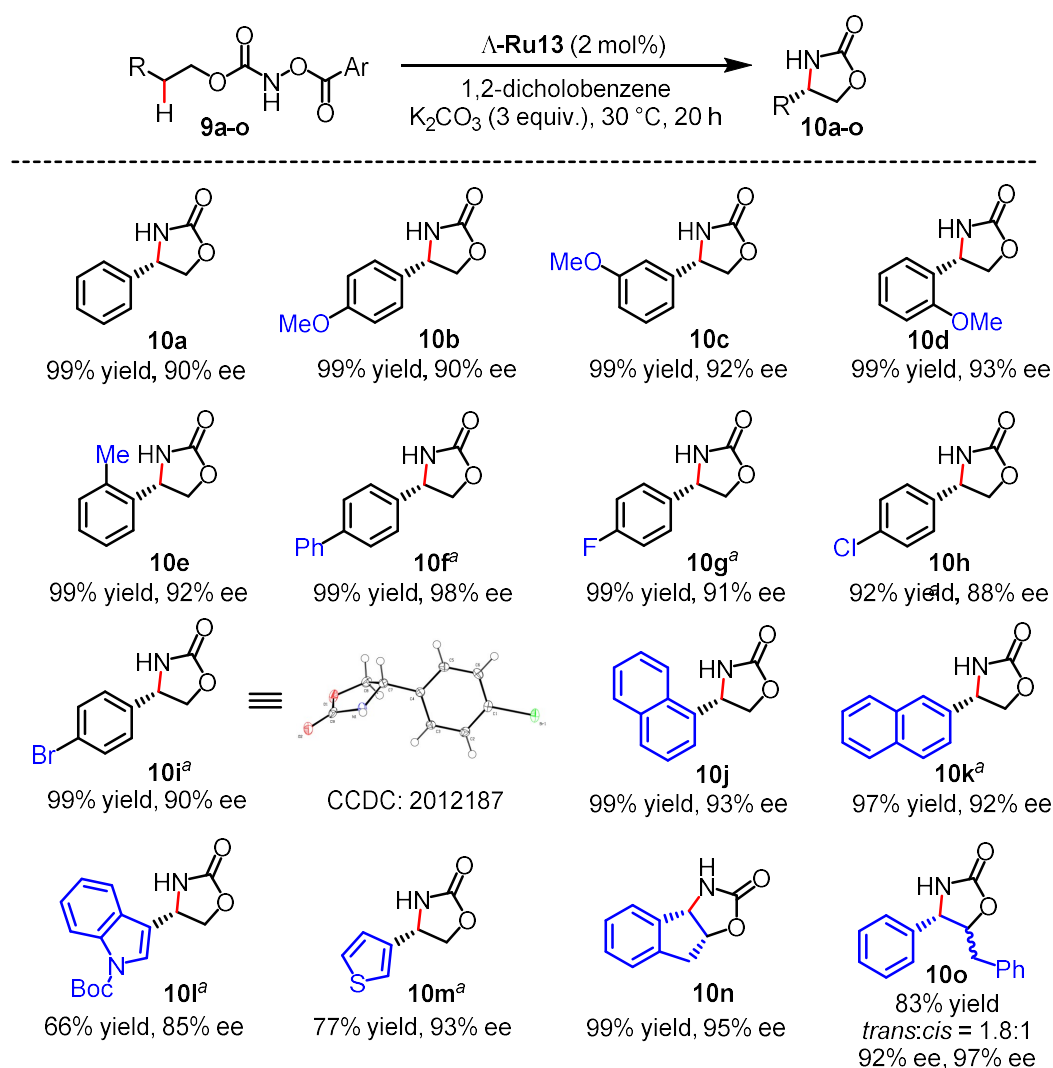


**Figure 64.** Substrate scope with respect to benzylic C–H aminations. Ar = 2,4-difluorophenyl unless noted otherwise. <sup>a</sup>Modified substrate and reaction conditions: Ar = 3,4,5-trimethoxyphenyl and reacted at 40 °C.

Non-benzylic C–H amination reactions are of particular interest since they are more difficult to

achieve in high yields and with high enantioselectivities. In fact, previous reported ruthenium catalyzed enantioselective intramolecular C–H aminations at non-benzylic positions from our group often failed to get satisfactory results. As shown in **Figure 64**, we investigated propargylic C–H aminations first and encouragingly found the product **10p** was formed in 91% yield and 91% ee under standard reaction conditions. An electron-donating methoxy substituent on the phenyl moiety provided cyclic carbamate **10q** with 91% yield and 94% ee while an electron-withdrawing fluorine substituent provided cyclic carbamate **10r** with slightly reduced 85% yield and 90% ee. Replacement of the phenyl moiety with an alkyl group is also accommodated as shown by the alkyne product **10s** (84% yield and 90% ee). The aminated C(sp<sup>3</sup>)–H bond can also be flanked by an alkenyl group. While (*E*)-**9t** converted to (*E*)-**10t** under complete retention of the alkene configuration (88% yield, 63% ee), (*Z*)-**9t** (*Z/E* ratio > 20:1) was converted to (*Z/E*)-**10t** with an eroded *Z/E* diastereomeric ratio of 10.3:1 (56% yield, 45% ee). This can be explained with an isomerization from the thermodynamically less stable *Z*-isomer to the preferred *E*-isomer in the course of the C–H amination through an intermediate allyl radical. However, the radical is apparently not long-lived enough to furnish complete isomerization. We were delighted to find that a cyclohexene substituent provided cyclic carbamate **10u** in 96% yield and 92% ee. It is noteworthy that the late-stage functionalization of (*R*)-nopol provided cyclic carbamate **10v** in 87% yield with 96:4 d.r.. In this example, the stereoselectivity of the C–N bond formation was controlled only by chiral ruthenium catalyst since the racemic ruthenium catalyst lead to the formation of **10v** with only 1:1 d.r.. In addition, C–H amination next to a small isopropenyl substituent, provided the product **10w** in 79% yield with 61% ee. Beside C(sp<sup>3</sup>)–H aminations at propargylic and allylic positions, ring-closing C–H amination was also possible at aliphatic methylene groups without any adjacent activating group. The adamantyl substituted cyclic carbamate **10x** was formed in 99% yield with 99% ee. The *n*-butyl substituted oxazolidin-2-one **10y** was formed in 53% yield with 80% ee. The late-stage functionalization of 10-undecen-1-ol provided **10z** in 41% yield and 79% ee. Finally, a substrate bearing an adjacent chiral center was also employed, which is the late-stage functionalization of (*S*)-catronnellol, providing **10za** in 18% yield and > 20:1 d.r. as determined by <sup>1</sup>H NMR.

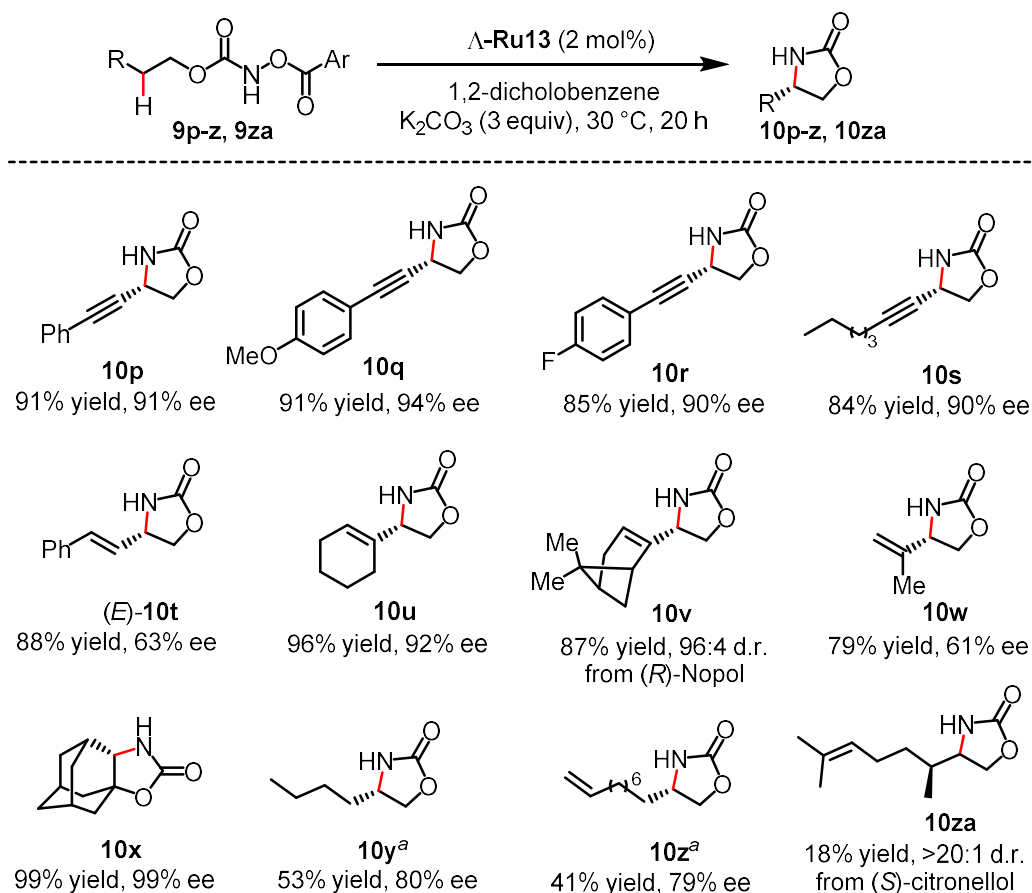
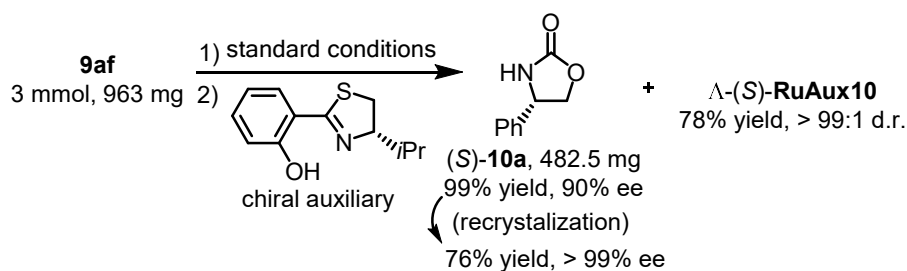


**Figure 65.** Substrate scope with respect to non-benzylic C–H aminations. Ar = 2,4-difluorophenyl unless noted otherwise. <sup>a</sup>Ar = Ph.

### 2.4.5 Synthetic Applications

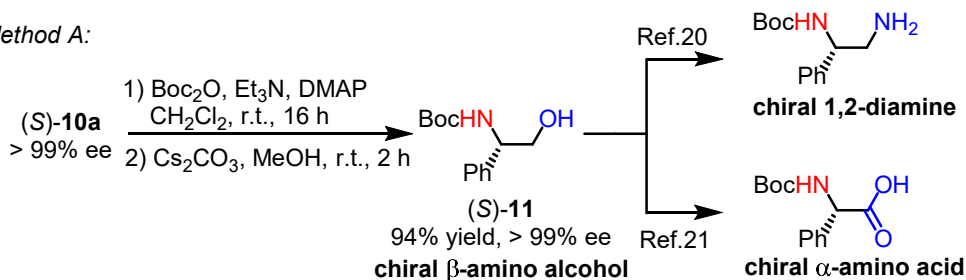
For practical purposes it is important to note that the catalytic intramolecular C–H amination of substrate **9af** was tested on a gram scale and proceeded smoothly under standard reaction conditions to provide (*S*)-**10a** in 99% yield with 90% ee (**Figure 66a**). Upon a following simple recrystallization step, (*S*)-**10a** could even be obtained with > 99% ee. Furthermore, upon addition of the auxiliary after the reaction, the chiral-at-Ru catalyst was recycled in 78% yield and with >99:1 d.r. as the auxiliary complex  $\Delta$ -(*S*)-RuAux10. We also investigated follow-up conversions of the carbamate products. Accordingly, the oxazolidin-2-one (*S*)-**10a** (recrystallized with > 99% ee) was converted to the Boc-protected  $\beta$ -amino alcohol (*S*)-**11** without any loss of enantiomeric excess (**Figure 66b**, method A). The aminoalcohol (*S*)-**11** was reported as a valuable synthetic intermediate for the synthesis of chiral 1,2-diamine<sup>20</sup> and also the chiral  $\alpha$ -amino acid<sup>21</sup>. In another follow-up chemistry using bis(2-aminoethyl)amine as the ring-opening reagent, the oxazolidin-2-one **10n**, bearing two vicinal stereocenters, was converted to the corresponding chiral amino alcohol (*1S,2R*)-**12** which is a building block for the frequently used chiral Box-ligand (**Figure 66b**, method B).<sup>22</sup>

(a) Gram-scale synthesis of (*S*)-**16a** and catalyst recovery:



(b) Synthesis of chiral  $\beta$ -amino alcohol and further transformations:

Method A:



Method B:

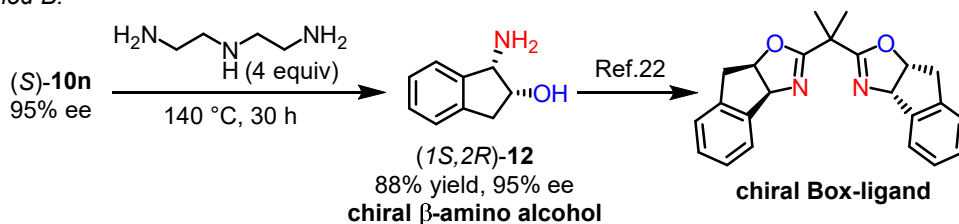
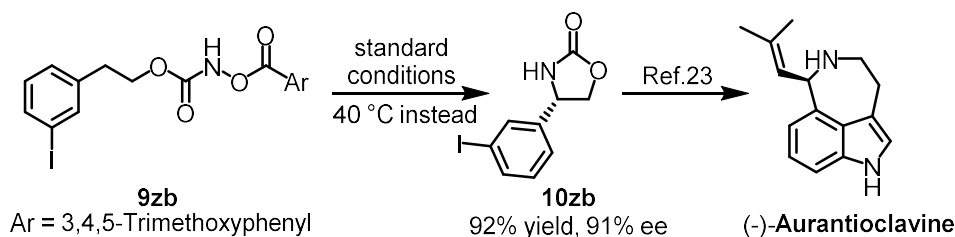


**Figure 66.** Gram-scale reaction and ring opening of chiral cyclic carbamates.

The utility of our new method for the straightforward synthesis of natural products is shown in **Figure 67**. Substrate **9zb** undergoes an intramolecular enantioselective cyclization to provide in 92% yield and with 91% ee (*S*)-**10zb** which was reported as an intermediate for the synthesis of the natural product (-)-aurantioclavine (**Figure 67a**).<sup>23</sup> A second example provides a concise route to the bisindole alkaloids hamacanthin A and dragmacidin A. Accordingly, ring-closing C–H amination of the indole containing substrate **9zc** provided under standard conditions the cyclic carbamate intermediate (*S*)-**10zc** in 74% yield and 94% ee. Further ring-opening provided the chiral  $\beta$ -amino alcohol **13** in 88% yield with 94% ee which was reported as an intermediate for the synthesis of natural products hamacanthin A and dragmacidin A (**Figure 67b**).<sup>24</sup>

(a) Synthesis of (-)-Aurantioclavine:



(b) Synthesis of Dragmacidin A and Hamacanthin A:

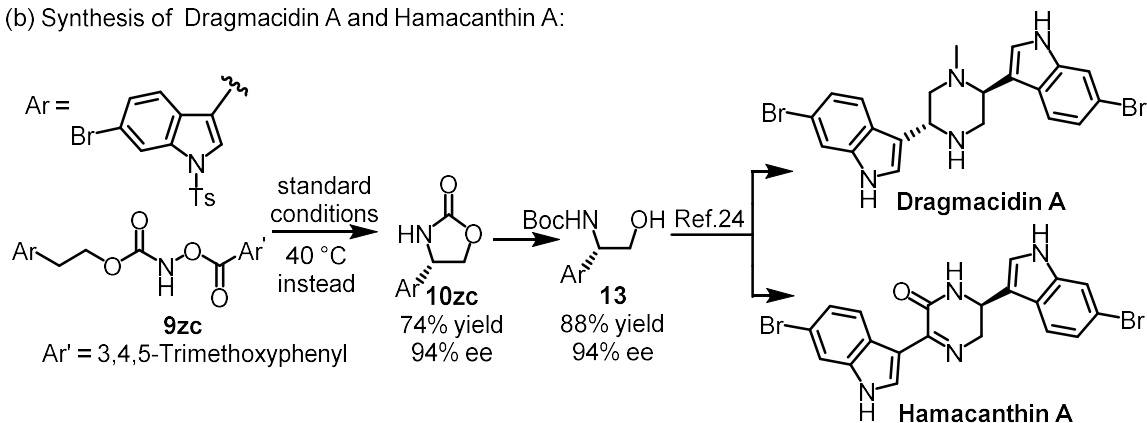


**Figure 67.** Synthetic application to natural products.

## 2.4.6 Conclusions

In summary, we here reported an economic and practical method to chiral oxazolidin-2-ones and corresponding  $\beta$ -amino alcohols, both of which are highly valuable chiral building blocks. The method is based on a ring-closing  $C(sp^3)$ -H amination of *N*-benzoyloxycarbamates using a new benzimidazol-2-ylidene carbene chiral-at-ruthenium catalyst. 2,4-Difluorobenzoate and 3,4,5-trimethoxy benzoate leaving groups afford for most substrates the best results. The intramolecular C-H amination provides cyclic carbamates in up to 99% yield and with up to 99% ee for benzylic, allylic, and propargylic C-H bonds. Completely non-activated  $C(sp^3)$ -H bonds provide somewhat reduced yields and enantioselectivities. We demonstrated the synthetic value of this new method with the catalytic enantioselective synthesis of chiral oxazolidin-2-ones as intermediates of the natural products aurantiolavine, hamacanthin A and dragmacidin A, a chiral amino acids, and a chiral Box ligand.

## Reference

1. S. C. Bergmeier, *Tetrahedron* **2000**, *56*, 2561.
2. E. Anakabe, D. Badia, L. Carrillo, E. Reyes, J. L. Vicario, *Targets in Heterocyclic Systems* **2002**, *6*, 270.
3. M. M. Heravi, T. B. Lashaki, B. Fattahi, V. Zadsirjan, *RSC Adv.* **2018**, *8*, 6634.
4. F. Fache, E. Schulz, M. L. Tommasino, M. Lemaire, *Chem. Rev.* **2000**, *100*, 2159.
5. J. Málek, Part II. Carboxylic acids and derivatives, nitrogen compounds, and sulfur compounds. *Organic Reactions* **1988**, *36*, 249.
6. M. T. Robak, M. A. Herbage, J. A. Ellman, *Chem. Rev.* **2010**, *110*, 3600.
7. J. Rudolph, P. C. Sennhenn, C. P. Vlaar, K. B. Sharpless, *Angew. Chem. Int. Ed.* **1996**, *35*, 2813.
8. I. V. Pavlidis, M. S. Weiß, M. Genz, P. Spurr, S. P. Hanlon, B. Wirz, H. Iding, U. T. Bornscheuer, *Nat. Chem.* **2016**, *8*, 1076.
9. K. M. Nakafuku, Z. Zhang, E. A. Wappes, *Nat. Chem.* **2020**, doi.org/10.1038/s41557-020-0482-8.
10. F. Collet, R. H. Dodd, P. Dauban, *Chem. Commun.* **2009**, 5061.
11. C.-M. Che, V. K.-Y. Lo, C.-Y. Zhou, J.-S. Huang, *Chem. Soc. Rev.* **2011**, *40*, 1950.
12. G. Dequirez, V. Pons, P. Dauban, *Angew. Chem. Int. Ed.* **2012**, *51*, 7384.
13. J. L. Roizen, M. E. Harvey, J. Du Bois, *Acc. Chem. Res.* **2012**, *45*, 911.
14. Y. Park, Y. Kim, S. Chang, *Chem. Rev.* **2017**, *117*, 9247.
15. T. Shimbayashi, K. Sasakura, A. Eguchi, K. Okamoto, K. Ohe, *Chem. Eur. J.* **2019**, *25*, 3156.
16. J.-L. Liang, S.-X. Yuan, J.-S. Huang, W.-Y. Yu, C.-M. Che, *Angew. Chem. Int. Ed.* **2002**, *41*, 3465.
17. E. Milczek, N. Boudet, S. Blakey, *Angew. Chem. Int. Ed.* **2008**, *47*, 6825.
18. D. N. Zalatan, J. Du Bois, *J. Am. Chem. Soc.* **2008**, *130*, 9220.
19. R. P. Reddy, H. M. L. Davies, *Org. Lett.* **2006**, *8*, 5013.
20. C. K. Skepper, *J. Med. Chem.* **2018**, *61*, 3325.
21. P. Ermert, *Tetrahedron Lett.* **1988**, *29*, 1265.
22. D. P. Hari, J. Waser, *J. Am. Chem. Soc.* **2017**, *139*, 8420.
23. J. Park, D. Kim, T. Das, C. Cho, *Org. Lett.* **2016**, *18*, 5098.
24. C. Yang, J. Wang, X.-X. Tang, B. Jiang, *Tetrahedron: Asymmetry* **2002**, *13*, 383.



## Chapter 3: Summary and Outlook

### 3.1 Summary

The synthetic access to a variety of newly modified chiral-at-ruthenium asymmetric catalysts has been accomplished through a chiral-auxiliary-mediated synthetic strategy. These ruthenium catalysts are composed of two chelating inert NHC ligands, which generate metal-centered chirality, and two nitrile ligands. The dicationic complexes are complemented by two hexafluorophosphate or tetrafluoroborate anions.

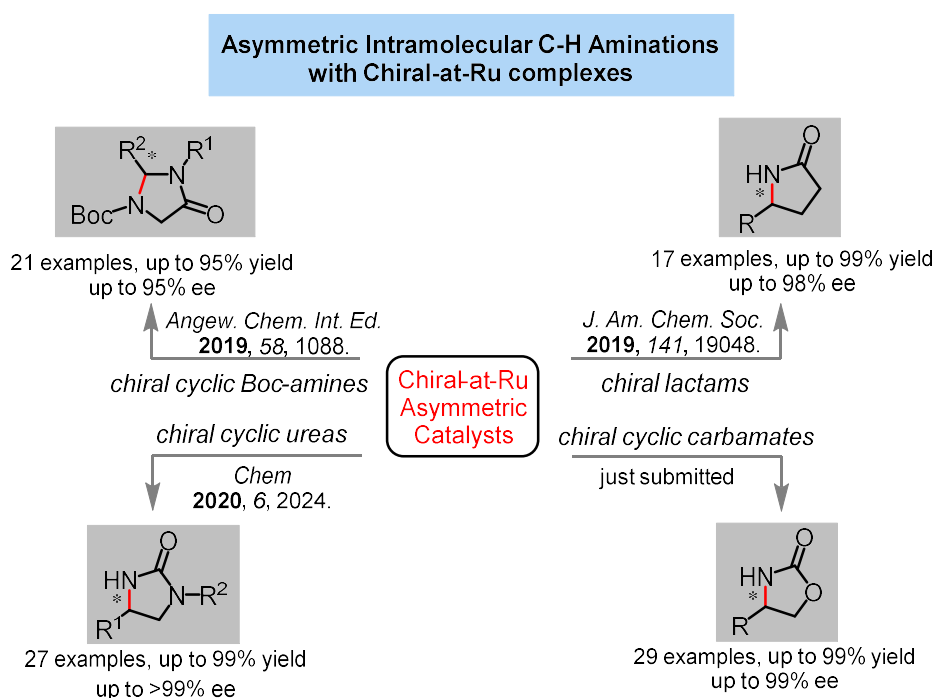


**Figure 68.** An overview of this thesis.

The excellent catalytic activity of these chiral ruthenium catalysts has been demonstrated through diverse asymmetric intramolecular C–H amination reactions. Accordingly, the efficient asymmetric intramolecular C–H aminations have been applied into the construction of chiral cyclic Boc-amines, lactams, cyclic ureas, and carbamates in high yields and excellent enantioselectivities. Further manipulation of these chiral nitrogen-containing heterocycles by performing the one-step ring-open transformations given rise to the formation of intermediates for the synthesis of drugs, natural products, chiral ligands, and chiral catalysts.

### 1) Catalytic enantioselective intramolecular C–H amination of 2-azidoacetamides

Asymmetric intramolecular C–H amination of 2-azidoacetamides was catalyzed by a newly modified ruthenium catalyst **Ru7**. The desired imidazolidin-4-one products were formed in excellent yields and enantioselectivities with up to 95% yield and 95% ee (错误!未找到引用源。). This work demonstrated our chiral-at-ruthenium asymmetric catalysts could be applied in challenging intramolecular C–H amination reactions.

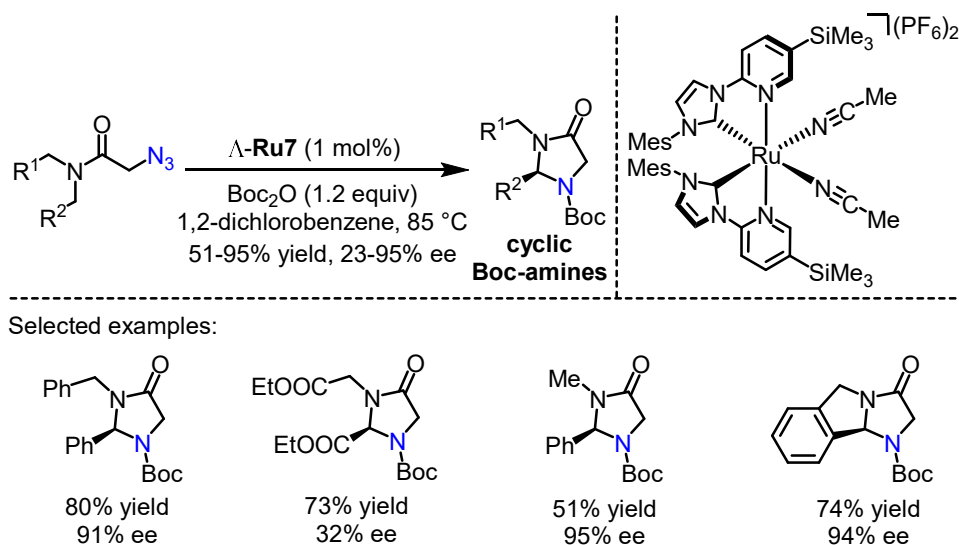


**Figure 69.** Catalytic enantioselective intramolecular C–H amination of 2-azidoacetamides.

### 2) Enantioselective synthesis of $\gamma$ -lactams by intramolecular C–H amidation

The exploration of the catalytic property of the non- $C_2$ -symmetric ruthenium catalyst **Ru10**, which was first synthesized by the group member Yubiao Hong, has been accomplished. The non- $C_2$ -symmetric chiral-at-ruthenium catalyst was applied in highly efficient enantioselective intramolecular C(sp<sup>3</sup>)-H amidation for the synthesis of chiral  $\gamma$ -lactams. Due to the strong electron-donating effect of the rNHC ligands, the metal center of the new ruthenium catalyst is more electron-rich compared with our previous chiral-at-ruthenium catalysts, which instead exhibited Curtius decomposition via transition-metal acyl-nitrenoid intermediates (**Figure 70**).

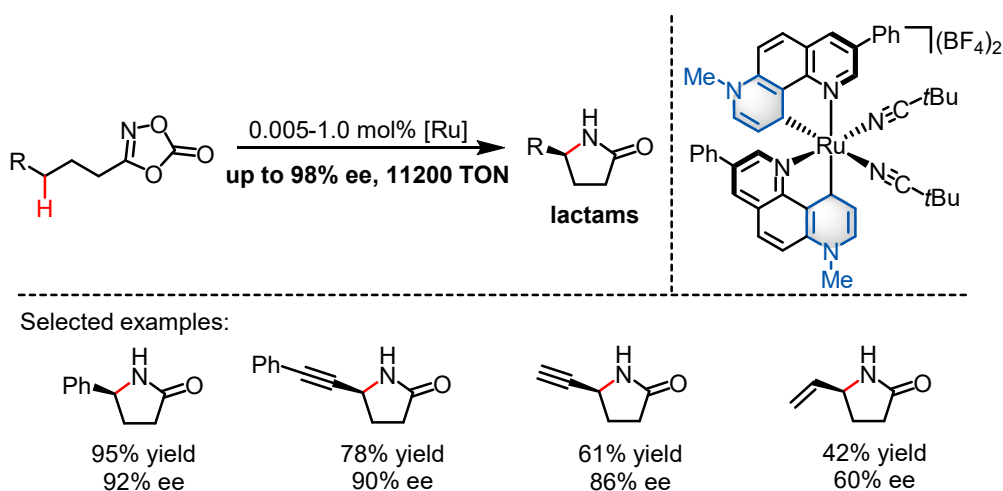


**Figure 70.** Enantioselective synthesis of  $\gamma$ -lactams by intramolecular C–H amidation.

### 3) Enantioselective synthesis of 2-imidazolidinones by intramolecular C–H amidation

The enantioselective synthesis of 2-imidazolidinones was accomplished by a chiral-at-metal ruthenium catalyst **Ru7**. It has been demonstrated for the first time on the synthesis of chiral cyclic ureas via ring-closing C–H aminations. The reaction proceeded smoothly and the target chiral cyclic ureas were formed in up to 99% yield and 99% ee (错误!未找到引用源。). Further ring-opening of cyclic ureas provided different chiral 1,2-diamines which were already been reported as intermediates for the synthesis of natural products, and a chiral organo-catalyst.

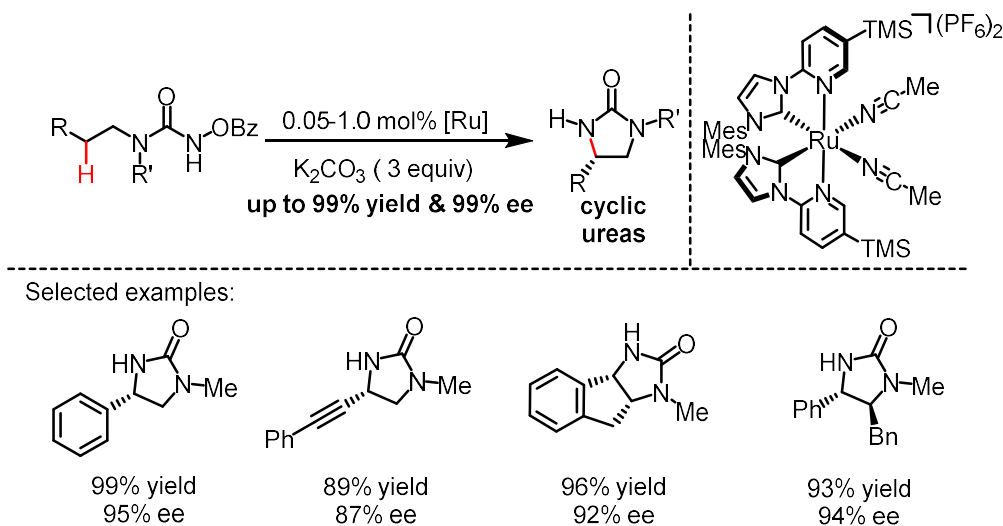


**Figure 71.** Enantioselective synthesis of cyclic ureas by intramolecular C–H amidation.

### 4) Enantioselective synthesis of $\beta$ -amino alcohols by nitrene insertion

The enantioselective synthesis of chiral cyclic carbamates was accomplished by a newly modified ruthenium catalyst **Ru13** catalyzed intramolecular C–H amination of *N*-benzoyloxycarbamates. The

desired chiral cyclic carbamates were obtained in up to 99% yield and 99% ee with broad substrate scope. It can be applied in the amination of benzylic, propargylic, allylic and even non-activated aliphatic C–H bonds. Further ring-opening of cyclic carbamates provided chiral  $\beta$ -amino alcohols as intermediates for the synthesis of natural products and chiral ligand used in asymmetric catalysis (Figure 72).

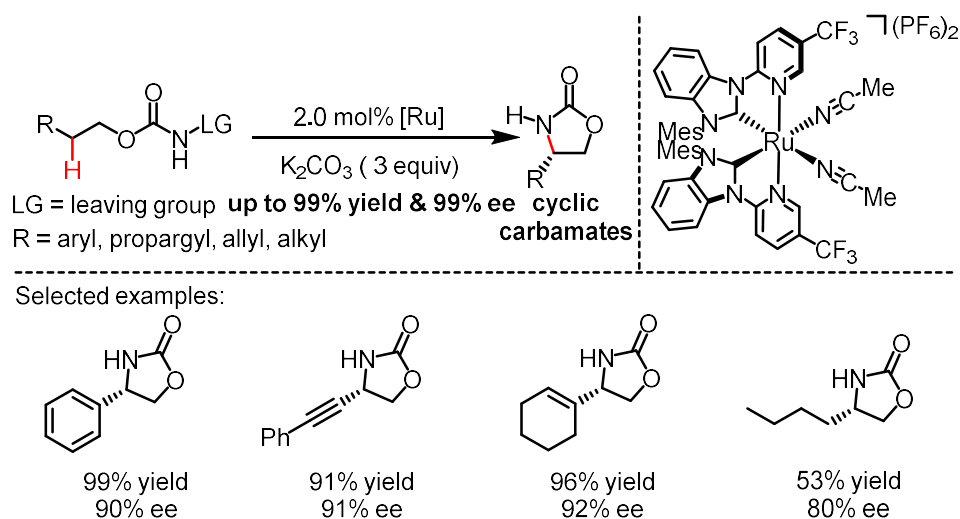
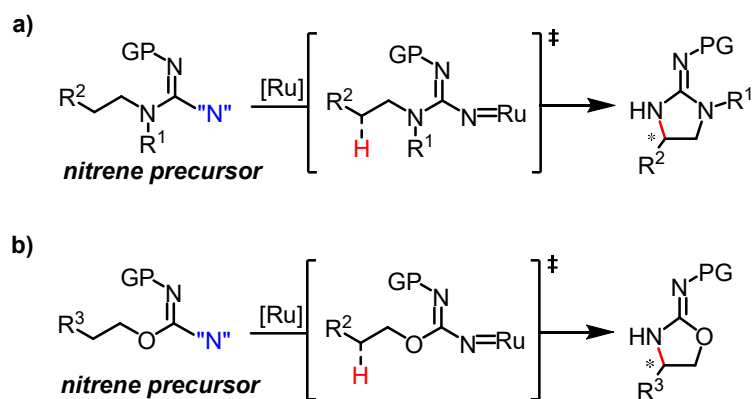


Figure 72. Enantioselective synthesis of cyclic carbamates by intramolecular C–H amidation.

### 3.2 Outlook

Considering the diverse synthetic applications of C–H amination products to drugs, natural products, chiral ligands, and chiral catalysts. Therefore, it should be of high synthetic value for further investigations on new types of C–H amination reactions.

**1) Synthesis of new chiral *N*-heterocycles by asymmetric intramolecular C–H aminations:** This thesis showed the synthesis of four different chiral *N*-heterocycles by asymmetric intramolecular C–H aminations, there are still some untapped structure motifs<sup>1</sup> which could be constructed through ruthenium catalyzed asymmetric intramolecular C–H aminations, such as the structures shown in Figure 73.



**Figure 73.** Synthesis of new chiral *N*-heterocycles via asymmetric intramolecular C–H aminations.

**2) Exploit asymmetric intermolecular C–H amination reactions:** Compared with intramolecular C–H amination reactions, the intermolecular version is more direct for the synthesis of chiral amines. Cyclic *N*-heterocycles synthesized via asymmetric intramolecular C–H aminations need further ring-opening to get final amine products. Thus, some functional groups are not well tolerated. The intermolecular version has its special advantages on the direct and rapid synthesis of chiral amines. Our ruthenium catalysts have been proved for asymmetric intramolecular C–H aminations, and the next stage should be asymmetric intermolecular C–H aminations<sup>2-5</sup>.

## Reference

1. M. Kim, J. V. Mulcahy, C. G. Espino, J. Du Bois, *Org. Lett.* **2006**, *8*, 1073.
2. S. Fukagawa, Y. Kato, R. Tanaka, M. Kojima, T. Yoshino, S. Matsunaga, *Angew. Chem. Int. Ed.* **2019**, *58*, 1153.
3. S. Fukagawa, M. Kojima, T. Yoshino, S. Matsunaga, *Angew. Chem. Int. Ed.* **2019**, *58*, 18154.
4. Y.-H. Liu, P.-X. Li, Q.-J. Yao, Z.-Z. Zhang, D.-Y. Huang, M. D. Le, H. Song, L. Liu, B.-F. Shi, *Org. Lett.* **2019**, *21*, 1895.
5. Y.-S. Jang, M. Dieckmann, N. Cramer, *Angew. Chem. Int. Ed.* **2017**, *56*, 15088.

## Chapter 4: Experimental Part

### 4.1 Materials and Methods

All reactions were carried out under an atmosphere of nitrogen with magnetic stirring. The catalysis reactions were performed using standard Schlenk glassware techniques.

#### Solvents and Reagents

Solvents were distilled under nitrogen from calcium hydride ( $\text{CH}_2\text{Cl}_2$ ,  $\text{CH}_3\text{CN}$ ) or sodium/benzophenone ( $\text{Et}_2\text{O}$ , THF and toluene). Super-dry solvents, such as 1,2-dichlorobenzene (from Acros) and DMF (from Sigma Aldrich) were purchased from commercial available source and used directly without further drying. All reagents purchased from Acros, Alfa Aesar, Sigma Aldrich, TCI, ChemPur, Merck and Fluorochem were used without any further purifications.

#### Chromatographic Methods

The course of the reactions and the column chromatographic elution were monitored by thin layer chromatography (TLC) [Macherey-Nagel (ALUGRAM®Xtra Sil G/UV254)]. Flash column chromatography was performed with silica gel from Merck (particle size 0.040-0.063 mm).

#### Nuclear Magnetic Resonance Spectroscopy (NMR)

$^1\text{H}$  NMR, proton decoupled  $^{13}\text{C}$  NMR, and proton coupled  $^{19}\text{F}$  NMR spectra were recorded on Bruker Avance 300 system ( $^1\text{H}$  NMR: 300 MHz and 500 MHz,  $^{13}\text{C}$  NMR: 75 MHz and 125 MHz,  $^{19}\text{F}$  NMR: 282 MHz) spectrometers at ambient temperature. Chemical shifts are given in ppm on the  $\delta$  scale, and were determined after calibration to the residual signals of the solvents, which were used as an internal standard. NMR standards were used are as follows:  $^1\text{H}$  NMR spectroscopy:  $\delta = 7.26$  ppm ( $\text{CDCl}_3$ ),  $\delta = 5.32$  ppm ( $\text{CD}_2\text{Cl}_2$ ),  $\delta = 2.50$  ppm ( $\text{DMSO-}d_6$ ),  $\delta = 3.31$  ppm ( $\text{CD}_3\text{OD}$ );  $^{13}\text{C}$ -NMR spectroscopy:  $\delta = 77.0$  ppm ( $\text{CDCl}_3$ ),  $\delta = 53.8$  ppm ( $\text{CD}_2\text{Cl}_2$ ),  $\delta = 118.26$ ,  $1.32$  ppm ( $\text{CD}_3\text{CN}$ ),  $\delta = 206.26$ ,  $\delta = 39.52$  ppm ( $\text{DMSO-}d_6$ ),  $\delta = 49.0$  ppm ( $\text{CD}_3\text{OD}$ ).  $^{19}\text{F}$  NMR spectroscopy:  $\delta = 0$  ppm ( $\text{CFCl}_3$ ). The characteristic signals were specified from the low field to high field with the chemical shifts ( $\delta$  in ppm).  $^1\text{H}$  NMR spectra peak multiplicities indicated as singlet (s), doublet (d), doublet of doublet (dd), doublet of doublet of doublet (ddd), triplet (t), doublet of triplet (dt), quartet (q), multiplet (m). The

coupling constant  $J$  indicated in hertz (Hz).

### High-Performance Liquid Chromatography (HPLC)

Chiral HPLC was performed with an Agilent 1200 Series, Agilent 1260 Series HPLC System or Shimadzu Lc-2030c. All the HPLC conditions were detailed in the individual procedures. The type of the columns, mobile phase and the flow rate were specified in the individual procedures.

### Infrared Spectroscopy (IR)

IR measurements were recorded on a Bruker Alpha-P FT-IR spectrometer. The absorption bands were indicated a wave numbers  $\nu$  ( $\text{cm}^{-1}$ ). All substances were measured as films or solids.

### Mass Spectrometry (MS)

High-resolution mass spectra were recorded on a Bruker En Apex Ultra 7.0 TFT-MS instrument using ESI or APCI or FD technique. Ionic masses are given in units of  $m/z$  for the isotopes with the highest natural abundance.

### Circular Dichroism Spectroscopy (CD)

CD spectra were recorded on a JASCO J-810 CD spectropolarimeter. The parameters we used as follows: from 600 nm to 200 nm; data pitch (0.5 nm); band with (1 nm); response (1 second); sensitivity (standard); scanning speed (50 nm/min); accumulation (5 times). The concentration of the compounds for the measurements was 0.2 mM. The formula for converting  $\theta$  to  $\epsilon$  is shown as below.

$$\Delta\epsilon = \frac{\theta[m\text{ deg}]}{32980 \times c(\text{mol}/L) \times L(\text{cm})}$$

C = concentration of the sample; L = thickness of the measurement vessel

### Crystal Structure Analysis

Crystal X-ray measurements and the crystal structure analysis were carried out by Dr. Klaus Harms (Chemistry Department, Philipps University of Marburg) and Sergei Ivlev (Chemistry Department, Philipps University of Marburg). X-ray data were collected with a Bruker 3 circuit D8 Quest diffractometer with MoK $\alpha$  radiation (microfocus tube with multilayer optics) and Photon 100 CMOS

detector. Scaling and absorption correction was performed by using the SADABS software package of Bruker. Structures were solved using direct methods in SHELXS and refined using the full matrix least squares procedure in SHELXL-2013 or SHELXL-2014. The Flack parameter is a factor used to estimate the absolute configuration of the compounds. Disorder of PF<sub>6</sub> ions, solvent molecules or methylene groups was refined using restraints for both the geometry and the anisotropic displacement factors.

### **Optical Rotation Polarimeter**

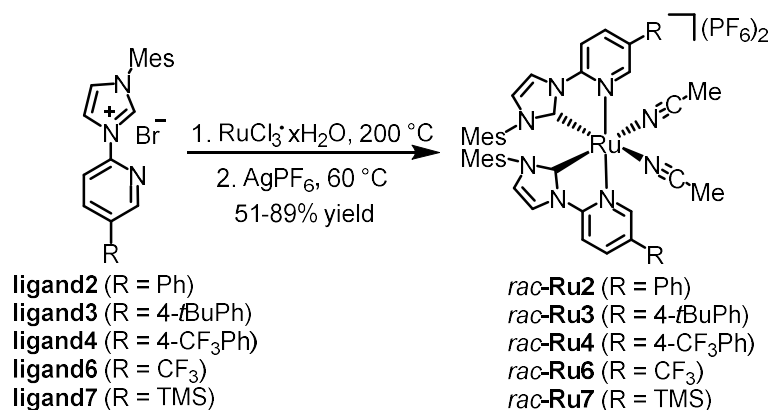
Optical rotations were measured on a Krüss P8000-T or Perkin-Elmer 241 polarimeter with  $[\alpha]_D^{20}$  or  $[\alpha]_D^{25}$  values reported in degrees with concentrations reported in g/100 mL.



## 4.2 Catalytic Enantioselective Intramolecular C–H Amination of 2-Azidoacetamides

## 4.2.1 Synthetic of the Ruthenium Catalysts

## 1) Synthesis of Racemic Ruthenium Catalysts:



**General procedure of racemic ruthenium catalysts synthesis:** A solution of RuCl<sub>3</sub>·xH<sub>2</sub>O (1 equiv, 0.24 mmol) and ligand (2 equiv, 0.48 mmol) in ethylene glycol (2.4 mL) was heated at 200 °C for 6 h. The reaction mixture was treated with saturated aqueous NH<sub>4</sub>PF<sub>6</sub> after cooling down to room temperature. A yellow precipitate was formed, which was dissolved and extracted with CH<sub>2</sub>Cl<sub>2</sub> for three times. The combined organic layers were washed with water and concentrated under reduced pressure to obtain an orange solid, which was dissolved in CH<sub>3</sub>CN (3 mL) followed by adding AgPF<sub>6</sub> (76 mg, 0.3 mmol). The mixture was stirred at 60 °C overnight. After cooling to room temperature, the mixture was filtered, and the filtrate was collected, evaporated to dryness and purified by column chromatography on silica gel (CH<sub>2</sub>Cl<sub>2</sub>:CH<sub>3</sub>CN = 200:1 to 20:1) to give pure racemic ruthenium catalyst.

*rac-Ru2*: pale yellow solid (204 mg, 74% yield) was obtained. <sup>1</sup>H NMR (300 MHz, CD<sub>2</sub>Cl<sub>2</sub>) δ 8.53 (d, *J* = 2.0 Hz, 2H), 8.08 (dd, *J* = 8.6, 2.1 Hz, 2H), 8.02 (d, *J* = 2.3 Hz, 2H), 7.65-7.52 (m, 12H), 6.93 (d, *J* = 2.3 Hz, 2H), 6.60 (d, *J* = 6.3 Hz, 4H), 2.31 (s, 6H), 2.01 (s, 6H), 1.97 (s, 6H), 1.52 (s, 6H). <sup>13</sup>C NMR (75 MHz, CD<sub>2</sub>Cl<sub>2</sub>) δ 189.6, 152.4, 149.2, 140.6, 137.1, 135.6, 135.3, 135.1, 134.3, 134.2, 130.2, 130.2, 129.8, 129.6, 127.0, 126.0, 125.0, 118.0, 111.8, 21.1, 17.7, 17.5, 4.0. <sup>19</sup>F NMR (282 MHz, CD<sub>2</sub>Cl<sub>2</sub>) δ -71.32, -73.84. IR (film): ν (cm<sup>-1</sup>) 2922, 2852, 1511, 1483, 1453, 1422, 1290, 1247, 1142, 1081, 1036, 952, 930, 835, 764, 745, 696, 678, 620, 591, 556, 542, 488, 457, 434, 388.

*rac-Ru3*: pale yellow solid (212 mg, 0.17 mmol, 56% yield) was obtained from **ligand 3** (0.6 mmol). <sup>1</sup>H NMR (300 MHz, CD<sub>2</sub>Cl<sub>2</sub>) δ 8.51 (d, *J* = 1.9 Hz, 2H), 8.07 (dd, *J* = 8.6, 2.1 Hz, 2H), 8.02 (d, *J* =

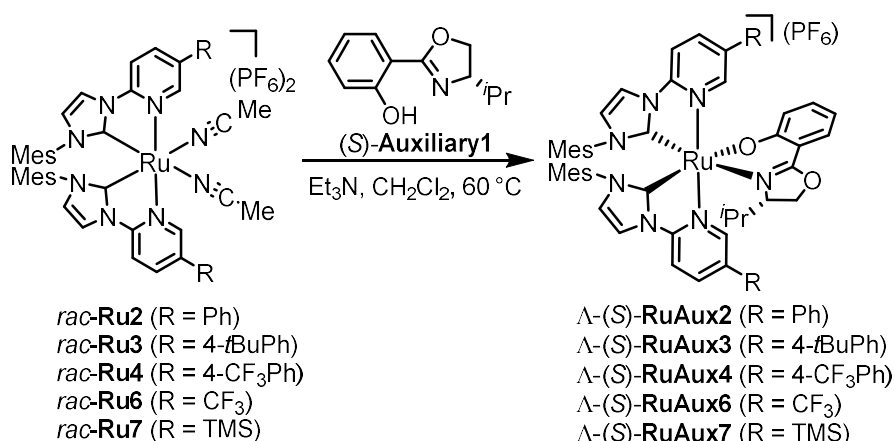
2.3 Hz, 2H), 7.68-7.52 (m, 10H), 6.93 (d,  $J = 2.3$  Hz, 2H), 6.60 (s, 4H), 2.31 (s, 6H), 2.03 (s, 6H), 1.95 (s, 6H), 1.51 (s, 6H), 1.41 (s, 18H).  $^{13}\text{C}$  NMR (75 MHz,  $\text{CD}_2\text{Cl}_2$ )  $\delta$  189.3, 153.0, 151.9, 148.7, 140.3, 136.5, 135.2, 135.0, 134.0, 134.0, 131.9, 130.0, 129.4, 127.0, 126.4, 125.6, 124.7, 117.8, 111.7, 35.1, 31.4, 20.8, 17.5, 17.2, 3.7.  $^{19}\text{F}$  NMR (282 MHz,  $\text{CD}_2\text{Cl}_2$ )  $\delta$  -72.21, -74.73. IR (film):  $\nu$  ( $\text{cm}^{-1}$ ) 3138, 2959, 1611, 1490, 1425, 1373, 1309, 1258, 1103, 1033, 932, 834, 738, 629, 588, 554, 434.

*rac*-Ru4: pale yellow solid (348 mg, 89% yield) was obtained from **ligand 4** (0.6 mmol).  $^1\text{H}$  NMR (300 MHz,  $\text{CD}_2\text{Cl}_2$ )  $\delta$  8.57 (d,  $J = 1.9$  Hz, 2H), 8.10 (dd,  $J = 8.7, 2.1$  Hz, 2H), 8.03 (d,  $J = 2.3$  Hz, 2H), 7.89 (d,  $J = 8.3$  Hz, 4H), 7.78 (d,  $J = 8.2$  Hz, 4H), 7.67 (d,  $J = 8.6$  Hz, 2H), 6.93 (d,  $J = 2.3$  Hz, 2H), 6.64 (s, 2H), 6.57 (s, 2H), 2.31 (s, 6H), 2.00 (s, 12H), 1.52 (s, 6H).  $^{13}\text{C}$  NMR (75 MHz,  $\text{CD}_2\text{Cl}_2$ )  $\delta$  189.7, 152.9, 149.4, 140.4, 138.6, 137.3, 135.2, 134.2, 134.1, 134.0, 131.6, 131.1, 130.2, 129.3, 127.5, 127.1, 127.0, 127.0, 126.9, 126.3, 126.0, 125.2, 122.7, 117.9, 111.9, 21.0, 17.5, 17.3, 3.7.  $^{19}\text{F}$  NMR (282 MHz,  $\text{CD}_2\text{Cl}_2$ )  $\delta$  -62.90, -71.13, -73.65. IR (film):  $\nu$  ( $\text{cm}^{-1}$ ) 1612, 1492, 1426, 1322, 1255, 1166, 1117, 1069, 823, 689, 552.

*rac*-Ru6: pale yellow solid (246 mg, 72% yield) was obtained from **ligand 6** (0.6 mmol).  $^1\text{H}$  NMR (300 MHz,  $\text{CD}_2\text{Cl}_2$ )  $\delta$  8.55 (s, 2H), 8.21-7.93 (m, 4H), 7.79 (d,  $J = 8.7$  Hz, 2H), 6.94 (d,  $J = 2.2$  Hz, 2H), 6.76 (s, 2H), 6.64 (s, 2H), 2.32 (s, 6H), 2.19 (s, 6H), 2.00 (s, 6H), 1.47 (s, 6H).  $^{13}\text{C}$  NMR (75 MHz,  $\text{CD}_2\text{Cl}_2$ )  $\delta$  189.9, 155.8, 148.6, 141.0, 136.6, 135.1, 134.0, 133.6, 130.2, 126.5, 125.8, 118.6, 112.5, 20.8, 17.3, 17.3, 3.9.  $^{19}\text{F}$  NMR (235 MHz,  $\text{CD}_2\text{Cl}_2$ )  $\delta$  -62.73, -71.10, -74.12. IR (film):  $\nu$  ( $\text{cm}^{-1}$ ) 3144, 2926, 2174, 1620, 1505, 1427, 1382, 1325, 1256, 1174, 1139, 1073, 1039, 929, 830, 736, 708, 626, 583, 554, 506, 463, 435.

*rac*-Ru7: pale yellow solid (175 mg, 51% yield) was obtained from **ligand 7** (0.6 mmol).  $^1\text{H}$  NMR (300 MHz,  $\text{CD}_2\text{Cl}_2$ )  $\delta$  8.43 (s, 2H), 7.97 (s, 2H), 7.88 (d,  $J = 8.1$  Hz, 2H), 7.48 (d,  $J = 8.1$  Hz, 2H), 6.86 (d,  $J = 1.8$  Hz, 2H), 6.63 (d,  $J = 6.5$  Hz, 4H), 2.31 (s, 6H), 2.17 (s, 6H), 1.98 (s, 6H), 1.49 (s, 6H), 0.40 (s, 18H).  $^{13}\text{C}$  NMR (75 MHz,  $\text{CD}_2\text{Cl}_2$ )  $\delta$  190.0, 154.7, 153.6, 143.8, 140.1, 135.0, 134.2, 134.0, 129.9, 129.7, 125.8, 124.6, 117.7, 111.0, 21.3, 17.6, 17.5, 3.6, -1.4.  $^{19}\text{F}$  NMR (235 MHz,  $\text{CD}_2\text{Cl}_2$ )  $\delta$  -71.14, -74.16. IR (film):  $\nu$  ( $\text{cm}^{-1}$ ) 2955, 2156, 2090, 2054, 2010, 1982, 1948, 1685, 1634, 1595, 1491, 1421, 1327, 1304, 1252, 1194, 1143, 1089, 1035, 931, 833, 760, 694, 627, 590, 553, 429.

## 2) Intermediate Ruthenium Auxiliary Complexes:



**General procedure of chiral ruthenium catalysts synthesis:** A mixture of racemic ruthenium catalyst (1 equiv, 0.11 mmol), chiral auxiliary (*S*)-Auxiliary1 (2 equiv, 62.2 mg, 0.22 mmol) and triethylamine (3 equiv, 50  $\mu$ L, 0.33 mmol) in CH<sub>2</sub>Cl<sub>2</sub> (3.6 mL) was heated at 60 °C for 18 h. The reaction mixture was cooled to room temperature and concentrated to dryness. The residue was subjected to flash silica gel chromatography (CH<sub>3</sub>CN:CH<sub>2</sub>Cl<sub>2</sub>= 1:600 to 1:50) to isolate the first diastereomer which was assigned as  $\Lambda\text{-(S)-RuAux2-4,6-7}$ . The absolute configuration of ruthenium auxiliary complexes were assigned as  $\Lambda\text{-(S)}$ -configuration, due to the auxiliary complexes after removal of auxiliary and got the final ruthenium catalyst's absolute configuration was  $\Lambda$ -configuration (see assignment of catalyst's absolute configuration as  $\Lambda$ -configuration on chapter 2.1.2, the catalyst's configuration was assigned by comparing the CD spectra with previous reported one), thus we assigned here the ruthenium auxiliary complexes as  $\Lambda\text{-(S)}$ -configuration.

$\Lambda\text{-(S)-RuAux2}$ : orange solid (33.8 mg, 28% yield). <sup>1</sup>H NMR (500 MHz, CD<sub>2</sub>Cl<sub>2</sub>)  $\delta$  8.74 (d, *J* = 2.0 Hz, 1H), 8.19 (d, *J* = 2.0 Hz, 1H), 7.95 (d, *J* = 2.3 Hz, 1H), 7.92 (dd, *J* = 8.6, 2.2 Hz, 1H), 7.87 (d, *J* = 2.3 Hz, 1H), 7.74 (dd, *J* = 8.6, 2.2 Hz, 1H), 7.54-7.43 (m, 7H), 7.42-7.38 (m, 3H), 7.37-7.31 (m, 3H), 7.00 (ddd, *J* = 8.7, 6.9, 1.9 Hz, 1H), 6.89 (d, *J* = 2.3 Hz, 1H), 6.84 (d, *J* = 2.2 Hz, 1H), 6.56 (s, 1H), 6.51 (s, 1H), 6.50-6.45 (m, 3H), 6.24-6.18 (m, 1H), 4.29 (dd, *J* = 9.3, 3.2 Hz, 1H), 4.12 (t, *J* = 9.1 Hz, 1H), 3.91 (dt, *J* = 8.9, 3.1 Hz, 1H), 2.28 (s, 3H), 2.05 (s, 3H), 2.00 (s, 3H), 1.95 (s, 3H), 1.61 (s, 3H), 1.42 (s, 3H), 0.55 (d, *J* = 7.0 Hz, 3H), 0.30-0.19 (m, 1H), -0.03 (d, *J* = 6.8 Hz, 3H). <sup>13</sup>C NMR (126 MHz, CD<sub>2</sub>Cl<sub>2</sub>)  $\delta$  197.5, 196.2, 172.0, 165.2, 153.0, 152.9, 148.5, 148.0, 139.5, 137.3, 135.8, 135.4, 135.1, 135.0, 134.7, 134.4, 134.2, 133.9, 133.9, 133.6, 133.4, 130.2, 129.8, 129.6, 129.4, 129.4, 129.1, 129.0, 126.4, 125.6, 125.1, 123.8, 116.6, 115.9, 112.7, 110.8, 110.5, 110.0, 74.9, 66.6, 30.1, 30.0, 20.9,

20.9, 18.8, 18.5, 17.9, 17.9, 17.4, 13.5.  $^{19}\text{F}$  NMR (282 MHz,  $\text{CD}_2\text{Cl}_2$ )  $\delta$  -71.73, -74.25. HRMS (ESI,  $m/z$ ) calcd. for  $\text{C}_{58}\text{H}_{56}\text{RuN}_7\text{O}_2$   $[\text{M-PF}_6]^+$ : 984.3533, found: 984.3565. IR (film):  $\nu$  ( $\text{cm}^{-1}$ ) 1605, 1537, 1507, 1471, 1413, 1355, 1322, 1250, 1222, 1067, 969, 921, 836, 756, 685, 580, 553.

$\Lambda$ -(*S*)-RuAux3: orange solid (45.9 mg, yield: 34%).  $^1\text{H}$  NMR (300 MHz,  $\text{CD}_2\text{Cl}_2$ )  $\delta$  8.73 (d,  $J = 2.0$  Hz, 1H), 8.20 (d,  $J = 1.9$  Hz, 1H), 7.95-7.82 (m, 3H), 7.75 (dd,  $J = 8.6, 2.1$  Hz, 1H), 7.49 (dt,  $J = 20.9, 9.3$  Hz, 6H), 7.40-7.22 (m, 5H), 6.99 (ddd,  $J = 8.7, 6.9, 1.9$  Hz, 1H), 6.87 (dd,  $J = 13.1, 2.3$  Hz, 2H), 6.61-6.37 (m, 5H), 6.22 (t,  $J = 7.1$  Hz, 1H), 4.29 (dd,  $J = 9.2, 3.2$  Hz, 1H), 4.15 (t,  $J = 9.0$  Hz, 1H), 3.96-3.87 (m, 1H), 2.28 (s, 3H), 2.06 (s, 3H), 1.99 (s, 3H), 1.93 (s, 3H), 1.60 (s, 3H), 1.42 (s, 3H), 1.39 (s, 9H), 1.35 (s, 9H), 0.55 (d,  $J = 6.9$  Hz, 3H), 0.33-0.16 (m, 1H), -0.03 (d,  $J = 6.8$  Hz, 3H).  $^{13}\text{C}$  NMR (75 MHz,  $\text{CD}_2\text{Cl}_2$ )  $\delta$  197.1, 195.9, 171.7, 165.0, 152.7, 152.7, 152.4, 152.3, 148.1, 147.7, 139.5, 139.5, 137.2, 135.0, 134.9, 134.7, 134.3, 134.1, 133.9, 133.8, 133.4, 133.3, 132.6, 132.4, 130.1, 129.7, 129.4, 129.4, 129.0, 126.8, 126.5, 126.0, 126.0, 125.5, 125.0, 123.8, 116.6, 115.8, 112.6, 110.8, 110.5, 109.9, 74.9, 66.5, 35.0, 34.9, 31.4, 31.3, 30.0, 20.9, 20.8, 18.8, 18.5, 17.9, 17.9, 17.4, 13.5.  $^{19}\text{F}$  NMR (282 MHz,  $\text{CD}_2\text{Cl}_2$ )  $\delta$  -71.68, -74.19. IR (film):  $\nu$  ( $\text{cm}^{-1}$ ) 2958, 1607, 1486, 1420, 1372, 1320, 1251, 1151, 1068, 1032, 926, 836, 747, 688, 553. HRMS (ESI,  $m/z$ ) calcd. for  $\text{C}_{66}\text{H}_{72}\text{RuN}_7\text{O}_2$   $[\text{M-PF}_6]^+$ : 1096.4786, found: 1096.4824.

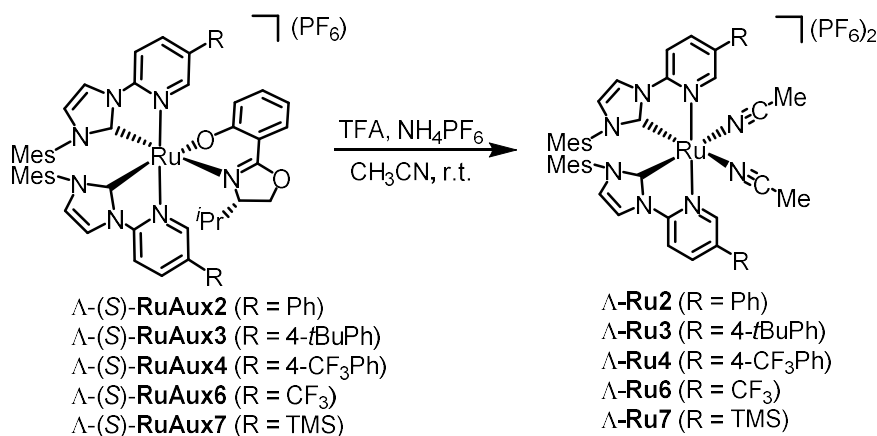
$\Lambda$ -(*S*)-RuAux4: orange solid (56.7 mg, yield: 41%).  $^1\text{H}$  NMR (300 MHz,  $\text{CD}_2\text{Cl}_2$ )  $\delta$  8.78 (d,  $J = 2.2$  Hz, 1H), 8.22-8.17 (m, 1H), 8.02-7.99 (m, 1H), 7.97 (dd,  $J = 8.6, 1.9$  Hz, 1H), 7.93-7.89 (m, 1H), 7.82-7.76 (m, 3H), 7.73 (s, 1H), 7.71 (s, 1H), 7.58 (d,  $J = 8.7$  Hz, 1H), 7.53-7.41 (m, 6H), 7.05-6.97 (m, 1H), 6.91 (d,  $J = 2.3$  Hz, 1H), 6.86 (d,  $J = 2.3$  Hz, 1H), 6.58 (s, 1H), 6.54 (s, 1H), 6.51-6.44 (m, 3H), 6.28-6.22 (m, 1H), 4.33-4.27 (m, 1H), 4.10 (t,  $J = 9.1$  Hz, 1H), 3.92-3.85 (m, 1H), 2.27 (s, 3H), 2.04 (s, 3H), 2.02 (s, 3H), 1.96 (s, 3H), 1.61 (s, 3H), 1.43 (s, 3H), 0.55 (d,  $J = 7.0$  Hz, 3H), 0.27-0.15 (m, 1H), -0.04 (d,  $J = 6.9$  Hz, 3H).  $^{13}\text{C}$  NMR (75 MHz,  $\text{CD}_2\text{Cl}_2$ )  $\delta$  197.5, 196.12 172.0, 165.3, 153.8, 153.6, 148.7, 148.2, 139.6, 139.5, 139.0, 137.2, 135.2, 134.9, 134.7, 134.7, 134.5, 134.4, 134.1, 134.0, 132.1, 131.8, 130.9, 130.8, 130.7, 130.5, 130.1, 129.9, 129.6, 129.2, 128.8, 126.9, 126.8, 126.8, 126.6, 126.6, 126.6, 126.5, 125.75, 125.56, 125.54, 125.34, 123.79, 123.40, 123.38, 116.84, 116.13, 112.87, 110.82, 110.32, 74.8, 66.6, 30.1, 20.9, 20.9, 18.8, 18.5, 17.9, 17.8, 17.4, 13.5.  $^{19}\text{F}$  NMR (282 MHz,  $\text{CD}_2\text{Cl}_2$ )  $\delta$  -63.02, -63.04, -71.64, -74.16. IR (film):  $\nu$  ( $\text{cm}^{-1}$ ) 2925, 1608, 1531, 1489, 1422, 1379, 1322, 1285, 1251, 1166, 1117, 1068, 1018, 925, 836, 757, 686, 596, 553, 507, 458, 429. HRMS (ESI,

$m/z$ ) calcd. for  $C_{60}H_{54}RuF_6N_7O_2 [M-PF_6]^+$ : 1120.3281, found: 1120.3317.

$\Lambda$ -(*S*)-**RuAux6**: orange solid (39.2 mg, yield: 32%).  $^1H$  NMR (300 MHz,  $CD_2Cl_2$ )  $\delta$  8.93 (s, 1H), 8.15 (s, 1H), 8.06 (d,  $J = 2.4$  Hz, 1H), 7.91 (dt,  $J = 5.3, 2.4$  Hz, 2H), 7.73 (dd,  $J = 8.6, 1.7$  Hz, 1H), 7.66 (d,  $J = 8.7$  Hz, 1H), 7.45 (d,  $J = 8.7$  Hz, 1H), 7.38 (dd,  $J = 8.1, 1.8$  Hz, 1H), 6.93 (ddd,  $J = 8.7, 6.3, 2.6$  Hz, 2H), 6.86 (d,  $J = 2.3$  Hz, 1H), 6.73 (d,  $J = 5.3$  Hz, 2H), 6.62 (s, 1H), 6.50 (s, 1H), 6.33 (dd,  $J = 8.6, 0.9$  Hz, 1H), 6.23 (ddd,  $J = 8.0, 6.9, 1.1$  Hz, 1H), 4.29 (dd,  $J = 9.4, 3.3$  Hz, 1H), 4.14 (t,  $J = 9.1$  Hz, 1H), 3.67 (dt,  $J = 8.7, 3.1$  Hz, 1H), 2.25 (s, 3H), 2.19 (s, 3H), 2.12 (s, 3H), 2.09 (s, 3H), 1.57 (s, 3H), 1.36 (s, 3H), 0.50 (d,  $J = 7.0$  Hz, 3H), 0.06 (d,  $J = 6.8$  Hz, 3H), -0.11-0.31 (m, 1H).  $^{13}C$  NMR (75 MHz,  $CD_2Cl_2$ )  $\delta$  172.2, 171.9, 165.6, 156.2, 155.7, 147.8, 147.4, 139.8, 137.0, 136.8, 134.5, 134.2, 134.1, 133.9, 133.9, 133.6, 133.5, 133.4, 130.0, 129.7, 129.4, 129.2, 125.9, 125.6, 122.9, 116.6, 116.2, 114.6, 113.0, 110.5, 110.3, 110.0, 74.1, 66.4, 30.0, 20.4, 20.3, 18.4, 17.8, 17.4, 17.2, 17.0, 16.9, 13.1.  $^{19}F$  NMR (235 MHz,  $CD_2Cl_2$ )  $\delta$  -62.73, -71.10, -74.12. IR (film):  $\nu$  ( $cm^{-1}$ ) 3141, 2965, 2924, 2868, 2120, 2083, 2050, 1976, 1928, 1608, 1536, 1500, 1472, 1421, 1381, 1321, 1253, 1225, 1170, 1134, 1066, 1035, 925, 834, 757, 706, 688, 627, 582, 555, 531, 504, 463, 435, 391. HRMS (ESI,  $m/z$ ) calcd. for  $C_{48}H_{46}F_6RuN_7O_2 [M-PF_6]^+$ : 968.2655, found: 968.2665.

$\Lambda$ -(*S*)-**RuAux7**: orange solid (44.4 mg, yield: 36%).  $^1H$  NMR (300 MHz,  $CD_2Cl_2$ )  $\delta$  8.53 (s, 1H), 8.05 (s, 1H), 7.90 (d,  $J = 2.3$  Hz, 1H), 7.82 (d,  $J = 2.2$  Hz, 1H), 7.70 (dd,  $J = 8.1, 1.3$  Hz, 1H), 7.60 (dd,  $J = 8.1, 1.3$  Hz, 1H), 7.45 (dd,  $J = 8.0, 1.6$  Hz, 1H), 7.35 (d,  $J = 8.1$  Hz, 1H), 7.26 (d,  $J = 8.1$  Hz, 1H), 7.02-6.91 (m, 1H), 6.85 (d,  $J = 2.3$  Hz, 1H), 6.78 (d,  $J = 2.2$  Hz, 1H), 6.57 (t,  $J = 9.2$  Hz, 4H), 6.36 (d,  $J = 8.4$  Hz, 1H), 6.17 (d,  $J = 6.8$  Hz, 1H), 4.26 (dd,  $J = 9.2, 3.2$  Hz, 1H), 4.11 (dd,  $J = 11.3, 6.8$  Hz, 1H), 3.88 (d,  $J = 8.5$  Hz, 1H), 2.24 (s, 3H), 1.60 (s, 3H), 1.41 (s, 3H), 0.50 (d,  $J = 6.8$  Hz, 3H), 0.22 (s, 9H), 0.17 (s, 9H), 0.02 (dd,  $J = 14.3, 7.9$  Hz, 1H), -0.09 (d,  $J = 6.6$  Hz, 3H).  $^{13}C$  NMR (75 MHz,  $CD_2Cl_2$ )  $\delta$  154.5, 154.5, 154.4, 154.3, 141.3, 141.1, 139.3, 139.2, 137.4, 135.2, 135.0, 134.9, 134.4, 134.0, 133.7, 132.5, 131.9, 130.1, 129.9, 129.6, 129.4, 129.2, 125.4, 125.0, 123.8, 116.6, 115.8, 110.0, 109.4, 74.9, 66.4, 30.0, 21.2, 21.1, 18.9, 18.7, 18.2, 17.9, 17.6, 13.7, -1.3, -1.4. HRMS (ESI,  $m/z$ ) calcd. for  $C_{52}H_{64}RuN_7O_2Si_2 [M-PF_6]^+$ : 976.3698, found: 978.3719. IR (film):  $\nu$  ( $cm^{-1}$ ) 2953, 2158, 2117, 2024, 1605, 1537, 1487, 1415, 1379, 1353, 1321, 1249, 1142, 1064, 1035, 960, 924, 836, 754, 687, 622, 584, 554, 505, 413.

## 3) Enantiopure Ruthenium Catalysts:



**General Procedure:** To a mixture of single ruthenium auxiliary complex (0.044 mmol) in CH<sub>3</sub>CN (4.4 mL) was added CF<sub>3</sub>COOH (0.44 mmol). The reaction mixture was stirred at room temperature for 5 min, then concentrated under reduced pressure. The residue was subjected to flash silica gel chromatography (CH<sub>3</sub>CN:CH<sub>2</sub>Cl<sub>2</sub> = 1:100 to 1:10) and added 2 g NH<sub>4</sub>PF<sub>6</sub> above the seasand band (to change the counter anion on the column) to afford chiral ruthenium catalyst as pale yellow solid. The counter anion exchange will lead to two yellow bands on the column but they are the same compound. It should be purified within 30 min (It should be eluted fast!).

**$\Lambda$ -Ru2:** pale yellow solid (44.8 mg, 88% yield) All other spectroscopic data of enantiopure ruthenium catalyst  $\Lambda$ -Ru2 were in agreement with the racemic catalyst *rac*-Ru2.

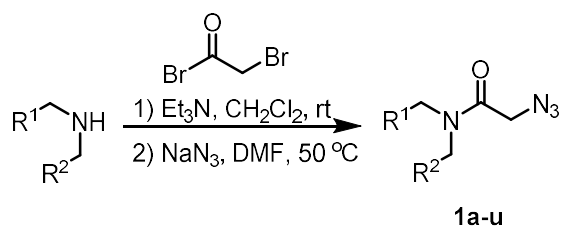
**$\Lambda$ -Ru3:** pale yellow solid (46 mg, yield: 82%). All other spectroscopic data of enantiopure ruthenium catalyst  $\Lambda$ -Ru3 were in agreement with the racemic catalyst *rac*-Ru3.

**$\Lambda$ -Ru4:** pale yellow solid (54 mg, yield: 95%). All other spectroscopic data of enantiopure ruthenium catalyst  $\Lambda$ -Ru4 were in agreement with the one of racemic catalyst *rac*-Ru4.

**$\Lambda$ -Ru6:** pale yellow solid (43.8 mg, 87% yield). All other spectroscopic data of enantiopure ruthenium catalyst  $\Lambda$ -Ru6 were in agreement with the racemic catalyst *rac*-Ru6.

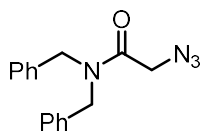
**$\Lambda$ -Ru7:** pale yellow solid (41.6 mg, 82% yield). All other spectroscopic data of enantiopure ruthenium catalyst  $\Lambda$ -Ru7 were in agreement with the racemic catalyst *rac*-Ru7.

## 4.2.2 Synthesis of Substrates



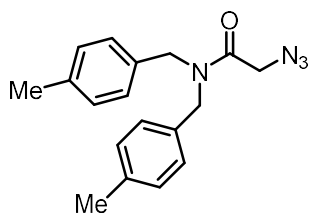
**General procedure for the preparation 2-azidoacetamides.** To a solution of amines (1.0 equiv, 5 mmol) and Et<sub>3</sub>N (1.0 equiv, 5 mmol) in fresh distilled CH<sub>2</sub>Cl<sub>2</sub> (10 mL) was added bromoacetyl bromide (1.05 equiv, 5.25 mmol) in CH<sub>2</sub>Cl<sub>2</sub> (2 mL) dropwise at 0 °C. The resulting mixture was then reacted at room temperature for 4 h. After that, the reaction was quenched by saturated aqueous NaHCO<sub>3</sub> (10 mL) at 0 °C. The aqueous phase was extracted three times with diethyl ether. The combined organic phases were washed with brine, dried over Na<sub>2</sub>SO<sub>4</sub>. After removal of the solvent under reduced pressure, the crude mixture was used without any further purification.

To a solution of the above 2-bromoacetamide in DMF (10 mL, 0.5 M) was added sodium azide (650.1 mg, 2.0 equiv). The resulting solution was stirred at 50 °C overnight (14 h to 16 h, monitored by TLC). After that, a 1:1 mixture of H<sub>2</sub>O with diethyl ether were added to the reaction mixture, and the aqueous phase was extracted three times with 10 mL diethyl ether. The combined organic phases were washed several times (5-8 times) with 10 mL H<sub>2</sub>O (deionized) to remove DMF. Then it was washed with brine, and dried over anhydrous Na<sub>2</sub>SO<sub>4</sub>. After removal of the solvent under reduced pressure, the crude mixture was purified by flash column chromatography on a silica gel column (*n*-hexane:EtOAc = 1:5 to 1:3, R<sub>f</sub> value = 0.4 to 0.6) which resulted in the analytical pure azides.

**Compound 1a**

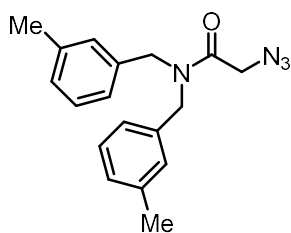
**1a:** white solid. Yield: 95%. <sup>1</sup>H NMR (300 MHz, CDCl<sub>3</sub>) δ 7.34 (m, 8H), 7.17 (m, 2H), 4.68 (s, 2H), 4.41 (s, 2H), 4.01 (s, 2H). <sup>13</sup>C NMR (75 MHz, CDCl<sub>3</sub>) δ 168.1, 136.6, 135.6, 129.3, 128.9, 128.6, 128.1, 127.9, 126.4, 50.8, 49.6, 49.1. **IR (film):** ν (cm<sup>-1</sup>) 3028, 2907, 2229, 2169, 2110, 1649, 1492, 1423, 1359, 1290, 1271, 1208, 1168, 1077, 1026, 993, 949, 816, 746, 697, 622, 570, 509, 456.

## Compound 1b



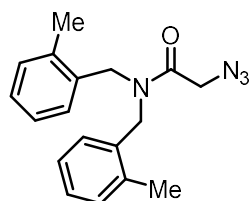
**1b:** white solid. Yield: 88%.  $^1\text{H NMR}$  (300 MHz,  $\text{CDCl}_3$ )  $\delta$  7.31-7.17 (m, 2H), 7.07 (dd,  $J = 17.3$ , 11.3 Hz, 4H), 6.93 (d,  $J = 6.6$  Hz, 2H), 4.62 (s, 2H), 4.34 (s, 2H), 3.97 (s, 2H), 2.35 (s, 6H).  $^{13}\text{C NMR}$  (75 MHz,  $\text{CDCl}_3$ )  $\delta$  168.1, 139.2, 138.7, 136.6, 135.7, 129.4, 129.2, 128.9, 128.7, 127.0, 125.7, 123.5, 50.9, 49.6, 49.2, 21.5. **IR (film):**  $\nu$  ( $\text{cm}^{-1}$ ) 3308, 2944, 2099, 1923, 1654, 1619, 1545, 1510, 1474, 1416, 1364, 1321, 1221, 1162, 1115, 1060, 1014, 974, 937, 816, 755, 711, 662, 632, 586, 549, 525, 490, 432, 392.

## Compound 1c



**1c:** white solid. Yield: 79%.  $^1\text{H NMR}$  (300 MHz,  $\text{CDCl}_3$ )  $\delta$  7.23-7.09 (m, 6H), 7.01 (d,  $J = 7.7$  Hz, 2H), 4.59 (s, 2H), 4.31 (s, 2H), 3.96 (s, 2H), 2.35 (s, 6H).  $^{13}\text{C NMR}$  (75 MHz,  $\text{CDCl}_3$ )  $\delta$  170.0, 137.0, 137.7, 133.7, 132.6, 130.0, 129.6, 128.7, 126.4, 50.1, 49.2, 48.7, 21.2. **IR (film):**  $\nu$  ( $\text{cm}^{-1}$ ) 2926, 2201, 2098, 1889, 1659, 1485, 1446, 1404, 1343, 1282, 1211, 1163, 1085, 1012, 981, 930, 833, 800, 717, 662, 613, 569, 547, 477, 445, 409.

## Compound 1d

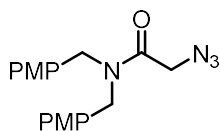


**1d:** white solid. Yield: 93%.  $^1\text{H NMR}$  (300 MHz,  $\text{CDCl}_3$ )  $\delta$  7.16 (t,  $J = 26.0$  Hz, 8H), 4.72 (s, 2H), 4.29 (s, 2H), 3.95 (s, 2H), 2.17 (d,  $J = 28.2$  Hz, 6H).  $^{13}\text{C NMR}$  (75 MHz,  $\text{CDCl}_3$ )  $\delta$  168.3, 136.9, 135.5, 134.0, 133.3, 130.8, 128.4, 127.9, 126.9, 126.4, 124.5, 50.8, 46.9, 19.0. **IR (film):**  $\nu$  ( $\text{cm}^{-1}$ )



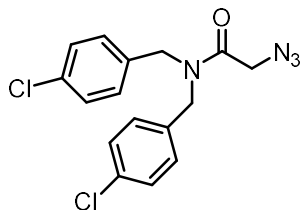
3024, 2919, 2100, 1656, 1608, 1420, 1349, 1277, 1210, 1175, 1093, 1038, 985, 949, 889, 822, 777, 741, 696, 644, 583, 550, 518, 476, 429.

### Compound 1e



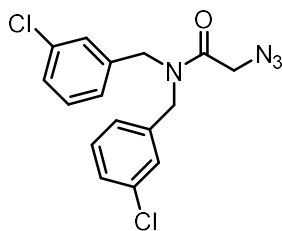
**1e:** white solid. Yield: 90%.  $^1\text{H NMR}$  (300 MHz,  $\text{CDCl}_3$ )  $\delta$  7.17 (d,  $J = 8.0$  Hz, 2H), 7.04 (d,  $J = 8.0$  Hz, 2H), 6.96-6.73 (m, 4H), 4.54 (s, 2H), 4.28 (s, 2H), 3.96 (s, 2H), 3.80 (s, 6H).  $^{13}\text{C NMR}$  (75 MHz,  $\text{CDCl}_3$ )  $\delta$  167.8, 159.4, 159.3, 130.0, 128.7, 127.7, 127.4, 114.6, 114.2, 55.4, 50.8, 48.8, 48.1. **IR (film):**  $\nu$  ( $\text{cm}^{-1}$ ) 2998, 2925, 2835, 2170, 2098, 1646, 1610, 1583, 1505, 1457, 1418, 1357, 1294, 1237, 1170, 1107, 1026, 926, 835, 808, 755, 709, 631, 598, 515, 474, 439, 395.

### Compound 1f



**1f:** white solid. Yield: 91%.  $^1\text{H NMR}$  (300 MHz,  $\text{CDCl}_3$ )  $\delta$  7.32 (dd,  $J = 15.9, 8.0$  Hz, 4H), 7.16 (d,  $J = 7.9$  Hz, 2H), 7.06 (d,  $J = 7.8$  Hz, 2H), 4.56 (s, 2H), 4.33 (s, 2H), 3.96 (s, 2H).  $^{13}\text{C NMR}$  (75 MHz,  $\text{CDCl}_3$ )  $\delta$  168.0, 134.9, 134.2, 133.9, 130.0, 129.6, 129.1, 127.9, 50.9, 49.2, 48.4. **IR (film):**  $\nu$  ( $\text{cm}^{-1}$ ) 3119, 2923, 2101, 1657, 1503, 1450, 1421, 1387, 1348, 1282, 1249, 1188, 1148, 1075, 1010, 940, 884, 813, 733, 636, 596, 552, 508, 416.

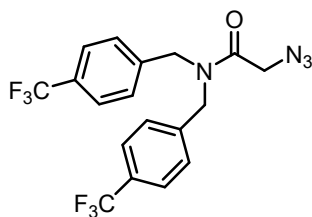
### Compound 1g



**1g:** white solid. Yield: 90%.  $^1\text{H NMR}$  (300 MHz,  $\text{CDCl}_3$ )  $\delta$  7.35-6.84 (m, 8H), 4.51 (s, 2H), 4.28 (s,

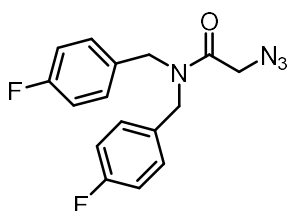
2H), 3.90 (s, 2H).  $^{13}\text{C}$  NMR (75 MHz,  $\text{CD}_2\text{Cl}_2$ )  $\delta$  168.4, 139.2, 138.2, 135.4, 134.9, 130.9, 130.5, 128.7, 128.6, 128.3, 127.0, 125.1, 51.0, 49.8, 49.2. IR (film):  $\nu$  ( $\text{cm}^{-1}$ ) 3066, 3042, 2923, 2217, 2098, 1647, 1603, 1505, 1460, 1417, 1353, 1279, 1210, 1154, 1097, 1022, 985, 928, 849, 816, 768, 709, 631, 583, 549, 519, 489, 423, 400.

### Compound 1h

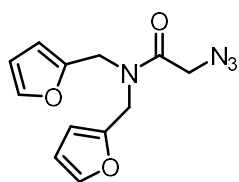


**1h**: white solid. Yield: 79%.  $^1\text{H}$  NMR (300 MHz,  $\text{CDCl}_3$ )  $\delta$  7.62 (dd,  $J$  = 17.3, 7.9 Hz, 4H), 7.34 (d,  $J$  = 7.7 Hz, 2H), 7.26 (d,  $J$  = 7.6 Hz, 2H), 4.68 (s, 2H), 4.46 (s, 2H), 4.00 (s, 2H).  $^{13}\text{C}$  NMR (75 MHz,  $\text{CDCl}_3$ )  $\delta$  168.2, 140.3, 139.4, 128.8, 126.8, 126.4, 125.9, 50.9, 49.8, 48.9.  $^{19}\text{F}$  NMR (235 MHz,  $\text{CD}_2\text{Cl}_2$ )  $\delta$  -62.90, -62.97. IR (film):  $\nu$  ( $\text{cm}^{-1}$ ) 3013, 2921, 2860, 2227, 2193, 2097, 1653, 1510, 1446, 1414, 1353, 1269, 1201, 1167, 1108, 1032, 983, 926, 798, 749, 697, 617, 591, 554, 527, 477, 417, 391.

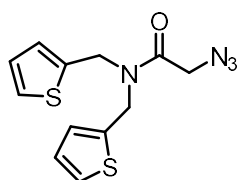
### Compound 1i



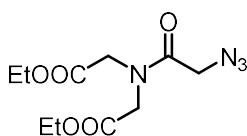
**1i**: white solid. Yield: 93%.  $^1\text{H}$  NMR (300 MHz,  $\text{CDCl}_3$ )  $\delta$  7.32-6.87 (m, 8H), 4.56 (s, 2H), 4.34 (s, 2H), 3.97 (s, 2H).  $^{13}\text{C}$  NMR (75 MHz,  $\text{CDCl}_3$ )  $\delta$  167.9, 164.1, 160.8, 132.3, 131.1, 130.4, 130.3, 128.2, 128.1, 116.4, 116.1, 115.9, 115.6, 50.8, 49.0, 48.2.  $^{19}\text{F}$  NMR (235 MHz,  $\text{CD}_2\text{Cl}_2$ )  $\delta$  -115.06, -115.44. IR (film):  $\nu$  ( $\text{cm}^{-1}$ ) 3023, 2944, 2912, 2183, 2099, 1649, 1606, 1450, 1352, 1284, 1215, 1105, 1049, 1024, 990, 948, 934, 875, 838, 811, 747, 713, 639, 583, 547, 512, 483, 435, 408.

**Compound 1j**

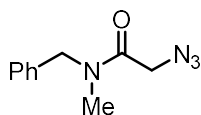
**1j**: colorless oil. Yield: 88%.  $^1\text{H NMR}$  (300 MHz,  $\text{CDCl}_3$ )  $\delta$  7.33 (d,  $J = 6.7$  Hz, 2H), 6.29 (s, 2H), 6.23 (d,  $J = 19.5$  Hz, 2H), 4.56 (s, 2H), 4.32 (s, 2H), 4.09 (s, 2H).  $^{13}\text{C NMR}$  (75 MHz,  $\text{CDCl}_3$ )  $\delta$  167.3, 150.0, 149.0, 143.0, 142.5, 110.5, 109.2, 108.8, 50.4, 43.0, 41.3. **IR (film)**:  $\nu$  ( $\text{cm}^{-1}$ ) 3103, 2921, 2100, 1653, 1536, 1446, 1421, 1367, 1331, 1280, 1239, 1203, 1152, 1077, 1041, 983, 934, 844, 825, 697, 586, 551, 514, 463, 408.

**Compound 1k**

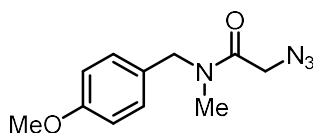
**1k**: colorless oil. Yield: 82%.  $^1\text{H NMR}$  (300 MHz,  $\text{CDCl}_3$ )  $\delta$  7.28-6.88 (m, 8H), 4.56 (s, 2H), 4.34 (s, 2H), 3.97 (s, 2H).  $^{13}\text{C NMR}$  (75 MHz,  $\text{CDCl}_3$ )  $\delta$  167.1, 138.6, 127.7, 127.3, 126.8, 126.3, 126.1, 125.9, 44.9, 43.3. **IR (film)**:  $\nu$  ( $\text{cm}^{-1}$ ) 2986, 2105, 1738, 1669, 1459, 1412, 1375, 1347, 1292, 1184, 1100, 1057, 1022, 966, 930, 867, 828, 736, 632, 556, 522, 436, 400.

**Compound 1l**

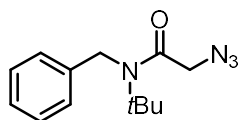
**1l**: colorless oil. Yield: 64%.  $^1\text{H NMR}$  (300 MHz,  $\text{CDCl}_3$ )  $\delta$  4.18 (m, 6H), 4.05 (s, 2H), 3.93 (s, 2H), 1.25 (q,  $J = 7.0$  Hz, 6H).  $^{13}\text{C NMR}$  (75 MHz,  $\text{CDCl}_3$ )  $\delta$  168.7, 168.4, 168.1, 62.1, 61.6, 50.5, 49.7, 48.4, 14.2. **IR (film)**:  $\nu$  ( $\text{cm}^{-1}$ ) 3061, 3027, 2923, 2853, 2196, 2150, 2098, 1951, 1700, 1644, 1485, 1449, 1419, 1369, 1263, 1223, 1180, 1150, 1080, 1030, 989, 920, 826, 792, 747, 699, 627, 598, 550, 496, 421.

**Compound 1m**

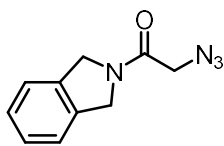
**1m**: colorless oil. Yield: 86%.  $^1\text{H NMR}$  (300 MHz,  $\text{CDCl}_3$ )  $\delta$  7.33 (m, 5H), 4.63 (s, 2H), 3.99 (s, 2H), 2.88 (s, 3H). with rotation ratio: 1.5:1.  $^{13}\text{C NMR}$  (75 MHz,  $\text{CDCl}_3$ )  $\delta$  167.8, 167.4, 136.6, 135.7, 129.3, 128.9, 128.4, 128.2, 127.9, 126.4, 53.0, 51.4, 50.8, 50.7, 34.5, 34.0. **IR (film)**:  $\nu$  ( $\text{cm}^{-1}$ ) 3047, 2956, 2919, 2860, 2283, 2196, 2152, 2099, 1727, 1648, 1418, 1353, 1320, 1272, 1227, 1172, 1147, 1087, 1010, 943, 912, 835, 797, 743, 649, 591, 559, 514, 419.

**Compound 1n**

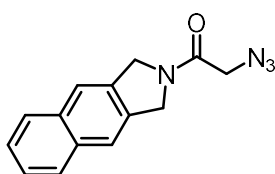
**1n**: colorless oil. Yield: 95%.  $^1\text{H NMR}$  (300 MHz,  $\text{CDCl}_3$ )  $\delta$  7.17 (d,  $J = 8.6$  Hz, 2H), 6.84 (d,  $J = 8.6$  Hz, 2H), 4.51 (s, 2H), 3.93 (s, 2H), 3.77 (s, 3H), 2.82 (s, 3H). With rotation ratio = 1.6:1.  $^{13}\text{C NMR}$  (75 MHz,  $\text{CDCl}_3$ )  $\delta$  167.6, 167.2, 159.4, 159.2, 129.7, 128.7, 127.7, 127.5, 114.6, 114.1, 55.4, 55.3, 52.3, 50.7, 50.6, 34.1, 33.7. **IR (film)**:  $\nu$  ( $\text{cm}^{-1}$ ) 3069, 3002, 2939, 2862, 2192, 2160, 2106, 2026, 1666, 1614, 1509, 1445, 1418, 1341, 1300, 1262, 1223, 1190, 1165, 1100, 1031, 994, 916, 864, 843, 774, 731, 646, 557, 505, 481, 391.

**Compound 1o**

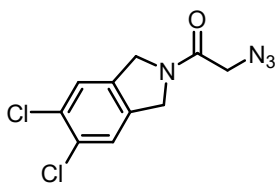
**1o**: white solid. Yield: 94%.  $^1\text{H NMR}$  (300 MHz,  $\text{CDCl}_3$ )  $\delta$  7.30 (dd,  $J = 10.0, 4.6$  Hz, 2H), 7.20 (dd,  $J = 9.2, 5.3$  Hz, 1H), 7.11 (d,  $J = 7.1$  Hz, 2H), 4.44 (s, 2H), 3.73 (s, 2H), 1.40 (s, 9H).  $^{13}\text{C NMR}$  (75 MHz,  $\text{CDCl}_3$ )  $\delta$  168.6, 138.3, 129.2, 127.6, 125.4, 58.9, 52.6, 48.0, 28.6. **IR (film)**:  $\nu$  ( $\text{cm}^{-1}$ ) 3099, 3027, 2928, 2902, 2854, 2225, 2176, 2147, 2103, 1744, 1659, 1573, 1439, 1416, 1339, 1253, 1183, 1153, 1114, 994, 932, 908, 867, 841, 816, 749, 693, 663, 634, 560, 488, 429.

**Compound 1p**

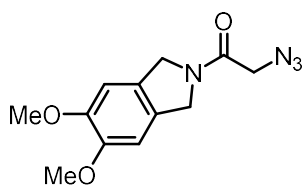
**1p:** white solid. Yield: 74%.  $^1\text{H NMR}$  (300 MHz,  $\text{CD}_2\text{Cl}_2$ )  $\delta$  7.31 (m, 4H), 4.81 (s, 2H), 4.73 (s, 2H), 3.94 (s, 2H).  $^{13}\text{C NMR}$  (75 MHz,  $\text{CD}_2\text{Cl}_2$ )  $\delta$  166.3, 136.4, 136.6, 128.4, 128.0, 123.4, 123.1, 52.8, 52.1, 51.2. **IR (film):**  $\nu$  ( $\text{cm}^{-1}$ ) 3062, 3014, 2959, 2920, 2857, 2262, 2185, 2104, 1765, 1652, 1502, 1431, 1339, 1312, 1270, 1235, 1171, 993, 911, 873, 836, 775, 747, 639, 576, 541, 478, 454, 395.

**Compound 1q**

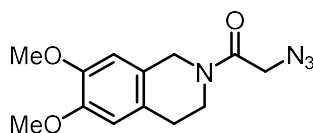
**1q:** white solid. Yield: 61%.  $^1\text{H NMR}$  (300 MHz,  $\text{CD}_2\text{Cl}_2$ )  $\delta$  7.90-7.81 (m, 2H), 7.78 (s, 1H), 7.74 (s, 1H), 7.53-7.43 (m, 2H), 4.96 (s, 2H), 4.87 (s, 2H), 3.99 (s, 2H).  $^{13}\text{C NMR}$  (75 MHz,  $\text{CD}_2\text{Cl}_2$ )  $\delta$  166.4, 135.2, 135.0, 133.8, 133.5, 128.2, 128.1, 126.5, 126.4, 121.9, 121.7, 52.3, 51.5, 51.3. **IR (film):**  $\nu$  ( $\text{cm}^{-1}$ ) 3062, 3030, 2925, 2100, 1652, 1486, 1447, 1406, 1355, 1265, 1216, 1111, 1025, 990, 948, 920, 817, 736, 699, 619, 583, 550, 514, 458, 398.

**Compound 1r**

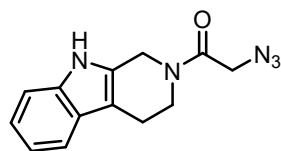
**1r:** white solid. Yield: 81%.  $^1\text{H NMR}$  (300 MHz,  $\text{CDCl}_3$ )  $\delta$  7.42 (s, 1H), 7.35 (s, 1H), 4.80 (s, 2H), 4.73 (s, 2H), 3.95 (s, 2H).  $^{13}\text{C NMR}$  (75 MHz,  $\text{CDCl}_3$ )  $\delta$  166.2, 136.1, 135.8, 132.7, 132.3, 125.2, 124.8, 52.1, 51.2, 51.1. **IR (film):**  $\nu$  ( $\text{cm}^{-1}$ ) 3002, 2931, 2838, 2101, 1652, 1611, 1509, 1461, 1407, 1354, 1242, 1176, 1112, 1030, 989, 928, 812, 756, 693, 587, 550, 516, 444, 397.

**Compound 1s**

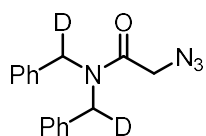
**1s:** white solid. Yield: 82%.  $^1\text{H NMR}$  (300 MHz,  $\text{CDCl}_3$ )  $\delta$  6.79 (s, 1H), 6.73 (s, 1H), 4.77 (s, 2H), 4.69 (s, 2H), 3.95 (s, 2H), 3.88 (s, 3H), 3.86 (s, 3H).  $^{13}\text{C NMR}$  (75 MHz,  $\text{CDCl}_3$ )  $\delta$  166.1, 149.8, 149.5, 127.7, 127.0, 105.9, 105.6, 56.3, 56.3, 52.7, 52.0, 51.0. **IR (film):**  $\nu$  ( $\text{cm}^{-1}$ ) 2987, 2947, 2900, 2838, 2149, 2103, 1650, 1607, 1515, 1454, 1363, 1335, 1281, 1250, 1201, 1107, 1060, 1014, 965, 912, 850, 821, 787, 747, 683, 606, 550, 484, 444, 402.

**Compound 1t**

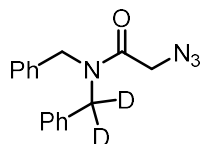
**1t:** white solid. Yield: 92%.  $^1\text{H NMR}$  (300 MHz,  $\text{CDCl}_3$ )  $\delta$  6.61 (m, 2H), 4.65 (s, 2H), 3.99 (s, 2H), 3.87-3.77 (m, 6H), 3.56 (t,  $J = 5.9$  Hz, 2H), 2.86-2.70 (m, 2H). With rotation ratio = 4:3.  $^{13}\text{C NMR}$  (75 MHz,  $\text{CDCl}_3$ )  $\delta$  166.2, 148.3, 148.2, 126.9, 125.7, 124.9, 123.5, 112.0, 111.5, 109.7, 109.2, 56.2, 51.2, 46.6, 44.4, 43.1, 40.4, 29.0, 28.1. **IR (film):**  $\nu$  ( $\text{cm}^{-1}$ ) 2985, 2949, 2900, 2838, 2205, 2162, 2105, 1651, 1607, 1515, 1454, 1362, 1337, 1282, 1251, 1201, 1106, 1060, 1015, 966, 913, 851, 821, 787, 747, 684, 606, 550, 486, 443, 401.

**Compound 1u**

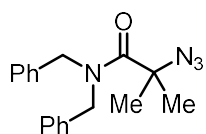
**1u:** white solid. Yield: 73%.  $^1\text{H NMR}$  (300 MHz,  $\text{CD}_2\text{Cl}_2$ )  $\delta$  8.08 (d,  $J = 61.5$  Hz, 1H), 7.48 (t,  $J = 7.5$  Hz, 1H), 7.36 (d,  $J = 7.8$  Hz, 1H), 7.12 (ddd,  $J = 14.8, 13.8, 6.9$  Hz, 2H), 4.71 (d,  $J = 78.7$  Hz, 2H), 4.15-3.99 (m, 2H), 3.98-3.57 (m, 2H), 2.86 (dd,  $J = 11.5, 5.9$  Hz, 2H).  $^{13}\text{C NMR}$  (75 MHz,  $\text{CD}_2\text{Cl}_2$ )  $\delta$  166.8, 136.7, 130.3, 127.2, 122.2, 120.0, 118.2, 111.4, 108.2, 51.3, 43.8, 41.2, 22.3. **IR (film):**  $\nu$  ( $\text{cm}^{-1}$ ) 3292, 3058, 2914, 2846, 2099, 1642, 1446, 1375, 1277, 1215, 1163, 1051, 985, 950, 919, 894, 848, 787, 735, 682, 656, 613, 577, 550, 499, 470, 429.

**Compound 1a-d2-1**

**1a-d2-1:** colorless oil. Yield: 87%.  $^1\text{H NMR}$  (300 MHz,  $\text{CD}_2\text{Cl}_2$ )  $\delta$  7.45-7.29 (m, 6H), 7.25 (d,  $J = 7.2$  Hz, 2H), 7.16 (d,  $J = 7.1$  Hz, 2H), 4.61 (s, 1H), 4.36 (s, 1H), 3.97 (s, 2H).  $^{13}\text{C NMR}$  (75 MHz,  $\text{CD}_2\text{Cl}_2$ )  $\delta$  168.3, 137.2, 136.1, 129.5, 129.1, 128.7, 128.3, 128.0, 126.9, 51.0, 50.0, 49.7, 49.4, 49.1, 48.9. **IR (film):**  $\nu$  ( $\text{cm}^{-1}$ ) 3060, 3031, 2915, 2099, 1653, 1492, 1443, 1415, 1358, 1266, 1211, 1079, 1020, 981, 920, 837, 814, 726, 699, 612, 553, 502, 454, 396.

**Compound 1a-d2-2**

**1a-d2-2:** colorless oil. Yield: 91%.  $^1\text{H NMR}$  (300 MHz,  $\text{CDCl}_3$ )  $\delta$  7.34-7.20 (m, 6H), 7.16 (d,  $J = 5.2$  Hz, 2H), 7.05 (d,  $J = 6.9$  Hz, 2H), 4.56 (s, 1H), 4.28 (s, 1H), 3.89 (s, 2H).  $^{13}\text{C NMR}$  (75 MHz,  $\text{CDCl}_3$ )  $\delta$  168.0, 136.6, 135.6, 135.5, 129.3, 128.9, 128.6, 128.1, 127.9, 126.4, 50.8, 49.5, 49.0. **IR (film):**  $\nu$  ( $\text{cm}^{-1}$ ) 3061, 3029, 2917, 2101, 1653, 1493, 1441, 1414, 1357, 1267, 1211, 1077, 1018, 982, 921, 834, 811, 730, 696, 609, 551, 500, 452, 399.

**Compound 1aMe<sub>2</sub>**

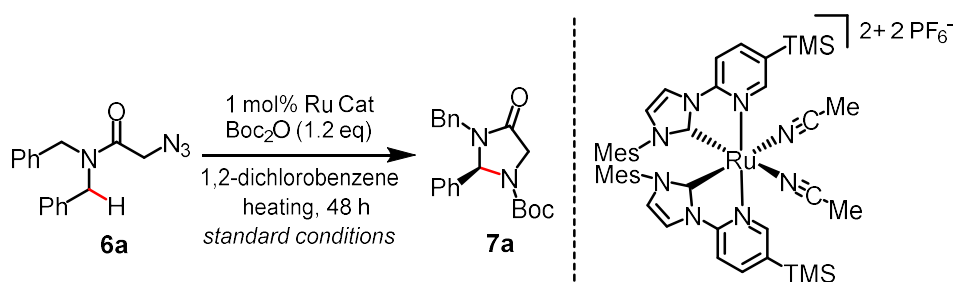
**1aMe<sub>2</sub>:** white solid. Yield: 87%  $^1\text{H NMR}$  (300 MHz,  $\text{CDCl}_3$ )  $\delta$  7.57-6.96 (m, 10H), 4.88 (s, 2H), 4.54 (s, 2H), 1.64 (s, 6H).  $^{13}\text{C NMR}$  (75 MHz,  $\text{CDCl}_3$ )  $\delta$  172.1, 136.9, 128.9, 128.2, 127.6, 127.1, 64.3, 50.8, 48.9, 25.7. **IR (film):**  $\nu$  ( $\text{cm}^{-1}$ ) 3062, 3033, 2978, 2925, 2857, 2469, 2100, 1629, 1494, 1444, 1416, 1361, 1315, 1245, 1172, 1144, 1077, 1025, 944, 896, 849, 816, 739, 696, 615, 589, 555, 508, 470, 429, 413.

## 4.2.3 Catalytic Asymmetric Intramolecular C–H Aminations

**General procedure:** A pre-dried (using heating gun to dry for 3 times per tube) 10 mL Schlenk tube was charged with azides **1a-v** (0.2 mmol) and  $\Lambda$ -**Ru7** (2.3 mg, 0.002 mmol, 1 mol%) under N<sub>2</sub> atmosphere. Boc<sub>2</sub>O (55  $\mu$ L, 0.24 mmol) and super dried 1,2-dichlorobenzene (0.2 mL, 1.0 M) bought from “Acros” was added via syringe in sequence. The reaction mixture was stirred at the indicated temperature for the indicated time under N<sub>2</sub> atmosphere. Afterwards, the mixture was directly transferred to a column and purified by flash chromatography on silica gel (*n*-Hexane/EtOAc= 10:1 to 3:1) to afford the analytically pure products **2a-l**, **2n-v**, and **2a'**. Enantiomeric excess was determined by HPLC analysis on chiral stationary phase. The absolute configuration of the product **2f** was measured by single-crystal X-ray analysis as *S*-configuration.

*Additional experimental informations:*

**Is the solvent 1,2-dichlorobenzene special?** It can be replaced by other solvents with little bit drop of the catalytic performance.



entry	catalyst	conditions <sup>b</sup>	T (°C)	NMR yield (%) <sup>c</sup>	ee (%) <sup>d</sup>
1	$\Lambda$ - <b>Ru7</b>	standard	85	84 (80) <sup>e</sup>	91
2	$\Lambda$ - <b>Ru7</b>	Dioxane as Sol.	85	82	90
3	$\Lambda$ - <b>Ru7</b>	Chlorobenzene as Sol.	85	79	91

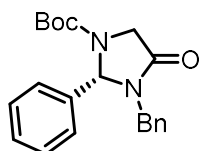
<sup>a</sup>Standard reaction conditions: **6a** (0.2 mmol), Boc<sub>2</sub>O (0.24 mmol), Ruthenium catalyst (0.002 mmol) in 1,2-dichlorobenzene (0.2 mL) stirred at 85 °C for 48 h under N<sub>2</sub> unless noted otherwise. <sup>b</sup>Deviations from standard conditions are shown. <sup>c</sup>Determined by <sup>1</sup>H NMR of the crude products using Cl<sub>2</sub>CHCHCl<sub>2</sub> as internal standard. <sup>d</sup>Enantiomeric excess determined by HPLC analysis of the crude main product on a chiral stationary phase. <sup>e</sup>Isolated yield in the brackets.

**How was the reaction executed?** All catalytic reactions were carried with a 10 mL Schlenk tube made by “Synthware” and the vial was sealed under N<sub>2</sub> atmosphere (see following picture on the left).



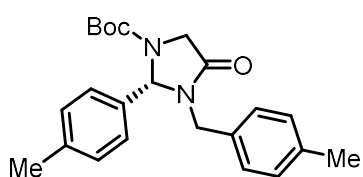
TLC of the reaction involved with standard substrate **1a** was monitored after 24 h (*n*-hexane:EtOAc = 3:1, Product  $R_f = 0.45$ , see following picture on the right). When the reaction time was 48 h, the starting material was fully consumed (>99% conversion).

### Compound 2a



Starting from **1a** (56.0 mg, 0.20 mmol) according to the general procedure to provide **2a** as a white solid (56.2 mg, 80% yield). Enantiomeric excess was established by HPLC analysis as 91% ee (column: Daicel Chiralpak IG column 250 x 4.6 mm, absorption:  $\lambda = 220$  nm, mobile phase: *n*-Hexane/isopropanol = 85:15, flow rate 1.0 mL/min, column temperature: 25 °C, retention times:  $t_r$  (major) = 19.7 min,  $t_r$  (minor) = 15.3 min).  $[\alpha]_D^{22} = +21.6^\circ$  ( $c = 1.0$ ,  $\text{CH}_2\text{Cl}_2$ ).  **$^1\text{H}$  NMR (300 MHz,  $\text{CD}_2\text{Cl}_2$ )**  $\delta$  7.44-7.36 (m,  $J = 6.2, 3.6$  Hz, 3H), 7.34-7.19 (m, 5H), 7.18-7.09 (m, 2H), 5.62 (br, m, 1H), 5.00 (br, m, 1H), 4.17 (s, 2H), 3.39 (br, m, 1H), 1.42-0.96 (br, m, 9H).  **$^{13}\text{C}$  NMR (75 MHz,  $\text{CD}_2\text{Cl}_2$ )**  $\delta$  167.4, 148.2, 138.3, 135.6, 129.3, 128.7, 128.4, 127.8, 127.4, 80.8, 74.7, 48.9, 48.4, 43.2, 27.9, 27.7. **HRMS (ESI,  $m/z$ )** calcd. for  $\text{C}_{21}\text{H}_{24}\text{N}_2\text{O}_3\text{Na}[\text{M}+\text{Na}]^+$ : 375.1679, found: 375.1687.

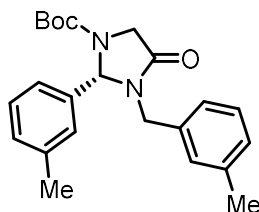
### Compound 2b



Starting from **1b** (61.7 mg, 0.20 mmol) according to the general procedure to provide **2b** as a colorless oil (61.4 mg, 81% yield). Enantiomeric excess was established by HPLC analysis as 90% ee (Enantiomeric excess was established by HPLC analysis as 91% ee (column: Daicel Chiralpak ASH column 250 x 4.6 mm, absorption:  $\lambda = 220$  nm, mobile phase: *n*-Hexane/isopropanol = 90:10, flow rate 1.0 mL/min, column temperature: 30 °C, retention times:  $t_r$  (major) = 14.9 min,  $t_r$  (minor) = 36.4 min).  $[\alpha]_D^{22} = +78.6^\circ$  ( $c = 1.0$ ,  $\text{CH}_2\text{Cl}_2$ ).  **$^1\text{H}$  NMR (300 MHz,  $\text{CD}_2\text{Cl}_2$ )**  $\delta$  7.31-7.15 (m, 3H), 7.13-6.97 (m, 3H), 6.93 (d,  $J = 6.2$  Hz, 2H), 5.57 (br, m, 1H), 4.92 (br, m, 1H), 4.16 (s, 2H), 3.36 (br, m, 1H), 2.35 (s, 3H), 2.32 (s, 3H), 1.27 (br, m, 9H).  **$^{13}\text{C}$  NMR (75 MHz,  $\text{CD}_2\text{Cl}_2$ )**  $\delta$  167.7, 152.7, 139.0, 135.9,

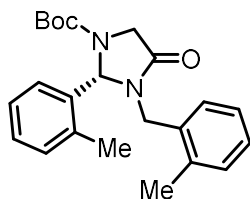
130.4, 129.5, 128.9, 128.4, 125.9, 125.1, 81.2, 75.3, 49.5, 48.8, 43.7, 28.4, 28.2, 21.5. **HRMS (ESI,  $m/z$ )** calcd. for  $C_{23}H_{28}N_2O_3Na[M+Na]^+$ : 403.1992, found: 403.2004.

### Compound 2c



Starting from **1c** (61.7 mg, 0.20 mmol) according to the general procedure to provide **2c** as a white solid (63.8 mg, 84% yield). Enantiomeric excess was established by HPLC analysis as 90% ee (column: Daicel Chiralpak ASH column 250 x 4.6 mm, absorption:  $\lambda = 220$  nm, mobile phase: *n*-Hexane/isopropanol = 70:30, flow rate 1.0 mL/min, column temperature: 25 °C, retention times:  $t_r$  (major) = 8.0 min,  $t_r$  (minor) = 22.0 min).  $[\alpha]_D^{22} = +86.6^\circ$  ( $c = 1.0$ ,  $CH_2Cl_2$ ).  **$^1H$  NMR (300 MHz,  $CD_2Cl_2$ )**  $\delta$  7.12 (d,  $J = 7.8$  Hz, 2H), 7.05 (d,  $J = 7.9$  Hz, 4H), 6.94 (d,  $J = 8.0$  Hz, 2H), 5.47 (br, m, 1H), 4.90 (br, m, 1H), 4.02 (s, 2H), 3.21 (br, m, 1H), 2.28 (s, 3H), 2.25 (s, 3H), 1.33-0.97 (br, m, 9H).  **$^{13}C$  NMR (75 MHz,  $CD_2Cl_2$ )**  $\delta$  167.7, 152.7, 139.7, 138.1, 135.6, 135.3, 133.0, 129.8, 128.8, 127.8, 81.1, 74.9, 74.7, 49.4, 48.9, 43.3, 28.2, 21.4, 21.3. **HRMS (ESI,  $m/z$ )** calcd. for  $C_{23}H_{28}N_2O_3Na[M+Na]^+$ : 403.1992, found: 403.2006.

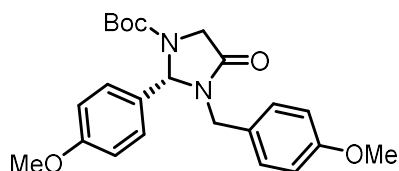
### Compound 2d



Starting from **1d** (61.7 mg, 0.20 mmol) according to the general procedure to provide **2d** as a white solid (39.6 mg, 52% yield). Enantiomeric excess was established by HPLC analysis as 87% ee (column: Daicel Chiralpak ASH column 250 x 4.6 mm, absorption:  $\lambda = 220$  nm, mobile phase: *n*-Hexane/isopropanol = 85:15, flow rate 1.0 mL/min, column temperature: 30 °C, retention times:  $t_r$  (major) = 13.9 min,  $t_r$  (minor) = 20.9 min).  $[\alpha]_D^{22} = +88.4^\circ$  ( $c = 1.0$ ,  $CH_2Cl_2$ ).  **$^1H$  NMR (300 MHz,  $CD_2Cl_2$ )**  $\delta$  7.27-7.08 (m, 7H), 6.88 (m, 1H), 5.83 (s, 1H), 5.09-4.88 (br, m, 1H), 4.20 (s, 2H), 3.38 (br, m, 1H), 2.10-1.92 (m, 6H), 1.48-0.96 (br, m, 9H).  **$^{13}C$  NMR (75 MHz,  $CD_2Cl_2$ )**  $\delta$  168.0, 153.0, 137.2,

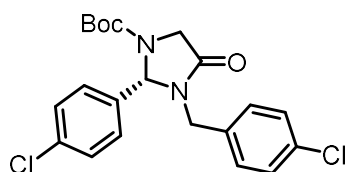
136.1, 133.3, 131.3, 131.0, 130.7, 129.4, 128.3, 127.8, 126.9, 126.5, 81.3, 72.2, 49.5, 49.3, 41.6, 28.4, 28.3, 19.2, 18.6. **HRMS (ESI,  $m/z$ )** calcd. for  $C_{23}H_{28}N_2O_3Na[M+Na]^+$ : 403.1992, found: 403.2003.

### Compound 2e



Starting from **1e** (68.1 mg, 0.20 mmol) according to the general procedure to provide **2e** as a colorless oil (78.3 mg, 95% yield). Enantiomeric excess was established by HPLC analysis as 90% ee (column: Daicel Chiralpak ASH column 250 x 4.6 mm, absorption:  $\lambda = 220$  nm, mobile phase: *n*-Hexane/isopropanol = 50:50, flow rate 1.0 mL/min, column temperature: 40 °C, retention times:  $t_r$  (major) = 10.0 min,  $t_r$  (minor) = 14.0 min).  $[\alpha]_D^{22} = +22.4^\circ$  ( $c = 1.0$ ,  $CH_2Cl_2$ ).  **$^1H$  NMR (300 MHz,  $CD_2Cl_2$ )**  $\delta$  7.16 (s, 2H), 7.09-7.00 (m, 2H), 6.91 (d,  $J = 8.6$  Hz, 2H), 6.86 (dd,  $J = 6.7, 4.8$  Hz, 2H), 5.55 (br, m, 1H), 4.93 (br, m, 1H), 4.13 (s, 2H), 3.83 (s, 3H), 3.78 (s, 3H), 3.32 (br, m, 1H), 1.44-0.99 (br, m, 9H).  **$^{13}C$  NMR (75 MHz,  $CD_2Cl_2$ )**  $\delta$  167.5, 160.8, 159.8, 152.8, 130.2, 129.2, 128.0, 114.5, 81.1, 74.7, 55.7, 55.7, 49.4, 48.9, 43.0, 28.3. **HRMS (ESI,  $m/z$ )** calcd. for  $C_{23}H_{28}N_2O_5Na[M+Na]^+$ : 435.1890, found: 435.1901.

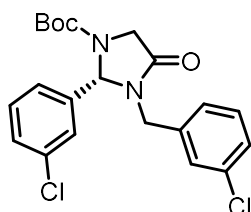
### Compound 2f



Starting from **1f** (69.6 mg, 0.20 mmol) according to the general procedure to provide **2f** as a white solid (65.5 mg, 78% yield). Enantiomeric excess was established by HPLC analysis as 90% ee (column: Daicel Chiralpak ASH column 250 x 4.6 mm, absorption:  $\lambda = 220$  nm, mobile phase: *n*-Hexane/isopropanol = 70:30, flow rate 1.0 mL/min, column temperature: 25 °C, retention times:  $t_r$  (major) = 8.9 min,  $t_r$  (minor) = 12.9 min).  $[\alpha]_D^{22} = +4.2^\circ$  ( $c = 1.0$ ,  $CH_2Cl_2$ ).  **$^1H$  NMR (300 MHz,  $CD_2Cl_2$ )**  $\delta$  7.43-7.34 (m, 2H), 7.30 (d,  $J = 8.4$  Hz, 2H), 7.17 (s, 2H), 7.07 (d,  $J = 8.4$  Hz, 2H), 5.74-5.38 (br, m, 1H), 4.97-4.81 (br, m, 1H), 4.16 (s, 2H), 3.56-3.20 (br, m, 1H), 1.47-1.04 (br, m, 9H).

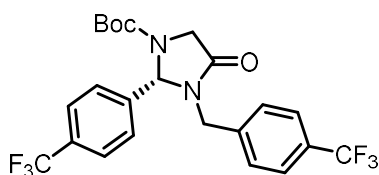
$^{13}\text{C}$  NMR (75 MHz,  $\text{CD}_2\text{Cl}_2$ )  $\delta$  167.8, 152.9, 146.5, 137.1, 135.5, 134.4, 134.1, 130.3, 129.4, 129.3, 81.6, 74.5, 48.7, 43.2, 28.2. HRMS (ESI,  $m/z$ ) calcd. for  $\text{C}_{21}\text{H}_{22}\text{N}_2\text{O}_3\text{Cl}_2[\text{M}+\text{Na}]^+$ : 443.0900, found: 443.0911.

### Compound 2g



Starting from **1g** (69.6 mg, 0.20 mmol) according to the general procedure to provide **2g** as a white solid (68.8 mg, 82% yield). Enantiomeric excess was established by HPLC analysis as 91% ee (column: Daicel Chiralpak ASH column 250 x 4.6 mm, absorption:  $\lambda = 220$  nm, mobile phase: *n*-Hexane/isopropanol = 75:25, flow rate 1.0 mL/min, column temperature: 40 °C, retention times:  $t_r$  (major) = 10.1 min,  $t_r$  (minor) = 12.2 min).  $[\alpha]_D^{22} = +6.2^\circ$  ( $c = 1.0$ ,  $\text{CH}_2\text{Cl}_2$ ).  $^1\text{H}$  NMR (300 MHz,  $\text{CD}_2\text{Cl}_2$ )  $\delta$  7.43-7.07 (m, 7H), 7.03 (d,  $J = 3.9$  Hz, 1H), 5.74-5.46 (br, m, 1H), 4.98-4.74 (br, m, 1H), 4.18 (s, 2H), 3.73-3.34 (br, m, 1H), 1.56-1.05 (br, m, 9H).  $^{13}\text{C}$  NMR (75 MHz,  $\text{CD}_2\text{Cl}_2$ )  $\delta$  167.8, 153.0, 152.4, 140.7, 137.9, 134.9, 130.5, 130.0, 128.8, 128.5, 128.1, 127.0, 126.2, 81.7, 74.8, 49.2, 48.6, 43.5, 28.2. HRMS (ESI,  $m/z$ ) calcd. for  $\text{C}_{21}\text{H}_{22}\text{N}_2\text{O}_3\text{Cl}_2[\text{M}+\text{Na}]^+$ : 443.0900, found: 443.0910.

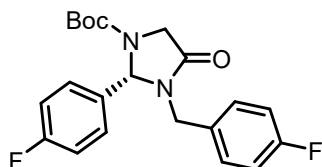
### Compound 2h



Starting from **1h** (83.2 mg, 0.20 mmol) according to the general procedure to provide **2h** as a white solid (49.8 mg, 51% yield). Enantiomeric excess was established by HPLC analysis as 94% ee (column: Daicel Chiralpak ASH column 250 x 4.6 mm, absorption:  $\lambda = 220$  nm, mobile phase: *n*-Hexane/isopropanol = 70:30, flow rate 1.0 mL/min, column temperature: 30 °C, retention times:  $t_r$  (major) = 4.9 min,  $t_r$  (minor) = 6.4 min).  $[\alpha]_D^{22} = +18.4^\circ$  ( $c = 1.0$ ,  $\text{CH}_2\text{Cl}_2$ ).  $^1\text{H}$  NMR (300 MHz,  $\text{CD}_2\text{Cl}_2$ )  $\delta$  7.64 (d,  $J = 8.1$  Hz, 2H), 7.56 (d,  $J = 8.1$  Hz, 2H), 7.36 (s, 2H), 7.24 (d,  $J = 8.0$  Hz, 2H), 5.82-5.51 (br, m, 1H), 5.01-4.78 (br, m, 1H), 4.22 (s, 2H), 3.81-3.55 (br, m, 1H), 1.50-0.97 (br, m, 9H).

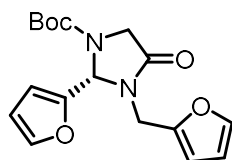
$^{13}\text{C}$  NMR (75 MHz,  $\text{CD}_2\text{Cl}_2$ )  $\delta$  168.0, 153.0, 152.4, 142.7, 142.2, 140.1, 132.05, 131.3, 130.6, 130.4-129.6 (m), 129.2, 128.4, 126.7-125.6 (m), 122.7 (d,  $J = 13.4$  Hz), 81.9, 74.9, 60.7, 49.1, 48.6, 43.7, 28.2.  $^{19}\text{F}$  NMR (235 MHz,  $\text{CD}_2\text{Cl}_2$ )  $\delta$  -63.01, -63.08. HRMS (ESI,  $m/z$ ) calcd. for  $\text{C}_{23}\text{H}_{22}\text{N}_2\text{O}_3\text{F}_6\text{Na}[\text{M}+\text{Na}]^+$ : 511.1427, found: 511.1441.

### Compound 2i



Starting from **1i** (63.2 mg, 0.20 mmol) according to the general procedure to provide **2i** as a white solid (56.5 mg, 73% yield). Enantiomeric excess was established by HPLC analysis as 91% ee (column: Daicel Chiralpak ASH column 250 x 4.6 mm, absorption:  $\lambda = 220$  nm, mobile phase: *n*-Hexane/isopropanol = 70:30, flow rate 1.0 mL/min, column temperature: 30 °C, retention times:  $t_r$  (major) = 8.4 min,  $t_r$  (minor) = 11.4 min).  $[\alpha]_D^{22} = +29.2^\circ$  ( $c = 1.0$ ,  $\text{CH}_2\text{Cl}_2$ ).  $^1\text{H}$  NMR (300 MHz,  $\text{CD}_2\text{Cl}_2$ )  $\delta$  7.38-6.82 (m, 8H), 5.79-5.43 (br, m, 1H), 5.02-4.78 (br, m, 1H), 4.16 (s, 2H), 3.59-3.28 (br, m, 1H), 1.43-1.00 (br, m, 9H).  $^{13}\text{C}$  NMR (75 MHz,  $\text{CD}_2\text{Cl}_2$ )  $\delta$  167.8, 165.3, 164.5, 162.0, 161.2, 152.6, 134.5, 131.8, 130.7, 130.6, 129.9, 129.8, 116.2, 116.1, 115.9, 115.8, 81.5, 74.6, 49.2, 48.7, 41.6, 43.1, 28.3.  $^{19}\text{F}$  NMR (235 MHz,  $\text{CD}_2\text{Cl}_2$ )  $\delta$  -112.77, -115.06. HRMS (ESI,  $m/z$ ) calcd. for  $\text{C}_{21}\text{H}_{22}\text{F}_2\text{N}_2\text{O}_3\text{Na}[\text{M}+\text{Na}]^+$ : 411.1491, found: 411.1491.

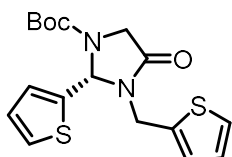
### Compound 2j



Starting from **1j** (52.0 mg, 0.20 mmol) according to the general procedure to provide **2j** as a colorless oil (42.5 mg, 64% yield). Enantiomeric excess was established by HPLC analysis as 88% ee (column: Daicel Chiralpak ASH column 250 x 4.6 mm, absorption:  $\lambda = 220$  nm, mobile phase: *n*-Hexane/isopropanol = 70:30, flow rate 1.0 mL/min, column temperature: 30 °C, retention times:  $t_r$  (major) = 8.6 min,  $t_r$  (minor) = 18.3 min).  $[\alpha]_D^{22} = +18.6^\circ$  ( $c = 1.0$ ,  $\text{CH}_2\text{Cl}_2$ ).  $^1\text{H}$  NMR (300 MHz,  $\text{CD}_2\text{Cl}_2$ )  $\delta$  7.41 (dd,  $J = 12.8, 1.0$  Hz, 2H), 6.49 (d,  $J = 15.0$  Hz, 1H), 6.37 (ddd,  $J = 20.3, 3.1, 1.8$  Hz,

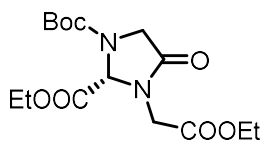
2H), 6.21 (d,  $J = 3.2$  Hz, 1H), 5.98-5.69 (br, m, 1H), 4.99-4.75 (br, m, 1H), 4.17-3.94 (br, m, 2H), 3.76-3.56 (br, m, 1H), 1.45-1.20 (br, m, 9H).  $^{13}\text{C}$  NMR (75 MHz,  $\text{CD}_2\text{Cl}_2$ )  $\delta$  167.8, 150.0, 149.5, 143.7, 143.2, 110.8, 110.8, 109.4, 81.4, 68.6, 68.4, 48.8, 48.1, 36.6, 28.3. HRMS (ESI,  $m/z$ ) calcd. for  $\text{C}_{17}\text{H}_{20}\text{N}_2\text{O}_5\text{Na}[\text{M}+\text{Na}]^+$ : 355.1264, found: 355.1274.

### Compound 2k



Starting from **1k** (58.4 mg, 0.20 mmol) according to the general procedure to provide **2k** as a white solid (54.6 mg, 75% yield). Enantiomeric excess was established by HPLC analysis as 82% ee (column: Daicel Chiralpak ASH column 250 x 4.6 mm, absorption:  $\lambda = 220$  nm, mobile phase: *n*-Hexane/isopropanol = 60:40, flow rate 1.0 mL/min, column temperature: 40 °C, retention times:  $t_r$  (major) = 6.4 min,  $t_r$  (minor) = 15.1 min).  $[\alpha]_D^{22} = +71.6^\circ$  ( $c = 1.0$ ,  $\text{CH}_2\text{Cl}_2$ ).  $^1\text{H}$  NMR (300 MHz,  $\text{CD}_2\text{Cl}_2$ )  $\delta$  7.40 (d,  $J = 5.0$  Hz, 1H), 7.29 (dd,  $J = 5.1, 1.0$  Hz, 1H), 7.17 (s, 1H), 7.03 (dd,  $J = 5.0, 3.5$  Hz, 1H), 6.97 (dd,  $J = 5.1, 3.5$  Hz, 1H), 6.92 (d,  $J = 3.4$  Hz, 1H), 6.18-5.90 (br, m, 1H), 5.16-5.00 (br, m, 1H), 4.15-3.98 (br, m, 2H), 3.93-3.75 (br, m, 1H), 1.45-1.19 (br, m, 9H).  $^{13}\text{C}$  NMR (75 MHz,  $\text{CD}_2\text{Cl}_2$ )  $\delta$  167.1, 152.6, 142.6, 138.1, 128.4, 127.9, 127.4, 127.2, 126.4, 81.6, 70.3, 48.6, 48.1, 38.1, 28.3. HRMS (ESI,  $m/z$ ) calcd. for  $\text{C}_{17}\text{H}_{20}\text{N}_2\text{O}_3\text{S}_2\text{Na}[\text{M}+\text{Na}]^+$ : 387.0808, found: 387.0818.

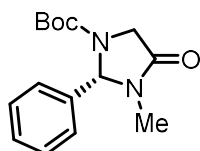
### Compound 2l



Starting from **1l** (54.4 mg, 0.20 mmol) according to the general procedure to provide **2l** as a colorless oil (50.3 mg, 73% yield, 32% ee). It's noteworthy that when treated with  $\Lambda$ -**Ru5** instead under general procedure provided **2l** (49.0 mg, 71% yield, 70% ee). Enantiomeric excess was established by HPLC analysis (column: Daicel Chiralpak ASH column 250 x 4.6 mm, absorption:  $\lambda = 210$  nm, mobile phase: *n*-Hexane/isopropanol = 70:30, flow rate 1.0 mL/min, column temperature: 30 °C, retention times:  $t_r$  (major) = 9.76 min,  $t_r$  (minor) = 15.78 min).  $[\alpha]_D^{22} = +7.6^\circ$  ( $c = 1.0$ ,  $\text{CH}_2\text{Cl}_2$ ).  $^1\text{H}$  NMR (300 MHz,  $\text{CDCl}_3$ )  $\delta$  5.43-5.31 (m, 1H), 4.43-4.32 (m, 1H), 4.32-4.15 (m, 4H), 4.12-4.00 (m, 2H), 3.95-3.76 (m,

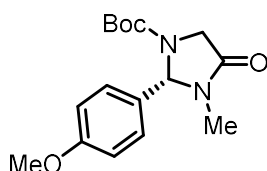
1H), 1.52-1.38 (m, 9H), 1.35-1.21 (m, 6H).  $^{13}\text{C}$  NMR (75 MHz,  $\text{CD}_2\text{Cl}_2$ )  $\delta$  169.2, 168.9, 167.9, 82.1, 72.6, 62.7, 62.2, 62.1, 61.8, 50.0, 49.1, 42.3, 30.1, 28.4, 28.3, 14.3. HRMS (ESI,  $m/z$ ) calcd. for  $\text{C}_{15}\text{H}_{24}\text{N}_2\text{O}_7\text{Na}[\text{M}+\text{Na}]^+$ : 367.1476, found: 367.1485.

### Compound 2m



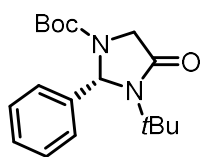
Starting from **1m** (40.8 mg, 0.20 mmol) according to the general procedure to provide **2m** as a colorless oil (28.2 mg, 51% yield). Enantiomeric excess was established by HPLC as 95% ee (column: Daicel Chiralpak IA column 250 x 4.6 mm, absorption:  $\lambda = 220$  nm, mobile phase: *n*-Hexane/isopropanol = 90:10, flow rate 1.0 mL/min, column temperature: 25 °C, retention times:  $t_r$  (major) = 9.3 min,  $t_r$  (minor) = 10.9 min).  $[\alpha]_D^{22} = +46.2^\circ$  ( $c = 1.0$ ,  $\text{CH}_2\text{Cl}_2$ ).  $^1\text{H}$  NMR (300 MHz,  $\text{CD}_2\text{Cl}_2$ )  $\delta$  7.50-7.17 (m, 5H), 5.90-5.55 (br, m, 1H), 4.09 (s, 2H), 2.60 (s, 3H), 1.55-1.06 (br, m, 9H).  $^{13}\text{C}$  NMR (75 MHz,  $\text{CD}_2\text{Cl}_2$ )  $\delta$  167.7, 152.9, 138.8, 129.6, 129.1, 127.6, 81.3, 77.4, 49.2, 48.7, 28.3, 26.7. HRMS (ESI,  $m/z$ ) calcd. for  $\text{C}_{15}\text{H}_{20}\text{N}_2\text{O}_3\text{Na}[\text{M}+\text{Na}]^+$ : 299.1366, found: 299.1366.

### Compound 2n



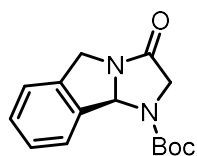
Starting from **1n** (46.8 mg, 0.20 mmol) according to the general procedure to provide **2n** as a colorless oil (39.1 mg, 64% yield). Enantiomeric excess was established by HPLC analysis as 94% ee (column: Daicel Chiralpak IA column 250 x 4.6 mm, absorption:  $\lambda = 220$  nm, mobile phase: *n*-Hexane/isopropanol = 90:10, flow rate 1.0 mL/min, column temperature: 30 °C, retention times:  $t_r$  (major) = 10.0 min,  $t_r$  (minor) = 13.0 min).  $[\alpha]_D^{22} = +52^\circ$  ( $c = 1.0$ ,  $\text{CH}_2\text{Cl}_2$ ).  $^1\text{H}$  NMR (300 MHz,  $\text{CD}_2\text{Cl}_2$ )  $\delta$  7.23 (s, 2H), 6.91 (d,  $J = 8.7$  Hz, 2H), 5.81-5.53 (br, m, 1H), 4.06 (s, 2H), 3.81 (s, 3H), 2.59 (s, 3H), 1.51-1.10 (br, m, 9H).  $^{13}\text{C}$  NMR (75 MHz,  $\text{CD}_2\text{Cl}_2$ )  $\delta$  167.6, 160.8, 152.9, 130.6, 128.9, 114.4, 81.1, 77.0, 55.7, 49.1, 48.6, 28.4, 26.7. HRMS (ESI,  $m/z$ ) calcd. for  $\text{C}_{16}\text{H}_{22}\text{N}_2\text{O}_4\text{Na}[\text{M}+\text{Na}]^+$ : 329.1472, found: 329.1481.

## Compound 2o



Starting from **1o** (49.2 mg, 0.20 mmol) according to the general procedure to provide **2o** as a white solid (51.5 mg, 81% yield). Enantiomeric excess was established by HPLC analysis as 23% ee (column: Daicel Chiralpak ADH column 250 x 4.6 mm, absorption:  $\lambda = 220$  nm, mobile phase: *n*-Hexane/isopropanol = 98:2 flow rate 1.0 mL/min, column temperature: 25 °C, retention times:  $t_r$  (major) = 17.0 min,  $t_r$  (minor) = 20.8 min).  $[\alpha]_D^{22} = +11.0^\circ$  ( $c = 1.0$ , CH<sub>2</sub>Cl<sub>2</sub>). <sup>1</sup>H NMR (300 MHz, CD<sub>2</sub>Cl<sub>2</sub>)  $\delta$  7.38 (d,  $J = 11.8$  Hz, 5H), 6.26-5.90 (br, m, 1H), 4.12-3.84 (br, m, 2H), 1.42-1.32 (br, m, 9H), 1.30 (s, 9H). <sup>13</sup>C NMR (75 MHz, CD<sub>2</sub>Cl<sub>2</sub>)  $\delta$  169.3, 169.0, 152.4, 152.0, 141.3, 129.1, 128.8, 127.7, 127.5, 81.3, 81.0, 75.3, 74.9, 55.7, 49.6, 49.1, 28.4, 28.1. HRMS (ESI,  $m/z$ ) calcd. for C<sub>18</sub>H<sub>26</sub>N<sub>2</sub>O<sub>3</sub>Na[M+Na]<sup>+</sup>: 341.1836, found: 341.1836.

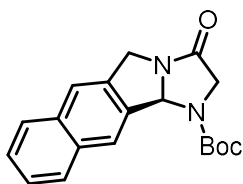
## Compound 2p



Starting from **1p** (40.4 mg, 0.20 mmol) according to the general procedure to provide **2p** as a white solid (40.5 mg, 74% yield). Enantiomeric excess was established by HPLC analysis as 94% ee (column: Daicel Chiralpak OJH column 250 x 4.6 mm, absorption:  $\lambda = 220$  nm, mobile phase: *n*-Hexane/isopropanol = 95:5, flow rate 1.0 mL/min, column temperature: 40 °C, retention times:  $t_r$  (major) = 16.9 min,  $t_r$  (minor) = 19.2 min).  $[\alpha]_D^{22} = +123.4^\circ$  ( $c = 1.0$ , CH<sub>2</sub>Cl<sub>2</sub>). <sup>1</sup>H NMR (300 MHz, CD<sub>2</sub>Cl<sub>2</sub>)  $\delta$  7.77 (s, 1H), 7.42-7.11 (m, 3H), 6.41 (s, 1H), 5.03-4.93 (br, m, 1H), 4.32-4.12 (br, m, 2H), 3.89-3.59 (br, m, 1H), 1.70-1.44 (br, m, 9H). <sup>13</sup>C NMR (75 MHz, CD<sub>2</sub>Cl<sub>2</sub>)  $\delta$  174.1, 154.7, 140.3, 139.6, 129.4, 128.4, 128.0, 123.3, 79.6, 50.7, 49.5, 28.6, 28.4, 28.3. HRMS (ESI,  $m/z$ ) calcd. for C<sub>15</sub>H<sub>18</sub>N<sub>2</sub>O<sub>3</sub>Na[M+Na]<sup>+</sup>: 297.1210, found: 297.1221.

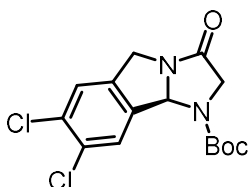


## Compound 2q



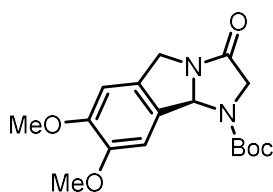
Starting from **1q** (50.4 mg, 0.20 mmol) according to the general procedure to provide **2q** as a white solid (42.5 mg, 66% yield). Enantiomeric excess was established by HPLC analysis as 88% ee (column: Daicel Chiralpak ASH column 250 x 4.6 mm, absorption:  $\lambda = 220$  nm, mobile phase: *n*-Hexane/isopropanol = 60:40, flow rate 1.0 mL/min, column temperature: 40 °C, retention times:  $t_r$  (major) = 7.3 min,  $t_r$  (minor) = 5.7 min).  $[\alpha]_D^{22} = +193.8^\circ$  ( $c = 1.0$ ,  $\text{CH}_2\text{Cl}_2$ ).  $^1\text{H NMR}$  (300 MHz,  $\text{CD}_2\text{Cl}_2$ )  $\delta$  8.43-8.03 (m, 1H), 7.98-7.80 (m, 2H), 7.73 (s, 1H), 7.62-7.38 (m, 2H), 6.55 (br, s, 1H), 5.25-5.11 (br, m, 1H), 4.45-4.14 (br, m, 2H), 3.89-3.65 (br, m, 1H), 1.78-1.47 (br, m, 9H).  $^{13}\text{C NMR}$  (75 MHz,  $\text{CD}_2\text{Cl}_2$ )  $\delta$  173.7, 138.6, 137.5, 134.2, 133.7, 128.9, 128.2, 127.0, 126.5, 124.3, 121.9, 81.7, 79.0, 50.8, 48.8, 28.6. HRMS (ESI,  $m/z$ ) calcd. for  $\text{C}_{19}\text{H}_{20}\text{N}_2\text{O}_3\text{Na}[\text{M}+\text{Na}]^+$ : 347.1366, found: 347.1379.

## Compound 2r



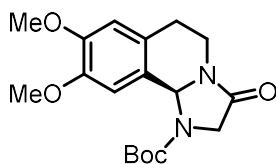
Starting from **1r** (54.0 mg, 0.20 mmol) according to the general procedure to provide **2r** as a white solid (39.0 mg, 57% yield). Enantiomeric excess was established by HPLC analysis as 94% ee (column: Daicel Chiralpak IB column 250 x 4.6 mm, absorption:  $\lambda = 220$  nm, mobile phase: *n*-Hexane/isopropanol = 90:10, flow rate 1.0 mL/min, column temperature: 25 °C, retention times:  $t_r$  (major) = 10.6 min,  $t_r$  (minor) = 8.6 min).  $[\alpha]_D^{22} = +62.0^\circ$  ( $c = 1.0$ ,  $\text{CH}_2\text{Cl}_2$ ).  $^1\text{H NMR}$  (300 MHz,  $\text{CD}_2\text{Cl}_2$ )  $\delta$  7.99-7.66 (m, 1H), 7.39 (s, 1H), 6.44-6.20 (br, m, 1H), 5.03-4.86 (br, m, 1H), 4.35-4.04 (br, m, 2H), 3.89-3.60 (br, m, 1H), 1.70-1.47 (br, m, 9H).  $^{13}\text{C NMR}$  (75 MHz,  $\text{CD}_2\text{Cl}_2$ )  $\delta$  173.8, 154.8, 140.5, 139.6, 133.5, 132.4, 127.3, 126.4, 125.2, 100.5, 82.1, 78.8, 50.6, 48.9, 28.5, 28.4, 28.3. HRMS (ESI,  $m/z$ ) calcd. for  $\text{C}_{15}\text{H}_{17}\text{N}_2\text{O}_3\text{Cl}_2[\text{M}+\text{H}]^+$ : 343.0611, found: 343.0624.

## Compound 2s



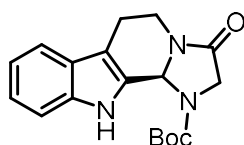
Starting from **1s** (52.4 mg, 0.20 mmol) according to the general procedure to provide **2s** as a white solid (50.4 mg, 75% yield). Enantiomeric excess was established by HPLC analysis as 89% ee (column: Daicel Chiralpak IA column 250 x 4.6 mm, absorption:  $\lambda = 220$  nm, mobile phase: *n*-Hexane/isopropanol = 90:10, flow rate 1.0 mL/min, column temperature: 40 °C, retention times:  $t_r$  (major) = 11.7 min,  $t_r$  (minor) = 10.7 min).  $[\alpha]_D^{22} = +199.6^\circ$  ( $c = 1.0$ ,  $\text{CH}_2\text{Cl}_2$ ).  **$^1\text{H}$  NMR (300 MHz,  $\text{CD}_2\text{Cl}_2$ )**  $\delta$  7.25 (d,  $J = 49.2$  Hz, 1H), 6.76 (s, 1H), 6.33 (s, 1H), 5.04-4.83 (br, m, 1H), 4.31-4.01 (br, m, 2H), 3.91-3.57 (m, 7H), 1.69-1.40 (br, m, 9H).  **$^{13}\text{C}$  NMR (75 MHz,  $\text{CD}_2\text{Cl}_2$ )**  $\delta$  174.2, 150.9, 149.9, 132.0, 131.4, 108.3, 107.1, 106.1, 81.6, 79.8, 56.4, 56.4, 50.7, 50.4, 49.6, 28.7. **HRMS (ESI,  $m/z$ )** calcd. for  $\text{C}_{17}\text{H}_{23}\text{N}_2\text{O}_5[\text{M}+\text{H}]^+$ : 335.1601, found: 335.1613.

## Compound 2t



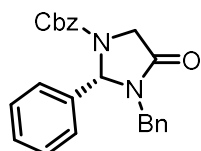
Starting from **1t** (55.2 mg, 0.20 mmol) according to the general procedure to provide **2t** as a white powder (33.4 mg, 48% yield). Enantiomeric excess was established by HPLC analysis as 92% ee (column: Daicel Chiralpak IA column 250 x 4.6 mm, absorption:  $\lambda = 220$  nm, mobile phase: *n*-Hexane/isopropanol = 90:10, flow rate 1.0 mL/min, column temperature: 40 °C, retention times:  $t_r$  (major) = 11.9 min,  $t_r$  (minor) = 15.3 min).  $[\alpha]_D^{22} = +56.4^\circ$  ( $c = 1.0$ ,  $\text{CH}_2\text{Cl}_2$ ).  **$^1\text{H}$  NMR (300 MHz,  $\text{CD}_2\text{Cl}_2$ )**  $\delta$  7.36-6.84 (m, 1H), 6.67-6.55 (m, 1H), 6.21 (s, 1H), 4.33-4.04 (m, 2H), 3.80 (s, 7H), 3.72-3.51 (m, 1H), 3.39-3.13 (m, 1H), 3.08-2.89 (m, 1H), 2.73-2.57 (m, 1H), 1.54 (s, 9H).  **$^{13}\text{C}$  NMR (75 MHz,  $\text{CD}_2\text{Cl}_2$ )**  $\delta$  168.9, 149.5, 148.5, 128.8, 126.9, 111.8, 110.1, 109.5, 81.6, 71.1, 56.2, 56.1, 49.4, 38.3, 28.5, 27.0. **HRMS (ESI,  $m/z$ )** calcd. for  $\text{C}_{18}\text{H}_{24}\text{N}_2\text{O}_5\text{Na}[\text{M}+\text{Na}]^+$ : 371.1577, found: 371.1588

## Compound 2u



Starting from **1u** (51.0 mg, 0.20 mmol) according to the general procedure to provide **2u** as a white solid (20.2 mg, 31% yield). Enantiomeric excess was established by HPLC analysis as 89% ee (column: Daicel Chiralpak IA column 250 x 4.6 mm, absorption:  $\lambda = 220$  nm, mobile phase: *n*-Hexane/isopropanol = 90:10, flow rate 1.0 mL/min, column temperature: 30 °C, retention times:  $t_r$  (major) = 7.7 min,  $t_r$  (minor) = 8.7 min).  $[\alpha]_D^{22} = +43.0^\circ$  ( $c = 1.0$ ,  $\text{CH}_2\text{Cl}_2$ ).  **$^1\text{H}$  NMR (300 MHz,  $\text{CDCl}_3$ )**  $\delta$  9.36 (s, 1H), 7.50 (d,  $J = 7.7$  Hz, 1H), 7.39 (d,  $J = 8.1$  Hz, 1H), 7.25-7.17 (m, 1H), 7.12 (t,  $J = 7.0$  Hz, 1H), 6.36 (s, 1H), 4.62 (dd,  $J = 13.2, 5.3$  Hz, 1H), 4.19-4.05 (m, 1H), 3.92 (dd,  $J = 15.8, 2.0$  Hz, 1H), 3.19 (td,  $J = 12.2, 4.6$  Hz, 1H), 3.08-2.90 (m, 1H), 2.80 (dd,  $J = 15.3, 4.8$  Hz, 1H), 1.55 (s, 9H).  **$^{13}\text{C}$  NMR (75 MHz,  $\text{CDCl}_3$ )**  $\delta$  167.6, 155.2, 136.1, 126.1, 123.1, 119.9, 118.9, 111.7, 109.6, 82.4, 68.6, 49.3, 38.7, 28.4, 20.8. **HRMS (ESI,  $m/z$ )** calcd. for  $\text{C}_{18}\text{H}_{21}\text{N}_3\text{O}_3\text{Na}[\text{M}+\text{Na}]^+$ : 350.1475, found: 350.1475.

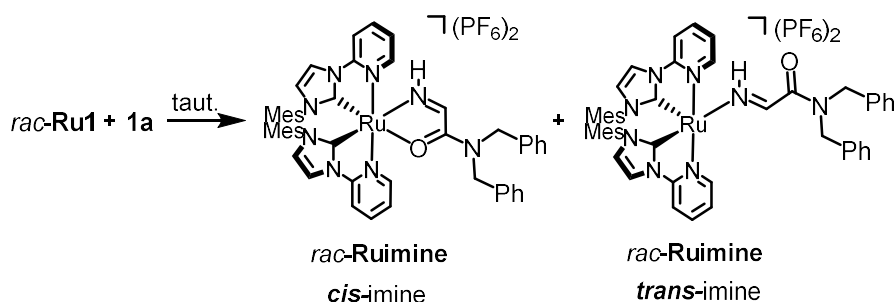
## Compound 2a'



Starting from **1a** (56.0 mg, 0.20 mmol) according to the general procedure using  $\text{Cbz}_2\text{O}$  instead of  $\text{Boc}_2\text{O}$  to provide **2a'** as a white solid (45.6 mg, 59% yield). Enantiomeric excess was established by HPLC analysis as 91% ee (column: Daicel Chiralpak ASH column 250 x 4.6 mm, absorption:  $\lambda = 220$  nm, mobile phase: *n*-Hexane/isopropanol = 40:60, flow rate 1.0 mL/min, column temperature: 30 °C, retention times:  $t_r$  (major) = 11.6 min,  $t_r$  (minor) = 40.8 min).  $[\alpha]_D^{22} = +30.6^\circ$  ( $c = 1.0$ ,  $\text{CH}_2\text{Cl}_2$ ).  **$^1\text{H}$  NMR (300 MHz,  $\text{CD}_2\text{Cl}_2$ )**  $\delta$  7.53-7.08 (m, 14H), 6.88 (s, 1H), 5.89-5.57 (m, 1H), 5.19-4.79 (m, 3H), 4.26 (s, 2H), 3.52-3.27 (m, 1H).  **$^{13}\text{C}$  NMR (75 MHz,  $\text{CD}_2\text{Cl}_2$ )**  $\delta$  167.5, 153.5, 137.7, 136.7, 135.8, 131.0, 129.9, 129.3, 129.2, 128.8, 128.6, 128.6, 128.3, 128.0, 75.1, 67.7, 49.0, 43.7. **HRMS (ESI,  $m/z$ )** calcd. for  $\text{C}_{24}\text{H}_{22}\text{N}_2\text{O}_3\text{Na}[\text{M}+\text{Na}]^+$ : 409.1523, found: 409.1519.

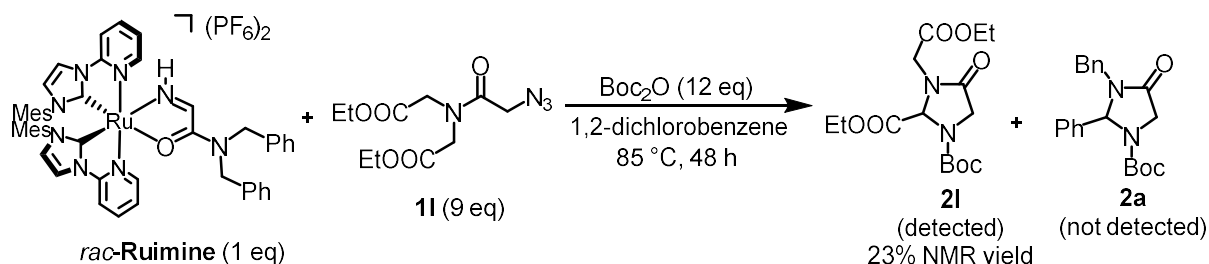
## 4.2.4 Mechanistic Studies

## a) Ru-imine complex formation under mild conditions



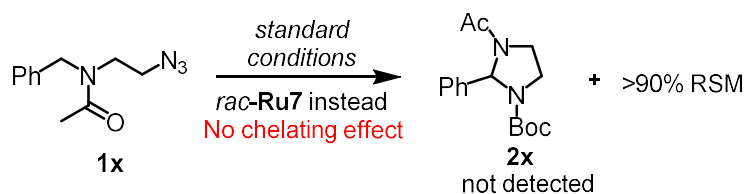
**Reaction at room temperature:** To a solution of *rac*-**Ru1** (50.1 mg, 0.05 mmol) in 0.5 mL mixed solvent (CH<sub>2</sub>Cl<sub>2</sub>:1,2-dichlorobenzene = 1:1) was added **1a** (28.0 mg, 0.05 mmol). After stirring at room temperature for 24 h, the above solution was concentrated under reduced pressure and subsequently purified by fast flash column (CH<sub>2</sub>Cl<sub>2</sub>:EtOAc = 2:1) to afford *rac*-**Ruimine** (58.7 mg, quantitative yield). The <sup>1</sup>H NMR analysis of the crude reaction solution showed only *cis*-imine formation. Spectrum analysis of *rac*-**Ruimine**: <sup>1</sup>H NMR (300 MHz, CD<sub>2</sub>Cl<sub>2</sub>) δ 12.09 (d, *J* = 11.7 Hz, 1H), 8.99 (d, *J* = 11.7 Hz, 1H), 8.00 (d, *J* = 2.3 Hz, 1H), 7.90 (d, *J* = 2.3 Hz, 1H), 7.86-7.70 (m, 2H), 7.54 (dd, *J* = 18.1, 5.0 Hz, 3H), 7.44 -7.31 (m, 4H), 7.18-7.02 (m, 5H), 6.92 (td, *J* = 5.5, 2.9 Hz, 4H), 6.75 (d, *J* = 7.3 Hz, 2H), 6.65 (d, *J* = 5.3 Hz, 2H), 6.52 (d, *J* = 7.0 Hz, 2H), 5.00-4.77 (m, 3H), 4.43 (d, *J* = 14.9 Hz, 1H), 2.16 (d, *J* = 5.9 Hz, 6H), 2.02 (s, 3H), 1.89 (s, 3H), 1.51 (s, 3H), 1.47 (s, 3H). <sup>13</sup>C NMR (75 MHz, CD<sub>2</sub>Cl<sub>2</sub>) δ 192.2, 190.8, 169.5, 163.8, 153.4, 153.1, 151.6, 149.6, 140.3, 138.5, 138.1, 135.8, 135.6, 134.6, 134.4, 134.2, 134.1, 134.0, 133.7, 132.8, 130.2, 130.1, 129.6, 129.6, 128.7, 127.7, 127.6, 125.9, 125.7, 123.2, 122.7, 117.5, 117.1, 111.4, 110.7, 52.2, 21.0, 20.9, 17.8, 17.5, 17.2, 17.1. <sup>19</sup>F NMR (282 MHz, CD<sub>2</sub>Cl<sub>2</sub>) δ -71.97, -74.50. HRMS (ESI, *m/z*) calcd. for C<sub>50</sub>H<sub>50</sub>N<sub>8</sub>OP<sub>1</sub>F<sub>6</sub>[M-PF<sub>6</sub>]<sup>+</sup>: 1025.2787, found: 1025.2823. IR (film): ν (cm<sup>-1</sup>) 3670, 3294, 2921, 2249, 2178, 2096, 2012, 1650, 1609, 1484, 1451, 1421, 1376, 1330, 1301, 1255, 1158, 1130, 1081, 1030, 931, 831, 766, 741, 698, 587, 554, 500, 453, 411.

**Reaction at 85 °C:** To a solution of *rac*-**Ru1** (50.1 mg, 0.05 mmol) in 0.5 mL 1,2-dichlorobenzene was added **1a** (28.0 mg, 0.1 mmol). After stirring at 85 °C for 1 h the reaction was complete. <sup>1</sup>H NMR analysis showed a ratio of *cis*-imine to *trans*-imine at 1:1.5 (*trans*-imine is not stable enough to be purified). Thus, this indicates that the amide group dissociates at high temperature which is in consistent with our mechanistic proposal.

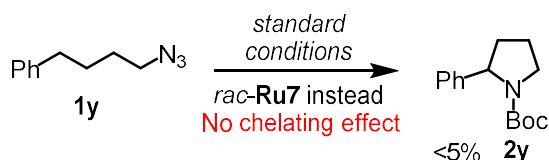


To a solution of *rac*-**Ruimine** (11.7 mg, 0.01 mmol) in 0.5 mL 1,2-dichlorobenzene was added **11** (24.5 mg, 0.18 mmol). After stirring at 85 °C for 48 h only **21** was detected from <sup>1</sup>H NMR. It was noteworthy that **2a** was not detected which indicates that the Ru-nitrene→imine tautomerization is irreversible.

### b) Probing presence and position of the amide group

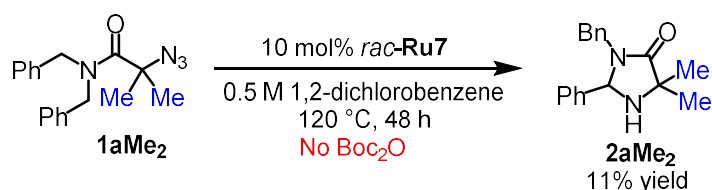


**1x** (43.6 mg, 0.2 mmol) and *rac*-**Ru7** (2.3 mg, 0.002 mmol) in 0.2 mL 1,2-dichlorobenzene were stirred at 85 °C under N<sub>2</sub> atmosphere for 24 h. To the resulting solution was added Cl<sub>2</sub>CHCHCl<sub>2</sub> as internal standard. The <sup>1</sup>H NMR analysis of the above solution showed >90% remaining starting material.



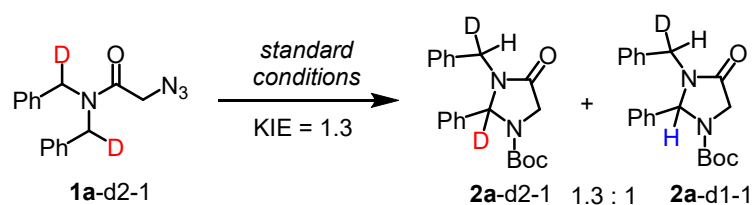
**1y** (35.1 mg, 0.2 mmol) and *rac*-**Ru7** (2.3 mg, 0.002 mmol) in 0.2 mL 1,2-dichlorobenzene were stirred at 85 °C under N<sub>2</sub> atmosphere for 24 h. To the resulting solution was added Cl<sub>2</sub>CHCHCl<sub>2</sub> as internal standard. The <sup>1</sup>H NMR analysis of the above solution showed <5% formation of **2y** and >90% remained starting material.

### c) Isolated C–H amination product without Boc<sub>2</sub>O



**1aMe<sub>2</sub>** (30.8 mg, 0.1 mmol) and *rac*-**Ru7** (11.5 mg, 0.01 mmol) in 0.2 mL 1,2-dichlorobenzene were stirred at 120 °C under N<sub>2</sub> atmosphere for 48 h. The above solution was transformed to a flash silica gel column and purified (*n*-hexane:EtOAc:Et<sub>3</sub>N = 1:1:0.001) to afford **2aMe<sub>2</sub>** (3.1 mg, 11% yield). **2aMe<sub>2</sub>**: <sup>1</sup>H NMR (300 MHz, CDCl<sub>3</sub>) δ 7.44-7.37 (m, 3H), 7.30-7.26 (m, 1H), 7.25-7.20 (m, 4H), 7.06-6.94 (m, 2H), 5.05 (s, 1H), 5.01 (d, *J* = 14.5 Hz, 1H), 3.53 (d, *J* = 14.5 Hz, 1H), 1.82 (s, br, 1H), 1.46 (s, 3H), 1.28 (s, 3H). <sup>13</sup>C NMR (75 MHz, CDCl<sub>3</sub>) δ 178.2, 138.2, 136.0, 129.5, 129.1, 128.6, 128.4, 127.7, 127.4, 73.2, 59.5, 44.5, 25.7, 24.5. HRMS (ESI, *m/z*) calcd. for C<sub>18</sub>H<sub>21</sub>N<sub>2</sub>O [M+H]<sup>+</sup>: 281.1648, found: 281.1657.

#### d) Kinetic isotope effects



**1a-d2-1** (56.0 mg, 0.2 mmol) and *rac*-**Ru7** (2.3 mg, 0.002 mmol) in 0.2 mL 1,2-dichlorobenzene were stirred at 85 °C under N<sub>2</sub> atmosphere for 48 h (standard conditions). The <sup>1</sup>H NMR analysis of the above solution showed a ratio of **2a-d2-1**:**2a-d1-1** = 1.3:1. The peaks from 5.5 to 5.7 ppm belong to **2a-d2-1** (blue H), and the peaks from 4.1 to 4.2 belong to **2a-d2-1** and **2a-d1-1** (green dot). Thus, we calculated the ratio of **2a-d2-1** to **2a-d1-1** as 1.3 to 1.

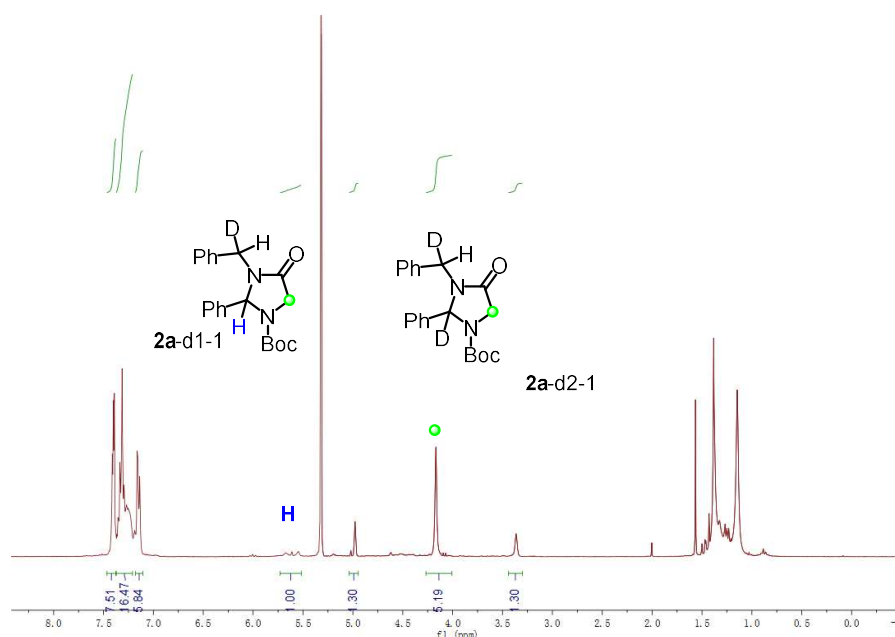
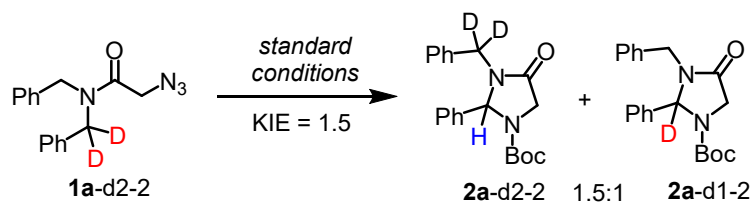


**Figure 74.** <sup>1</sup>H NMR of **2a-d2-1** reaction analysis.



**1a-d2-2** (56.0 mg, 0.2 mmol) and *rac*-**Ru7** (2.3 mg, 0.002 mmol) in 0.2 mL 1,2-dichlorobenzene were stirred at 85 °C under N<sub>2</sub> atmosphere for 48 h. The <sup>1</sup>H NMR analysis of the above solution showed a ratio of **2a-d2-2**:**2a-d1-2** = 1.5:1. The peaks from 4.1 to 4.2 ppm belong to **2a-d2-2** and **2a-d1-2** (green dot), and the peak from 3.25 to 3.35 ppm belongs to **2a-d1-2** (blue H). Thus, we calculated the ratio of **2a-d2-2** to **2a-d1-2** as 1.5 to 1.

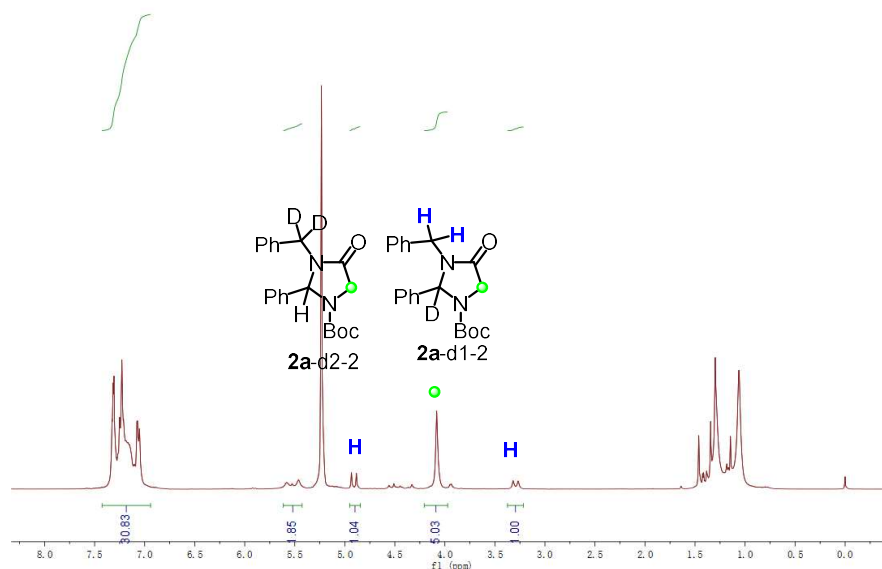
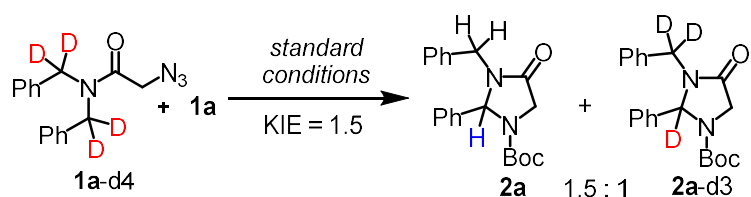


**Figure 75.** <sup>1</sup>H NMR of **2a-d2-2** reaction analysis.



**1a-d4** (56.0 mg, 0.2 mmol) and *rac*-**Ru7** (2.3 mg, 0.002 mmol) in 0.2 mL 1,2-dichlorobenzene were stirred at 85 °C under N<sub>2</sub> atmosphere for 16 h. The <sup>1</sup>H NMR analysis of the above solution showed a ratio of **2a**:**2a-d3** = 1.5:1. The peak from 4.1 to 4.2 ppm belongs to **2a** and **2a-d3** (green dot), and the peak from 3.25 to 3.35 ppm belongs to **2a** (blue H). Thus, we calculated the ratio of **2a** to **2a-d3** as 1.5 to 1.

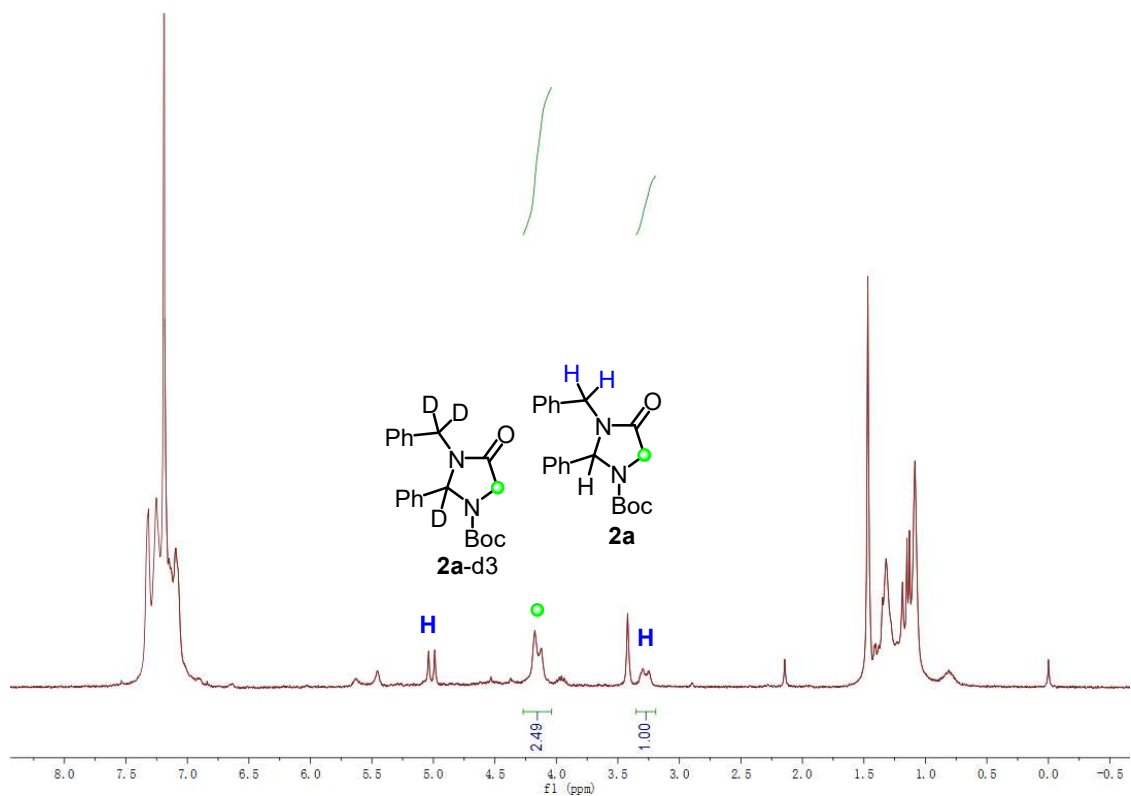
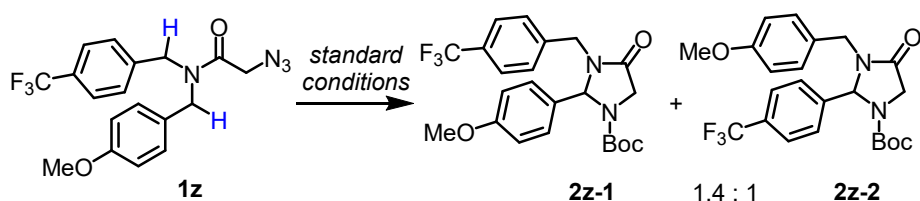


Figure 76.  $^1\text{H}$  NMR of **2a** and **2a-d4** reaction analysis.

### e) Competition experiment



**1z** (75.6 mg, 0.2 mmol) and *rac*-**Ru7** (2.3 mg, 0.002 mmol) in 0.2 mL 1,2-dichlorobenzene were stirred at 85 °C under  $\text{N}_2$  atmosphere for 48 h. The resulting solution was concentrated under vacuo and purified by flash silical gel column (*n*-hexane:EtOAc = 3:1) to afford a mixture of **2z-1** and **2z-2** (79% total yield).  $^1\text{H}$  NMR analysis showed a ratio of the products of 1.4:1.



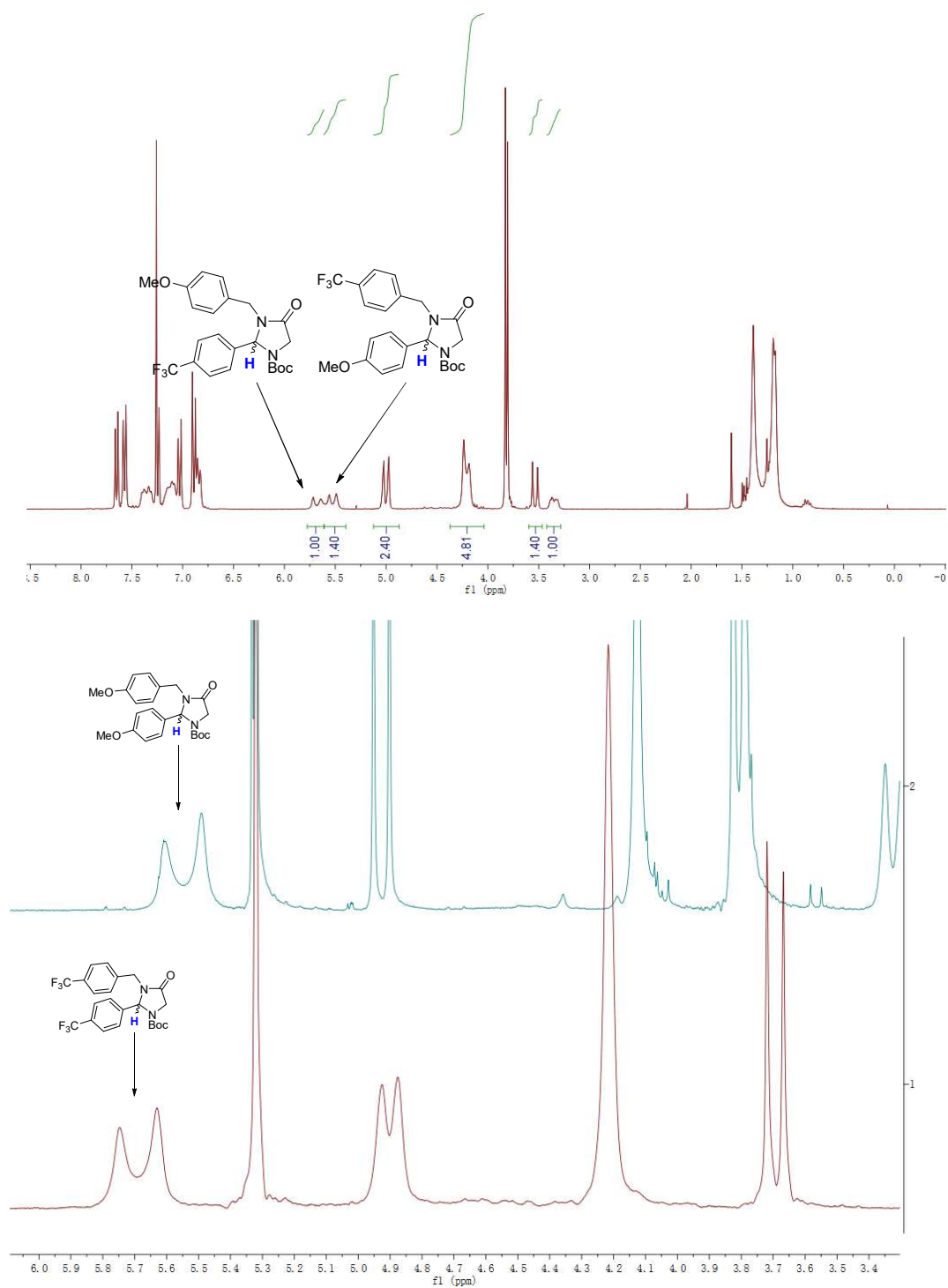


Figure 77.  $^1\text{H}$  NMR of competition experiment analysis.

### 4.2.5 Single Crystal X-Ray Diffraction Studies

Single crystals of (*S*)-**2e** were obtained by slow diffusion from the solution in EtOAc layered with *n*-hexane at room temperature.

Single crystals of *rac*-**Ruimine** were obtained by slow volatilization from the solution in CDCl<sub>3</sub> and CH<sub>2</sub>Cl<sub>2</sub> (ratio = 1:1) at room temperature.

Data was collected with an STOE STADIVARI diffractometer equipped with with CuK<sub>α</sub> radiation, a graded multilayer mirror monochromator ( $\lambda = 1.54178 \text{ \AA}$ ) and a DECTRIS PILATUS 300K detector using an oil-coated shock-cooled crystal at 100(2) K. Absorption effects were corrected semi-empirical using multiscanned reflexions (STOE LANA, absorption correction by scaling of reflection intensities.). Cell constants were refined using 72887 of observed reflections of the data collection. The structure was solved by direct methods by using the program XT V2014/1 (Bruker AXS Inc., 2014) and refined by full matrix least squares procedures on  $F^2$  using SHELXL-2018/3 (Sheldrick, 2018). The non-Hydrogen atoms have been refined anisotropically, carbon bonded hydrogen atoms were included at calculated positions and refined using the 'riding model' with isotropic temperature factors at 1.2 times (for CH<sub>3</sub> groups 1.5 times) that of the preceding carbon atom. CH<sub>3</sub> groups were allowed to rotate about the bond to their next atom to fit the electron density. Nitrogen bonded hydrogen atoms were located and allowed to refine isotropically. Disordered solvent contribution to the calculated structure factors were calculated by using the PLATON/SQUEEZE procedure. Crystallographic data for *rac*-**Ruimine** has been deposited with the Cambridge Crystallographic Data Centre as supplementary publication number CCDC 1857105. Absolute configuration could be established: The Flack parameter refined to -0.005(14). Crystallographic data for (*S*)-**2e** has been deposited with the Cambridge Crystallographic Data Centre as supplementary publication number CCDC 1857104.

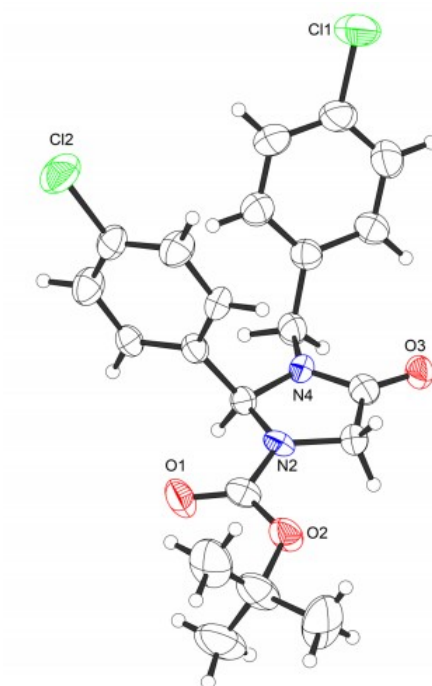


Figure 78. Crystal structure of compound (S)-2e.

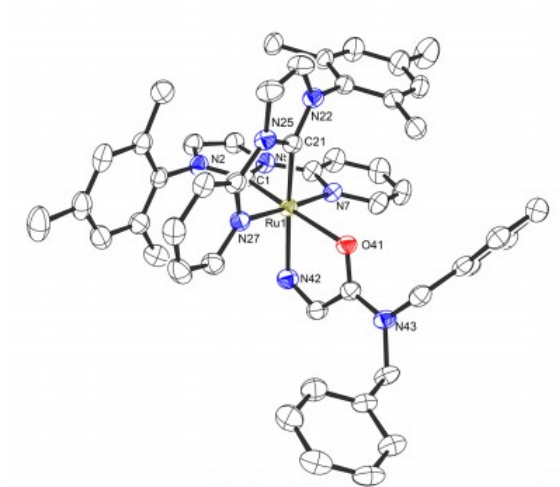


Figure 79. Crystal structure of compound *rac*-Ruimine.

**Table 5.** Crystal data and structure refinement for (*S*)-**2e**.

Habitus, colour	needle, colourless
Crystal size	0.21 x 0.06 x 0.04 mm <sup>3</sup>
Crystal system	Monoclinic
Space group	P2 <sub>1</sub> <span style="float: right;">Z = 4</span>
Unit cell dimensions	a = 12.8650(8) Å <span style="float: right;">= 90°.</span> b = 6.1505(3) Å <span style="float: right;">= 101.330(5)°.</span> c = 27.0802(15) Å <span style="float: right;">= 90°.</span>
Volume	2101.0(2) Å <sup>3</sup>
Cell determination	6303 peaks with Theta 3.5 to 67.1°.
Empirical formula	C <sub>21</sub> H <sub>22</sub> Cl <sub>2</sub> N <sub>2</sub> O <sub>3</sub>
Moiety formula	C <sub>21</sub> H <sub>22</sub> Cl <sub>2</sub> N <sub>2</sub> O <sub>3</sub>
Formula weight	421.30
Density (calculated)	1.332 Mg/m <sup>3</sup>
Absorption coefficient	2.978 mm <sup>-1</sup>
F(000)	880
Diffraction type	STOE STADIVARI
Wavelength	1.54186 Å
Temperature	230(2) K
Theta range for data collection	3.504 to 68.472°.
Index ranges	-14<=h<=14, -7<=k<=7, -31<=l<=32
Data collection software	X-Area Pilatus3_SV 1.31.127.0 (STOE, 2016) <sup>2</sup>
Cell refinement software	X-Area Recipe 1.33.0.0 (STOE, 2015) <sup>3</sup>
Data reduction software	X-Area Integrate 1.71.0.0 (STOE, 2016) <sup>4</sup> X-Area LANA 1.68.2.0 (STOE, 2016) <sup>5</sup> MERGEHKL5 (Lutz, 2016) <sup>6</sup>
Reflections collected	38035
Independent reflections	8441 [R(int) = 0.0686]
Completeness to theta = 67.686°	98.2 %
Observed reflections	5312[I > 2σ(I)]
Reflections used for refinement	8441
Extinction coefficient	X = 0.0033(3)
Absorption correction	Semi-empirical from equivalents <sup>7</sup>
Max. and min. transmission	0.7032 and 0.1984
Flack parameter (absolute struct.)	-0.005(14) <sup>8</sup>
Largest diff. peak and hole	0.279 and -0.252 e.Å <sup>-3</sup>
Solution	dual space <sup>9</sup>
Refinement	Full-matrix least-squares on F <sup>2</sup>

## Chapter 4. Experimental Part

---

Treatment of hydrogen atoms	Calculated positions, constr. ref.
Programs used	XT V2014/1 (Bruker AXS Inc., 2014) <sup>10</sup> SHELXL-2018/1 (Sheldrick, 2018) DIAMOND (Crystal Impact) ShelXle (Hübschle, Sheldrick, Dittrich, 2011)
Data / restraints / parameters	8441 / 1 / 513
Goodness-of-fit on $F^2$	0.899
R index (all data)	wR2 = 0.1031
R index conventional [I>2sigma(I)]	R1 = 0.0449

**Table 6.** Crystal data and structure refinement for *rac*-Ruimine.

Habitus, colour	prism, red
Crystal size	0.17 x 0.14 x 0.06 mm
Crystal system	Monoclinic
Space group	P2 <sub>1</sub> /c <span style="float: right;">Z = 4</span>
Unit cell dimensions	a = 19.4935(2) Å <span style="float: right;">= 90°.</span> b = 25.6083(3) Å <span style="float: right;">= 97.5930(10)°.</span> c = 23.9361(3) Å <span style="float: right;">= 90°.</span>
Volume	11844.0(2) Å <sup>3</sup>
Cell determination	72887 peaks with Theta 2.5 to 76.2°.
Empirical formula	C <sub>103</sub> H <sub>104.50</sub> Cl <sub>7.50</sub> F <sub>24</sub> N <sub>16</sub> O <sub>2</sub> P <sub>4</sub> Ru <sub>2</sub>
Moiety formula	2(C <sub>50</sub> H <sub>49</sub> N <sub>8</sub> O Ru), 4(F <sub>6</sub> P), 1.5(C H Cl <sub>3</sub> ), 1.5(C H <sub>2</sub> Cl <sub>2</sub> )
Formula weight	2646.41
Density (calculated)	1.484 Mg/m <sup>3</sup>
Absorption coefficient	4.930 mm <sup>-1</sup>
F(000)	5368
Diffractometer type	STOE STADIVARI
Wavelength	1.54178 Å
Temperature	100(2) K
Theta range for data collection	2.539 to 75.866°.
Index ranges	-24 ≤ h ≤ 23, -30 ≤ k ≤ 32, -18 ≤ l ≤ 29
Data collection software	X-Area Pilatus3_SV 1.31.127.0 (STOE, 2016) <sup>2</sup>
Cell refinement software	X-Area Recipe 1.33.0.0 (STOE, 2015) <sup>3</sup>
Data reduction software	X-Area Integrate 1.71.0.0 (STOE, 2016) <sup>4</sup> X-Area LANA 1.68.2.0 (STOE, 2016) <sup>5</sup> PLATON/SQUEEZE (Spek, 2015) <sup>6</sup>
Reflections collected	130276
Independent reflections	24295 [R(int) = 0.0654]
Completeness to theta = 67.679°	99.8 %
Observed reflections	18362 [I > 2σ(I)]
Reflections used for refinement	24295
Absorption correction	Semi-empirical from equivalents <sup>7</sup>
Max. and min. transmission	0.3444 and 0.0969
Largest diff. peak and hole	1.721 and -0.919 e.Å <sup>-3</sup>
Solution	intrinsic phases <sup>8</sup>
Refinement	Full-matrix least-squares on F <sup>2</sup> <sup>9</sup>
Treatment of hydrogen atoms	CH calculated, “riding”, NH located, isotr. ref.
Programs used	XT V2014/1 (Bruker AXS Inc., 2014) <sup>10</sup> SHELXL-2018/3 (Sheldrick, 2018)

## Chapter 4. Experimental Part

---

	DIAMOND (Crystal Impact)
	ShelXle (Hübschle, Sheldrick, Dittrich, 2011)
Data / restraints / parameters	24295 / 32 / 1524
Goodness-of-fit on $F^2$	1.052
R index (all data)	wR2 = 0.1293
R index conventional [I>2sigma(I)]	R1 = 0.0470

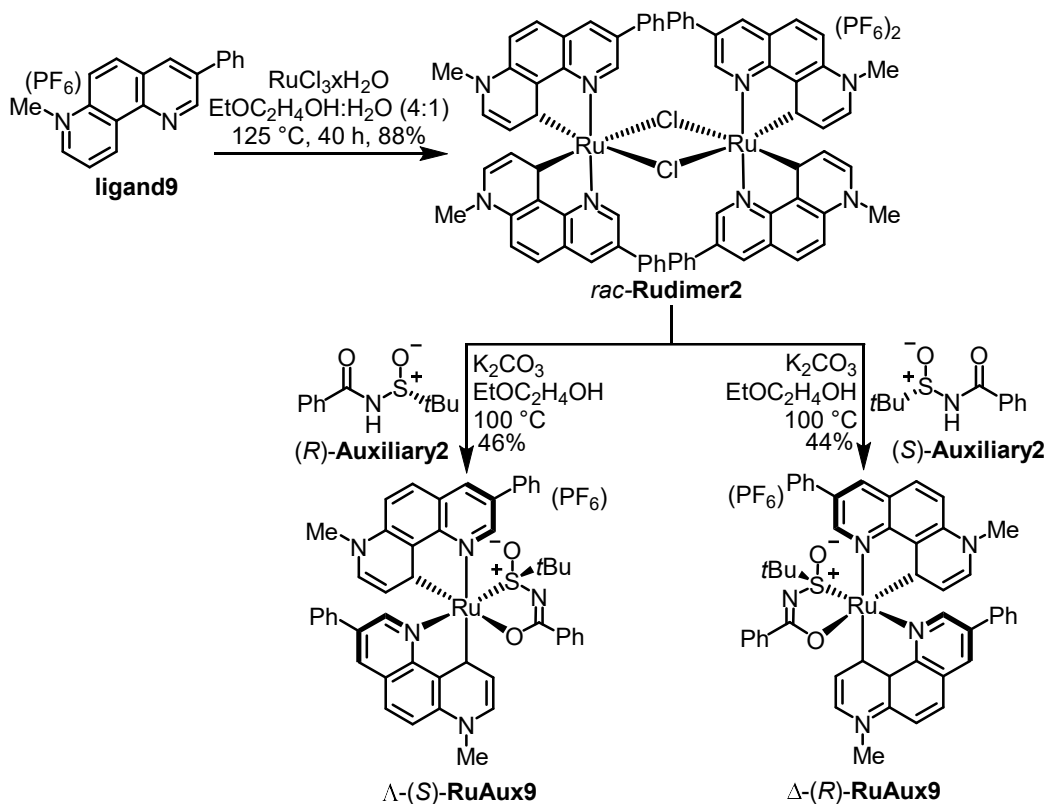
## References

1. *X-Area Recipe*, STOE & Cie GmbH, Darmstadt, Germany, **2015**.
2. *X-Area Pilatus3\_SV*, STOE & Cie GmbH, Darmstadt, Germany, **2016**.
3. *X-Area Integrate*, STOE & Cie GmbH, Darmstadt, Germany, **2016**.
4. *X-Area LANA*, STOE & Cie GmbH, Darmstadt, Germany, **2016**.
5. Martin Lutz, *MERGEHKL5*, Laboratory for Crystal and Structural Chemistry, Bijvoet Center for Biomolecular Research, Padualaan 8, NL-3584 CH Utrecht, The Netherlands., **2016**.
6. S. Parsons, H. D. Flack, T. Wagner, *Acta Crystallogr., Sect. B: Struct. Sci., Cryst. Eng. Mater.* **2013**, *69*, 249.
7. G. M. Sheldrick, *Acta Crystallogr A Found Adv* **2015**, *71*, 3.
8. G. M. Sheldrick, *Acta crystallographica. Section C, Structural chemistry* **2015**, *71*, 3.
9. K. Brandenburg, *Diamond - Crystal and Molecular Structure Visualization*, Crystal Impact - Dr. H. Putz & Dr. K. Brandenburg GbR, Bonn, Germany, **2014**.
10. C. B. Hübschle, G. M. Sheldrick, B. Dittrich, *Journal of applied crystallography* **2011**, *44*, 1281.



4.3 Enantioselective Synthesis of  $\gamma$ -Lactams by Intramolecular C–H Amidation

## 4.3.1 Synthesis of the Ruthenium Catalysts

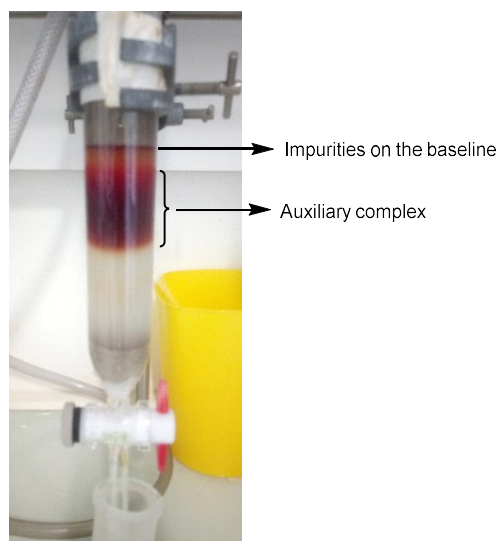


**Synthesis of *rac*-Rudimer2:** To a 10 mL Schlenk tube was added **ligand9** (125 mg, 0.3 mmol),  $RuCl_3 \cdot xH_2O$  (31 mg, 0.15 mmol) and 3.0 mL solvent mixture ( $EtOC_2H_4OH:H_2O = 4:1$ ). The resulting solution was heated at  $125^\circ C$  for 40 h. After that, 50 mg  $NH_4PF_6$  dissolved in 0.5 mL deionized  $H_2O$  was added to the reaction solution. Ultrasonic was used for 3 min to achieve counteranion exchange. The liquid phase was removed by filtration and the resulting residue was washed with water (3 x 3 mL) and  $Et_2O$  (3 x 5 mL). The resulting residue was dried under high *vacuo* to provide crude *rac*-**Rudimer2** (108 mg, 88% yield) as dark purple solid for the next step without further purification.

**Synthesis of  $\Delta$ -(S)-RuAux9:** To a 10 mL Schlenk tube was added *rac*-**Rudimer2** (164 mg, 0.1 mmol), (*R*)-*N*-(*tert*-butylsulfinyl)benzamide (34 mg, 0.15 mmol),  $K_2CO_3$  (27.6 mg, 0.2 mmol) and  $EtOC_2H_4OH$  (3 mL) in sequence. The resulting solution was heated at  $100^\circ C$  for 16 h. After that, solvent was removed under high *vacuo*. After cooling to room temperature,  $NH_4PF_6$  (50 mg) in MeOH (3 mL) was added and stirred at room temperature for 30 min. Organic solvent was removed under *vacuo*. The resulting residue was diluted with  $CH_2Cl_2$  and purified by flash chromatography (see

details below) to provide analytical pure  $\Lambda$ -(*S*)-**RuAux9** (93 mg, 46% yield) as dark red solid.

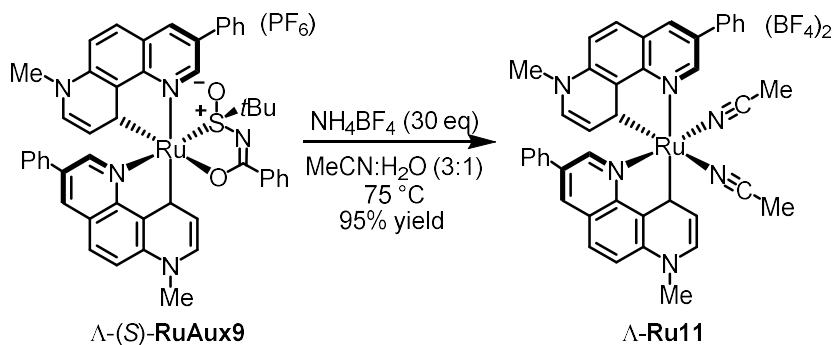
Procedures for the purification of  $\Lambda$ -(*S*)-**RuAux9**: First, 400 mL CH<sub>2</sub>Cl<sub>2</sub>:MeOH = 50:1 was used as eluent. After that, 300 mL CH<sub>2</sub>Cl<sub>2</sub>:MeOH = 20:1 was used. Next, 300 mL CH<sub>2</sub>Cl<sub>2</sub>:MeOH = 10:1 was used to provide the desired compound  $\Lambda$ -(*S*)-**RuAux9** with 95% <sup>1</sup>H NMR purity. A second short flash column was performed to remove some ruthenium complex decomposition products during the first column. For this second column, 600 mL CH<sub>2</sub>Cl<sub>2</sub>:MeOH = 15:1 was used to remove impurities on the baseline (see below).



$\Lambda$ -(*S*)-**RuAux9**: <sup>1</sup>H NMR (500 MHz, CD<sub>3</sub>CN)  $\delta$  10.11 (d, *J* = 6.9 Hz, 1H), 9.50 (d, *J* = 2.0 Hz, 1H), 9.00 (d, *J* = 2.0 Hz, 1H), 8.49 (d, *J* = 9.3 Hz, 1H), 8.43 (d, *J* = 1.9 Hz, 1H), 8.22-8.12 (m, 3H), 8.09 (d, *J* = 9.3 Hz, 1H), 7.99 (dd, *J* = 13.3, 8.1 Hz, 2H), 7.73-7.64 (m, 2H), 7.56 (d, *J* = 1.9 Hz, 1H), 7.48 (ddd, *J* = 22.7, 10.4, 5.4 Hz, 5H), 7.34 (dddd, *J* = 11.8, 8.9, 6.1, 4.7 Hz, 6H), 7.19-7.07 (m, 2H), 4.13 (s, 3H), 3.97 (s, 3H), 0.56 (s, 9H). <sup>13</sup>C NMR (126 MHz, CD<sub>3</sub>CN)  $\delta$  177.6, 151.8, 151.5, 150.7, 150.3, 142.2, 141.8, 138.1, 137.1, 136.8, 136.2, 136.1, 136.0, 135.7, 135.6, 135.6, 135.3, 135.3, 134.3, 133.4, 132.1, 131.9, 130.5, 130.3, 130.2, 130.1, 129.7, 129.0, 128.2, 127.6, 127.2, 125.9, 120.7, 120.4, 68.0, 55.3, 43.1, 42.9, 28.4, 23.7. <sup>19</sup>F NMR (283 MHz, CD<sub>3</sub>CN)  $\delta$  -71.02, -73.52. IR (film):  $\nu$  (cm<sup>-1</sup>) 1612, 1531, 1504, 1455, 1330, 1173, 830, 779, 718, 669, 586, 556, 491, 428, 398. HRMS (ESI, *m/z*) calcd. for C<sub>49</sub>H<sub>42</sub>N<sub>5</sub>O<sub>2</sub>Ru<sub>1</sub>S<sub>1</sub> [M-PF<sub>6</sub>]<sup>+</sup>: 866.2110, found: 866.2117.

**Synthesis of  $\Delta$ -(*R*)-**RuAux9****: Identical synthetic procedures as for  $\Lambda$ -(*S*)-**RuAux10** but with slightly reduced yield (89 mg, 44% yield).

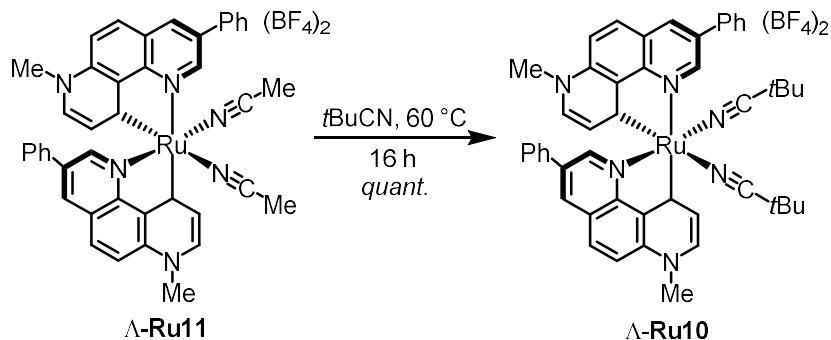
$\Delta$ -(*R*)-**RuAux9**: Dark red solid. Analytical data of  $\Delta$ -(*R*)-**RuAux10** identical with  $\Lambda$ -(*S*)-**RuAux10**.



**Synthesis of  $\Lambda$ -Ru11:** To a 10 mL Schlenk tube was added  $\Lambda$ -(S)-RuAux9 (50.6 mg, 0.05 mmol) and  $\text{NH}_4\text{BF}_4$  (157 mg, 1.5 mmol) in  $\text{MeCN:H}_2\text{O} = 3:1$  (3 mL). The resulting solution was heated at 75 °C for 16 h. After that, the solution was directly transferred to a column and purified by flash chromatography (see details below) to provide analytical pure  $\Lambda$ -Ru11 (42.7 mg, 95% yield) as dark red solid.

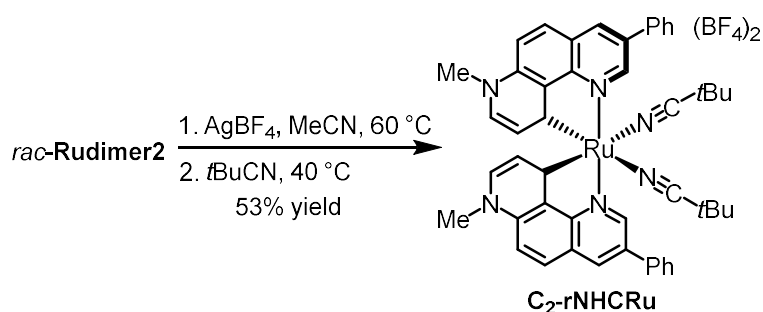
Procedures for the purification of  $\Lambda$ -Ru11: First,  $\text{CH}_2\text{Cl}_2:\text{MeCN} = 20:1$  (300 mL) was used as eluent to remove the recovered auxiliary. Secondly, pure MeCN (200 mL) was used as eluent to provide the desired compound  $\Lambda$ -Ru11 mixed with  $\text{NH}_4\text{BF}_4$ . Finally, the excess  $\text{NH}_4\text{BF}_4$  was removed by running a short celite column using  $\text{CH}_2\text{Cl}_2:\text{MeCN} = 20:1$  (60 mL). The solvent was removed under *vacuo* to provide analytical pure  $\Lambda$ -Ru11 as red solid.

**$\Lambda$ -Ru11:**  $^1\text{H NMR}$  (500 MHz,  $\text{CD}_3\text{CN}$ )  $\delta$  9.98 (d,  $J = 2.0$  Hz, 1H), 9.04 (d,  $J = 2.0$  Hz, 1H), 8.68 (d,  $J = 6.5$  Hz, 1H), 8.53 (dd,  $J = 16.6, 5.6$  Hz, 2H), 8.35 (d,  $J = 9.3$  Hz, 1H), 8.20 (d,  $J = 9.3$  Hz, 1H), 8.13-8.04 (m, 4H), 8.02 (d,  $J = 1.9$  Hz, 1H), 7.74-7.66 (m, 2H), 7.61 (ddd,  $J = 7.4, 4.0, 1.2$  Hz, 1H), 7.41-7.23 (m, 6H), 7.04 (d,  $J = 6.5$  Hz, 1H), 4.30 (s, 3H), 4.04 (s, 3H), 2.17 (s, 3H), 1.96 (s, 3H).  $^{13}\text{C NMR}$  (126 MHz,  $\text{CD}_3\text{CN}$ )  $\delta$  154.1, 153.8, 151.9, 150.6, 142.7, 142.1, 138.2, 137.6, 137.6, 137.1, 136.7, 136.0, 135.8, 135.1, 134.9, 134.6, 133.9, 133.7, 132.9, 132.4, 130.6, 130.2, 130.0, 129.7, 128.7, 128.0, 127.0, 126.6, 126.1, 125.4, 120.3, 119.9, 43.3, 43.1, 4.2.  $^{19}\text{F NMR}$  (283 MHz,  $\text{CD}_3\text{CN}$ )  $\delta$  -151.08, -151.13.



**Synthesis of  $\Lambda\text{-Ru10}$ :**  $\Lambda\text{-Ru11}$  (20 mg) was dissolved in 3 mL pivalonitrile and heated at 60 °C for 16 h. After that, the solvent was removed under *vacuo* to provide  $\Lambda\text{-Ru10}$  as a red solid in quantitative yield.

**$\Lambda\text{-Ru10}$ :**  $^1\text{H NMR}$  (300 MHz,  $\text{CD}_3\text{CN}$ )  $\delta$  9.97 (d,  $J = 2.0$  Hz, 1H), 9.04 (d,  $J = 2.0$  Hz, 1H), 8.59-8.50 (m, 3H), 8.35 (d,  $J = 9.3$  Hz, 1H), 8.20 (d,  $J = 9.3$  Hz, 1H), 8.14-7.99 (m, 5H), 7.70 (t,  $J = 7.4$  Hz, 2H), 7.62 (d,  $J = 7.3$  Hz, 1H), 7.38-7.26 (m, 6H), 7.02 (d,  $J = 6.4$  Hz, 1H), 4.30 (s, 3H), 4.04 (s, 3H), 1.34 (s, 9H), 1.17 (s, 9H).  $^{13}\text{C NMR}$  (126 MHz,  $\text{CD}_3\text{CN}$ )  $\delta$  154.0, 153.8, 151.8, 150.5, 142.6, 142.1, 138.3, 137.8, 137.6, 137.1, 136.7, 136.1, 135.8, 135.2, 134.9, 134.4, 133.9, 133.8, 133.4, 133.0, 132.0, 130.6, 130.2, 130.1, 129.7, 128.7, 128.7, 128.0, 127.0, 126.2, 120.3, 119.9, 79.2, 78.9, 78.6, 43.4, 43.2, 28.4, 28.2.  $^{19}\text{F NMR}$  (235 MHz,  $\text{CD}_3\text{CN}$ )  $\delta$  -151.82, -151.87. **IR** (film):  $\nu$  ( $\text{cm}^{-1}$ ) 1624, 1584, 1535, 1460, 1393, 1353, 1304, 1229, 1170, 1022, 931, 871, 814, 761, 726, 696, 651, 569, 518, 446.

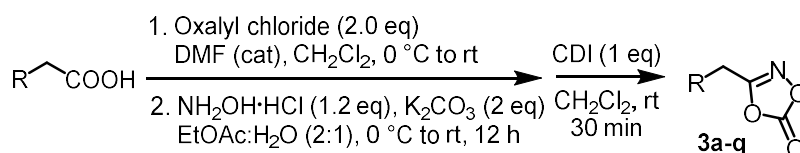


**Synthesis of  $\text{C}_2\text{-rNHCRu}$ :** To a 10 mL Schlenk tube were added *rac-Rudimer2* (33 mg, 0.02 mmol) and  $\text{AgBF}_4$  (9.7 mg, 0.05 mmol) in 3 mL MeCN. The resulting solution was heated at 60 °C for 16 h. After that, the above solution was directly transferred to a column and purified by flash chromatography ( $\text{CH}_2\text{Cl}_2\text{:MeCN} = 5\text{:}1$ ) to provide analytical pure ruthenium intermediate. The intermediate was dissolved in 2 mL pivalonitrile. The resulting solution was heated at 40 °C for 10

min. After that, organic solvent was removed under *vacuo* to provide analytical pure **C<sub>2</sub>-rNHCRu** (20.9 mg, 53% yield) as a brown solid.

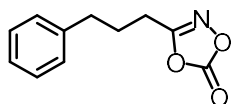
**C<sub>2</sub>-rNHCRu**: <sup>1</sup>H NMR (300 MHz, CD<sub>3</sub>CN) δ 9.86 (d, *J* = 1.8 Hz, 1H), 8.93 (d, *J* = 1.8 Hz, 1H), 8.55 (d, *J* = 9.3 Hz, 1H), 8.15 (d, *J* = 9.3 Hz, 1H), 8.09-8.03 (m, 2H), 7.73 (t, *J* = 7.4 Hz, 2H), 7.65 (d, *J* = 7.3 Hz, 1H), 7.50 (d, *J* = 6.5 Hz, 1H), 6.81 (d, *J* = 6.4 Hz, 1H), 4.08 (s, 3H), 1.38 (s, 9H). <sup>13</sup>C NMR (75 MHz, CD<sub>3</sub>CN) δ 154.6, 154.4, 142.2, 138.5, 137.9, 137.5, 134.9, 133.7, 133.4, 131.0, 130.6, 130.3, 130.1, 128.8, 128.2, 127.1, 112.0, 43.3, 28.5. <sup>19</sup>F NMR (235 MHz, CD<sub>3</sub>CN) δ -152.37, -152.42. IR (film): 1624, 1584, 1535, 1460, 1422, 1393, 1353, 1304, 1229, 1170, 1022, 931, 871, 814, 761, 726, 696, 651, 569, 518, 446.

### 4.3.2 Synthesis of the Substrates

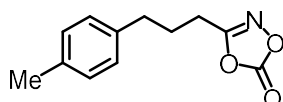


All substrates were synthesized according to the published procedures.<sup>1-3</sup>

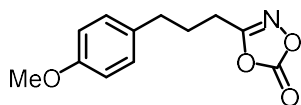
**General procedure:** Oxalyl chloride (4.0 mmol) and DMF (2 drops) were added to a solution of the carboxylic acid (2.0 mmol) in dichloromethane (30 mL) at 0 °C. The mixture was allowed to stir at room temperature for 2.5-4 h. Then, the reaction mixture was concentrated, and the crude product was used directly in the next reaction. Hydroxylamine hydrochloride (1.2 equiv) was added to a biphasic mixture of K<sub>2</sub>CO<sub>3</sub> (2.0 equiv) in a 2:1 mixture of EtOAc (16 mL) and H<sub>2</sub>O (8 mL). The resulting solution was cooled to 0 °C followed by dropwise addition of the unpurified acid chloride dissolved in a minimum amount of EtOAc under air. The flask containing the acid chloride was then rinsed with additional EtOAc. The reaction was warmed to room temperature for stirring additional 12 h. The phases were separated and the aqueous phase was extracted twice with EtOAc. The combined organic layers were dried over MgSO<sub>4</sub>, filtered, and evaporated under reduced pressure. The resulting solid was dissolved in CH<sub>2</sub>Cl<sub>2</sub> (10 mL), CDI (1 equiv) was added, and the reaction stirred at room temperature for 30 min. After that, 10 mL 1 N HCl<sub>(aq)</sub> was added to the resulting solution. The organic layer was collected and dried over MgSO<sub>4</sub>. The resulting solid was purified by flash chromatography (CH<sub>2</sub>Cl<sub>2</sub>, R<sub>f</sub> value = 0.95) to provide the desired analytical pure 1,4,2-dioxazol-5-ones.

**Compound 3a**

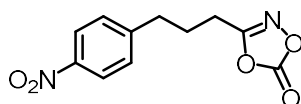
**3a**, 72% yield, colorless oil.  $^1\text{H NMR}$  (300 MHz,  $\text{CDCl}_3$ )  $\delta$  7.28-7.20 (m, 2H), 7.19-7.07 (m, 3H), 2.67 (t,  $J = 7.4$  Hz, 2H), 2.54 (t,  $J = 7.5$  Hz, 2H), 1.99 (p,  $J = 7.5$  Hz, 2H).  $^{13}\text{C NMR}$  (75 MHz,  $\text{CDCl}_3$ )  $\delta$  166.6, 154.2, 139.9, 128.8, 128.6, 126.7, 34.7, 26.0, 24.2.

**Compound 3b**

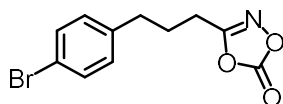
**3b**, 78% yield, white solid.  $^1\text{H NMR}$  (300 MHz,  $\text{CDCl}_3$ )  $\delta$  7.13 (d,  $J = 8.0$  Hz, 2H), 7.07 (d,  $J = 8.1$  Hz, 2H), 2.71 (t,  $J = 7.3$  Hz, 2H), 2.61 (t,  $J = 7.5$  Hz, 2H), 2.34 (s, 3H), 2.05 (p,  $J = 7.5$  Hz, 2H).  $^{13}\text{C NMR}$  (75 MHz,  $\text{CDCl}_3$ )  $\delta$  166.6, 154.2, 136.8, 136.2, 129.5, 128.5, 34.2, 26.1, 24.1, 21.1.

**Compound 3c**

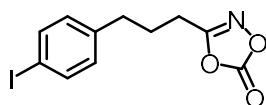
**3c**, 65% yield, colorless oil.  $^1\text{H NMR}$  (300 MHz,  $\text{CDCl}_3$ )  $\delta$  7.09 (d,  $J = 8.6$  Hz, 2H), 6.85 (d,  $J = 8.7$  Hz, 2H), 3.80 (s, 3H), 2.69 (t,  $J = 7.3$  Hz, 2H), 2.60 (t,  $J = 7.5$  Hz, 2H), 2.03 (p,  $J = 7.4$  Hz, 2H).  $^{13}\text{C NMR}$  (75 MHz,  $\text{CDCl}_3$ )  $\delta$  166.6, 158.5, 154.2, 131.9, 129.5, 114.3, 55.4, 33.8, 26.3, 24.1.

**Compound 3d**

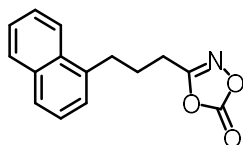
**3d**, 80% yield, white solid.  $^1\text{H NMR}$  (300 MHz,  $\text{CDCl}_3$ )  $\delta$  8.17 (d,  $J = 8.7$  Hz, 2H), 7.36 (d,  $J = 8.7$  Hz, 2H), 2.93-2.80 (m, 2H), 2.68 (t,  $J = 7.4$  Hz, 2H), 2.19-2.03 (m, 2H).  $^{13}\text{C NMR}$  (75 MHz,  $\text{CDCl}_3$ )  $\delta$  166.1, 154.0, 147.7, 147.0, 129.4, 124.1, 34.5, 25.5, 24.2.

**Compound 3e**

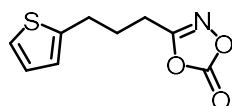
**3e**, 82% yield, white solid.  $^1\text{H NMR}$  (300 MHz,  $\text{CDCl}_3$ )  $\delta$  7.44 (d,  $J = 8.4$  Hz, 2H), 7.06 (d,  $J = 8.4$  Hz, 2H), 2.70 (t,  $J = 7.4$  Hz, 2H), 2.62 (t,  $J = 7.5$  Hz, 2H), 2.04 (p,  $J = 7.5$  Hz, 2H).  $^{13}\text{C NMR}$  (75 MHz,  $\text{CDCl}_3$ )  $\delta$  166.4, 154.1, 138.9, 131.9, 130.3, 120.5, 34.1, 25.9, 24.1.

**Compound 3f**

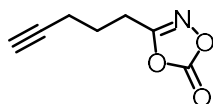
**3f**, 58% yield, white solid.  $^1\text{H NMR}$  (300 MHz,  $\text{CDCl}_3$ )  $\delta$  7.63 (d,  $J = 8.3$  Hz, 2H), 6.94 (d,  $J = 8.3$  Hz, 2H), 2.69 (t,  $J = 7.5$  Hz, 2H), 2.61 (t,  $J = 7.5$  Hz, 2H), 2.04 (p,  $J = 7.5$  Hz, 2H).  $^{13}\text{C NMR}$  (75 MHz,  $\text{CDCl}_3$ )  $\delta$  166.4, 154.1, 139.6, 137.9, 130.6, 91.8, 34.2, 25.8, 24.1.

**Compound 3g**

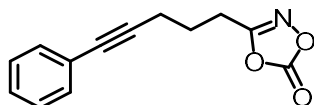
**3g**, 74% yield, white solid.  $^1\text{H NMR}$  (300 MHz,  $\text{CDCl}_3$ )  $\delta$  7.99 (d,  $J = 8.0$  Hz, 1H), 7.93-7.86 (m, 1H), 7.77 (d,  $J = 8.2$  Hz, 1H), 7.53 (pd,  $J = 6.8, 1.5$  Hz, 2H), 7.46-7.38 (m, 1H), 7.32 (d,  $J = 6.8$  Hz, 1H), 3.21 (t,  $J = 7.4$  Hz, 2H), 2.68 (t,  $J = 7.5$  Hz, 2H), 2.21 (p,  $J = 7.5$  Hz, 2H).  $^{13}\text{C NMR}$  (75 MHz,  $\text{CDCl}_3$ )  $\delta$  166.6, 154.2, 136.0, 134.2, 131.7, 129.2, 127.6, 126.6, 126.4, 125.9, 125.6, 123.4, 31.9, 25.2, 24.5.

**Compound 3h**

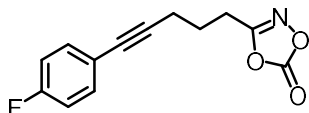
**3h**, 62% yield, colorless oil.  $^1\text{H NMR}$  (300 MHz,  $\text{CDCl}_3$ )  $\delta$  7.17 (dd,  $J = 5.1, 1.1$  Hz, 1H), 6.94 (dd,  $J = 5.1, 3.4$  Hz, 1H), 6.83 (dd,  $J = 3.4, 0.9$  Hz, 1H), 2.98 (t,  $J = 7.2$  Hz, 2H), 2.67 (t,  $J = 7.5$  Hz, 2H), 2.11 (p,  $J = 7.3$  Hz, 2H).  $^{13}\text{C NMR}$  (75 MHz,  $\text{CDCl}_3$ )  $\delta$  166.4, 154.2, 142.4, 127.1, 125.3, 124.0, 28.8, 26.4, 4.0.

**Compound 3i**

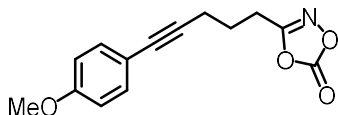
**3i**, 62% yield, colorless oil.  $^1\text{H NMR}$  (300 MHz,  $\text{CDCl}_3$ )  $\delta$  2.80 (t,  $J = 7.5$  Hz, 2H), 2.37 (td,  $J = 6.7$ , 2.6 Hz, 2H), 2.04 (t,  $J = 2.7$  Hz, 1H), 1.96 (dt,  $J = 18.0$ , 7.0 Hz, 2H).  $^{13}\text{C NMR}$  (75 MHz,  $\text{CDCl}_3$ )  $\delta$  166.2, 154.2, 81.8, 70.5, 23.8, 23.3, 17.8.

**Compound 3j**

**3j**, 70% yield, colorless oil.  $^1\text{H NMR}$  (300 MHz,  $\text{CDCl}_3$ )  $\delta$  7.44-7.35 (m, 2H), 7.33-7.27 (m, 3H), 2.85 (t,  $J = 7.5$  Hz, 2H), 2.59 (t,  $J = 6.7$  Hz, 2H), 2.04 (dt,  $J = 18.1$ , 7.0 Hz, 2H).  $^{13}\text{C NMR}$  (75 MHz,  $\text{CDCl}_3$ )  $\delta$  166.3, 154.2, 131.7, 128.5, 128.2, 123.3, 87.2, 82.7, 24.0, 23.6, 18.8.

**Compound 3k**

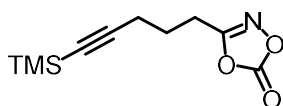
**3k**, 73% yield, colorless oil.  $^1\text{H NMR}$  (250 MHz,  $\text{CDCl}_3$ )  $\delta$  7.37 (dd,  $J = 8.8$ , 5.4 Hz, 2H), 6.99 (t,  $J = 8.7$  Hz, 2H), 2.84 (t,  $J = 7.5$  Hz, 2H), 2.58 (t,  $J = 6.7$  Hz, 2H), 2.10-1.96 (m, 2H).

**Compound 3l**

**3l**, 77% yield, colorless oil.  $^1\text{H NMR}$  (300 MHz,  $\text{CDCl}_3$ )  $\delta$  7.32 (d,  $J = 8.8$  Hz, 2H), 6.82 (d,  $J = 8.8$  Hz, 2H), 3.80 (s, 3H), 2.84 (t,  $J = 7.5$  Hz, 2H), 2.57 (t,  $J = 6.7$  Hz, 2H), 2.09-1.95 (m, 2H).  $^{13}\text{C NMR}$  (75 MHz,  $\text{CDCl}_3$ )  $\delta$  166.4, 159.6, 154.2, 133.1, 115.4, 114.1, 85.6, 82.5, 55.4, 24.0, 23.7, 18.8.

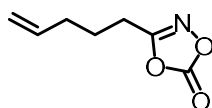


## Compound 3m



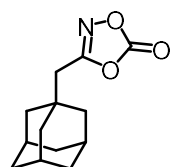
**3m**, 62% yield, colorless oil.  $^1\text{H NMR}$  (300 MHz,  $\text{CDCl}_3$ )  $\delta$  2.77 (t,  $J = 7.5$  Hz, 2H), 2.39 (t,  $J = 6.7$  Hz, 2H), 2.01-1.85 (m, 2H), 0.15 (s, 9H).  $^{13}\text{C NMR}$  (75 MHz,  $\text{CDCl}_3$ )  $\delta$  166.3, 154.2, 104.2, 87.1, 23.9, 23.4, 19.2, 0.1.

## Compound 3n



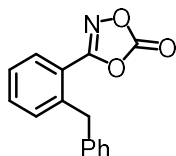
**3n**, 71% yield, colorless oil.  $^1\text{H NMR}$  (300 MHz,  $\text{CD}_2\text{Cl}_2$ )  $\delta$  5.79 (ddt,  $J = 17.0, 10.2, 6.7$  Hz, 1H), 5.18-4.94 (m, 2H), 2.64 (t,  $J = 7.5$  Hz, 2H), 2.18 (q,  $J = 7.0$  Hz, 2H), 1.82 (p,  $J = 7.4$  Hz, 2H).  $^{13}\text{C NMR}$  (75 MHz,  $\text{CD}_2\text{Cl}_2$ )  $\delta$  167.3, 154.7, 137.0, 116.5, 32.9, 24.4, 24.0.

## Compound 3o

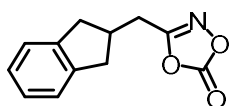


**3o**, 80% yield, white solid.  $^1\text{H NMR}$  (300 MHz,  $\text{CDCl}_3$ )  $\delta$  2.37 (s, 2H), 2.03 (s, 3H), 1.83-1.53 (m, 12H).  $^{13}\text{C NMR}$  (75 MHz,  $\text{CDCl}_3$ )  $\delta$  165.1, 154.5, 42.3, 39.0, 36.5, 33.3, 28.5.

## Compound 3p



**3p**, 58% yield, white solid.  $^1\text{H NMR}$  (300 MHz,  $\text{CDCl}_3$ )  $\delta$  7.79 (dd,  $J = 7.8, 1.2$  Hz, 1H), 7.56 (td,  $J = 7.6, 1.4$  Hz, 1H), 7.42 (td,  $J = 7.7, 1.0$  Hz, 1H), 7.35-7.17 (m, 4H), 7.14 (dd,  $J = 6.6, 5.2$  Hz, 2H), 4.35 (s, 2H).  $^{13}\text{C NMR}$  (75 MHz,  $\text{CDCl}_3$ )  $\delta$  163.9, 153.7, 141.9, 139.0, 133.4, 132.1, 129.5, 129.2, 128.8, 127.2, 126.7, 119.5, 40.0.

**Compound 3q**

**3q**, 84% yield, white solid.  $^1\text{H NMR}$  (300 MHz,  $\text{CDCl}_3$ )  $\delta$  7.25-7.14 (m, 4H), 3.22 (dd,  $J = 15.3, 7.5$  Hz, 2H), 2.91 (tt,  $J = 13.4, 6.9$  Hz, 1H), 2.83-2.75 (m, 3H), 2.72 (d,  $J = 6.3$  Hz, 1H).  $^{13}\text{C NMR}$  (75 MHz,  $\text{CDCl}_3$ )  $\delta$  166.1, 154.2, 141.5, 126.9, 124.8, 38.8, 35.7, 30.4.

**4.3.3 Ruthenium Catalyzed Enantioselective Intramolecular C–H Amidations**

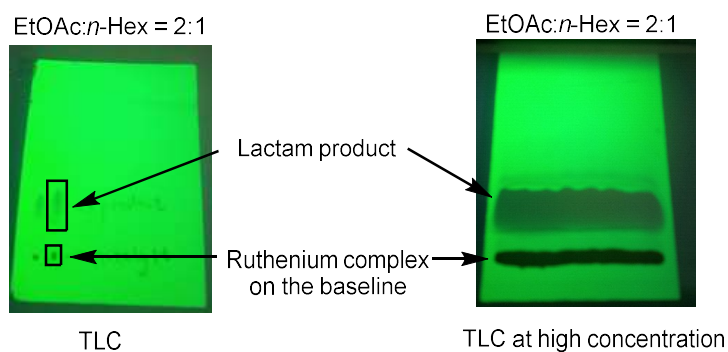
**General Procedures:** A pre-dried (using heating gun to dry for 3 times per tube) 10 mL Schlenk tube was charged with substrates **3a-q** (0.2 mmol) and  $\Lambda$ -**Ru10** (0.2 mg, 0.0002 mmol, 0.1 mol%) under an atmosphere of  $\text{N}_2$ . Pre-cooled (using an ice water bath) “super dried” (Acros) 1,2-dichlorobenzene (0.4 mL, 0.5 M) from “Acros” was added via syringe in sequence. The reaction mixture was stirred at the indicated temperature for the indicated time under an atmosphere of  $\text{N}_2$ . Afterwards, the mixture was directly transferred to a column (the Schlenk tube was rinsed with a minimal amount of  $\text{CH}_2\text{Cl}_2$  to transfer the reaction solution completely) and purified by flash chromatography on silica gel (EtOAc with 5% MeOH/*n*-Hexane = 1:2 to 2:1) to afford the analytical pure products **4a-q**. Enantiomeric ratios were determined by HPLC analysis on chiral stationary phase. The absolute configuration of the product **4e** was confirmed by single crystallography and X-ray structure analysis as *S*-configuration.

*Additional experimental informations:*

- Control of reaction temperature.** The catalytic reactions were set up in a cold room at 4 °C.
- Execution of the reactions.** All catalytic reactions were carried out in 10 mL Schlenk tubes from “Synthware” under  $\text{N}_2$  atmosphere (see image below).

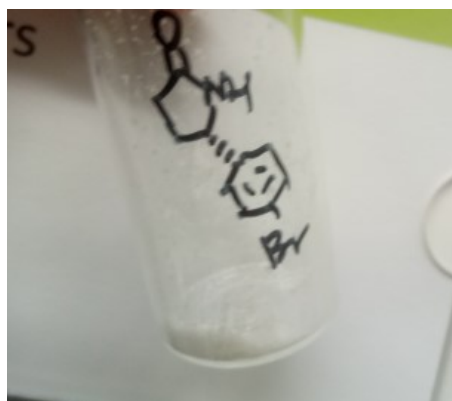


c) TLC monitoring of the final reaction solution. See images below.

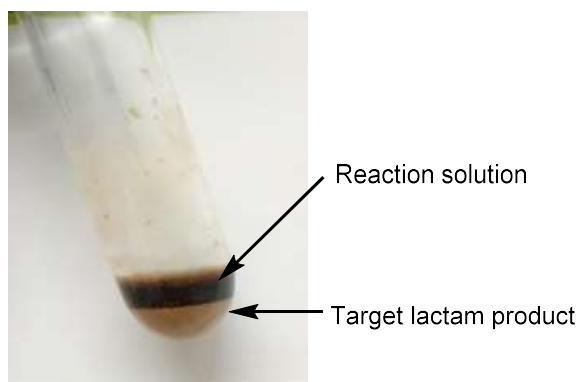


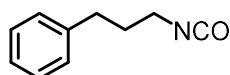
d) Isolation of the final product.

1) The C-H amidation products can be isolated by flash chromatography without any trace contaminations from the ruthenium catalyst as evident by the white color of the products (see image below).

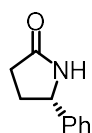


2) For the catalytic reactions of **3b**, **3e**, **3f**, **3g**, and **3q**. The lactam products can also be isolated without any chromatography by only filtration (see image below). This method was used for the gram-scale synthesis of **4e**.

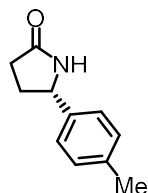


**Compound 5** (side product)

**5:** The Curtius-type decomposition pathway provide the formation of isocyanate **5** which can be isolated by flash chromatography on silica gel (pure CH<sub>2</sub>Cl<sub>2</sub>, R<sub>f</sub> value = 0.9-0.95). <sup>1</sup>H NMR (300 MHz, CD<sub>2</sub>Cl<sub>2</sub>) δ 7.41-7.26 (m, 2H), 7.25-7.08 (m, 3H), 3.32 (t, *J* = 6.6 Hz, 2H), 2.79-2.65 (m, 2H), 2.01-1.85 (m, 2H). <sup>13</sup>C NMR (75 MHz, CD<sub>2</sub>Cl<sub>2</sub>) δ 141.3, 128.87, 128.85, 126.5, 42.7, 33.1, 33.0.

**Compound (S)-4a**

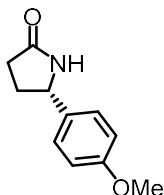
Starting from **3a** (41.0 mg, 0.20 mmol) according to the general procedure to provide **4a** as a white solid (30.6 mg, 95% yield) and with 96:4 e.r. as determined by HPLC analysis (column: Daicel Chiralpak IA 250 x 4.6 mm, absorption: λ = 220 nm, mobile phase: *n*-Hexane/isopropanol = 95:5, flow rate: 1.0 mL/min, column temperature: 30 °C, retention times: t<sub>r</sub> (major) = 18.6 min, t<sub>r</sub> (minor) = 21.6 min). [α]<sub>D</sub><sup>22</sup> = -24.2° (*c* = 1.0, CH<sub>2</sub>Cl<sub>2</sub>). <sup>1</sup>H NMR (300 MHz, CDCl<sub>3</sub>) δ 7.44-7.22 (m, 5H), 6.27 (s, 1H), 4.75 (t, *J* = 7.1 Hz, 1H), 2.69-2.31 (m, 3H), 1.97 (tdd, *J* = 9.1, 8.4, 4.4 Hz, 1H). <sup>13</sup>C NMR (75 MHz, CDCl<sub>3</sub>) δ 178.6, 142.6, 129.1, 128.1, 125.8, 58.2, 31.5, 30.4. HRMS (ESI, *m/z*) calcd. for C<sub>10</sub>H<sub>11</sub>N<sub>1</sub>O<sub>1</sub>Na<sub>1</sub>[M+Na]<sup>+</sup>: 184.0733, found: 184.0733.

**Compound (S)-4b**

Starting from **3b** (43.8 mg, 0.20 mmol) according to the general procedure to provide **4b** as a white solid (33.6 mg, 96% yield) and with 95:5 e.r. as determined by HPLC analysis (column: Daicel Chiralpak IA 250 x 4.6 mm, absorption: λ = 220 nm, mobile phase: *n*-Hexane/isopropanol = 90:10, flow rate: 1.0 mL/min, column temperature: 30 °C, retention times: t<sub>r</sub> (major) = 20.1 min, t<sub>r</sub> (minor) = 21.2 min). [α]<sub>D</sub><sup>22</sup> = -25.6° (*c* = 1.0, CH<sub>2</sub>Cl<sub>2</sub>). <sup>1</sup>H NMR (300 MHz, CDCl<sub>3</sub>) δ 7.21-7.10 (m, 4H), 6.14 (s,

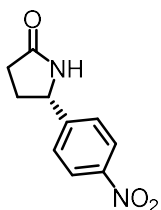
1H), 4.71 (t,  $J = 7.1$  Hz, 1H), 2.64-2.48 (m, 1H), 2.47-2.37 (m, 2H), 2.34 (s, 3H), 2.05-1.83 (m, 1H).  $^{13}\text{C}$  NMR (75 MHz,  $\text{CDCl}_3$ )  $\delta$  178.7, 139.4, 137.9, 129.7, 125.8, 58.2, 31.5, 30.5, 21.2. HRMS (ESI,  $m/z$ ) calcd. for  $\text{C}_{11}\text{H}_{13}\text{N}_1\text{O}_1\text{Na}_1[\text{M}+\text{Na}]^+$ : 198.0889, found: 198.0889.

#### Compound (S)-4c



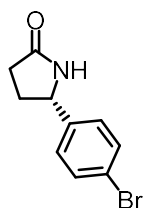
Starting from **3c** (47.0 mg, 0.20 mmol) according to the general procedure to provide **4c** as a white solid (37.9 mg, 99% yield) and with 89:11 e.r. as determined by HPLC analysis (column: Daicel Chiralpak IC column 250 x 4.6 mm, absorption:  $\lambda = 220$  nm, mobile phase: *n*-Hexane/isopropanol = 70:30, flow rate: 1.0 mL/min, column temperature: 30 °C, retention times:  $t_r$  (major) = 31.8 min,  $t_r$  (minor) = 21.2 min).  $[\alpha]_D^{22} = -28.4^\circ$  ( $c = 1.0$ ,  $\text{CH}_2\text{Cl}_2$ ).  $^1\text{H}$  NMR (300 MHz,  $\text{CDCl}_3$ )  $\delta$  7.20 (d,  $J = 8.6$  Hz, 2H), 6.88 (d,  $J = 8.7$  Hz, 2H), 6.45 (s, 1H), 4.70 (t,  $J = 7.0$  Hz, 1H), 3.79 (s, 3H), 2.62-2.31 (m, 3H), 2.03-1.84 (m, 12 1H).  $^{13}\text{C}$  NMR (75 MHz,  $\text{CDCl}_3$ )  $\delta$  178.6, 159.5, 134.5, 127.0, 114.4, 57.9, 55.5, 31.6, 30.5. HRMS (ESI,  $m/z$ ) calcd. for  $\text{C}_{11}\text{H}_{13}\text{N}_1\text{O}_2\text{Na}_1[\text{M}+\text{Na}]^+$ : 214.0838, found: 214.0838.

#### Compound (S)-4d



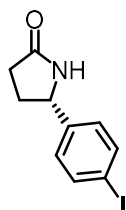
Starting from **3d** (50.0 mg, 0.20 mmol) according to the general procedure to provide **4d** as a white solid (34.5 mg, 84% yield) and with 95:5 e.r. as determined by HPLC analysis (column: Daicel Chiralpak IC column 250 x 4.6 mm, absorption:  $\lambda = 220$  nm, mobile phase: *n*-Hexane/isopropanol = 70:30, flow rate: 1.0 mL/min, column temperature: 30 °C, retention times:  $t_r$  (major) = 38.9 min,  $t_r$  (minor) = 46.1 min).  $[\alpha]_D^{22} = -47.4^\circ$  ( $c = 1.0$ ,  $\text{CH}_2\text{Cl}_2$ ).  $^1\text{H}$  NMR (300 MHz,  $\text{CD}_2\text{Cl}_2$ )  $\delta$  8.21 (d,  $J = 8.8$  Hz, 2H), 7.50 (d,  $J = 8.6$  Hz, 2H), 6.86 (s, 1H), 2.70-2.55 (m, 1H), 2.45-2.35 (m, 2H), 2.03-1.82 (m, 1H).  $^{13}\text{C}$  NMR (75 MHz,  $\text{CD}_2\text{Cl}_2$ )  $\delta$  178.8, 150.9, 148.0, 127.0, 124.5, 57.8, 31.4, 30.4. HRMS (ESI,  $m/z$ ) calcd. for  $\text{C}_{10}\text{H}_{10}\text{N}_2\text{O}_3\text{Na}_1[\text{M}+\text{Na}]^+$ : 229.0584, found: 229.0584.

## Compound (S)-4e

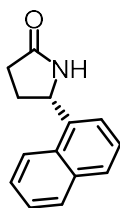


Starting from **3e** (56.6 mg, 0.20 mmol) according to the general procedure to provide **4e** as a white solid (45.8 mg, 96% yield) and with 93:7 e.r. as determined by HPLC analysis (column: Daicel Chiralpak IA column 250 x 4.6 mm, absorption:  $\lambda = 220$  nm, mobile phase: *n*-Hexane/isopropanol = 95:5, flow rate 1.0 mL/min, column temperature: 30 °C, retention times:  $t_r$  (major) = 26.8 min,  $t_r$  (minor) = 24.0 min).  $[\alpha]_D^{22} = -30.8^\circ$  ( $c = 1.0$ ,  $\text{CH}_2\text{Cl}_2$ ).  $^1\text{H NMR}$  (300 MHz,  $\text{CDCl}_3$ )  $\delta$  7.49 (d,  $J = 8.4$  Hz, 2H), 7.17 (d,  $J = 8.4$  Hz, 2H), 6.41 (s, 1H), 4.73 (t,  $J = 7.1$  Hz, 1H), 2.68-2.34 (m, 3H), 2.05-1.81 (m, 1H).  $^{13}\text{C NMR}$  (75 MHz,  $\text{CDCl}_3$ )  $\delta$  178.7, 141.5, 132.2, 127.5, 122.0, 57.8, 31.4, 30.3. **HRMS (ESI,  $m/z$ )** calcd. for  $\text{C}_{10}\text{H}_{10}\text{Br}_1\text{N}_1\text{O}_1\text{Na}_1[\text{M}+\text{Na}]^+$ : 261.9838, found: 261.9838.

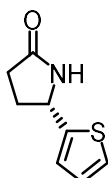
## Compound (S)-4f



Starting from **3f** (66.2 mg, 0.20 mmol) according to the general procedure to provide **4f** as a white solid (52.6 mg, 92% yield) and with 92:8 e.r. as determined by HPLC analysis (column: Daicel Chiralpak IA column 250 x 4.6 mm, absorption:  $\lambda = 220$  nm, mobile phase: *n*-Hexane/isopropanol = 95:5, flow rate: 1.0 mL/min, column temperature: 30 °C, retention times:  $t_r$  (major) = 29.7 min,  $t_r$  (minor) = 26.4 min).  $[\alpha]_D^{22} = -11.2^\circ$  ( $c = 1.0$ ,  $\text{CH}_2\text{Cl}_2$ ).  $^1\text{H NMR}$  (300 MHz,  $\text{CDCl}_3$ )  $\delta$  7.70 (d,  $J = 8.3$  Hz, 2H), 7.05 (d,  $J = 8.3$  Hz, 2H), 5.93 (s, 1H), 4.70 (t,  $J = 7.0$  Hz, 1H), 2.69-2.30 (m, 3H), 2.02-1.83 (m, 1H).  $^{13}\text{C NMR}$  (75 MHz,  $\text{CDCl}_3$ )  $\delta$  178.4, 142.4, 138.2, 127.7, 93.4, 57.7, 31.5, 30.2. **HRMS (ESI,  $m/z$ )** calcd. for  $\text{C}_{10}\text{H}_{10}\text{I}_1\text{N}_1\text{O}_1\text{Na}_1[\text{M}+\text{Na}]^+$ : 309.9699, found: 309.9698.

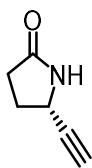
**Compound (S)-4g**

Starting from **3g** (51.0 mg, 0.20 mmol) according to the general procedure to provide **4g** as a white solid (40.0 mg, 95% yield) and with 92:8 e.r. as determined by HPLC analysis (column: Daicel Chiralpak IC column 250 x 4.6 mm, absorption:  $\lambda = 220$  nm, mobile phase: *n*-Hexane/isopropanol = 80:20, flow rate: 1.0 mL/min, column temperature: 30 °C, retention times:  $t_r$  (major) = 32.3 min,  $t_r$  (minor) = 37.1 min).  $[\alpha]_D^{22} = -142.2^\circ$  ( $c = 1.0$ ,  $\text{CH}_2\text{Cl}_2$ ).  $^1\text{H NMR}$  (300 MHz,  $\text{CDCl}_3$ )  $\delta$  8.01-7.86 (m, 2H), 7.80 (d,  $J = 7.9$  Hz, 1H), 7.61-7.42 (m, 4H), 6.60 (s, 1H), 5.54 (dd,  $J = 8.0, 5.1$  Hz, 1H), 2.81 (ddd,  $J = 15.7, 12.7, 8.2$  Hz, 1H), 2.54-2.34 (m, 2H), 2.14-1.98 (m, 1H).  $^{13}\text{C NMR}$  (75 MHz,  $\text{CDCl}_3$ )  $\delta$  179.0, 138.2, 134.1, 130.2, 129.2, 128.3, 126.6, 126.0, 125.6, 122.5, 121.4, 54.6, 30.1, 29.8. **HRMS (ESI,  $m/z$ )** calcd. for  $\text{C}_{14}\text{H}_{13}\text{N}_1\text{O}_1\text{Na}_1[\text{M}+\text{Na}]^+$ : 234.0889, found: 234.0888.

**Compound (S)-4h**

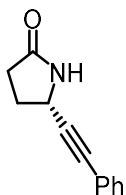
Starting from **3h** (42.2 mg, 0.20 mmol) according to the general procedure to provide **4h** as a white solid (22.1 mg, 66% yield) and with 94:6 e.r. as determined by HPLC analysis (column: Daicel Chiralpak IA column 250 x 4.6 mm, absorption:  $\lambda = 220$  nm, mobile phase: *n*-Hexane/isopropanol = 95:5, flow rate: 1.0 mL/min, column temperature: 30 °C, retention times:  $t_r$  (major) = 23.3 min,  $t_r$  (minor) = 27.9 min).  $[\alpha]_D^{22} = -6.2^\circ$  ( $c = 1.0$ ,  $\text{CH}_2\text{Cl}_2$ ).  $^1\text{H NMR}$   $\delta$  7.26 (dd,  $J = 6.2, 1.3$  Hz, 1H), 7.02-6.93 (m, 2H), 6.51 (s, 1H), 5.03 (t,  $J = 6.8$  Hz, 1H), 2.68-2.33 (m, 3H), 2.22-2.05 (m, 1H).  $^{13}\text{C NMR}$   $\delta$  177.9, 146.5, 127.1, 125.0, 124.3, 54.1, 31.8, 30.2. **HRMS (ESI,  $m/z$ )** calcd. for  $\text{C}_8\text{H}_9\text{N}_1\text{O}_1\text{S}_1$   $[\text{M}+\text{Na}]^+$ : 190.0297, found: 190.0296.

## Compound (S)-4i



Starting from **3i** (30.6 mg, 0.20 mmol) according to the general procedure to provide **4i** as a white solid (13.3 mg, 61% yield). and with 93:7 e.r. as determined by HPLC analysis (column: Daicel Chiralpak IC column 250 x 4.6 mm, absorption:  $\lambda = 220$  nm, mobile phase: *n*-Hexane/isopropanol = 80:20, flow rate: 1.0 mL/min, column temperature: 25 °C, retention times:  $t_r$  (major) = 27.8 min,  $t_r$  (minor) = 19.2 min).  $[\alpha]_D^{22} = -24.2^\circ$  ( $c = 1.0$ ,  $\text{CH}_2\text{Cl}_2$ ).  $^1\text{H NMR}$  (300 MHz,  $\text{CD}_2\text{Cl}_2$ )  $\delta$  6.58 (s, 1H), 4.37 (ddd,  $J = 7.2, 5.4, 2.1$  Hz, 1H), 2.53-2.07 (m, 5H).  $^{13}\text{C NMR}$  (75 MHz,  $\text{CD}_2\text{Cl}_2$ )  $\delta$  177.8, 83.6, 72.1, 44.9, 29.7, 29.3.

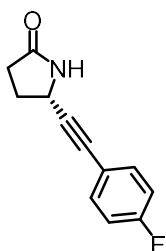
## Compound (S)-4j



Starting from **3j** (45.8 mg, 0.20 mmol) according to the general procedure to provide **4j** as a white solid (28.7 mg, 78% yield) and with 95:5 e.r. as determined by HPLC analysis (column: Daicel Chiralpak IC column 250 x 4.6 mm, absorption:  $\lambda = 220$  nm, mobile phase: *n*-Hexane/isopropanol = 70:30, flow rate: 1.0 mL/min, column temperature: 30 °C, retention times:  $t_r$  (major) = 16.0 min,  $t_r$  (minor) = 11.3 min).  $[\alpha]_D^{22} = -5.4^\circ$  ( $c = 1.0$ ,  $\text{CH}_2\text{Cl}_2$ ).  $^1\text{H NMR}$  (300 MHz,  $\text{CD}_2\text{Cl}_2$ )  $\delta$  7.49-7.38 (m, 2H), 7.37-7.25 (m, 3H), 6.52 (s, 1H), 4.60 (dd,  $J = 7.2, 5.2$  Hz, 1H), 2.59-2.38 (m, 2H), 2.38-2.17 (m, 2H).  $^{13}\text{C NMR}$  (75 MHz,  $\text{CD}_2\text{Cl}_2$ )  $\delta$  177.8, 132.0, 129.0, 128.8, 122.8, 88.8, 83.9, 45.7, 29.9, 29.6.

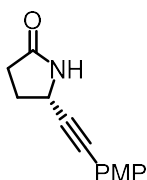


## Compound (S)-4k

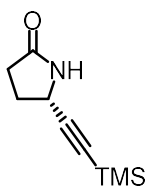


Starting from **3k** (49.4 mg, 0.20 mmol) according to the general procedure to provide **4k** as a white solid (29.9 mg, 74% yield) and with 95:5 e.r. as determined by HPLC analysis (column: Daicel Chiralpak IC column 250 x 4.6 mm, absorption:  $\lambda = 220$  nm, mobile phase: *n*-Hexane/isopropanol = 80:20, flow rate: 1.0 mL/min, column temperature: 30 °C, retention times:  $t_r$  (major) = 23.2 min,  $t_r$  (minor) = 14.7 min).  $[\alpha]_D^{22} = -26.6^\circ$  ( $c = 1.0$ ,  $\text{CH}_2\text{Cl}_2$ ).  $^1\text{H NMR}$  (300 MHz,  $\text{CDCl}_3$ )  $\delta$  7.47-7.30 (m, 2H), 7.10-6.89 (m, 2H), 6.14 (s, 1H), 4.65-4.51 (m, 1H), 2.62-2.44 (m, 2H), 2.43-2.20 (m, 2H).  $^{13}\text{C NMR}$  (75 MHz,  $\text{CDCl}_3$ )  $\delta$  177.5, 164.5, 161.2, 133.8, 133.7, 118.5, 118.4, 116.0, 115.7, 87.8, 83.2, 45.4, 29.6, 29.3.  $^{19}\text{F NMR}$  (235 MHz,  $\text{CDCl}_3$ )  $\delta$  -110.29.

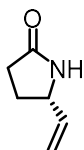
## Compound (S)-4l



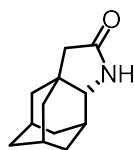
Starting from **3l** (51.8 mg, 0.20 mmol) according to the general procedure to provide **4l** as a white solid (34.6 mg, 82% yield) and with 90:10 e.r. as determined by HPLC analysis (column: Daicel Chiralpak IA column 250 x 4.6 mm, absorption:  $\lambda = 220$  nm, mobile phase: *n*-Hexane/isopropanol = 92 : 8, flow rate: 1.0 mL/min, column temperature: 30 °C, retention times:  $t_r$  (major) = 21.1 min,  $t_r$  (minor) = 19.5 min).  $[\alpha]_D^{22} = -25.4^\circ$  ( $c = 1.0$ ,  $\text{CH}_2\text{Cl}_2$ ).  $^1\text{H NMR}$  (300 MHz,  $\text{CDCl}_3$ )  $\delta$  7.34 (d,  $J = 8.9$  Hz, 2H), 6.83 (d,  $J = 8.9$  Hz, 2H), 6.05 (s, 1H), 4.59 (dd,  $J = 7.4, 5.1$  Hz, 1H), 3.79 (d,  $J = 7.6$  Hz, 3H), 2.58-2.17 (m, 4H).  $^{13}\text{C NMR}$  (75 MHz,  $\text{CDCl}_3$ )  $\delta$  177.6, 160.0, 133.3, 114.4, 114.1, 86.6, 84.1, 55.4, 45.5, 29.6, 29.4.

**Compound (S)-4m**

Starting from **3m** (45.0 mg, 0.20 mmol) according to the general procedure to provide **4m** as a white solid (25.3 mg, 70% yield) and with 94:6 e.r. as determined by HPLC analysis (column: Daicel Chiralpak IC column 250 x 4.6 mm, absorption:  $\lambda = 210$  nm, mobile phase: *n*-Hexane/isopropanol = 90:10, flow rate: 1.0 mL/min, column temperature: 25 °C, retention times:  $t_r$  (major) = 31.2 min,  $t_r$  (minor) = 17.2 min).  $[\alpha]_D^{22} = -9.0^\circ$  ( $c = 1.0$ ,  $\text{CH}_2\text{Cl}_2$ ).  $^1\text{H NMR}$  (300 MHz,  $\text{CD}_2\text{Cl}_2$ )  $\delta$  6.07 (s, 1H), 4.41-4.28 (m, 1H), 2.48-2.06 (m, 4H), 0.21-0.10 (m, 9H).  $^{13}\text{C NMR}$  (75 MHz,  $\text{CD}_2\text{Cl}_2$ )  $\delta$  177.5, 105.3, 88.7, 45.6, 29.7, 29.5, -0.1.

**Compound (S)-4n**

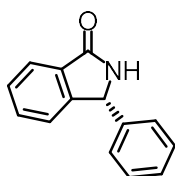
Starting from **3n** (32.0 mg, 0.20 mmol) according to the general procedure to provide **4n** as a white solid (9.3 mg, 42% yield) and with 80:20 e.r. as determined by HPLC analysis (column: Daicel Chiralpak ADH column 250 x 4.6 mm, absorption:  $\lambda = 210$  nm, mobile phase: *n*-Hexane/isopropanol = 96:4, flow rate: 0.8 mL/min, column temperature: 30 °C, retention times:  $t_r$  (major) = 17.4 min,  $t_r$  (minor) = 20.4 min).  $[\alpha]_D^{22} = -4.2^\circ$  ( $c = 1.0$ ,  $\text{CH}_2\text{Cl}_2$ ).  $^1\text{H NMR}$  (300 MHz,  $\text{CD}_2\text{Cl}_2$ )  $\delta$  6.57 (s, 1H), 5.82 (ddd,  $J = 17.0, 10.2, 6.7$  Hz, 1H), 5.15 (dd,  $J = 32.3, 13.6$  Hz, 2H), 4.19-4.00 (m, 1H), 2.36-2.16 (m, 3H), 1.88-1.72 (m, 1H).  $^{13}\text{C NMR}$  (75 MHz,  $\text{CD}_2\text{Cl}_2$ )  $\delta$  178.5, 139.6, 115.4, 57.0, 30.2, 28.5. **HRMS** (ESI,  $m/z$ ) calcd. for  $\text{C}_6\text{H}_9\text{N}_1\text{O}_1\text{Na}_1[\text{M}+\text{Na}]^+$ : 134.0576, found: 134.0577.

**Compound (R)-4o**

Starting from **3o** (47.0 mg, 0.20 mmol) according to the general procedure to provide **4o** as a white

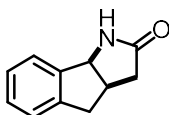
solid (5.3 mg, 14% yield) and with 96:4 e.r. as determined by HPLC analysis (column: Daicel Chiralpak ODH column 250 x 4.6 mm, absorption:  $\lambda = 210$  nm, mobile phase: *n*-Hexane/isopropanol = 90:10, flow rate: 0.7 mL/min, column temperature: 25 °C, retention times:  $t_r$  (major) = 14.5 min,  $t_r$  (minor) = 16.7 min).  $[\alpha]_D^{22} = -9.0^\circ$  ( $c = 1.0$ ,  $\text{CH}_2\text{Cl}_2$ ).  $^1\text{H NMR}$  (300 MHz,  $\text{CD}_2\text{Cl}_2$ )  $\delta$  5.59 (s, 1H), 3.45 (d,  $J = 2.2$  Hz, 1H), 2.10-1.95 (m, 3H), 1.91-1.80 (m, 5H), 1.79-1.55 (m, 6H), 1.42 (dd,  $J = 10.1$ , 2.3 Hz, 1H).  $^{13}\text{C NMR}$  (75 MHz,  $\text{CD}_2\text{Cl}_2$ )  $\delta$  179.0, 64.3, 46.6, 40.4, 38.9, 37.6, 37.5, 37.2, 30.1, 29.9, 29.6, 28.0. **HRMS** (ESI,  $m/z$ ) calcd. for  $\text{C}_{12}\text{H}_{17}\text{N}_1\text{O}_1\text{Na}_1[\text{M}+\text{Na}]^+$ : 214.1202, found: 214.1203.

#### Compound (*R*)-4p



Starting from **3p** (50.6 mg, 0.20 mmol) according to the general procedure to provide **4p** as a white solid (22.6 mg, 54% yield) and with 71.29 e.r. as determined by HPLC analysis (column: Daicel Chiralpak ODH column 250 x 4.6 mm, absorption:  $\lambda = 220$  nm, mobile phase: *n*-Hexane/isopropanol = 90:10, flow rate 1.0 mL/min, column temperature: 30 °C, retention times:  $t_r$  (major) = 14.5 min,  $t_r$  (minor) = 16.6 min).  $[\alpha]_D^{22} = -14.0^\circ$  ( $c = 1.0$ ,  $\text{CH}_2\text{Cl}_2$ ).  $^1\text{H NMR}$  (300 MHz,  $\text{CDCl}_3$ )  $\delta$  7.89 (dd,  $J = 6.2$ , 1.9 Hz, 1H), 7.57-7.42 (m, 2H), 7.40-7.30 (m, 3H), 7.30-7.20 (m, 3H), 6.71 (s, 1H), 5.63 (s, 1H).  $^{13}\text{C NMR}$  (75 MHz,  $\text{CDCl}_3$ )  $\delta$  171.1, 148.1, 138.6, 132.5, 130.9, 129.2, 128.7, 128.5, 127.0, 124.0, 123.5, 60.9. **HRMS** (ESI,  $m/z$ ) calcd. for  $\text{C}_{14}\text{H}_{11}\text{N}_1\text{O}_1\text{H}[\text{M}+\text{H}]^+$ : 210.0913, found: 210.0913.

#### Compound (*3R*, *8S*)-4q

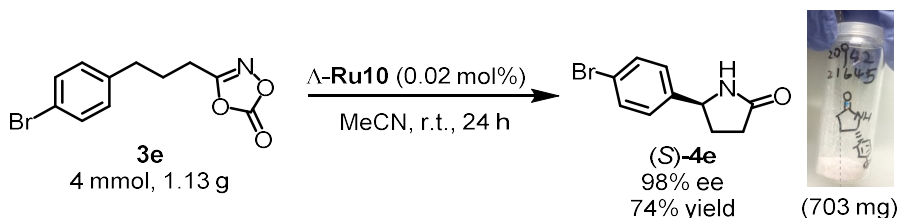


Starting from **3q** (43.4 mg, 0.20 mmol) according to the general procedure to provide **4q** as a white solid (31.8 mg, 92% yield) and with 90:10 e.r. as determined by HPLC analysis (column: Daicel Chiralpak IA column 250 x 4.6 mm, absorption:  $\lambda = 220$  nm, mobile phase: *n*-Hexane/isopropanol = 80:20, flow rate 1.0 mL/min, column temperature: 30 °C, retention times:  $t_r$  (major) = 6.9 min,  $t_r$  (minor) = 12.1 min).  $[\alpha]_D^{22} = +14.4^\circ$  ( $c = 1.0$ ,  $\text{CH}_2\text{Cl}_2$ ).  $^1\text{H NMR}$  (300 MHz,  $\text{CDCl}_3$ )  $\delta$  7.28-7.10 (m, 4H), 7.02 (s, 1H), 4.95 (d,  $J = 7.0$  Hz, 1H), 3.32-3.13 (m, 2H), 2.84-2.70 (m, 1H), 2.69-2.56 (m, 1H),

2.20-2.07 (m, 1H).  $^{13}\text{C}$  NMR (75 MHz,  $\text{CDCl}_3$ )  $\delta$  177.8, 142.6, 141.7, 128.8, 127.4, 125.5, 124.9, 63.6, 38.6, 37.7, 37.7. HRMS (ESI,  $m/z$ ) calcd. for  $\text{C}_{11}\text{H}_{11}\text{N}_1\text{O}_1\text{Na}[\text{M}+\text{Na}]^+$ : 196.0733, found: 196.0732.

#### 4.3.4 Gram-Scale Reactions and Mechanistic Study

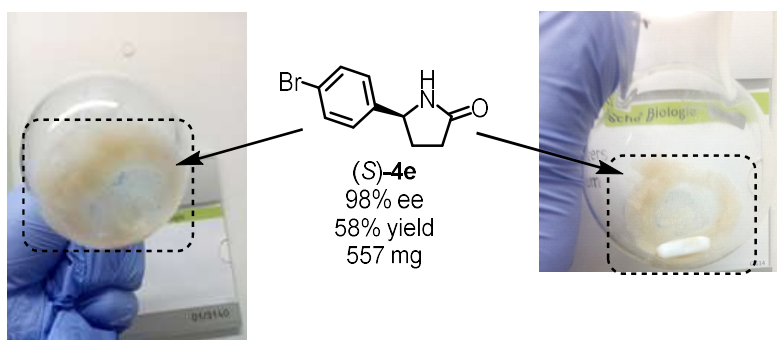
##### 1) Gram-Scale Synthesis of (*S*)-4e, (*R*)-4e and (*S*)-4i



**Procedure:** To a 100 mL round bottom Schlenk flask was added **3e** (1.13 g, 4 mmol) and  $\Delta\text{-Ru10}$  (0.8 mg, 0.0008 mmol, 0.02 mol% catalyst loading). Freshly distilled MeCN (8 mL) was added to the flask and the resulting reaction solution was stirred at room temperature for 24 h under an atmosphere of  $\text{N}_2$ . After complete consumption of **3e** monitored by TLC, (*S*)-**4e** was isolated without column chromatography by precipitation and crystallization.

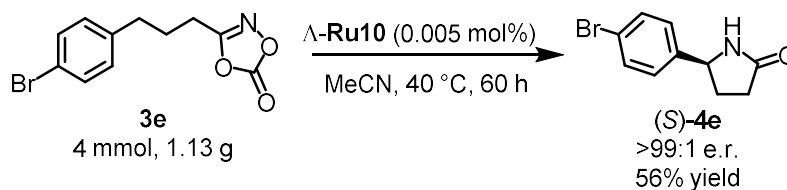
*Work-up of the above reaction:*

Enantiopure (*S*)-**4e** directly precipitated (557 mg, 58% yield) during the reaction and was isolated easily by removal of the remaining solution via syringe since the product was sticking to the wall of the flask (see image below). Enantiomeric ratio was established by HPLC analysis as 98% ee



The remaining solution was cooled with an ice-water bath and (*S*)-**4e** crystals were formed and collected (146 mg).

The combined two batches of (*S*)-**4e** provided a total yield of 74% (703 mg). Enantiomeric ratio was established by HPLC analysis as 98% ee

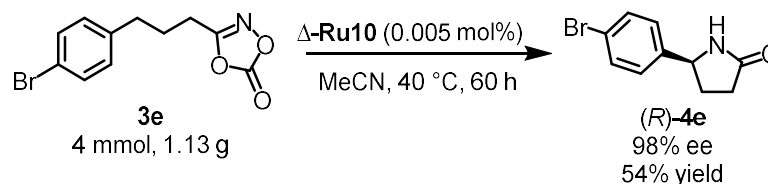


**Procedure:** To a 25 mL round bottom flask was added **3e** (1.13 g, 4 mmol) and  $\Delta\text{-Ru10}$  (0.2 mg, 0.0002 mmol, 0.005 mol% catalyst loading). Freshly distilled MeCN (4 mL) was added to the flask and the resulting reaction solution was stirred at 40 °C for 60 h under an atmosphere of  $\text{N}_2$ . Afterwards,  $(S)\text{-4e}$  was isolated without column chromatography by crystallization upon cooling with an ice-water bath (Note: No precipitation of  $(S)\text{-4e}$  occurred at the elevated temperature of 40 °C).

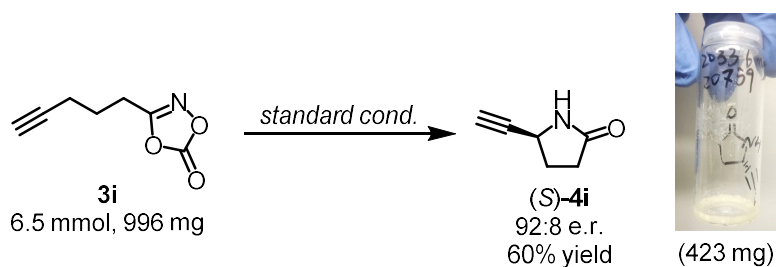


$(S)\text{-4e}$  crystal formed

*Work up of the above reaction:* The reaction solution was cooled with an ice-water bath and  $(S)\text{-4e}$  crystals were formed and collected by filtration. The resulting filtrate was washed with MeCN (pre-cooled to 0 °C) (3 x 2 mL) to provide analytical pure  $(S)\text{-4e}$  (535 mg, 56% yield) with 98% ee.

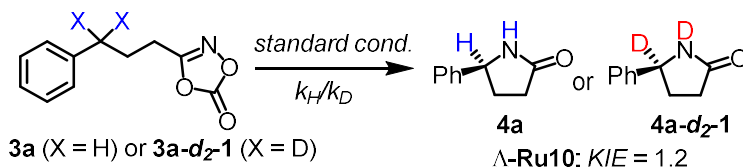


**Procedure:** The same transformation of **3e** to **4e** by using 0.005 mol%  $\Delta$ -configuration **Ru10** catalyst provided lactam product **4e** in 54% yield with 98% ee as  $(R)$ -configuration.



**Procedure:** To a 50 mL round bottom Schlenk flask (pre-dried for 3 times by using heating gun) was added **3i** (996 mg, 6.5 mmol) and  $\Lambda$ -**Ru10** (6.5 mg, 0.0065 mmol, 0.1 mol% catalyst loading). 1,2-Dichlorobenzene (13 mL) was added to the flask and the resulting reaction solution was stirred in a cold room for 30 h under an atmosphere of  $N_2$ . After that, the reaction solution was directly transferred to flash column chromatography (*n*-Hexane:EtOAc = 1:1  $R_f$  = 0.3-0.4) to provide analytical pure (*S*)-**4i** as white solid (423 mg, 60% yield) with 84% ee.

## 2) Kinetic Isotope Effects



**Procedure:** **3a** (21.0 mg, 0.2 mmol) and **3a- $d_2$ -1** (21.0 mg, 0.2 mmol) were separated as individual reactions. **3a** or **3a- $d_2$ -1** was added to a solution of  $\Lambda$ -**Ru10** (0.2 mg, 0.0002 mmol) in pre-cooled (using an ice water bath) super dried 1,2-dichlorobenzene (0.4 mL, 0.5 M). Then 10.6  $\mu$ L  $Cl_2CHCHCl_2$  was added as the internal standard. The reaction mixture was stirred at 0 °C under an atmosphere of nitrogen. Aliquots were taken at time intervals as indicated in the figure below. The aliquot was analyzed by  $^1H$  NMR spectroscopy for the formation of product (blue square for **4a**, red square for **4a- $d_2$ -1**).

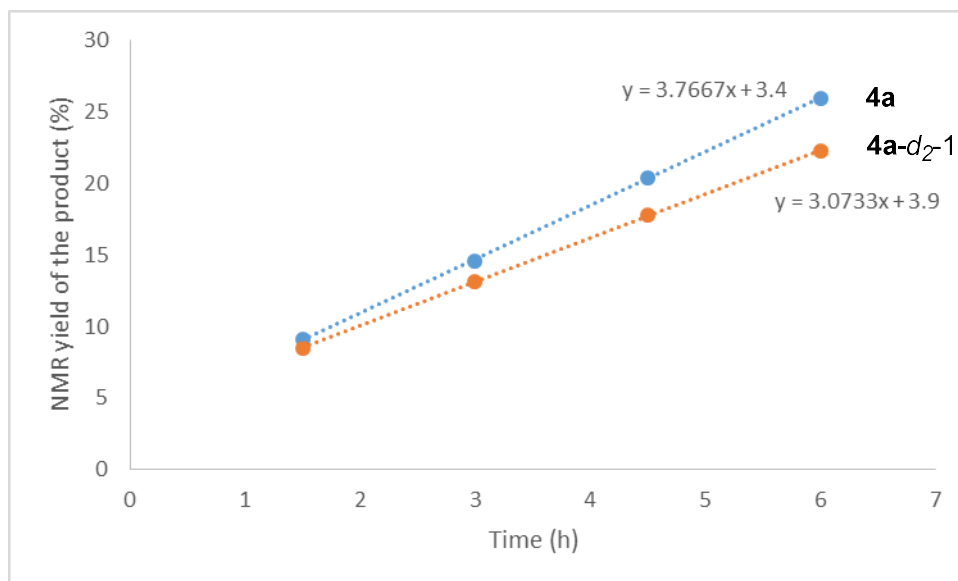
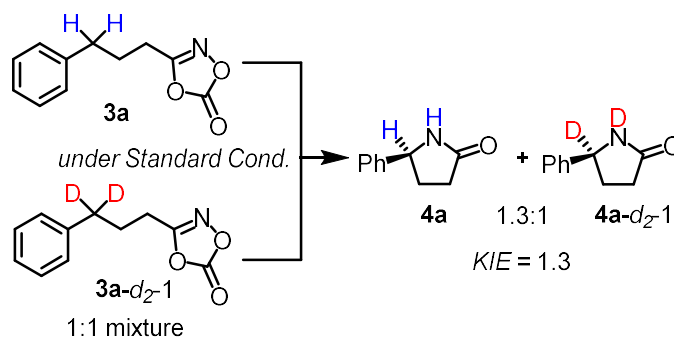
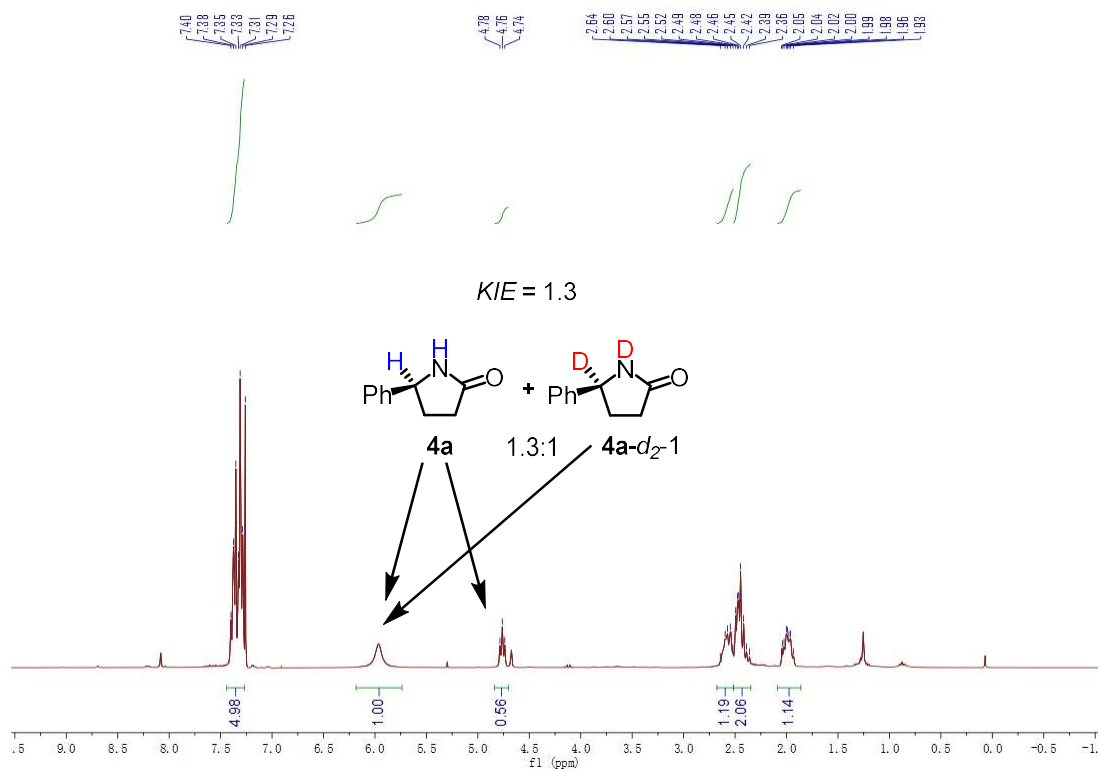


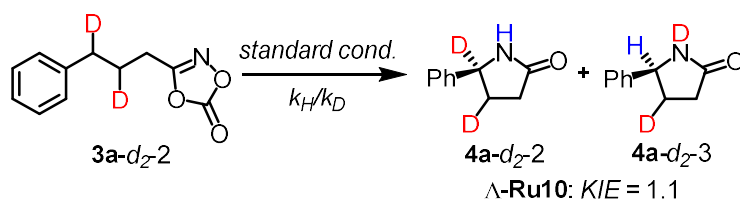
Figure 80. Initial rate of **4a** and **4a-d<sub>2</sub>-1** formation under the above reaction conditions.



**Procedure:** **3a** (21.0 mg, 0.1 mmol) and **3a-d<sub>2</sub>-1** (21.0 mg, 0.1 mmol) were added to a solution of  $\Lambda$ -**Ru10** (0.2 mg, 0.0002 mmol) in pre-cooled (using an ice water bath) super dried 1,2-dichlorobenzene (0.4 mL, 0.5 M). The reaction solution was set up in a cold room at 4 °C . After 6 h reaction time (<50% conv., monitored by crude <sup>1</sup>H NMR), the C–H amidation product was isolated. <sup>1</sup>H NMR analysis showed a ratio **4a**:**4a-d<sub>2</sub>-1** of 1.3:1. (Both **4a** and **4a-d<sub>2</sub>-1** have the same signal at 5.96 ppm but only **4a** has the signal at 4.76 ppm)



**Figure 81.**  $^1\text{H}$  NMR spectra for the analysis of KIE value.



**Procedure:** **3a-d<sub>2</sub>-2** (21.0 mg, 0.1 mmol) was added to a solution of  $\Lambda\text{-Ru10}$  (0.2 mg, 0.0002 mmol) in pre-cooled (using an ice water bath) super dried 1,2-dichlorobenzene (0.4 mL, 0.5 M). The reaction solution was setup in a cold room at 4 °C room temperature. After 30 h reaction time, the C–H amidation product was isolated.  $^1\text{H}$  NMR analysis showed a ratio **4a-d<sub>2</sub>-2**:**4a-d<sub>2</sub>-3** of 1.1:1.



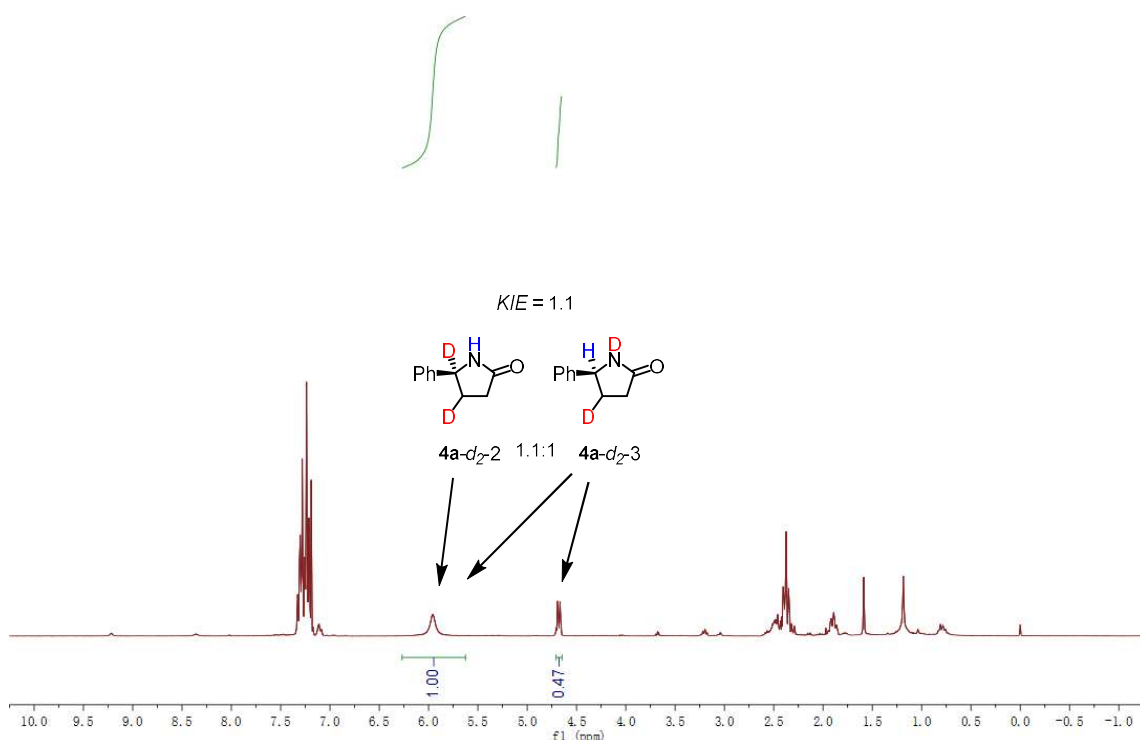
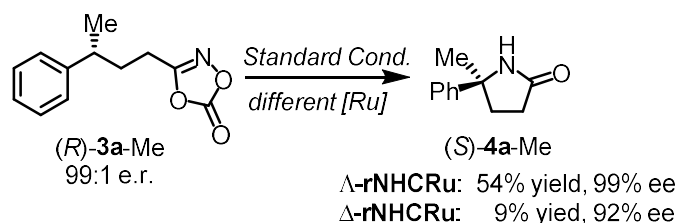


Figure 82. <sup>1</sup>H NMR spectra for the analysis of KIE value.

### 3) Probing the Stereochemistry



**Procedure:** A pre-dried (using heating gun to dry for 3 times per tube) 10 mL Schlenk tube was charged with substrate (*R*)-**3a-Me** (0.2 mmol) and  $\Lambda$  or  $\Delta$ -**Ru10** (0.2 mg, 0.0002 mmol, 0.1 mol%) under an atmosphere of N<sub>2</sub>. Pre-cooled (using an ice water bath) “super dried” (Acros) 1,2-dichlorobenzene (0.4 mL, 0.5 M) from “Acros” was added via syringe in sequence. The reaction mixture was stirred at 4 °C for 30 h under an atmosphere of N<sub>2</sub>. Afterwards, the mixture was directly transferred to a column (the Schlenk tube was rinsed with a minimal amount of CH<sub>2</sub>Cl<sub>2</sub> to transfer the reaction solution completely) and purified by flash chromatography on silica gel (EtOAc with 5% MeOH/*n*-Hexane = 1:2 to 2:1) to afford the analytical pure products (*S*)-**4a-Me**. Enantiomeric ratios were determined by HPLC analysis on chiral stationary phase. (column: Daicel Chiralpak IA column 250 x 4.6 mm, absorption:  $\lambda = 220$  nm, mobile phase: *n*-Hexane/isopropanol = 95:5, flow rate 1.0

mL/min, column temperature: 30 °C, retention times:  $t_r$  (major) = 16.9 min,  $t_r$  (minor) = 19.3 min). The HPLC spectrums were shown below. The observed results indicated a singlet nitrene was formed in our system rather than a triplet nitrene. Although, a triplet nitrene pathway cannot be totally excluded.

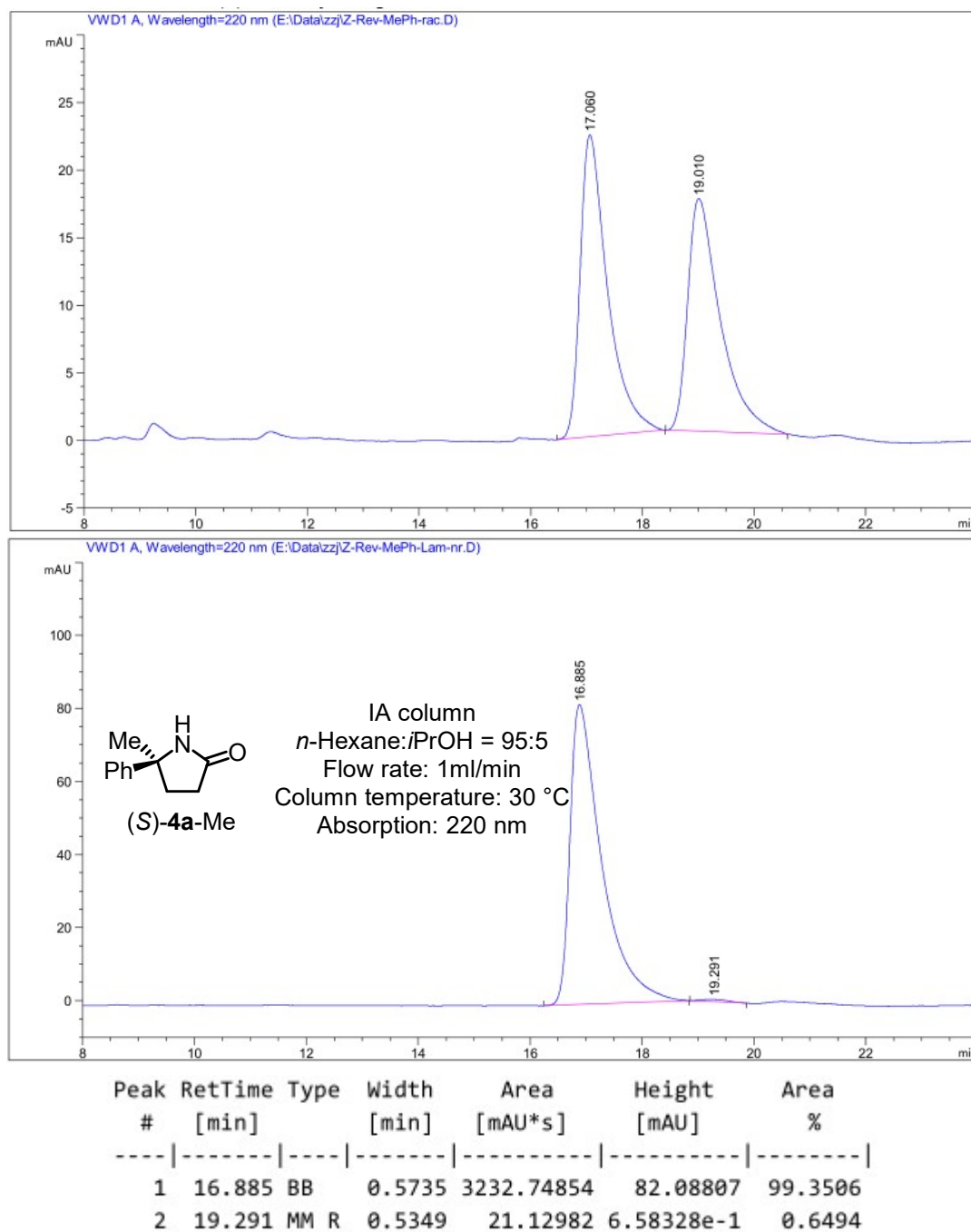


Figure 83. HPLC spectrums of *rac*-4a-Me and (S)-4a-Me obtained by using  $\Lambda$ -Ru10.

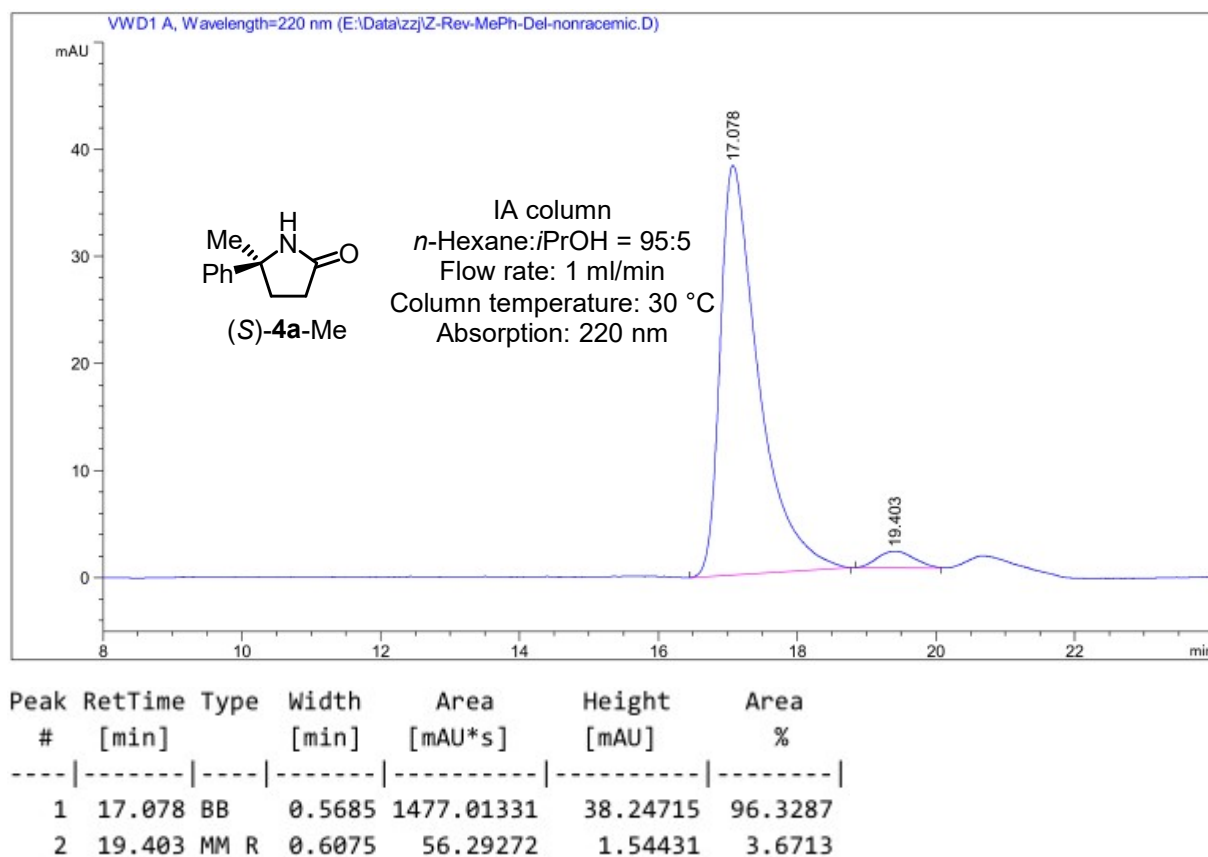
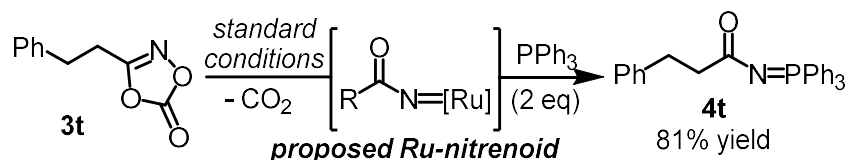


Figure 84. HPLC spectrum of (S)-4a-Me obtained by using  $\Delta$ -Ru10.

#### 4) Trapping of Ru-nitrenoid Intermediate



**Procedure:** A pre-dried (using heating gun to dry for 3 times per tube) 10 mL Schlenk tube was charged with substrate **3t** (38.2 mg, 0.2 mmol), PPh<sub>3</sub> (52.4 mg, 0.4 mmol) and  $\Delta$ -Ru10 (0.2 mg, 0.0002 mmol, 0.1 mol%) under an atmosphere of N<sub>2</sub>. Pre-cooled (using an ice water bath) “super dried” (Acros) 1,2-dichlorobenzene (0.4 mL, 0.5 M) from “Acros” was added via syringe in sequence. The reaction mixture was stirred at 4 °C for 30 h under an atmosphere of N<sub>2</sub>. Afterwards, the mixture was directly transferred to a column (the Schlenk tube was rinsed with a minimal amount of CH<sub>2</sub>Cl<sub>2</sub> to transfer the reaction solution completely) and purified by flash chromatography on silica gel (EtOAc:*n*-Hexane = 1:3 R<sub>f</sub> value = 0.4-0.45) to afford the analytical pure products **4t**.

**4t:** 81% yield, color less oil. <sup>1</sup>H NMR (300 MHz, CD<sub>3</sub>CN)  $\delta$  7.78-7.58 (m, 9H), 7.50 (ddd, *J* = 7.2, 5.4, 2.4 Hz, 6H), 7.31-7.13 (m, 5H), 3.01 (t, *J* = 7.4 Hz, 2H), 2.68 (td, *J* = 7.4, 1.5 Hz, 2H). <sup>13</sup>C NMR (75

MHz, CD<sub>3</sub>CN)  $\delta$  184.0, 183.8, 143.7, 133.9, 133.8, 133.3, 133.3, 130.2, 129.7, 129.6, 129.5, 129.1, 128.9, 126.6, 42.6, 42.3, 33.5, 33.4. <sup>31</sup>P NMR (122 MHz, CD<sub>3</sub>CN)  $\delta$  19.22. HRMS (ESI, *m/z*) calcd. for C<sub>27</sub>H<sub>24</sub>N<sub>1</sub>Na<sub>1</sub>O<sub>1</sub>P<sub>1</sub> [M+Na]<sup>+</sup>: 432.1488, found: 432.1484.

#### 4.3.5 Single Crystal X-Ray Diffraction Studies

**Crystallography of compound (*S*)-4e:** Single crystals of **4e** were obtained by recrystallization on EtOAc at 80 °C. Data was collected with an STOE STADIVARI diffractometer equipped with with CuK radiation, a graded multilayer mirror monochromator (1.54186 Å) and a DECTRIS PILATUS 300K detector using an oil-coated shock-cooled crystal at 100(2) K. Absorption effects were corrected semi-empirical using multiscanned reflections (STOE LANA, absorption correction by scaling of reflection intensities.). Cell constants were refined using 15678 of observed reflections of the data collection. The structure was solved by direct methods by using the program XT V2014/1 (Bruker AXS Inc., 2014) and refined by full matrix least squares procedures on F<sup>2</sup> using SHELXL-2018/3 (Sheldrick, 2018). The non-Hydrogen atoms have been refined anisotropically, carbon bonded hydrogen atoms were included at calculated positions and refined using the ‘riding model’ with isotropic temperature factors at 1.2 times (for CH<sub>3</sub> groups 1.5 times) that of the preceding carbon atom. CH<sub>3</sub> groups were allowed to rotate about the bond to their next atom to fit the electron density. Nitrogen or oxygen bonded hydrogen atoms were located and allowed to refine isotropically. The absolute configuration has been determined: The “Flack parameter” (Parsons, Flack, *et al.*, 2013) refined to -0.005(14). CCDC number: 1910815.

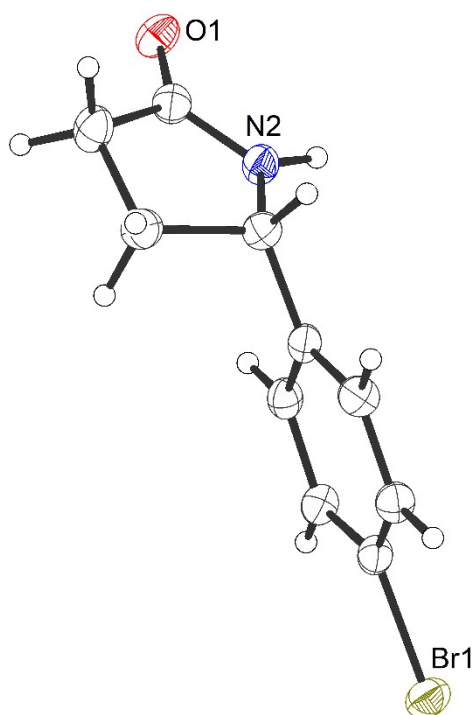


Figure 85. Crystal structure of (*S*)-4e.

Table 7. Crystal data and structure refinement for (*S*)-4e.

Crystal data		
Identification code	<i>(S)</i> -4e	
Habitus, colour	plate, colourless	
Crystal size	0.18 x 0.17 x 0.05 mm <sup>3</sup>	
Crystal system	Monoclinic	
Space group	P2 <sub>1</sub>	Z = 2
Unit cell dimensions	a = 4.8070(2) Å	= 90°.
	b = 7.0174(2) Å	= 96.901(3)°.
	c = 14.3984(6) Å	= 90°.
Volume	482.18(3) Å <sup>3</sup>	
Cell determination	15678 peaks with Theta 3.1 to 76.1°.	
Empirical formula	C <sub>10</sub> H <sub>10</sub> Br N O	
Moiety formula	C <sub>10</sub> H <sub>10</sub> Br N O	
Formula weight	240.10	
Density (calculated)	1.654 Mg/m <sup>3</sup>	

## Chapter 4. Experimental Part

---

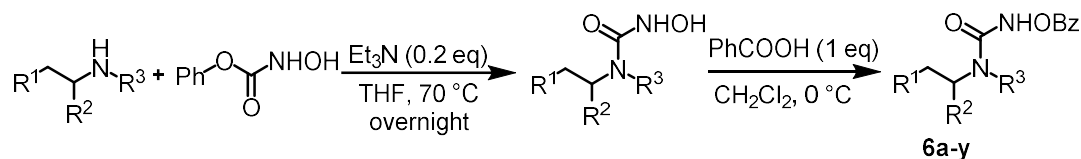
Absorption coefficient	5.468 mm <sup>-1</sup>
F(000)	240
Data collection:	
Diffraction type	STOE STADIVARI
Wavelength	1.54186 Å
Temperature	100(2) K
Theta range for data collection	3.092 to 75.455°.
Index ranges	-5<=h<=6, -6<=k<=8, -17<=l<=17
Data collection software	X-Area Pilatus3_SV 1.31.127.0 (STOE, 2016) <sup>4</sup>
Cell refinement software	X-Area Recipe 1.33.0.0 (STOE, 2015) <sup>5</sup>
Data reduction software	X-Area Integrate 1.71.0.0 (STOE, 2016) <sup>6</sup> X-Area LANA 1.68.2.0 (STOE, 2016) <sup>7</sup>
Solution and refinement:	
Reflections collected	8380
Independent reflections	1728 [R(int) = 0.0289]
Completeness to theta = 67.686°	100.0 %
Observed reflections	1725[I > 2σ(I)]
Reflections used for refinement	1728
Absorption correction	Semi-empirical from equivalents <sup>8</sup>
Max. and min. transmission	0.0516 and 0.0138
Flack parameter (absolute struct.)	-0.005(14) <sup>9</sup>
Largest diff. peak and hole	0.324 and -0.590 e.Å <sup>-3</sup>
Solution	intrinsic phases <sup>10</sup>
Refinement	Full-matrix least-squares on F <sup>2</sup> <sup>11</sup>
Treatment of hydrogen atoms	CH calculated positions, constr., NH located, isotr. ref.
Programs used	XT V2014/1 (Bruker AXS Inc., 2014) <sup>12</sup> SHELXL-2018/3 (Sheldrick, 2018) <sup>13</sup> DIAMOND (Crystal Impact) <sup>14</sup> ShelXle (Hübschle, Sheldrick, Dittrich, 2011) <sup>15</sup>
Data / restraints / parameters	1728 / 1 / 122
Goodness-of-fit on F <sup>2</sup>	1.098
R index (all data)	wR2 = 0.0625
R index conventional [I>2σ(I)]	R1 = 0.0235

## References

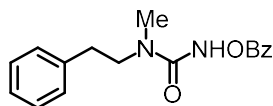
1. Y. Park, S. Chang, *Nat. Catal.* **2019**, *9*, 3360.
2. Q. Xing, C.-M. Chan, Y.-W. Yeung, W.-Y. Yu, *J. Am. Chem. Soc.* **2019**, *141*, 3849.
3. H. Wang, Y. Park, Z. Bai, S. Chang, G. He, G. Chen, *J. Am. Chem. Soc.* **2019**, *141*, 7194.
4. *X-Area Pilatus3\_SV*, STOE & Cie GmbH, Darmstadt, Germany, **2016**.
5. *X-Area Recipe*, STOE & Cie GmbH, Darmstadt, Germany, **2015**.
6. *X-Area Integrate*, STOE & Cie GmbH, Darmstadt, Germany, **2016**.
7. *X-Area LANA*, STOE & Cie GmbH, Darmstadt, Germany, **2016**.
8. S. Parsons, H. D.; Flack, T. Wagner, *Acta Cryst. B* **2013**, *69*, 249.
9. G. M. Sheldrick, *Acta Cryst. A* **2015**, *71*, 3.
10. G. M. Sheldrick, *Acta Cryst. C* **2015**, *71*, 3.
11. K. Brandenburg, *Diamond - Crystal and Molecular Structure Visualization*, Crystal Impact - Dr. Putz, H.; Dr. Brandenburg GbR, K. Bonn, Germany, **2014**.
12. C. B. Hübschle, G. M. Sheldrick, B. Dittrich, *J. Appl. Cryst.* **2011**, *44*, 1281.

## 4.4 Enantioselective Synthesis of 2-Imidazolidinones by Intramolecular C–H Amidation

## 4.4.1 Synthesis of Substrates



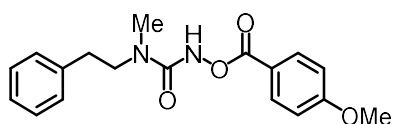
**General procedure:** Amine (3.0 mmol, 1 equiv) phenyl hydroxycarbamate (3.0 mmol, 1 equiv) and Et<sub>3</sub>N (0.6 mmol, 0.2 equiv) dissolved in THF (10 mL) were heated at 70 °C overnight (16-18 h, monitored by TLC) under N<sub>2</sub> atmosphere. After cooling to room temperature, the organic solvent was removed under reduced pressure. The resulting solid was dissolved in 20 mL EtOAc, and washed with brine (3 x 10 mL). The organic layer was collected and dried under anhydrous MgSO<sub>4</sub>. The organic solvent was removed and the residue was subjected to flash silica gel chromatography to provide crude intermediate (EtOAc, R<sub>f</sub> value = 0.3-0.4) as a white solid. The above intermediate (3.0 mmol, 1 equiv) together with benzoic acid (3.0 mmol, 1 equiv) were dissolved in 30 mL CH<sub>2</sub>Cl<sub>2</sub>. The resulting solution was cooled to 0 °C (ice-water bath). After that, DCC (3.0 mmol, 1 equiv) dissolved in 10 mL CH<sub>2</sub>Cl<sub>2</sub> was added dropwisely to the solution. After stirring at 0 °C for 3 h, 20 mL Et<sub>2</sub>O was added to the solution in one portion. The resulting solution was filtered and the filtrate was collected. The organic solvent was removed under reduced pressure. The residue was subjected to a flash silica gel chromatography to provide analytical pure *N*-benzoyloxyurea substrates.

**Compound 6aa**

**6aa**, 74% yield, white solid. <sup>1</sup>H NMR (300 MHz, CDCl<sub>3</sub>) 8.39 (s, 1H), 8.22-8.12 (m, 2H), 7.66 (t, *J* = 7.4 Hz, 1H), 7.52 (t, *J* = 7.7 Hz, 2H), 7.37 (dd, *J* = 10.2, 4.3 Hz, 2H), 7.32-7.23 (m, 3H), 3.62 (t, *J* = 7.4 Hz, 2H), 3.04-2.89 (m, 5H). <sup>13</sup>C NMR (75 MHz, CDCl<sub>3</sub>) δ 166.9, 157.7, 138.7, 134.1, 130.0, 128.9, 128.9, 128.7, 127.3, 126.7, 51.4, 34.8, 34.3. HRMS (ESI, *m/z*) calcd. for C<sub>17</sub>H<sub>18</sub>N<sub>2</sub>O<sub>3</sub>Na<sub>1</sub>[M+Na]<sup>+</sup>: 321.1210, found: 321.1207.

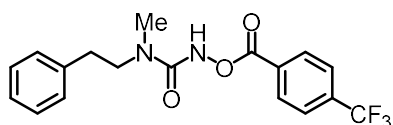


## Compound 6ab



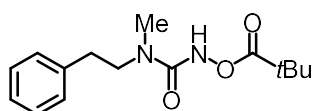
**6ab**, 78% yield, white solid.  $^1\text{H NMR}$  (300 MHz,  $\text{CDCl}_3$ )  $\delta$  8.34 (s, 1H), 8.18-8.07 (m, 2H), 7.33 (qd,  $J = 7.6, 2.2$  Hz, 5H), 7.05-6.93 (m, 2H), 3.93 (s, 3H), 3.67-3.57 (m, 2H), 3.02-2.91 (m, 5H).  $^{13}\text{C NMR}$  (75 MHz,  $\text{CDCl}_3$ )  $\delta$  166.7, 164.4, 157.9, 138.8, 132.2, 129.0, 128.9, 126.8, 119.5, 114.1, 55.7, 51.5, 34.9, 34.4. **HRMS (ESI,  $m/z$ )** calcd. for  $\text{C}_{18}\text{H}_{20}\text{N}_2\text{O}_4\text{Na}_1[\text{M}+\text{Na}]^+$ : 351.1315, found: 351.1313.

## Compound 6ac



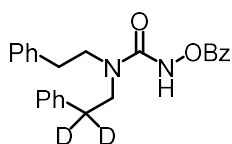
**6ac**, 75% yield, white solid.  $^1\text{H NMR}$  (300 MHz,  $\text{CDCl}_3$ )  $\delta$  8.14 (d,  $J = 8.0$  Hz, 3H), 7.67 (d,  $J = 8.3$  Hz, 2H), 7.35-7.21 (m, 2H), 7.17 (dd,  $J = 8.0, 4.6$  Hz, 3H), 3.50 (t,  $J = 7.3$  Hz, 2H), 2.90-2.79 (m, 5H).  $^{13}\text{C NMR}$  (75 MHz,  $\text{CDCl}_3$ )  $\delta$  165.7, 157.4, 138.6, 135.7, 135.3, 130.7, 130.5, 128.97, 128.95, 126.9, 125.87, 125.82, 125.8, 125.7, 125.4, 121.8, 51.5, 34.8, 34.3. **HRMS (ESI,  $m/z$ )** calcd. for  $\text{C}_{18}\text{H}_{17}\text{F}_3\text{N}_2\text{O}_3\text{Na}_1[\text{M}+\text{Na}]^+$ : 389.1083, found: 389.1086.

## Compound 6ad



**6ad**, 52% yield, white solid.  $^1\text{H NMR}$  (300 MHz,  $\text{CD}_3\text{CN}$ )  $\delta$  8.38 (s, 1H), 7.41-7.16 (m, 5H), 3.55-3.39 (m, 2H), 2.93-2.77 (m, 5H), 1.28 (s, 9H).  $^{13}\text{C NMR}$  (75 MHz,  $\text{CD}_3\text{CN}$ )  $\delta$  178.7, 158.5, 140.2, 129.8, 129.5, 127.3, 51.2, 38.8, 34.7, 34.5, 27.3. **HRMS (ESI,  $m/z$ )** calcd. for  $\text{C}_{15}\text{H}_{22}\text{N}_2\text{O}_3\text{Na}_1[\text{M}+\text{Na}]^+$ : 301.1523, found: 301.1520.

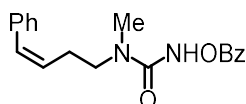
## Compound 6aa'



**6aa'**, 57% yield, white solid.  $^1\text{H NMR}$  (300 MHz,  $\text{CD}_3\text{CN}$ )  $\delta$  8.74 (s, 1H), 8.16-8.04 (m, 2H), 7.73 (t,

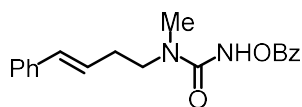
$J = 7.4$  Hz, 1H), 7.58 (t,  $J = 7.7$  Hz, 2H), 7.41-7.17 (m, 10H), 3.41 (dd,  $J = 9.5, 5.5$  Hz, 4H), 2.95-2.80 (m, 2H).  $^{13}\text{C}$  NMR (75 MHz,  $\text{CD}_3\text{CN}$ )  $\delta$  167.3, 158.2, 140.2, 140.1, 135.0, 130.4, 129.9, 129.9, 129.5, 128.8, 127.3, 55.3, 50.1, 50.0, 35.0. HRMS (ESI,  $m/z$ ) calcd. for  $\text{C}_{24}\text{H}_{22}\text{D}_2\text{N}_2\text{O}_3\text{Na}_1[\text{M}+\text{Na}]^+$ : 413.1805, found: 413.1805.

#### Compound (Z)-6b



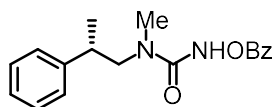
(Z)-6b, 77% yield, white solid.  $^1\text{H}$  NMR (300 MHz,  $\text{CDCl}_3$ )  $\delta$  8.38 (s, 1H), 8.09-7.97 (m, 2H), 7.61-7.49 (m, 1H), 7.40 (t,  $J = 7.6$  Hz, 2H), 7.34-7.09 (m, 5H), 6.52 (d,  $J = 11.6$  Hz, 1H), 5.60 (dt,  $J = 11.6, 7.4$  Hz, 1H), 3.38 (t,  $J = 7.2$  Hz, 2H), 2.85 (s, 3H), 2.56 (qd,  $J = 7.4, 1.6$  Hz, 2H).  $^{13}\text{C}$  NMR (75 MHz,  $\text{CDCl}_3$ )  $\delta$  167.0, 157.8, 137.2, 134.1, 132.0, 130.1, 128.8, 128.5, 128.0, 127.3, 127.1, 49.0, 34.1, 26.9. HRMS (ESI,  $m/z$ ) calcd. for  $\text{C}_{19}\text{H}_{20}\text{N}_2\text{O}_3\text{Na}_1[\text{M}+\text{Na}]^+$ : 347.1366, found: 347.1363.

#### Compound (E)-6b



(E)-6b, 63% yield, white solid.  $^1\text{H}$  NMR (300 MHz,  $\text{CDCl}_3$ )  $\delta$  8.38 (s, 1H), 8.09-7.98 (m, 2H), 7.54 (t,  $J = 7.4$  Hz, 1H), 7.40 (t,  $J = 7.7$  Hz, 2H), 7.33-7.09 (m, 6H), 6.43 (d,  $J = 15.8$  Hz, 1H), 6.20-6.04 (m, 1H), 3.42 (t,  $J = 7.2$  Hz, 2H), 2.97 (s, 3H), 2.47 (q,  $J = 7.2$  Hz, 2H).  $^{13}\text{C}$  NMR (75 MHz,  $\text{CDCl}_3$ )  $\delta$  167.0, 157.8, 137.3, 134.1, 132.9, 130.1, 128.8, 128.7, 127.5, 127.3, 126.3, 49.3, 34.7, 31.6. HRMS (ESI,  $m/z$ ) calcd. for  $\text{C}_{19}\text{H}_{20}\text{N}_2\text{O}_3\text{Na}_1[\text{M}+\text{Na}]^+$ : 347.1366, found: 347.1363.

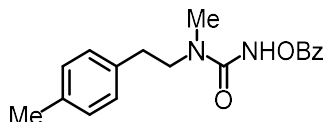
#### Compound (S)-6c



6c, 64% yield, colorless oil, and with 89% ee as determined by HPLC analysis (column: Daicel Chiralpak IC 250 x 4.6 mm, absorption:  $\lambda = 220$  nm, mobile phase: *n*-Hexane/isopropanol = 60:40, flow rate: 1.0 mL/min, column temperature: 30 °C, retention times:  $t_r$  (major) = 9.8 min,  $t_r$  (minor) = 8.5 min).  $^1\text{H}$  NMR (300 MHz,  $\text{CDCl}_3$ )  $\delta$  8.26 (s, 1H), 8.20-8.09 (m, 2H), 7.64 (t,  $J = 7.4$  Hz, 1H), 7.50

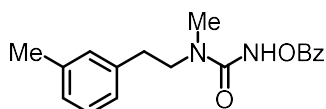
(t,  $J = 7.6$  Hz, 2H), 7.42-7.20 (m, 5H), 3.71 (dd,  $J = 13.7, 6.6$  Hz, 1H), 3.25 (ddd,  $J = 21.6, 14.3, 8.0$  Hz, 2H), 2.81 (s, 3H), 1.35 (d,  $J = 6.8$  Hz, 3H).  $^{13}\text{C}$  NMR (75 MHz,  $\text{CDCl}_3$ )  $\delta$  166.9, 158.0, 144.1, 134.1, 130.1, 128.9, 128.7, 127.4, 127.3, 127.0, 57.2, 38.8, 35.2, 18.7. HRMS (ESI,  $m/z$ ) calcd. for  $\text{C}_{18}\text{H}_{20}\text{N}_2\text{O}_3\text{Na}_1[\text{M}+\text{Na}]^+$ : 335.1366, found: 335.1363.

### Compound 6d



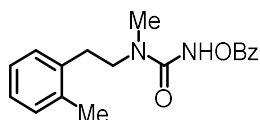
**6d**, 72% yield, white solid.  $^1\text{H}$  NMR (300 MHz,  $\text{CDCl}_3$ )  $\delta$  8.27 (s, 1H), 8.11 (d,  $J = 7.9$  Hz, 2H), 7.62 (t,  $J = 7.4$  Hz, 1H), 7.47 (t,  $J = 7.6$  Hz, 2H), 7.21 (t,  $J = 7.7$  Hz, 1H), 7.07 (t,  $J = 15.6$  Hz, 3H), 3.56 (t,  $J = 7.4$  Hz, 2H), 2.99-2.83 (m, 5H), 2.33 (d,  $J = 5.4$  Hz, 3H).  $^{13}\text{C}$  NMR (75 MHz,  $\text{CDCl}_3$ )  $\delta$  166.9, 157.7, 138.6, 134.1, 130.1, 129.8, 128.8, 128.8, 127.5, 127.3, 125.9, 51.5, 34.9, 34.3, 21.5. HRMS (ESI,  $m/z$ ) calcd. for  $\text{C}_{18}\text{H}_{20}\text{N}_2\text{O}_3\text{Na}_1[\text{M}+\text{Na}]^+$ : 335.1366, found: 335.1363.

### Compound 6e



**6e**, 68% yield, white solid.  $^1\text{H}$  NMR (300 MHz,  $\text{CDCl}_3$ )  $\delta$  8.28 (s, 1H), 8.11 (dd,  $J = 8.3, 1.2$  Hz, 2H), 7.61 (dd,  $J = 10.6, 4.3$  Hz, 1H), 7.47 (t,  $J = 7.7$  Hz, 2H), 7.25-7.00 (m, 4H), 3.65-3.44 (m, 2H), 2.99-2.81 (m, 5H), 2.33 (d,  $J = 5.5$  Hz, 3H).  $^{13}\text{C}$  NMR (75 MHz,  $\text{CDCl}_3$ )  $\delta$  166.9, 157.7, 136.3, 135.6, 134.1, 130.1, 129.6, 128.8, 128.7, 127.3, 77.6, 77.2, 76.7, 51.5, 34.8, 33.9, 21.2. HRMS (ESI,  $m/z$ ) calcd. for  $\text{C}_{18}\text{H}_{20}\text{N}_2\text{O}_3\text{Na}_1[\text{M}+\text{Na}]^+$ : 335.1366, found: 335.1363.

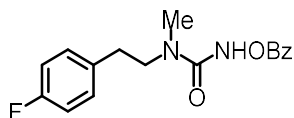
### Compound 6f



**6f**, 71% yield, white solid.  $^1\text{H}$  NMR (300 MHz,  $\text{CDCl}_3$ )  $\delta$  8.37 (s, 1H), 8.12 (dd,  $J = 8.4, 1.3$  Hz, 2H), 7.65-7.58 (m, 1H), 7.46 (dd,  $J = 10.6, 4.7$  Hz, 2H), 7.16 (s, 4H), 3.52 (dd,  $J = 8.4, 6.8$  Hz, 2H), 3.04-2.85 (m, 5H), 2.38 (s, 3H).  $^{13}\text{C}$  NMR (75 MHz,  $\text{CDCl}_3$ )  $\delta$  166.8, 157.7, 136.8, 136.3, 134.1,

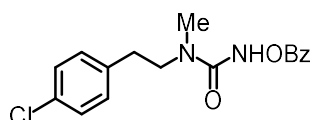
130.6, 130.0, 129.7, 128.7, 127.3, 126.9, 126.5, 50.3, 34.8, 31.6, 19.4. **HRMS (ESI,  $m/z$ )** calcd. for  $C_{18}H_{20}N_2O_3Na_1[M+Na]^+$ : 335.1366, found: 335.1363.

#### Compound 6g



**6g**, 72% yield, white solid.  **$^1H$  NMR** (300 MHz,  $CD_3CN$ )  $\delta$  8.71 (s, 1H), 8.07 (dd,  $J = 8.3, 1.2$  Hz, 2H), 7.78-7.67 (m, 1H), 7.57 (t,  $J = 7.7$  Hz, 2H), 7.37-7.24 (m, 2H), 7.13-7.00 (m, 2H), 3.61-3.41 (m, 2H), 2.98-2.79 (m, 5H).  **$^{13}C$  NMR** (75 MHz,  $CD_3CN$ )  $\delta$  167.2, 164.1, 160.9, 158.5, 136.2, 136.2, 135.0, 131.6, 131.5, 130.4, 129.9, 128.7, 116.2, 115.9, 51.2, 34.8, 33.6. **HRMS (ESI,  $m/z$ )** calcd. for  $C_{17}H_{17}F_1N_2O_3Na_1[M+Na]^+$ : 339.1115, found: 339.1113.

#### Compound 6h

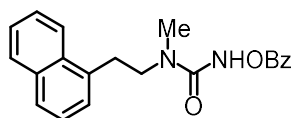


**6h**, 73% yield, white solid.  **$^1H$  NMR** (300 MHz,  $CDCl_3$ )  $\delta$  8.28 (s, 1H), 8.11-7.95 (m, 2H), 7.64-7.49 (m, 1H), 7.40 (t,  $J = 7.6$  Hz, 2H), 7.29-7.16 (m, 2H), 7.09 (d,  $J = 8.4$  Hz, 2H), 3.47 (t,  $J = 7.3$  Hz, 2H), 2.90-2.76 (m, 5H).  **$^{13}C$  NMR** (75 MHz,  $CDCl_3$ )  $\delta$  167.0, 157.7, 137.2, 134.2, 132.6, 130.3, 130.1, 129.0, 128.8, 127.2, 51.3, 34.9, 33.6. **HRMS (ESI,  $m/z$ )** calcd. for  $C_{17}H_{17}Cl_1N_2O_3Na_1[M+Na]^+$ : 355.0820, found: 355.0818.

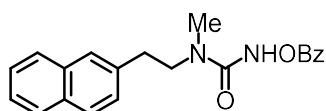
#### Compound 6i



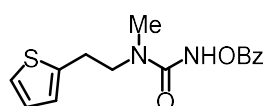
**6i**, 70% yield, white solid.  **$^1H$  NMR** (300 MHz,  $CDCl_3$ )  $\delta$  8.26 (s, 1H), 8.15-8.07 (m, 2H), 7.61 (dd,  $J = 10.6, 4.3$  Hz, 1H), 7.47 (t,  $J = 7.7$  Hz, 2H), 7.14 (t,  $J = 5.7$  Hz, 2H), 6.87 (dd,  $J = 6.7, 4.7$  Hz, 2H), 3.79 (s, 3H), 3.53 (t,  $J = 7.3$  Hz, 2H), 2.91 (s, 3H), 2.86 (t,  $J = 7.3$  Hz, 2H).  **$^{13}C$  NMR** (75 MHz,  $CDCl_3$ )  $\delta$  166.9, 158.6, 157.7, 134.1, 130.7, 130.1, 129.9, 128.7, 127.3, 114.4, 55.4, 51.2, 34.9, 33.4. **HRMS (ESI,  $m/z$ )** calcd. for  $C_{18}H_{20}N_2O_4Na_1[M+Na]^+$ : 351.1315, found: 351.1313.

**Compound 6j**

**6j**, 63% yield, white solid.  $^1\text{H NMR}$  (300 MHz,  $\text{CDCl}_3$ )  $\delta$  8.39 (s, 1H), 8.20-8.10 (m, 3H), 7.87 (d,  $J = 7.8$  Hz, 1H), 7.76 (d,  $J = 7.5$  Hz, 1H), 7.69-7.35 (m, 7H), 3.69 (dd,  $J = 8.5, 6.5$  Hz, 2H), 3.46-3.34 (m, 2H), 2.90 (s, 3H).  $^{13}\text{C NMR}$  (75 MHz,  $\text{CDCl}_3$ )  $\delta$  167.0, 157.7, 134.9, 134.2, 134.1, 132.0, 130.1, 129.0, 128.8, 127.6, 127.3, 127.2, 126.6, 125.9, 125.8, 123.6, 51.1, 35.1, 31.5. **HRMS (ESI,  $m/z$ )** calcd. for  $\text{C}_{21}\text{H}_{20}\text{N}_2\text{O}_3\text{Na}_1[\text{M}+\text{Na}]^+$ : 371.1366, found: 371.1367.

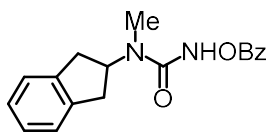
**Compound 6k**

**6k**, 71% yield, white solid.  $^1\text{H NMR}$  (300 MHz,  $\text{CDCl}_3$ )  $\delta$  8.38 (s, 1H), 8.15-8.04 (m, 2H), 7.81 (dd,  $J = 4.6, 3.3$  Hz, 3H), 7.69 (s, 1H), 7.62 (t,  $J = 7.5$  Hz, 1H), 7.54-7.41 (m, 4H), 7.38 (dd,  $J = 8.4, 1.5$  Hz, 1H), 3.66 (t,  $J = 7.4$  Hz, 2H), 3.08 (t,  $J = 7.4$  Hz, 2H), 2.91 (s, 3H).  $^{13}\text{C NMR}$  (75 MHz,  $\text{CDCl}_3$ )  $\delta$  166.9, 157.8, 136.2, 134.1, 133.8, 132.4, 130.1, 128.7, 128.5, 127.8, 127.7, 127.5, 127.3, 126.3, 125.7, 51.4, 35.0, 34.5. **HRMS (ESI,  $m/z$ )** calcd. for  $\text{C}_{21}\text{H}_{20}\text{N}_2\text{O}_3\text{Na}_1[\text{M}+\text{Na}]^+$ : 371.1366, found: 371.1364.

**Compound 6l**

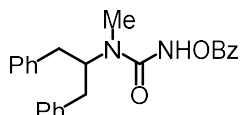
**6l**, 69% yield, white solid.  $^1\text{H NMR}$  (300 MHz,  $\text{CDCl}_3$ )  $\delta$  8.25 (s, 1H), 8.01 (dd,  $J = 8.2, 1.0$  Hz, 2H), 7.60-7.47 (m, 1H), 7.37 (t,  $J = 7.7$  Hz, 2H), 7.07 (dd,  $J = 5.1, 1.1$  Hz, 1H), 6.85 (dd,  $J = 5.1, 3.5$  Hz, 1H), 6.78 (d,  $J = 3.3$  Hz, 1H), 3.51 (t,  $J = 7.1$  Hz, 2H), 3.04 (t,  $J = 7.1$  Hz, 2H), 2.85 (s, 3H).  $^{13}\text{C NMR}$  (75 MHz,  $\text{CDCl}_3$ )  $\delta$  166.9, 157.8, 140.7, 134.1, 130.1, 128.8, 127.4, 127.3, 125.8, 124.3, 51.5, 34.9, 28.3. **HRMS (ESI,  $m/z$ )** calcd. for  $\text{C}_{15}\text{H}_{16}\text{N}_2\text{O}_3\text{S}_1\text{Na}_1[\text{M}+\text{Na}]^+$ : 327.0774, found: 327.0771.

## Compound 6m



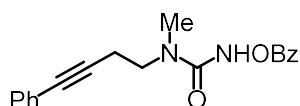
**6m**, 73% yield, white solid.  $^1\text{H NMR}$  (300 MHz,  $\text{CD}_3\text{CN}$ )  $\delta$  8.83 (s, 1H), 8.18-8.02 (m, 2H), 7.72 (t,  $J = 7.5$  Hz, 1H), 7.57 (t,  $J = 7.6$  Hz, 2H), 7.21 (ddd,  $J = 8.8, 7.0, 4.2$  Hz, 4H), 5.14-4.99 (m, 1H), 3.19 (dd,  $J = 16.3, 8.4$  Hz, 2H), 3.05 (dd,  $J = 16.3, 7.0$  Hz, 2H), 2.81 (s, 3H).  $^{13}\text{C NMR}$  (75 MHz,  $\text{CD}_3\text{CN}$ )  $\delta$  167.2, 158.7, 142.2, 135.0, 130.4, 129.9, 128.8, 127.6, 125.3, 56.3, 36.7, 29.2. **HRMS (ESI,  $m/z$ )** calcd. for  $\text{C}_{18}\text{H}_{18}\text{N}_2\text{O}_3\text{Na}_1[\text{M}+\text{Na}]^+$ : 333.1210, found: 333.1207.

## Compound 6n



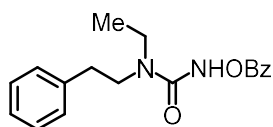
**6n**, 58% yield, colorless oil.  $^1\text{H NMR}$  (300 MHz,  $\text{CDCl}_3$ )  $\delta$  8.16-8.05 (m, 2H), 8.00 (s, 1H), 7.63 (dd,  $J = 10.6, 4.3$  Hz, 1H), 7.48 (t,  $J = 7.6$  Hz, 2H), 7.39-7.19 (m, 10H), 4.51 (s, 1H), 3.21-2.86 (m, 4H), 2.75 (s, 3H).  $^{13}\text{C NMR}$  (75 MHz,  $\text{CDCl}_3$ )  $\delta$  166.5, 158.0, 138.4, 134.0, 130.0, 129.0, 128.9, 128.7, 127.4, 126.8, 38.5. **HRMS (ESI,  $m/z$ )** calcd. for  $\text{C}_{24}\text{H}_{24}\text{N}_2\text{O}_3\text{Na}_1[\text{M}+\text{Na}]^+$ : 411.1679, found: 411.1690.

## Compound 6o



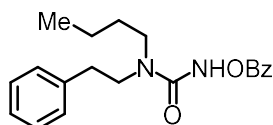
**6o**, 75% yield, white solid.  $^1\text{H NMR}$  (300 MHz,  $\text{CDCl}_3$ )  $\delta$  8.59 (s, 1H), 8.06 (dd,  $J = 8.1, 1.0$  Hz, 2H), 7.57 (ddd,  $J = 6.9, 2.5, 1.2$  Hz, 1H), 7.47-7.33 (m, 4H), 7.28-7.20 (m, 3H), 3.57 (t,  $J = 6.7$  Hz, 2H), 3.09 (s, 3H), 2.70 (t,  $J = 6.7$  Hz, 2H).  $^{13}\text{C NMR}$  (75 MHz,  $\text{CDCl}_3$ )  $\delta$  166.7, 157.8, 134.1, 131.8, 130.0, 128.7, 128.4, 128.1, 127.3, 123.4, 86.8, 82.7, 48.6, 35.1, 19.1. **HRMS (ESI,  $m/z$ )** calcd. for  $\text{C}_{19}\text{H}_{18}\text{N}_2\text{O}_3\text{Na}_1[\text{M}+\text{Na}]^+$ : 345.1221, found: 345.1210.

## Compound 6p



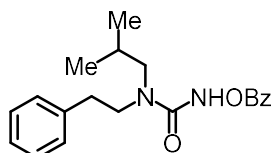
**6p**, 77% yield, white solid.  $^1\text{H NMR}$  (300 MHz,  $\text{CDCl}_3$ )  $\delta$  8.29 (s, 1H), 8.04 (dd,  $J = 5.2, 3.3$  Hz, 2H), 7.62-7.49 (m, 1H), 7.39 (dd,  $J = 10.6, 4.7$  Hz, 2H), 7.31-7.21 (m, 2H), 7.20-7.10 (m, 3H), 3.53-3.38 (m, 2H), 3.20 (q,  $J = 7.2$  Hz, 2H), 2.93-2.81 (m, 2H), 1.12 (t,  $J = 7.2$  Hz, 3H).  $^{13}\text{C NMR}$  (75 MHz,  $\text{CDCl}_3$ )  $\delta$  167.1, 157.4, 138.8, 134.1, 130.1, 129.0, 128.9, 128.7, 127.3, 126.8, 49.2, 42.6, 34.9, 13.4. **HRMS (ESI,  $m/z$ )** calcd. for  $\text{C}_{18}\text{H}_{20}\text{N}_2\text{O}_3\text{Na}_1[\text{M}+\text{Na}]^+$ : 335.1377, found: 335.1363.

## Compound 6q

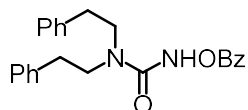


**6q**, 71% yield, colorless oil.  $^1\text{H NMR}$  (300 MHz,  $\text{CDCl}_3$ )  $\delta$  8.30 (s, 1H), 8.12-7.99 (m, 2H), 7.53 (dd,  $J = 10.6, 4.3$  Hz, 1H), 7.40 (t,  $J = 7.6$  Hz, 2H), 7.31-7.10 (m, 5H), 3.53-3.38 (m, 2H), 3.19-3.05 (m, 2H), 2.96-2.80 (m, 2H), 1.51 (dt,  $J = 12.2, 7.2$  Hz, 2H), 1.27 (dt,  $J = 15.0, 7.3$  Hz, 2H), 0.86 (t,  $J = 7.3$  Hz, 3H).  $^{13}\text{C NMR}$  (75 MHz,  $\text{CDCl}_3$ )  $\delta$  167.1, 157.6, 138.8, 134.1, 130.1, 129.0, 128.9, 128.7, 127.3, 126.8, 49.6, 47.7, 34.7, 30.4, 20.2, 13.9. **HRMS (ESI,  $m/z$ )** calcd. for  $\text{C}_{20}\text{H}_{24}\text{N}_2\text{O}_3\text{Na}_1[\text{M}+\text{Na}]^+$ : 363.1690, found: 363.1680.

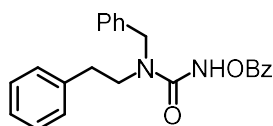
## Compound 6r



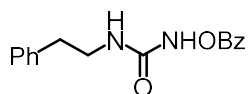
**6r**, 62% yield, colorless oil.  $^1\text{H NMR}$  (300 MHz,  $\text{CDCl}_3$ )  $\delta$  8.50 (s, 1H), 8.16 (dd,  $J = 8.4, 1.3$  Hz, 2H), 7.65 (ddd,  $J = 6.8, 2.5, 1.3$  Hz, 1H), 7.50 (t,  $J = 7.7$  Hz, 2H), 7.44-7.22 (m, 5H), 3.64-3.48 (m, 2H), 3.07 (d,  $J = 7.6$  Hz, 2H), 3.02-2.92 (m, 2H), 2.13-1.95 (m, 1H), 0.98 (d,  $J = 6.7$  Hz, 6H).  $^{13}\text{C NMR}$  (75 MHz,  $\text{CDCl}_3$ )  $\delta$  167.1, 157.8, 138.8, 134.1, 130.1, 128.9, 128.9, 128.7, 127.3, 126.7, 55.2, 50.1, 34.4, 27.7, 20.3. **HRMS (ESI,  $m/z$ )** calcd. for  $\text{C}_{20}\text{H}_{24}\text{N}_2\text{O}_3\text{Na}_1[\text{M}+\text{Na}]^+$ : 363.1690, found: 363.1679.

**Compound 6s**

**6s**, 61% yield, white solid.  $^1\text{H NMR}$  (300 MHz,  $\text{CDCl}_3$ )  $\delta$  8.14 (dd,  $J = 10.0, 2.9$  Hz, 3H), 7.65 (t,  $J = 7.5$  Hz, 1H), 7.51 (t,  $J = 7.7$  Hz, 2H), 7.35 (t,  $J = 7.1$  Hz, 4H), 7.30-7.18 (m, 7H), 3.47 (t,  $J = 7.4$  Hz, 4H), 2.92 (t,  $J = 7.4$  Hz, 4H).  $^{13}\text{C NMR}$  (75 MHz,  $\text{CDCl}_3$ )  $\delta$  166.8, 157.6, 138.7, 134.1, 130.1, 128.9, 128.7, 127.3, 126.8, 50.1, 34.7. **HRMS (ESI,  $m/z$ )** calcd. for  $\text{C}_{20}\text{H}_{24}\text{N}_2\text{O}_3\text{Na}_1[\text{M}+\text{Na}]^+$ : 363.1690, found: 363.1680. **HRMS (ESI,  $m/z$ )** calcd. for  $\text{C}_{24}\text{H}_{24}\text{N}_2\text{O}_3\text{Na}_1[\text{M}+\text{Na}]^+$ : 411.1690, found: 411.1680.

**Compound 6t**

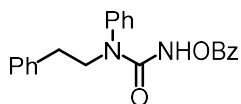
**6t**, 68% yield, white solid.  $^1\text{H NMR}$  (300 MHz,  $\text{CD}_3\text{CN}$ )  $\delta$  8.81 (s, 1H), 8.08 (dd,  $J = 5.2, 3.3$  Hz, 2H), 7.80-7.65 (m, 1H), 7.57 (dd,  $J = 10.6, 4.7$  Hz, 2H), 7.44-7.20 (m, 10H), 4.46 (s, 2H), 3.58-3.41 (m, 2H), 3.01-2.83 (m, 2H).  $^{13}\text{C NMR}$  (75 MHz,  $\text{CD}_3\text{CN}$ )  $\delta$  167.3, 158.7, 140.0, 138.6, 135.0, 130.4, 129.9, 129.8, 129.6, 129.5, 128.7, 128.4, 127.4, 51.0, 49.3, 34.8. **HRMS (ESI,  $m/z$ )** calcd. for  $\text{C}_{23}\text{H}_{22}\text{N}_2\text{O}_3\text{Na}_1[\text{M}+\text{Na}]^+$ : 397.1534, found: 397.1522.

**Compound 6u**

**6u**, 82% yield, white solid.  $^1\text{H NMR}$  (300 MHz,  $\text{CDCl}_3$ )  $\delta$  8.56 (s, 1H), 8.01-7.90 (m, 2H), 7.66 (ddd,  $J = 7.0, 2.5, 1.3$  Hz, 1H), 7.57-7.44 (m, 2H), 7.25-7.08 (m, 5H), 5.39 (s, 1H), 3.56 (dd,  $J = 12.8, 6.6$  Hz, 2H), 2.84 (t,  $J = 6.8$  Hz, 2H).  $^{13}\text{C NMR}$  (75 MHz,  $\text{CDCl}_3$ )  $\delta$  164.9, 158.3, 138.6, 134.5, 129.8, 129.0, 128.9, 128.8, 126.8, 126.7, 41.1, 35.9. **HRMS (ESI,  $m/z$ )** calcd. for  $\text{C}_{16}\text{H}_{16}\text{N}_2\text{O}_3\text{Na}_1[\text{M}+\text{Na}]^+$ : 307.1053, found: 307.1050.

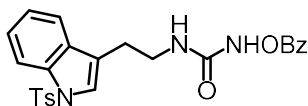


## Compound 6v



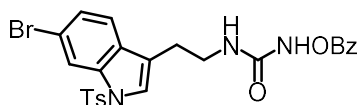
**6v**, 57% yield, colorless oil.  $^1\text{H NMR}$  (300 MHz,  $\text{CDCl}_3$ )  $\delta$  8.15-8.08 (m, 2H), 8.02 (s, 1H), 7.63 (t,  $J = 7.4$  Hz, 1H), 7.55-7.39 (m, 5H), 7.37-7.17 (m, 7H), 4.04-3.89 (m, 2H), 2.98 (dd,  $J = 8.9, 6.9$  Hz, 2H).  $^{13}\text{C NMR}$  (75 MHz,  $\text{CDCl}_3$ )  $\delta$  166.9, 156.8, 140.1, 138.6, 134.1, 130.4, 130.1, 129.0, 128.8, 128.7, 128.6, 128.3, 127.2, 126.5, 52.2, 34.5.

## Compound 6w

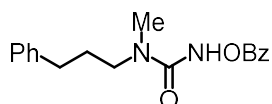


**6w**, 48% yield, white solid.  $^1\text{H NMR}$  (300 MHz,  $\text{CD}_3\text{CN}$ )  $\delta$  8.40 (s, 1H), 8.17-8.01 (m, 2H), 7.93 (d,  $J = 8.1$  Hz, 1H), 7.78 (d,  $J = 8.4$  Hz, 2H), 7.71 (t,  $J = 7.5$  Hz, 1H), 7.64-7.46 (m, 4H), 7.41-7.20 (m, 4H), 6.16 (s, 1H), 3.49 (q,  $J = 6.6$  Hz, 2H), 2.89 (t,  $J = 6.7$  Hz, 2H), 2.32 (s, 3H).  $^{13}\text{C NMR}$  (75 MHz,  $\text{CD}_3\text{CN}$ )  $\delta$  166.3, 159.4, 146.5, 135.9, 135.6, 135.0, 132.1, 130.9, 130.6, 129.7, 128.3, 127.6, 125.6, 124.9, 124.2, 121.4, 120.6, 114.4, 39.8, 25.8, 21.4. **HRMS (ESI,  $m/z$ )** calcd. for  $\text{C}_{25}\text{H}_{23}\text{N}_3\text{O}_5\text{S}_1\text{Na}_1[\text{M}+\text{Na}]^+$ : 500.1251, found: 500.1252.

## Compound 6x



**6x**, 52% yield, white solid.  $^1\text{H NMR}$  (300 MHz,  $\text{CDCl}_3$ )  $\delta$  8.47 (s, 1H), 8.04 (d,  $J = 1.2$  Hz, 1H), 7.89-7.79 (m, 2H), 7.65 (d,  $J = 8.4$  Hz, 2H), 7.58 (t,  $J = 7.5$  Hz, 1H), 7.41 (t,  $J = 7.7$  Hz, 2H), 7.25 (dd,  $J = 13.8, 5.9$  Hz, 3H), 7.21-7.11 (m, 3H), 5.38 (t,  $J = 5.7$  Hz, 1H), 3.50 (q,  $J = 6.7$  Hz, 2H), 2.83 (t,  $J = 6.8$  Hz, 2H), 2.26 (s, 3H).  $^{13}\text{C NMR}$  (75 MHz,  $\text{CDCl}_3$ )  $\delta$  164.9, 158.3, 145.5, 136.0, 135.1, 134.6, 130.2, 129.7, 129.6, 129.1, 126.9, 126.8, 126.5, 124.1, 120.6, 119.4, 118.8, 117.0, 39.9, 25.4, 21.7. **HRMS (ESI,  $m/z$ )** calcd. for  $\text{C}_{25}\text{H}_{22}\text{N}_3\text{O}_5\text{S}_1\text{Br}_1\text{Na}_1[\text{M}+\text{Na}]^+$ : 578.0356, 580.0338, found: 578.0357, 580.0337.

**Compound 6y**

**6y**, 63% yield, white solid.  $^1\text{H NMR}$  (300 MHz,  $\text{CD}_3\text{CN}$ )  $\delta$  8.72 (s, 1H), 8.07 (d,  $J = 7.3$  Hz, 2H), 7.72 (t,  $J = 7.4$  Hz, 1H), 7.56 (t,  $J = 7.7$  Hz, 2H), 7.37-7.16 (m, 5H), 3.41-3.24 (m, 2H), 2.94 (s, 3H), 2.74-2.57 (m, 2H), 1.88 (dd,  $J = 15.2, 7.5$  Hz, 2H).  $^{13}\text{C NMR}$  (75 MHz,  $\text{CD}_3\text{CN}$ )  $\delta$  167.2, 158.5, 142.9, 134.8, 130.3, 129.8, 129.3, 129.2, 128.7, 126.7, 49.0, 34.1, 33.4, 30.0. **HRMS (ESI,  $m/z$ )** calcd. for  $\text{C}_{18}\text{H}_{20}\text{N}_2\text{O}_3\text{Na}_1[\text{M}+\text{Na}]^+$ : 335.1377, found: 335.1364.

**4.4.2 Ruthenium Catalyzed Intramolecular C–H Amidations**

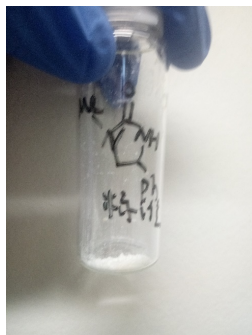
**General procedure:** A pre-dried (using heating gun to dry for 3 times per tube) 10 mL Schlenk tube was charged with substrates **6a-y** (0.2 mmol), chiral ruthenium catalyst (0.002 mmol, 1 mol%) and  $\text{K}_2\text{CO}_3$  (82.8 mg, 0.6 mmol) under an atmosphere of  $\text{N}_2$ . Fresh distilled dichloromethane (2.0 mL) was added via syringe. The reaction mixture was stirred at the indicated temperature for the indicated time under an atmosphere of  $\text{N}_2$ . Afterwards, the mixture was directly transferred to a column (the Schlenk tube was rinsed with a minimal amount of  $\text{CH}_2\text{Cl}_2$  to transfer the reaction solution completely) and purified by flash chromatography on silica gel (EtOAc/*n*-Hexane = 2:1 to EtOAc/MeOH 95:5) to afford the analytical pure products **7a-y**. Enantiomeric ratios were determined by HPLC analysis on chiral stationary phase. The absolute configuration of the product **7h** was confirmed by X-ray analysis (CCDC number: 1972573) as *S*-configuration. Racemic samples were obtained by the same catalytic reactions using racemic ruthenium catalyst instead of chiral ruthenium catalyst.

*Additional experimental informations:*

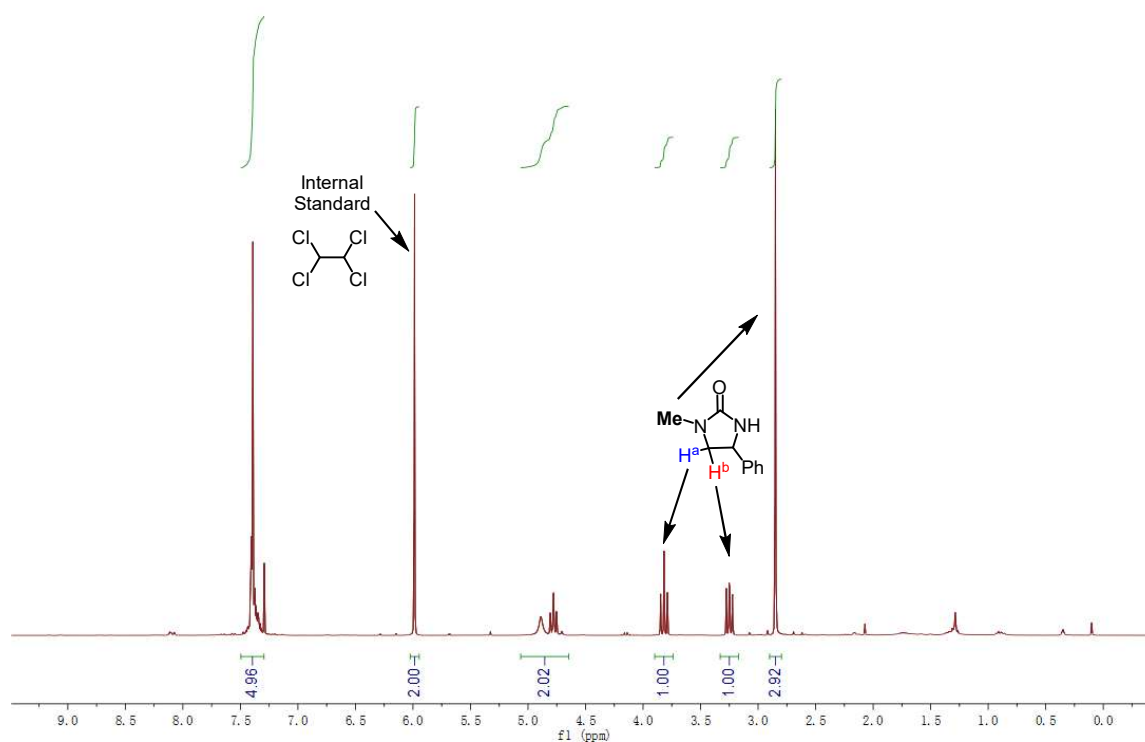
- a) **Execution of the reactions.** All catalytic reactions were carried out in 10 mL Schlenk tubes from “Synthware” under  $\text{N}_2$  atmosphere (see image below).



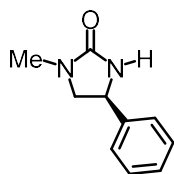
**b) Isolation of the final product.** The C-H amination products can be isolated by flash chromatography without any trace contaminations from the ruthenium catalyst as evident by the white color of the products (see image below).



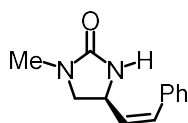
**c) Crude  $^1\text{H}$  NMR spectra analysis of the standard reaction solution.** See image below.



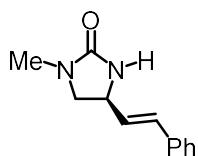
The above crude  $^1\text{H}$  NMR analysis shows quantitative yield of the target cyclic urea product **7a** (Table 3, entry 5).

**Compound (S)-7a**

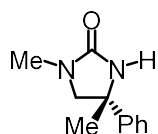
Starting from **6aa** (59.6 mg, 0.20 mmol) according to the general procedure to provide **7a** as a white solid (34.9 mg, 99% yield) and with 95% ee as determined by HPLC analysis (column: Daicel Chiralpak IA 250 x 4.6 mm, absorption:  $\lambda = 220$  nm, mobile phase: *n*-Hexane/isopropanol = 90:10, flow rate: 1.0 mL/min, column temperature: 30 °C, retention times:  $t_r$  (major) = 13.2 min,  $t_r$  (minor) = 11.4 min).  $[\alpha]_D^{22} = 10.6^\circ$  ( $c = 1.0$ ,  $\text{CH}_2\text{Cl}_2$ ).  $^1\text{H NMR}$  (300 MHz,  $\text{CD}_3\text{CN}$ )  $\delta$  7.46-7.28 (m, 5H), 5.54 (s, 1H), 4.82-4.63 (m, 1H), 3.77 (t,  $J = 8.8$  Hz, 1H), 3.12 (dd,  $J = 8.7, 7.5$  Hz, 1H), 2.71 (s, 3H).  $^{13}\text{C NMR}$  (75 MHz,  $\text{CD}_3\text{CN}$ )  $\delta$  163.2, 143.6, 129.6, 128.7, 127.1, 56.5, 54.1, 30.8. **HRMS (ESI,  $m/z$ )** calcd. for  $\text{C}_{10}\text{H}_{12}\text{N}_2\text{O}_1\text{Na}_1[\text{M}+\text{Na}]^+$ : 199.0842, found: 199.0842.

**Compound (S,Z)-7b**

Starting from (*Z*)-**6b** (62.8 mg, 0.20 mmol) according to the general procedure to provide (*S,Z*)-**7b** as a white solid (29.5 mg, 73% yield) and with 91% ee as determined by HPLC analysis (column: Daicel Chiralpak IG 250 x 4.6 mm, absorption:  $\lambda = 220$  nm, mobile phase: *n*-Hexane/isopropanol = 80:20, flow rate: 1.0 mL/min, column temperature: 30 °C, retention times:  $t_r$  (major) = 15.5 min,  $t_r$  (minor) = 14.6 min).  $[\alpha]_D^{22} = 47.0^\circ$  ( $c = 1.0$ ,  $\text{CH}_2\text{Cl}_2$ ).  $^1\text{H NMR}$  (300 MHz,  $\text{CD}_3\text{CN}$ )  $\delta$  7.44-7.36 (m, 2H), 7.35-7.30 (m, 1H), 7.30-7.23 (m, 2H), 6.65 (d,  $J = 11.6$  Hz, 1H), 5.72 (dd,  $J = 11.5, 9.3$  Hz, 1H), 5.14 (s, 1H), 4.57 (dd,  $J = 16.4, 8.7$  Hz, 1H), 3.63 (t,  $J = 8.6$  Hz, 1H), 3.14 (dd,  $J = 8.7, 7.4$  Hz, 1H), 2.69 (s, 3H).  $^{13}\text{C NMR}$  (75 MHz,  $\text{CD}_3\text{CN}$ )  $\delta$  162.9, 137.2, 133.3, 132.4, 129.6, 129.4, 128.4, 54.3, 48.1, 30.8. **HRMS (ESI,  $m/z$ )** calcd. for  $\text{C}_{12}\text{H}_{14}\text{N}_2\text{O}_1\text{Na}_1[\text{M}+\text{Na}]^+$ : 225.0998, found: 225.0997.

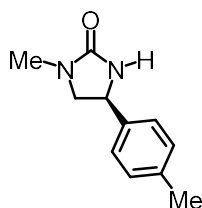
**Compound (*S,E*)-7b**

Starting from (*E*)-**6b** (62.8 mg, 0.20 mmol) according to the general procedure to provide (*S,E*)-**7b** as a white solid (32.2 mg, 80% yield) and with 76% ee as determined by HPLC analysis (column: Daicel Chiralpak IG 250 x 4.6 mm, absorption:  $\lambda = 220$  nm, mobile phase: *n*-Hexane/isopropanol = 80:20, flow rate: 1.0 mL/min, column temperature: 30 °C, retention times:  $t_r$  (major) = 15.5 min,  $t_r$  (minor) = 17.8 min).  $[\alpha]_D^{22} = -15.4^\circ$  ( $c = 1.0$ ,  $\text{CH}_2\text{Cl}_2$ ).  $^1\text{H NMR}$  (300 MHz,  $\text{CD}_3\text{CN}$ )  $\delta$  7.49-7.42 (m, 2H), 7.41-7.24 (m, 3H), 6.61 (d,  $J = 15.9$  Hz, 1H), 6.28 (dd,  $J = 15.9, 7.3$  Hz, 1H), 5.15 (s, 1H), 4.29 (q,  $J = 7.3$  Hz, 1H), 3.60 (t,  $J = 8.7$  Hz, 1H), 3.14 (dd,  $J = 8.8, 7.1$  Hz, 1H), 2.70 (s, 3H).  $^{13}\text{C NMR}$  (75 MHz,  $\text{CD}_3\text{CN}$ )  $\delta$  162.9, 137.6, 132.0, 130.7, 129.7, 128.8, 127.4, 54.0, 52.8, 30.8. **HRMS (ESI,  $m/z$ )** calcd. for  $\text{C}_{12}\text{H}_{14}\text{N}_2\text{O}_1\text{Na}_1[\text{M}+\text{Na}]^+$ : 225.0998, found: 225.0998.

**Compound (*R*)-7c**

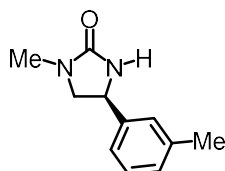
Starting from (*S*)-**6c** (62.4 mg, 0.20 mmol) according to the general procedure to provide (*R*)-**7c** as a white solid (33.7 mg, 89% yield) and with 85% ee ( $\Delta$ -**Ru5** was applied), enantioselectivity was determined by HPLC analysis (column: Daicel Chiralpak IC 250 x 4.6 mm, absorption:  $\lambda = 215$  nm, mobile phase: *n*-Hexane/isopropanol = 60:40, flow rate: 1.0 mL/min, column temperature: 30 °C, retention times:  $t_r$  (major) = 11.6 min,  $t_r$  (minor) = 8.9 min).  $^1\text{H NMR}$  (300 MHz,  $\text{CDCl}_3$ )  $\delta$  7.43-7.32 (m, 4H), 7.29 (dd,  $J = 5.7, 2.9$  Hz, 1H), 4.83 (s, 1H), 3.45 (dd,  $J = 20.1, 8.6$  Hz, 2H), 2.80 (s, 3H), 1.68 (s, 3H).  $^{13}\text{C NMR}$  (75 MHz,  $\text{CDCl}_3$ )  $\delta$  161.3, 145.9, 128.9, 127.5, 124.9, 62.1, 57.1, 30.6, 28.7. **HRMS (ESI,  $m/z$ )** calcd. for  $\text{C}_{11}\text{H}_{14}\text{N}_2\text{O}_1\text{Na}_1[\text{M}+\text{Na}]^+$ : 213.0998, found: 213.0999.

## Compound (S)-7d



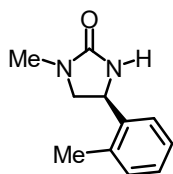
Starting from **6d** (62.4 mg, 0.20 mmol) according to the general procedure to provide **7d** as a white solid (35.0 mg, 92% yield) and with 95% ee as determined by HPLC analysis (column: Daicel Chiralpak IA 250 x 4.6 mm, absorption:  $\lambda = 220$  nm, mobile phase: *n*-Hexane/isopropanol = 95:5, flow rate: 1.0 mL/min, column temperature: 40 °C, retention times:  $t_r$  (major) = 21.1 min,  $t_r$  (minor) = 16.9 min).  $[\alpha]_D^{22} = 18.0^\circ$  ( $c = 1.0$ ,  $\text{CH}_2\text{Cl}_2$ ).  $^1\text{H NMR}$  (300 MHz,  $\text{CDCl}_3$ )  $\delta$  7.26-6.97 (m, 4H), 4.76-4.47 (m, 2H), 3.70 (t,  $J = 8.9$  Hz, 1H), 3.14 (dd,  $J = 8.6, 7.5$  Hz, 1H), 2.75 (s, 3H), 2.29 (s, 3H).  $^{13}\text{C NMR}$  (75 MHz,  $\text{CDCl}_3$ )  $\delta$  162.3, 141.7, 138.9, 129.7, 129.1, 129.0, 126.8, 126.2, 123.3, 56.2, 53.8, 30.7, 21.5. **HRMS (ESI,  $m/z$ )** calcd. for  $\text{C}_{11}\text{H}_{14}\text{N}_2\text{O}_1\text{Na}_1[\text{M}+\text{Na}]^+$ : 213.0998, found: 213.0999.

## Compound (S)-7e



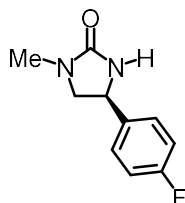
Starting from **6e** (62.4 mg, 0.20 mmol) according to the general procedure to provide **7e** as a white solid (37.7 mg, 99% yield) and with 96% ee as determined by HPLC analysis (column: Daicel Chiralpak IC 250 x 4.6 mm, absorption:  $\lambda = 220$  nm, mobile phase: *n*-Hexane/isopropanol = 50:50, flow rate: 1.0 mL/min, column temperature: 25 °C, retention times:  $t_r$  (major) = 11.4 min,  $t_r$  (minor) = 12.6 min).  $[\alpha]_D^{22} = 5.6^\circ$  ( $c = 1.0$ ,  $\text{CH}_2\text{Cl}_2$ ).  $^1\text{H NMR}$  (300 MHz,  $\text{CD}_3\text{CN}$ )  $\delta$  7.27 (d,  $J = 8.1$  Hz, 2H), 7.23-7.12 (m, 2H), 5.43 (s, 1H), 4.67 (t,  $J = 8.1$  Hz, 1H), 3.74 (dd,  $J = 10.9, 6.5$  Hz, 1H), 3.10 (dd,  $J = 8.7, 7.6$  Hz, 1H), 2.71 (s, 3H), 2.35 (s, 3H).  $^{13}\text{C NMR}$  (75 MHz,  $\text{CD}_3\text{CN}$ )  $\delta$  163.1, 140.5, 138.5, 130.2, 127.1, 56.6, 53.9, 30.8, 21.1. **HRMS (ESI,  $m/z$ )** calcd. for  $\text{C}_{11}\text{H}_{14}\text{N}_2\text{O}_1\text{Na}_1[\text{M}+\text{Na}]^+$ : 213.0998, found: 213.0999.

## Compound (S)-7f



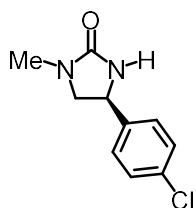
Starting from **6f** (62.4 mg, 0.20 mmol) according to the general procedure to provide **7f** as a white solid (36.6 mg, 96% yield) and with 97% ee as determined by HPLC analysis (column: Daicel Chiralpak IA 250 x 4.6 mm, absorption:  $\lambda = 220$  nm, mobile phase: *n*-Hexane/isopropanol = 85:15, flow rate: 1.0 mL/min, column temperature: 30 °C, retention times:  $t_r$  (major) = 8.8 min,  $t_r$  (minor) = 7.6 min).  $[\alpha]_D^{22} = 151.0^\circ$  ( $c = 1.0$ ,  $\text{CH}_2\text{Cl}_2$ ).  $^1\text{H NMR}$  (300 MHz,  $\text{CDCl}_3$ )  $\delta$  7.50-7.37 (m, 1H), 7.24-7.04 (m, 3H), 4.92 (dd,  $J = 8.8, 7.4$  Hz, 2H), 3.78 (t,  $J = 8.8$  Hz, 1H), 3.05 (dd,  $J = 8.5, 7.3$  Hz, 1H), 2.72 (s, 3H), 2.24 (s, 3H).  $^{13}\text{C NMR}$  (75 MHz,  $\text{CDCl}_3$ )  $\delta$  162.4, 139.7, 134.7, 130.8, 127.8, 126.8, 125.1, 54.9, 50.5, 30.6, 19.1. **HRMS (ESI,  $m/z$ )** calcd. for  $\text{C}_{11}\text{H}_{14}\text{N}_2\text{O}_1\text{Na}_1[\text{M}+\text{Na}]^+$ : 213.0998, found: 213.0998.

## Compound (S)-7g



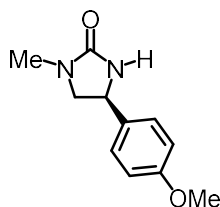
Starting from **6g** (63.2 mg, 0.20 mmol) according to the general procedure to provide **7g** as a white solid (34.8 mg, 90% yield) and with 93% ee as determined by HPLC analysis (column: Daicel Chiralpak IC 250 x 4.6 mm, absorption:  $\lambda = 220$  nm, mobile phase: *n*-Hexane/isopropanol = 50:50, flow rate: 1.0 mL/min, column temperature: 40 °C, retention times:  $t_r$  (major) = 8.9 min,  $t_r$  (minor) = 9.8 min).  $[\alpha]_D^{22} = 63.2^\circ$  ( $c = 1.0$ ,  $\text{CH}_2\text{Cl}_2$ ).  $^1\text{H NMR}$  (300 MHz,  $\text{CDCl}_3$ )  $\delta$  7.39-7.28 (m, 2H), 7.12-6.95 (m, 2H), 5.36 (s, 1H), 4.73 (t,  $J = 8.1$  Hz, 1H), 3.75 (t,  $J = 8.8$  Hz, 1H), 3.16 (dd,  $J = 8.7, 7.4$  Hz, 1H), 2.78 (s, 3H).  $^{13}\text{C NMR}$  (75 MHz,  $\text{CDCl}_3$ )  $\delta$  164.3, 162.4, 161.0, 137.5, 137.5, 127.9, 127.8, 116.0, 115.7, 56.2, 53.2, 30.6.  $^{19}\text{F NMR}$  (235 MHz,  $\text{CDCl}_3$ )  $\delta$  -114.16. **HRMS (ESI,  $m/z$ )** calcd. for  $\text{C}_{10}\text{H}_{11}\text{F}_1\text{N}_2\text{O}_1\text{Na}_1[\text{M}+\text{Na}]^+$ : 217.0748, found: 217.0748.

## Compound (S)-7h



Starting from **6h** (66.4 mg, 0.20 mmol) according to the general procedure to provide **7h** as a white solid (39.1 mg, 93% yield) and with 90% ee as determined by HPLC analysis (column: Daicel Chiralpak ODH 250 x 4.6 mm, absorption:  $\lambda = 220$  nm, mobile phase: *n*-Hexane/isopropanol = 85:15, flow rate: 1.0 mL/min, column temperature: 30 °C, retention times:  $t_r$  (major) = 12.1 min,  $t_r$  (minor) = 14.1 min).  $[\alpha]_D^{22} = 23.2^\circ$  ( $c = 1.0$ ,  $\text{CH}_2\text{Cl}_2$ ).  $^1\text{H NMR}$  (300 MHz,  $\text{CDCl}_3$ )  $\delta$  7.31-7.17 (m, 4H), 5.22 (s, 1H), 4.72-4.59 (m, 1H), 3.70 (t,  $J = 8.9$  Hz, 1H), 3.09 (dd,  $J = 8.5, 7.5$  Hz, 1H), 2.72 (s, 3H).  $^{13}\text{C NMR}$  (75 MHz,  $\text{CDCl}_3$ )  $\delta$  162.4, 140.3, 134.1, 129.2, 127.6, 56.1, 53.2, 30.6. **HRMS (ESI,  $m/z$ )** calcd. for  $\text{C}_{10}\text{H}_{11}\text{Cl}_1\text{N}_2\text{O}_1\text{Na}_1[\text{M}+\text{Na}]^+$ : 233.0452, found: 233.0451.

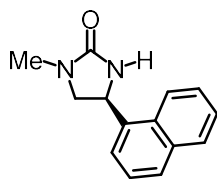
## Compound (S)-7i



Starting from **6i** (65.6 mg, 0.20 mmol) according to the general procedure to provide **7i** as a white solid (41.0 mg, 99% yield) and with 92% ee as determined by HPLC analysis (column: Daicel Chiralpak IA 250 x 4.6 mm, absorption:  $\lambda = 220$  nm, mobile phase: *n*-Hexane/isopropanol = 90:10, flow rate: 1.0 mL/min, column temperature: 30 °C, retention times:  $t_r$  (major) = 19.4 min,  $t_r$  (minor) = 16.9 min).  $[\alpha]_D^{22} = 56.4^\circ$  ( $c = 1.0$ ,  $\text{CH}_2\text{Cl}_2$ ).  $^1\text{H NMR}$  (300 MHz,  $\text{CDCl}_3$ )  $\delta$  7.34-7.18 (m, 2H), 6.88 (d,  $J = 8.7$  Hz, 2H), 4.97 (s, 1H), 4.68 (t,  $J = 8.1$  Hz, 1H), 3.79 (s, 3H), 3.73 (t,  $J = 8.8$  Hz, 1H), 3.17 (dd,  $J = 8.6, 7.6$  Hz, 1H), 2.79 (s, 3H).  $^{13}\text{C NMR}$  (75 MHz,  $\text{CDCl}_3$ )  $\delta$  162.3, 159.6, 133.7, 127.4, 114.4, 56.4, 55.4, 53.3, 30.7. **HRMS (ESI,  $m/z$ )** calcd. for  $\text{C}_{11}\text{H}_{14}\text{N}_2\text{O}_2\text{Na}_1[\text{M}+\text{Na}]^+$ : 229.0947, found: 229.0948.

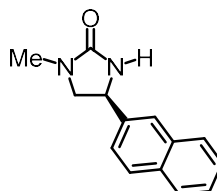


## Compound (S)-7j



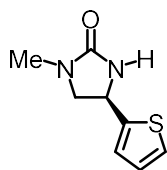
Starting from **6j** (69.6 mg, 0.20 mmol) according to the general procedure to provide **7j** as a white solid (45.0 mg, 99% yield) and with 99% ee as determined by HPLC analysis (column: Daicel Chiralpak IA 250 x 4.6 mm, absorption:  $\lambda = 220$  nm, mobile phase: *n*-Hexane/isopropanol = 85:15, flow rate: 1.0 mL/min, column temperature: 30 °C, retention times:  $t_r$  (major) = 10.9 min,  $t_r$  (minor) = 9.5 min).  $[\alpha]_D^{22} = 106.6^\circ$  ( $c = 1.0$ ,  $\text{CH}_2\text{Cl}_2$ ).  $^1\text{H NMR}$  (300 MHz,  $\text{CDCl}_3$ )  $\delta$  7.90 (dd,  $J = 11.5$ , 6.2 Hz, 2H), 7.82 (d,  $J = 8.2$  Hz, 1H), 7.70 (d,  $J = 7.1$  Hz, 1H), 7.60-7.44 (m, 3H), 5.53 (t,  $J = 7.9$  Hz, 1H), 5.04 (s, 1H), 4.07 (t,  $J = 9.0$  Hz, 1H), 3.26 (dd,  $J = 8.7$ , 6.9 Hz, 1H), 2.82 (s, 3H).  $^{13}\text{C NMR}$  (75 MHz,  $\text{CDCl}_3$ )  $\delta$  162.2, 137.1, 134.1, 130.4, 129.4, 128.5, 126.7, 126.0, 125.8, 122.6, 122.3, 55.3, 50.4, 30.6. **HRMS (ESI,  $m/z$ )** calcd. for  $\text{C}_{14}\text{H}_{14}\text{N}_2\text{O}_1\text{Na}_1[\text{M}+\text{Na}]^+$ : 249.0998, found: 249.0997.

## Compound (S)-7k



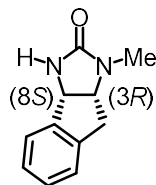
Starting from **6k** (69.6 mg, 0.20 mmol) according to the general procedure to provide **7k** as a white solid (43.9 mg, 97% yield) and with 90% ee as determined by HPLC analysis (column: Daicel Chiralpak IC 250 x 4.6 mm, absorption:  $\lambda = 220$  nm, mobile phase: *n*-Hexane/isopropanol = 60:40, flow rate: 1.0 mL/min, column temperature: 30 °C, retention times:  $t_r$  (major) = 19.4 min,  $t_r$  (minor) = 31.8 min).  $[\alpha]_D^{22} = 97.6^\circ$  ( $c = 1.0$ ,  $\text{CH}_2\text{Cl}_2$ ).  $^1\text{H NMR}$  (300 MHz,  $\text{CDCl}_3$ )  $\delta$  7.91-7.74 (m, 4H), 7.57-7.38 (m, 3H), 5.35 (s, 1H), 4.89 (t,  $J = 8.1$  Hz, 1H), 3.82 (t,  $J = 8.9$  Hz, 1H), 3.27 (dd,  $J = 8.7$ , 7.2 Hz, 1H), 2.81 (s, 3H).  $^{13}\text{C NMR}$  (75 MHz,  $\text{CDCl}_3$ )  $\delta$  162.4, 139.1, 133.4, 133.3, 129.0, 128.0, 127.8, 126.6, 126.3, 125.1, 123.9, 56.0, 53.8, 30.7. **HRMS (ESI,  $m/z$ )** calcd. for  $\text{C}_{14}\text{H}_{14}\text{N}_2\text{O}_1\text{Na}_1[\text{M}+\text{Na}]^+$ : 249.0998, found: 249.0999.

## Compound (S)-7l

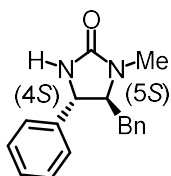


Starting from **6l** (60.8 mg, 0.20 mmol) according to the general procedure to provide **7l** as a white solid (36.1 mg, 99% yield) and with 88% ee as determined by HPLC analysis (column: Daicel Chiralpak IA 250 x 4.6 mm, absorption:  $\lambda = 220$  nm, mobile phase: *n*-Hexane/isopropanol = 90:10, flow rate: 1.0 mL/min, column temperature: 30 °C, retention times:  $t_r$  (major) = 16.0 min,  $t_r$  (minor) = 13.3 min).  $[\alpha]_D^{22} = 8.6^\circ$  ( $c = 1.0$ ,  $\text{CH}_2\text{Cl}_2$ ).  $^1\text{H NMR}$  (300 MHz,  $\text{CDCl}_3$ )  $\delta$  7.29 (dd,  $J = 4.8, 1.1$  Hz, 1H), 7.05 (d,  $J = 2.9$  Hz, 1H), 6.99 (dd,  $J = 5.0, 3.6$  Hz, 1H), 5.05 (dd,  $J = 15.4, 7.1$  Hz, 2H), 3.80 (t,  $J = 8.7$  Hz, 1H), 3.36 (dd,  $J = 8.8, 7.1$  Hz, 1H), 2.85 (s, 3H).  $^{13}\text{C NMR}$  (75 MHz,  $\text{CDCl}_3$ )  $\delta$  161.6, 145.5, 127.1, 125.4, 124.8, 56.4, 49.9, 30.6. **HRMS (ESI,  $m/z$ )** calcd. for  $\text{C}_8\text{H}_{10}\text{S}_1\text{N}_2\text{O}_1\text{Na}_1[\text{M}+\text{Na}]^+$ : 245.0406, found: 245.0406.

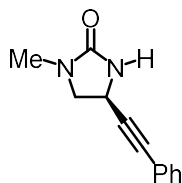
## Compound (3R,8S)-7m



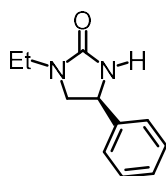
Starting from **6m** (62.0 mg, 0.20 mmol) according to the general procedure to provide **7m** as a white solid (10.9 mg, 29% yield) and with 89% ee as determined by HPLC analysis (column: Daicel Chiralpak IA 250 x 4.6 mm, absorption:  $\lambda = 220$  nm, mobile phase: *n*-Hexane/isopropanol = 90:10, flow rate: 1.0 mL/min, column temperature: 25 °C, retention times:  $t_r$  (major) = 26.2 min,  $t_r$  (minor) = 16.2 min).  $[\alpha]_D^{22} = -131.8^\circ$  ( $c = 1.0$ ,  $\text{CH}_2\text{Cl}_2$ ).  $^1\text{H NMR}$  (300 MHz,  $\text{CDCl}_3$ )  $\delta$  7.19 (s, 5H), 5.03 (s, 1H), 4.94 (d,  $J = 7.8$  Hz, 1H), 4.31 (ddd,  $J = 7.8, 5.1, 2.8$  Hz, 1H), 3.18-3.01 (m, 2H), 2.75 (s, 3H).  $^{13}\text{C NMR}$  (75 MHz,  $\text{CDCl}_3$ )  $\delta$  161.2, 142.1, 140.5, 128.9, 127.7, 125.7, 124.5, 62.3, 58.8, 36.6, 28.8. **HRMS (ESI,  $m/z$ )** calcd. for  $\text{C}_{11}\text{H}_{12}\text{N}_2\text{O}_1\text{Na}_1[\text{M}+\text{Na}]^+$ : 211.0842, found: 211.0842.

Compound (4*S*,5*S*)-7n

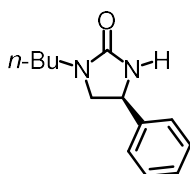
Starting from **6n** (77.6 mg, 0.20 mmol) according to the general procedure to provide **7n** as a white solid (49.3 mg, 93% yield) and with 94% ee as determined by HPLC analysis (column: Daicel Chiralpak ODH 250 x 4.6 mm, absorption:  $\lambda = 220$  nm, mobile phase: *n*-Hexane/isopropanol = 85:15, flow rate: 1.0 mL/min, column temperature: 30 °C, retention times:  $t_r$  (major) = 11.1 min,  $t_r$  (minor) = 9.7 min).  $[\alpha]_D^{22} = -8.2^\circ$  ( $c = 1.0$ ,  $\text{CH}_2\text{Cl}_2$ ).  $^1\text{H NMR}$  (300 MHz,  $\text{CDCl}_3$ )  $\delta$  7.30-7.14 (m, 6H), 7.14-7.05 (m, 2H), 7.02-6.90 (m, 2H), 4.76 (s, 1H), 4.27 (d,  $J = 5.4$  Hz, 1H), 3.54 (dt,  $J = 7.4, 5.3$  Hz, 1H), 3.01 (dd,  $J = 13.9, 5.1$  Hz, 1H), 2.90-2.68 (m, 4H).  $^{13}\text{C NMR}$  (75 MHz,  $\text{CDCl}_3$ )  $\delta$  161.3, 141.9, 136.6, 129.8, 128.9, 128.8, 128.1, 127.1, 126.2, 68.4, 58.0, 38.3, 29.3. **HRMS (ESI,  $m/z$ )** calcd. for  $\text{C}_{17}\text{H}_{18}\text{N}_2\text{O}_1\text{Na}_1$   $[\text{M}+\text{Na}]^+$ : 289.1311, found: 289.1318.

Compound (*S*)-7o

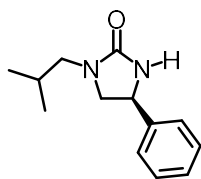
Starting from **6o** (64.4 mg, 0.20 mmol) according to the general procedure to provide **7o** as a white solid (35.7 mg, 89% yield) and with 87% ee as determined by HPLC analysis (column: Daicel Chiralpak IA 250 x 4.6 mm, absorption:  $\lambda = 220$  nm, mobile phase: *n*-Hexane/isopropanol = 90:10, flow rate: 1.0 mL/min, column temperature: 30 °C, retention times:  $t_r$  (major) = 10.8 min,  $t_r$  (minor) = 13.3 min).  $[\alpha]_D^{22} = 11.0^\circ$  ( $c = 1.0$ ,  $\text{CH}_2\text{Cl}_2$ ).  $^1\text{H NMR}$  (300 MHz,  $\text{CDCl}_3$ )  $\delta$  7.40-7.29 (m, 2H), 7.29-7.13 (m, 3H), 5.17 (s, 1H), 4.52 (dd,  $J = 8.6, 5.8$  Hz, 1H), 3.61 (t,  $J = 8.6$  Hz, 1H), 3.42 (dd,  $J = 8.6, 5.8$  Hz, 1H), 2.74 (s, 3H).  $^{13}\text{C NMR}$  (75 MHz,  $\text{CDCl}_3$ )  $\delta$  161.6, 131.8, 128.8, 128.4, 122.2, 87.6, 83.9, 53.8, 41.5, 30.6. **HRMS (ESI,  $m/z$ )** calcd. for  $\text{C}_{12}\text{H}_{13}\text{N}_2\text{O}_1$   $[\text{M}+\text{H}]^+$ : 201.1022, found: 201.1022.

Compound (*S*)-7p

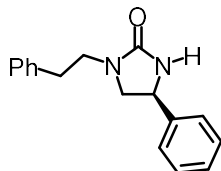
Starting from **6p** (62.4 mg, 0.20 mmol) according to the general procedure to provide **7p** as a white solid (37.9 mg, 99% yield) and with 93% ee as determined by HPLC analysis (column: Daicel Chiralpak IA 250 x 4.6 mm, absorption:  $\lambda = 220$  nm, mobile phase: *n*-Hexane/isopropanol = 90:10, flow rate: 1.0 mL/min, column temperature: 30 °C, retention times:  $t_r$  (major) = 12.1 min,  $t_r$  (minor) = 11.2 min).  $[\alpha]_D^{22} = 79.4^\circ$  ( $c = 1.0$ ,  $\text{CH}_2\text{Cl}_2$ ).  $^1\text{H NMR}$  (300 MHz,  $\text{CDCl}_3$ )  $\delta$  7.47-7.28 (m, 5H), 4.93-4.67 (m, 2H), 3.79 (t,  $J = 8.8$  Hz, 1H), 3.47-3.14 (m, 3H), 1.11 (t,  $J = 7.2$  Hz, 3H).  $^{13}\text{C NMR}$  (75 MHz,  $\text{CDCl}_3$ )  $\delta$  161.8, 141.8, 129.1, 128.3, 126.2, 54.0, 53.2, 38.1, 12.8. **HRMS (ESI,  $m/z$ )** calcd. for  $\text{C}_{11}\text{H}_{15}\text{N}_2\text{O}_1$   $[\text{M}+\text{H}]^+$ : 191.1179, found: 191.1178.

Compound (*S*)-7q

Starting from **6q** (68.0 mg, 0.20 mmol) according to the general procedure to provide **7q** as a white solid (35.7 mg, 82% yield) and with 93% ee as determined by HPLC analysis (column: Daicel Chiralpak IC 250 x 4.6 mm, absorption:  $\lambda = 220$  nm, mobile phase: *n*-Hexane/isopropanol = 50:50, flow rate: 1.0 mL/min, column temperature: 25 °C, retention times:  $t_r$  (major) = 9.7 min,  $t_r$  (minor) = 12.8 min).  $[\alpha]_D^{22} = -61.0^\circ$  ( $c = 1.0$ ,  $\text{CH}_2\text{Cl}_2$ ).  $^1\text{H NMR}$  (300 MHz,  $\text{CDCl}_3$ )  $\delta$  7.41-7.28 (m, 5H), 4.93 (s, 1H), 4.81-4.66 (m, 1H), 3.78 (t,  $J = 8.9$  Hz, 1H), 3.34-3.08 (m, 3H), 1.55-1.42 (m, 2H), 1.40-1.27 (m, 2H), 0.92 (t,  $J = 7.2$  Hz, 3H).  $^{13}\text{C NMR}$  (75 MHz,  $\text{CDCl}_3$ )  $\delta$  162.1, 141.9, 129.0, 128.3, 126.2, 54.0, 53.7, 43.2, 29.8, 20.1, 13.9. **HRMS (ESI,  $m/z$ )** calcd. for  $\text{C}_{13}\text{H}_{19}\text{N}_2\text{O}_1$   $[\text{M}+\text{H}]^+$ : 219.1492, found: 219.1492.

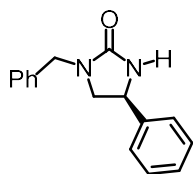
Compound (*S*)-7r

Starting from **6r** (68.0 mg, 0.20 mmol) according to the general procedure to provide **7r** as a white solid (29.7 mg, 68% yield) and with 95% ee as determined by HPLC analysis (column: Daicel Chiralpak IC 250 x 4.6 mm, absorption:  $\lambda = 220$  nm, mobile phase: *n*-Hexane/isopropanol = 50:50, flow rate: 1.0 mL/min, column temperature: 25 °C, retention times:  $t_r$  (major) = 8.3 min,  $t_r$  (minor) = 11.7 min).  $[\alpha]_D^{22} = 13.0^\circ$  ( $c = 1.0$ ,  $\text{CH}_2\text{Cl}_2$ ).  $^1\text{H NMR}$  (300 MHz,  $\text{CDCl}_3$ )  $\delta$  7.51-7.25 (m, 5H), 5.04 (s, 1H), 4.75 (dd,  $J = 8.6, 7.6$  Hz, 1H), 3.79 (t,  $J = 8.9$  Hz, 1H), 3.29-3.15 (m, 1H), 3.01 (qd,  $J = 13.7, 7.5$  Hz, 2H), 1.93-1.71 (m, 1H), 0.90 (dd,  $J = 6.6, 4.0$  Hz, 6H).  $^{13}\text{C NMR}$  (75 MHz,  $\text{CDCl}_3$ )  $\delta$  162.4, 142.0, 129.0, 128.3, 126.1, 54.4, 54.0, 51.2, 27.1, 20., 20.1. **HRMS (ESI,  $m/z$ )** calcd. for  $\text{C}_{13}\text{H}_{19}\text{N}_2\text{O}_1$   $[\text{M}+\text{H}]^+$ : 219.1492, found: 219.1492.

Compound (*S*)-7s

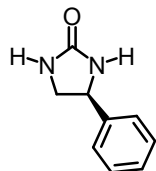
Starting from **6s** (77.6 mg, 0.20 mmol) according to the general procedure to provide **7s** as a white solid (47.8 mg, 90% yield) and with 92% ee as determined by HPLC analysis (column: Daicel Chiralpak IC 250 x 4.6 mm, absorption:  $\lambda = 220$  nm, mobile phase: *n*-Hexane/isopropanol = 50:50, flow rate: 1.0 mL/min, column temperature: 40 °C, retention times:  $t_r$  (major) = 8.9 min,  $t_r$  (minor) = 10.2 min).  $[\alpha]_D^{22} = -2.0^\circ$  ( $c = 1.0$ ,  $\text{CH}_2\text{Cl}_2$ ).  $^1\text{H NMR}$  (300 MHz,  $\text{CDCl}_3$ )  $\delta$  7.33-7.08 (m, 10H), 4.96 (s, 1H), 4.59 (t,  $J = 8.0$  Hz, 1H), 3.59 (t,  $J = 8.8$  Hz, 1H), 3.50-3.30 (m, 2H), 3.05 (dd,  $J = 8.6, 7.2$  Hz, 1H), 2.75 (t,  $J = 7.4$  Hz, 3H).  $^{13}\text{C NMR}$  (75 MHz,  $\text{CDCl}_3$ )  $\delta$  161.9, 141.8, 139.0, 129.0, 128.9, 128.8, 128.6, 128.2, 126.5, 126.2, 54.1, 53.9, 44.9, 34.4. **HRMS (ESI,  $m/z$ )** calcd. for  $\text{C}_{17}\text{H}_{19}\text{N}_2\text{O}_1$   $[\text{M}+\text{H}]^+$ : 267.1492, found: 267.1492.

## Compound (S)-7t



Starting from **6t** (74.8 mg, 0.20 mmol) according to the general procedure to provide **7t** as a white solid (18.7 mg, 37% yield) and with 93% ee as determined by HPLC analysis (column: Daicel Chiralpak IA 250 x 4.6 mm, absorption:  $\lambda = 220$  nm, mobile phase: *n*-Hexane/isopropanol = 95:5, flow rate: 1.0 mL/min, column temperature: 30 °C, retention times:  $t_r$  (major) = 33.9 min,  $t_r$  (minor) = 30.2 min).  $[\alpha]_D^{22} = -9.2^\circ$  ( $c = 1.0$ ,  $\text{CH}_2\text{Cl}_2$ ).  $^1\text{H NMR}$  (300 MHz,  $\text{CDCl}_3$ )  $\delta$  7.29-7.11 (m, 10H), 4.87 (s, 1H), 4.66 (t,  $J = 8.2$  Hz, 1H), 4.42 (d,  $J = 14.9$  Hz, 1H), 4.24 (d,  $J = 14.9$  Hz, 1H), 3.59 (t,  $J = 8.9$  Hz, 1H), 3.03 (dd,  $J = 8.8, 7.5$  Hz, 1H).  $^{13}\text{C NMR}$  (75 MHz,  $\text{CDCl}_3$ )  $\delta$  161.9, 141.6, 137.0, 129.0, 128.8, 128.3, 128.2, 127.7, 126.2, 53.9, 53.3, 47.7. **HRMS (ESI,  $m/z$ )** calcd. for  $\text{C}_{16}\text{H}_{16}\text{N}_2\text{O}_1\text{Na}_1$   $[\text{M}+\text{Na}]^+$ : 275.1155, found: 275.1155.

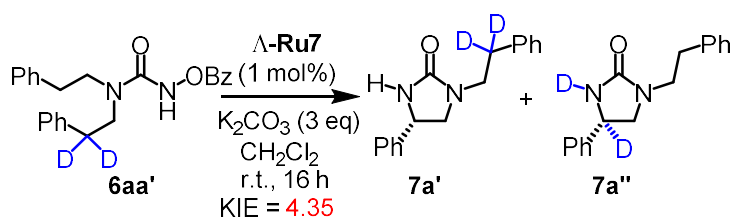
## Compound (S)-7u



Starting from **6u** (56.8 mg, 0.20 mmol) according to the general procedure to provide **7u** as a white solid (29.6 mg, 91% yield) and with 91% ee as determined by HPLC analysis (column: Daicel Chiralpak IA 250 x 4.6 mm, absorption:  $\lambda = 210$  nm, mobile phase: *n*-Hexane/isopropanol = 90:10, flow rate: 1.0 mL/min, column temperature: 30 °C, retention times:  $t_r$  (major) = 15.2 min,  $t_r$  (minor) = 12.6 min).  $[\alpha]_D^{22} = 23.8^\circ$  ( $c = 1.0$ ,  $\text{CH}_2\text{Cl}_2$ ).  $^1\text{H NMR}$  (300 MHz,  $\text{CDCl}_3$ )  $\delta$  7.46-7.27 (m, 5H), 4.95 (dd,  $J = 49.5, 41.5$  Hz, 3H), 3.87 (t,  $J = 8.8$  Hz, 1H), 3.35 (t,  $J = 8.1$  Hz, 1H).  $^{13}\text{C NMR}$  (75 MHz,  $\text{CDCl}_3$ )  $\delta$  141.5, 129.1, 128.4, 126.2, 56.9, 49.8. **HRMS (ESI,  $m/z$ )** calcd. for  $\text{C}_9\text{H}_{10}\text{N}_2\text{O}_1$   $[\text{M}+\text{H}]^+$ : 163.0866, found: 163.0866.

## 4.4.3 Mechanistic Experiments

## 1) Kinetic Isotope Experiment



**Procedure:** A pre-dried (using heating gun to dry for 3 times per tube) 10 mL Schlenk tube was charged with substrates **1aa'** (0.2 mmol),  $\Delta$ -**Ru7** (0.002 mmol, 1 mol%) and  $K_2CO_3$  (82.8 mg, 0.6 mmol) under an atmosphere of  $N_2$ . Fresh distilled dichloromethane (2.0 mL, 0.1 M) was added via syringe. The reaction mixture was stirred at room temperature for 16 h under an atmosphere of  $N_2$ . Afterwards, the mixture was directly transferred to a column and purified by flash chromatography on silica gel (EtOAc/*n*-Hexane = 2:1 to EtOAc/MeOH = 95:5) to afford the mixture of products **7a'** and **7a''**. The ratio was determined by  $^1H$  NMR analysis, resulting in KIE = 4.35 (**Figure 86**).

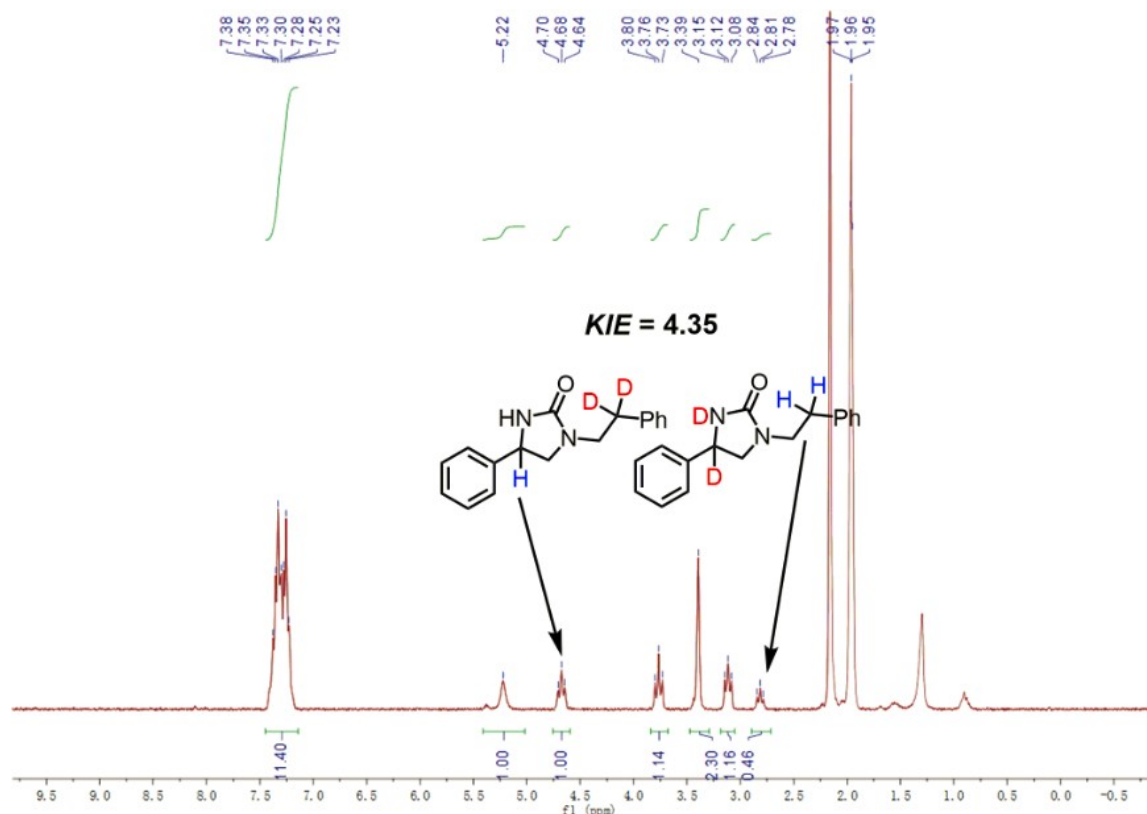
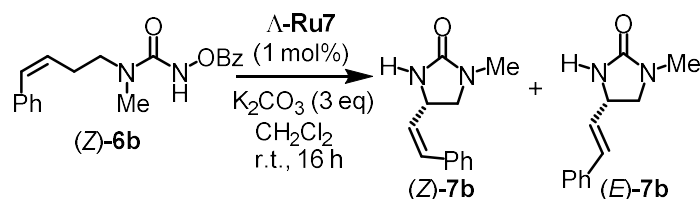


**Figure 86.**  $^1H$  NMR spectrum analysis of the kinetic isotope experiment.

## 2) Olefin Isomerization



**Procedure:** A pre-dried (using heating gun to dry for 3 times per tube) 10 mL Schlenk tube was charged with substrates (Z)-6b (0.2 mmol),  $\Delta$ -Ru7 (0.002 mmol, 1 mol%) and  $K_2CO_3$  (82.8 mg, 0.6 mmol) under an atmosphere of  $N_2$ . Fresh distilled dichloromethane (2.0 mL, 0.1 M) was added via syringe in sequence. The reaction mixture was stirred at room temperature for 16 h under an atmosphere of  $N_2$ . Afterwards, the crude reaction solution was filtered through a thin layer of celite and washed with 5 mL EtOAc. Filtrate was collected and organic solvent was removed under vacuo. The ratios of (Z)-7b and (E)-7b were analyzed by  $^1H$  NMR of crude reaction solutions (see attached spectrums). The ratios of (Z)-7b : (E)-7b are 4.4:1 (at room temperature), 5.1:1 (at 4 °C) and 2.9:1 (at 40 °C).

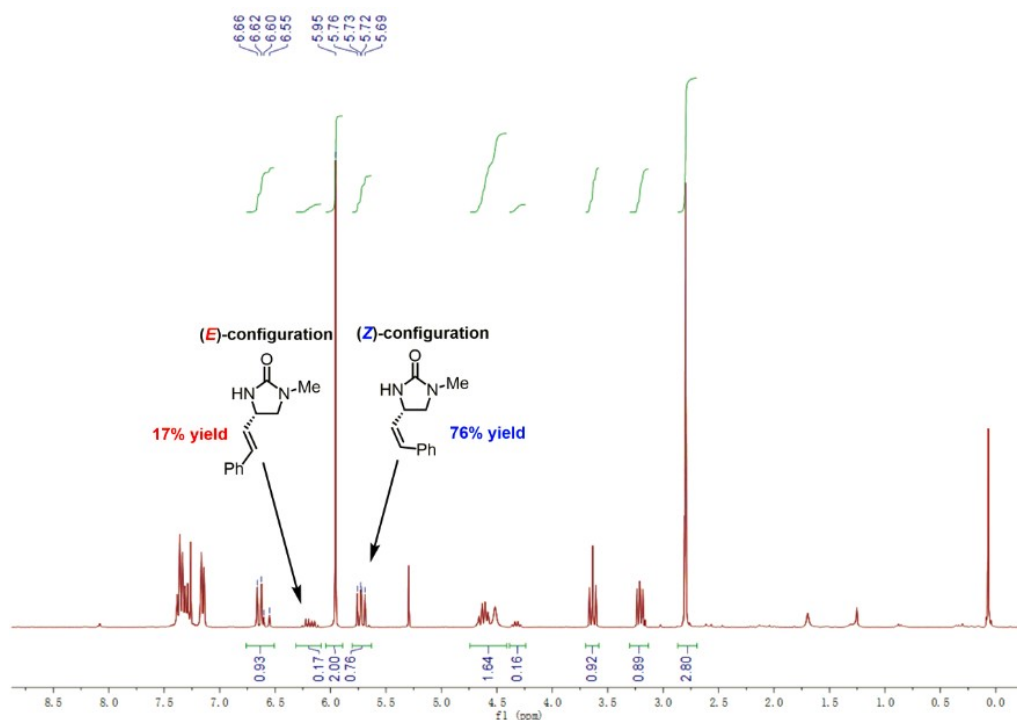


**Figure 87.**  $^1H$  NMR spectrum analysis of crude reaction solution (at room temperature).



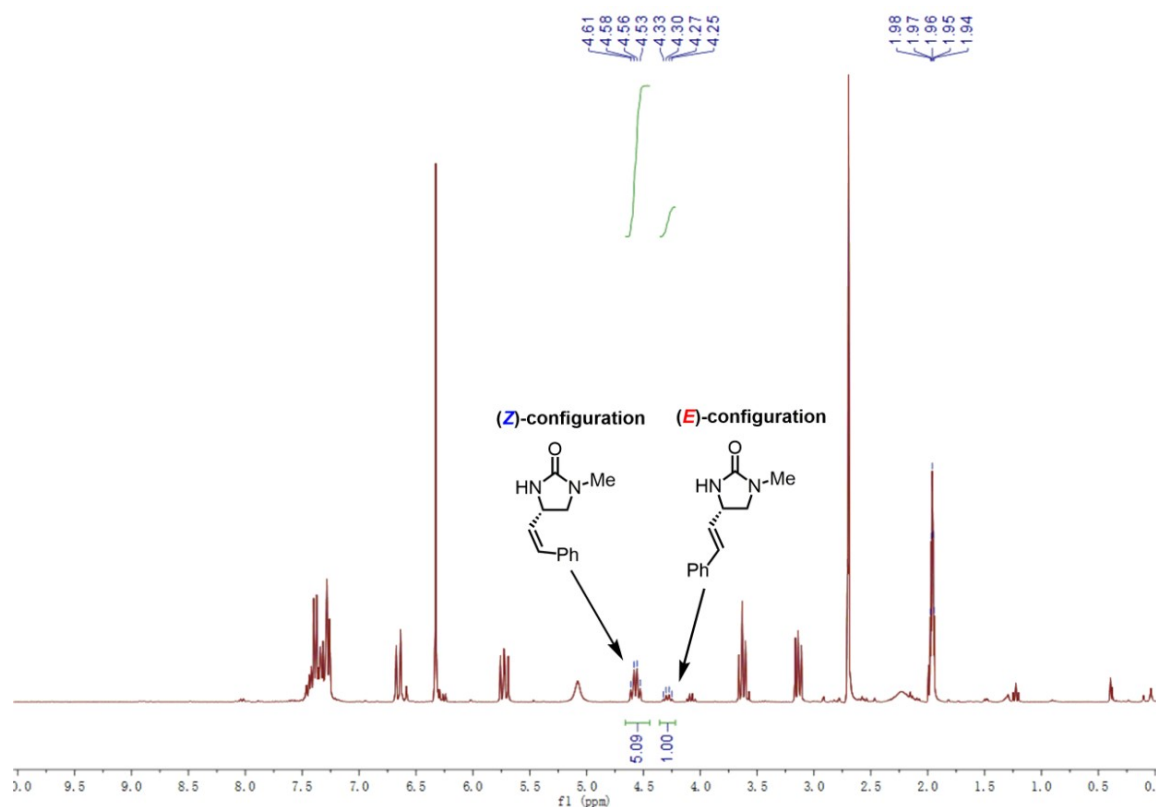


**Figure 88.**  $^1\text{H}$  NMR spectrum analysis of crude reaction solution (at 4 °C).

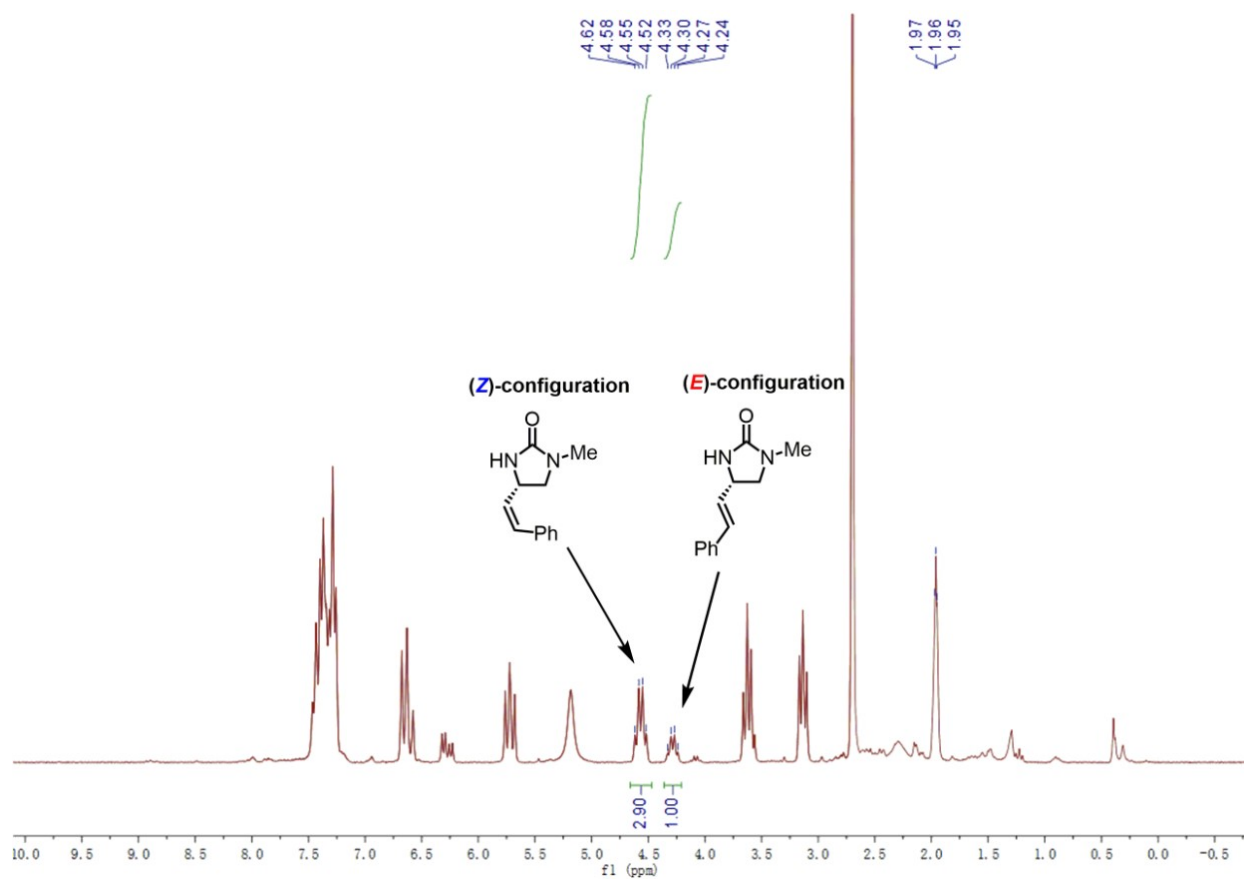
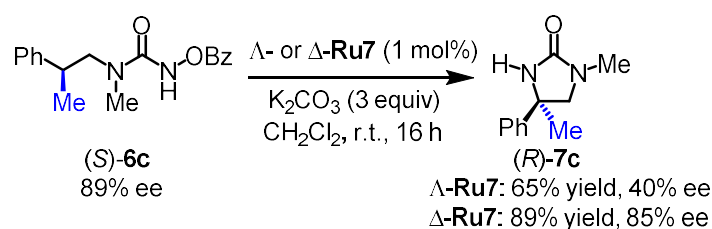


**Figure 89.**  $^1\text{H}$  NMR spectrum analysis of crude reaction solution (at 40 °C).

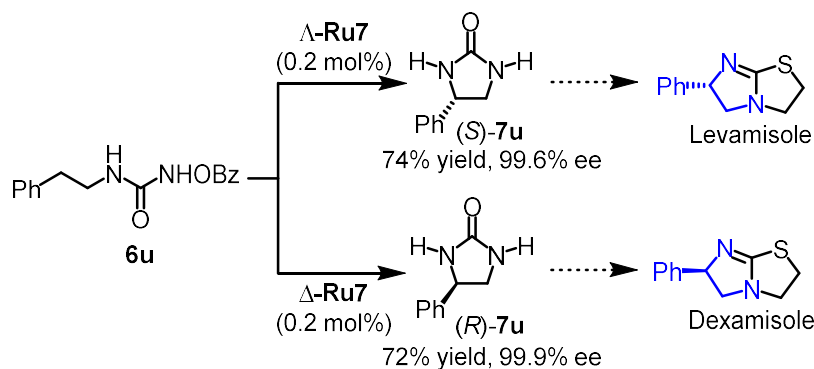
## 3) Stereochemistry



**Procedure:** A pre-dried (using heating gun to dry for 3 times per tube) 10 mL Schlenk tube was charged with substrates (*S*)-**6c** (0.2 mmol),  $\Lambda$ -Ru7 or  $\Delta$ -Ru7 (0.002 mmol, 1 mol%) and  $\text{K}_2\text{CO}_3$  (82.8 mg, 0.6 mmol) under an atmosphere of  $\text{N}_2$ . Fresh distilled dichloromethane (2.0 mL, 0.1 M) was added via syringe in sequence. The reaction mixture was stirred at room temperature for 16 h under an atmosphere of  $\text{N}_2$ . Afterwards, the mixture was directly transferred to a column (the Schlenk tube was rinsed with a minimal amount of  $\text{CH}_2\text{Cl}_2$  to transfer the reaction solution completely) and purified by flash chromatography on silica gel (EtOAc/*n*-Hexane = 2:1 to EtOAc/MeOH = 95:5) to afford the analytical pure product (*R*)-**7c**.

## 4.4.4 Synthetic applications

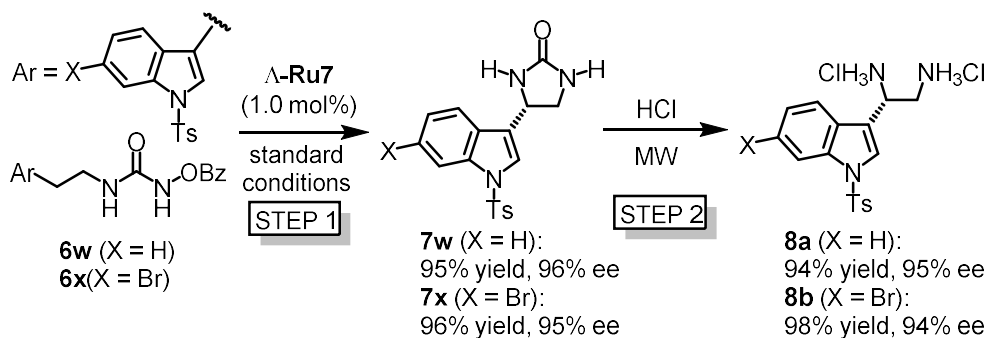
## 1) Synthetic Application to Drugs



**Procedure:** A pre-dried (using heating gun to dry for 3 times per tube) 25 mL Schlenk tube was charged with substrates **6u** (0.5 mmol),  $\Lambda$ -Ru7 or  $\Delta$ -Ru7 (0.001 mmol, 0.2 mol%) and  $\text{K}_2\text{CO}_3$  (207.0 mg, 1.5 mmol) under an atmosphere of  $\text{N}_2$ . Fresh distilled dichloromethane (5.0 mL, 0.1 M) was added via syringe in sequence. The reaction mixture was stirred at room temperature for 40 h under an atmosphere of  $\text{N}_2$ . Afterwards, the mixture was filtered and washed with 5 mL dichloromethane for 3 times. The filtrate was collected. Organic solvent was removed under *vacuo*. The resulting residue was dissolved in a minimum of EtOAc at 80 °C. After that, *n*-Hexane was added dropwisely until some precipitate formed. Subsequently, a minimum amount of EtOAc was added dropwisely until the solution became clear again. The resulting solution was cooled to 0 °C in freezer for 30 min. After that,

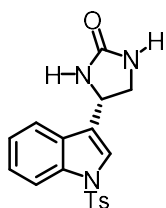
the precipitate was collected to provide enantiomeric pure (*S*)-**7u** with 74% yield, 99.6% ee and (*R*)-**7u** with 72% yield, 99.9% ee. The analytical data of compound **7u** was already shown on page 189.

## 2) Synthetic Application to Natural Products



**Step 1: Enantioselective C–H amination.** A pre-dried (using heating gun to dry 3 times) 10 mL Schlenk tube was charged with substrates **6w** or **6x** (0.2 mmol), chiral ruthenium catalyst (0.002 mmol, 1 mol%) and  $K_2CO_3$  (82.8 mg, 0.6 mmol) under an atmosphere of  $N_2$ . Fresh distilled dichloromethane (2.0 mL) was added via syringe. The reaction mixture was stirred at the indicated temperature for the indicated time under an atmosphere of  $N_2$ . Afterwards, the mixture was directly transferred to a column (the Schlenk tube was rinsed with a minimal amount of  $CH_2Cl_2$  to transfer the reaction solution completely) and purified by flash chromatography on silica gel (EtOAc/*n*-Hexane = 2:1 to EtOAc/MeOH 95:5) to afford the analytical pure products **7w** and **7x**.

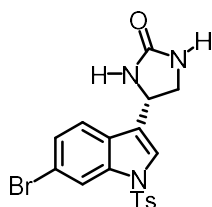
### Compound (*S*)-**7w**



Starting from **6w** (95.4 mg, 0.20 mmol) according to the general procedure to provide **7w** as a white solid (67.5 mg, 95% yield) and with 96% ee as determined by HPLC analysis (column: Daicel Chiralpak IG 250 x 4.6 mm, absorption:  $\lambda = 210$  nm, mobile phase: *n*-Hexane/isopropanol = 60:40, flow rate: 1.0 mL/min, column temperature: 30 °C, retention times:  $t_r$  (major) = 16.9 min,  $t_r$  (minor) = 21.1 min).  $[\alpha]_D^{22} = 17.8^\circ$  ( $c = 1.0$ ,  $CH_2Cl_2$ ).  $^1H$  NMR (300 MHz,  $CDCl_3$ )  $\delta$  8.02 (d,  $J = 8.3$  Hz, 1H), 7.81 (d,  $J = 8.3$  Hz, 2H), 7.61 (d,  $J = 6.9$  Hz, 2H), 7.37 (t,  $J = 7.7$  Hz, 1H), 7.31-7.22 (m, 3H), 5.25 (s,

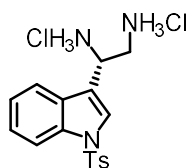
1H), 5.19-5.08 (m, 2H), 3.93 (t,  $J = 8.9$  Hz, 1H), 3.52 (t,  $J = 7.9$  Hz, 1H), 2.37 (s, 3H).  $^{13}\text{C}$  NMR (75 MHz,  $\text{CDCl}_3$ )  $\delta$  163.5, 145.3, 135.9, 135.3, 130.1, 128.2, 127.1, 125.4, 123.5, 122.6, 119.9, 114.1, 49.7, 47.5, 21.7. HRMS (ESI,  $m/z$ ) calcd. for  $\text{C}_{18}\text{H}_{17}\text{S}_1\text{N}_3\text{O}_3\text{Na}_1[\text{M}+\text{Na}]^+$ : 378.0833, found: 378.0885.

#### Compound (S)-7x

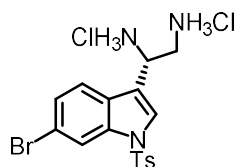


Starting from **6x** (111.0 mg, 0.20 mmol) according to the general procedure to provide **7x** as a white solid (83.2 mg, 96% yield) and with 95% ee as determined by HPLC analysis (column: Daicel Chiralpak IG 250 x 4.6 mm, absorption:  $\lambda = 220$  nm, mobile phase: *n*-Hexane/isopropanol = 50:50, flow rate: 1.0 mL/min, column temperature: 30 °C, retention times:  $t_r$  (major) = 9.5 min,  $t_r$  (minor) = 11.5 min).  $[\alpha]_D^{22} = 28.2^\circ$  ( $c = 1.0$ ,  $\text{CH}_2\text{Cl}_2$ ).  $^1\text{H}$  NMR (300 MHz,  $\text{CDCl}_3$ )  $\delta$  8.10 (d,  $J = 1.2$  Hz, 1H), 7.71 (d,  $J = 8.3$  Hz, 2H), 7.48 (s, 1H), 7.38 (d,  $J = 8.4$  Hz, 1H), 7.29 (dd,  $J = 8.5, 1.5$  Hz, 1H), 7.20 (d,  $J = 8.0$  Hz, 3H), 5.23 (s, 1H), 5.13-4.89 (m, 2H), 3.83 (t,  $J = 8.9$  Hz, 1H), 3.39 (t,  $J = 7.9$  Hz, 1H), 2.30 (s, 3H).  $^{13}\text{C}$  NMR (75 MHz,  $\text{CDCl}_3$ )  $\delta$  163.5, 145.7, 136.5, 135.0, 130.4, 130.1, 128.5, 127.1, 127.0, 124.0, 122.4, 121.1, 119.2, 117.2, 49.6, 47.5, 21.8. HRMS (ESI,  $m/z$ ) calcd. for  $\text{C}_{18}\text{H}_{16}\text{Br}_1\text{S}_1\text{N}_3\text{O}_3\text{Na}_1[\text{M}+\text{Na}]^+$ : 455.9988, 457.9969, found: 455.9989, 457.9969.

**Step 2: Hydrolysis.** **7w** or **7x** (10.0 mg) dissolved in 0.5 mL concentrated HCl together with 0.5 mL acetic acid was placed in a sealed tube (CEM designed 20 mL pressure-rated reaction vial) with a stirring bar, and the reaction mixture was exposed to microwave irradiation for 10 min at 85 °C. After that, the resulting mixture was evaporated to dryness, redissolved with water (2 mL) and evaporated to dryness to remove traces of HCl. Redissolving with water and evaporation to dryness was repeated once. Water (2 mL) was added and the solution washed with  $\text{CH}_2\text{Cl}_2$  (3 x 2 mL) and dried under *vacuo* to provide analytical pure products **8a** with 94% yield, 95% ee and **8b** with 98% yield, 94% ee.

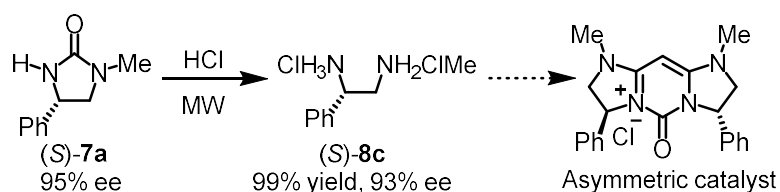
Compound (*S*)-**8a**

(*S*)-**8a**: 94% yield, 95% ee. light brown solid.  $^1\text{H NMR}$  (500 MHz, DMSO)  $\delta$  9.18 (s, 3H), 8.59 (s, 3H), 8.28 (s, 1H), 7.99-7.93 (m, 4H), 7.44 (dd,  $J = 10.7, 4.5$  Hz, 3H), 7.41-7.35 (m, 1H), 5.06 (d,  $J = 4.5$  Hz, 1H), 3.62-3.53 (m, 1H), 3.51-3.41 (m, 1H), 2.37 (s, 3H).  $^{13}\text{C NMR}$  (126 MHz, DMSO)  $\delta$  145.8, 133.9, 133.9, 130.4, 128.3, 128.1, 127.2, 126.7, 125.5, 125.4, 123.5, 120.3, 115.4, 113.1, 108.6, 44.5, 41.2, 21.1. **HRMS (ESI,  $m/z$ )** calcd. for  $\text{C}_{17}\text{H}_{17}\text{N}_2\text{O}_2\text{S}_1$   $[\text{M}-\text{NH}_3\text{Cl}_2]^+$ : 313.1005, found: 313.1007.

Compound (*S*)-**8b**

(*S*)-**8b**: 98% yield, 94% ee. light brown solid.  $^1\text{H NMR}$  (500 MHz, DMSO)  $\delta$  9.16 (s, 3H), 8.53 (s, 3H), 8.33 (s, 1H), 8.06 (s, 1H), 8.01 (d,  $J = 7.9$  Hz, 2H), 7.93 (d,  $J = 8.4$  Hz, 1H), 7.58 (d,  $J = 8.2$  Hz, 1H), 7.48 (d,  $J = 8.0$  Hz, 2H), 5.05 (s, 1H), 3.53 (s, 2H), 2.39 (s, 3H).  $^{13}\text{C NMR}$  (126 MHz, DMSO)  $\delta$  142.5, 130.8, 130.0, 126.9, 123.9, 123.6, 122.9, 118.6, 114.4, 111.7, 111.7, 40.6, 37.4, 17.5. **HRMS (ESI,  $m/z$ )** calcd. for  $\text{C}_{17}\text{H}_{19}\text{Br}_1\text{N}_3\text{O}_2\text{S}_1$   $[\text{M}-\text{HCl}_2]^+$ : 408.0376, 410.0355 found: 408.0379, 410.0357.

## 3) Synthetic Application to Asymmetric Catalyst



**Hydrolysis.** **7a** (10.0 mg) dissolved in 1.0 mL concentrated HCl was placed in a sealed tube (CEM designed 20 mL pressure-rated reaction vial) with a stirring bar, and the reaction mixture was exposed to microwave irradiation for 15 min at 120 °C. After that, the resulting mixture was evaporated to dryness, redissolved with water (2 mL) and evaporated to dryness to remove traces of HCl to provide analytical pure products **8c** with 99% yield, 93% ee.

(*S*)-**8c**: 99% yield, 93% ee. white solid.  $^1\text{H}$  NMR (300 MHz,  $\text{CD}_3\text{OD\_SPE}$ )  $\delta$  7.66-7.38 (m, 5H), 3.74-3.54 (m, 2H), 3.25 (s, 1H), 2.70 (s, 3H).  $^{13}\text{C}$  NMR (75 MHz,  $\text{CD}_3\text{OD\_SPE}$ )  $\delta$  133.9, 132.0, 131.3, 129.3, 53.3, 52.0, 34.7. HRMS (ESI,  $m/z$ ) calcd. for  $\text{C}_9\text{H}_{15}\text{N}_2$   $[\text{M}-\text{HCl}_2]^+$ : 151.1230 found: 151.1234.

**Note:** The vicinal diamines were transformed back to the corresponding cyclic ureas for the determination of the ee values using a reported method starting from the bis-Hydrochloride salt.<sup>1</sup>

*Additional informations about the set up of microwave irradiation reaction:*



**Figure 90.** Reaction set up in the microwave reactor.

### 4.4.5 Single Crystal X-Ray Diffraction Studies

**Crystallography of compound (*S*)-7h:** Single crystals of (*S*)-**7h** were obtained by slow diffusion from the solution in  $\text{CH}_2\text{Cl}_2$  layered with  $\text{Et}_2\text{O}$  at room temperature.

A suitable crystal of  $\text{C}_{10}\text{H}_{11}\text{ClN}_2\text{O}$  was selected under inert oil and mounted using a MiTeGen loop. Intensity data of the crystal were recorded with a STADIVARI diffractometer (Stoe & Cie). The diffractometer was operated with  $\text{Cu-K}\alpha$  radiation (1.54186 Å, microfocus source) and equipped with a Dectris PILATUS 300K detector. Evaluation, integration and reduction of the diffraction data was carried out using the X-Area software suite.<sup>2</sup> Multi-scan and numerical absorption corrections were applied with the X-Red32 and LANA modules of the X-Area software suite.<sup>3,4</sup> The structure was solved using dual-space methods (SHELXT-2014/5) and refined against  $F^2$  (SHELXL-2018/3 using ShelXle interface).<sup>5-7</sup> All non-Hydrogen atoms were refined with anisotropic displacement parameters. The hydrogen atoms bonded to carbon atoms were refined using the “riding model” approach with isotropic displacement parameters 1.2 times (for  $\text{CH}_3$  groups 1.5 times) of that of the preceding carbon atom. The hydrogen atom bonded to the nitrogen atom was refined isotropic without restraints. CCDC

1972573 contains the supplementary crystallographic data for this compound.

**Table 8.** Selected crystallographic data and details of the structure determination for (S)-7h.

Identification code	(S)-7h
Empirical formula	C <sub>10</sub> H <sub>11</sub> ClN <sub>2</sub> O
Molar mass / g·mol <sup>-1</sup>	210.66
Space group (No.)	P2 <sub>1</sub> 2 <sub>1</sub> 2 <sub>1</sub> (19)
<i>a</i> / Å	5.66680(10)
<i>b</i> / Å	7.92950(10)
<i>c</i> / Å	21.8819(5)
<i>V</i> / Å <sup>3</sup>	983.26(3)
<i>Z</i>	4
$\rho_{calc.}$ / g·cm <sup>-3</sup>	1.423
$\mu$ / mm <sup>-1</sup>	3.172
Color	colorless
Crystal habitus	needle
Crystal size / mm <sup>3</sup>	0.510 x 0.190 x 0.104
<i>T</i> / K	100
$\lambda$ / Å	1.54186 (Cu-K $\alpha$ )
$\theta$ range / °	4.041 to 75.585
Range of Miller indices	-6 ≤ <i>h</i> ≤ 2 -8 ≤ <i>k</i> ≤ 9 -27 ≤ <i>l</i> ≤ 27
Absorption correction	multi-scan and numerical
<i>T</i> <sub>min</sub> , <i>T</i> <sub>max</sub>	0.1354, 0.3599
<i>R</i> <sub>int</sub> , <i>R</i> <sub>σ</sub>	0.0179, 0.0090
Completeness of the data set	0.995
No. of measured reflections	10354
No. of independent reflections	1981
No. of parameters	133
No. of restraints	0
<i>S</i> (all data)	1.044
<i>R</i> ( <i>F</i> ) ( <i>I</i> ≥ 2σ( <i>I</i> ), all data)	0.0236, 0.0237
<i>wR</i> ( <i>F</i> <sup>2</sup> ) ( <i>I</i> ≥ 2σ( <i>I</i> ), all data)	0.0644, 0.0645
Extinction coefficient	0.0032(7)
Flack parameter <i>x</i>	0.002(6)
$\Delta\rho_{max}$ , $\Delta\rho_{min}$ / e·Å <sup>-3</sup>	0.269, -0.148

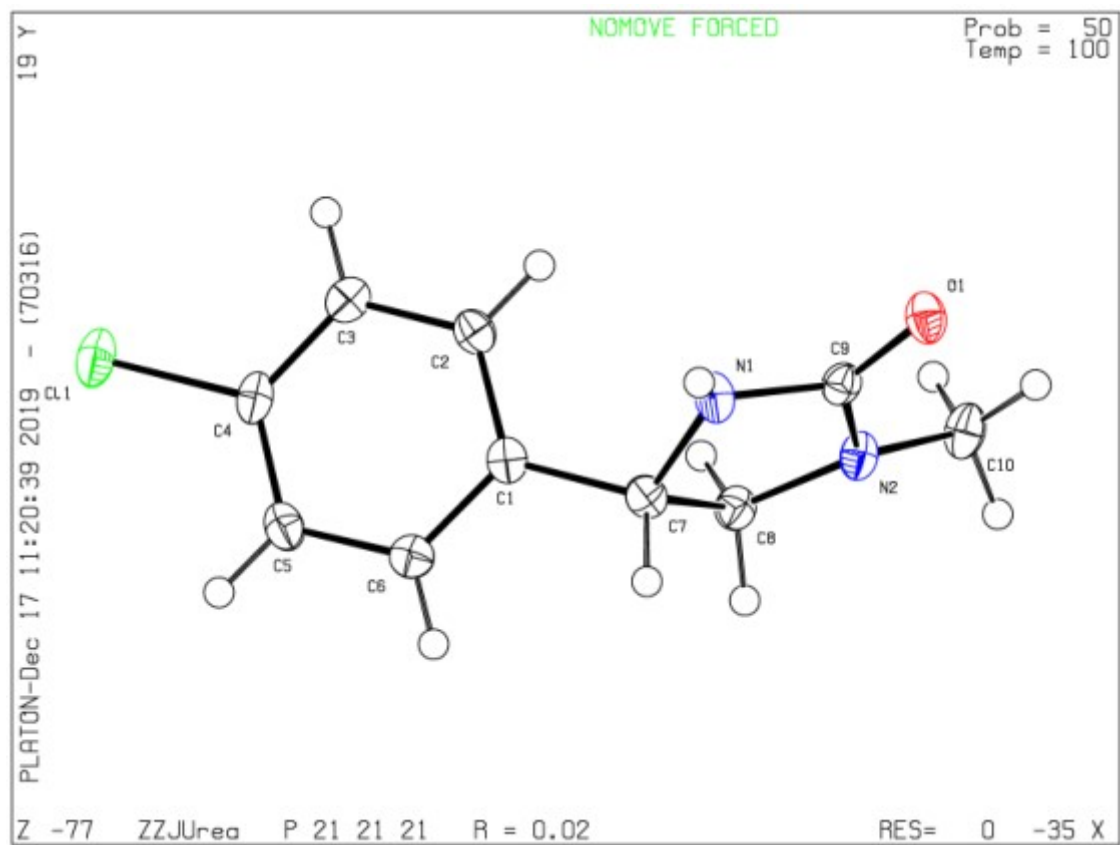


Figure 91. X-ray structure analysis of compound (S)-7h.

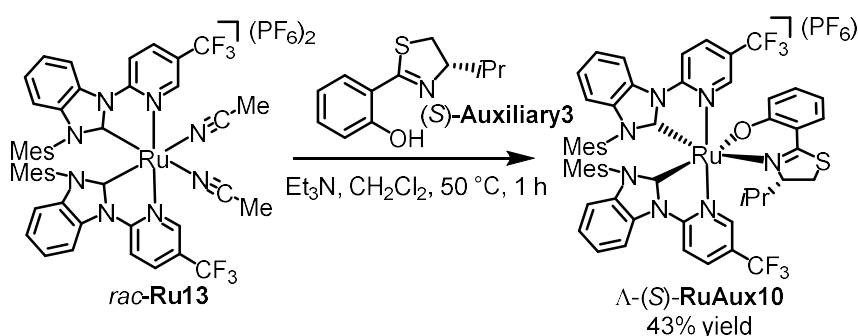


### Reference

1. Y. Liu, K. Ding, *J. Am. Chem. Soc.* **2005**, *127*, 10488-10489.
2. X-Area, STOE & Cie GmbH, Darmstadt, Germany, **2018**.
3. X-RED32, STOE & Cie GmbH, Darmstadt, Germany, **2018**.
4. LANA - Laue Analyzer, STOE & Cie GmbH, Darmstadt, Germany, **2019**.
5. G. M. Sheldrick, *Acta Cryst. A* **2015**, *71*, 3.
6. G. M. Sheldrick, *Acta Cryst. C* **2015**, *71*, 3.
7. C. B. Hübschle, G. M. Sheldrick, B. Dittrich, *J. Appl. Cryst.* **2011**, *44*, 1281.

## 4.5 Enantioselective Synthesis of Cyclic Carbamates by Intramolecular C–H Amidation

## 4.5.1 Synthesis of the Ruthenium Catalyst



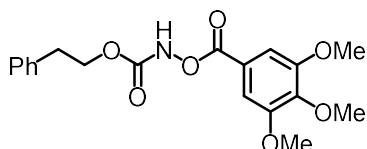
A mixture of racemic ruthenium complex *rac*-**Ru13** (1 equiv, 494.5 mg, 0.4 mmol), chiral auxiliary (*S*)-**5** (1 equiv, 88.5 mg, 0.4 mmol) and triethylamine (5 equiv, 278  $\mu\text{L}$ , 2.0 mmol) in  $\text{CH}_2\text{Cl}_2$  (4 mL) was heated at 50  $^\circ\text{C}$  for 1 h (*Note*: longer time will decrease the yield!). The reaction mixture was cooled to room temperature and concentrated to dryness. The residue was subjected to a flash silica gel chromatography ( $\text{CH}_3\text{CN}:\text{CH}_2\text{Cl}_2 = 1:50$  to  $1:20$ ) to separate the first colorful eluent which was assigned as  $\Delta$ -(*S*)-**RuAux10**.

$\Delta$ -(*S*)-**RuAux10**: red solid (236.4 mg, 43% yield).  $^1\text{H NMR}$  (300 MHz,  $\text{CD}_2\text{Cl}_2$ )  $\delta$  9.26 (s, 1H), 8.26 (s, 1H), 8.16 (t,  $J = 5.8$  Hz, 3H), 8.04 (d,  $J = 8.3$  Hz, 1H), 7.88 (dt,  $J = 8.9, 5.4$  Hz, 2H), 7.63–7.47 (m, 2H), 7.32 (ddd,  $J = 10.9, 9.8, 4.6$  Hz, 3H), 6.93–6.75 (m, 3H), 6.66 (dd,  $J = 12.4, 5.0$  Hz, 3H), 6.51 (s, 1H), 6.36–6.21 (m, 2H), 3.91 (dd,  $J = 8.4, 2.3$  Hz, 1H), 3.21 (dd,  $J = 11.9, 9.0$  Hz, 1H), 3.05 (d,  $J = 11.9$  Hz, 1H), 2.28 (s, 3H), 2.18 (s, 3H), 2.13 (s, 3H), 2.03 (s, 3H), 1.19 (s, 3H), 0.93 (s, 3H), 0.38 (d,  $J = 7.1$  Hz, 6H), -0.44–0.64 (m, 1H).  $^{13}\text{C NMR}$  (75 MHz,  $\text{CD}_2\text{Cl}_2$ )  $\delta$  207.7, 205.4, 174.4, 169.9, 157.4, 156.7, 149.1, 147.6, 141.0, 137.7, 137.3, 137.1, 135.2, 134.8, 134.7, 134.5, 134.0, 133.0, 131.4, 131.2, 131.10, 131.07, 130.5, 130.2, 130.1, 126.3, 125.5, 125.4, 124.1, 123.6, 123.6, 123.0, 122.5, 119.0, 114.5, 111.8, 111.6, 111.4, 111.0, 110.6, 85.3, 32.2, 28.5, 20.9, 20.8, 19.7, 17.9, 17.5, 17.3, 16.9, 15.2.  $^{19}\text{F NMR}$  (283 MHz,  $\text{CD}_2\text{Cl}_2$ )  $\delta$  -62.15, -62.79, -71.40, -73.92. **HRMS** (ESI,  $m/z$ ) calcd for  $\text{C}_{50}\text{H}_{50}\text{F}_6\text{N}_7\text{O}_1\text{Ru}_1\text{S}_1$   $[\text{M-PF}_6]^+$ : 1084.2754, found: 1084.2791.



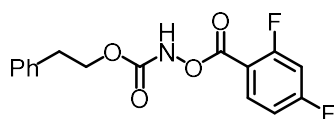
stirring for 2-3 hours (monitored by TLC), the reaction mixture was diluted by Et<sub>2</sub>O (10 mL/mmol). The byproduct precipitated out and was removed by filtration. The solvent was removed in *vacuo* and the residue was purified by column chromatography on silica gel (*n*-hexane/CH<sub>2</sub>Cl<sub>2</sub> = 1:1 to pure CH<sub>2</sub>Cl<sub>2</sub>).

#### Compound 9ae



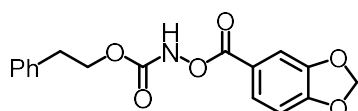
**9ae**: white solid. <sup>1</sup>H NMR (300 MHz, CDCl<sub>3</sub>) δ 8.27 (s, 1H), 7.50-7.13 (m, 7H), 4.47 (t, *J* = 7.0 Hz, 2H), 4.06-3.83 (m, 9H), 3.03 (t, *J* = 7.0 Hz, 2H). <sup>13</sup>C NMR (75 MHz, CDCl<sub>3</sub>) δ 165.8, 156.8, 153.3, 143.6, 137.3, 129.1, 128.7, 126.9, 121.5, 107.5, 67.4, 61.2, 56.5, 35.3. **HRMS** (ESI, *m/z*) calcd for C<sub>19</sub>H<sub>21</sub>N<sub>1</sub>O<sub>7</sub>Na [M+Na]<sup>+</sup>: 398.1210, found: 398.1210.

#### Compound 9af



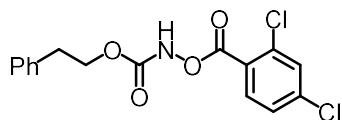
**9af**: white solid. <sup>1</sup>H NMR (300 MHz, CDCl<sub>3</sub>) δ 8.33 (s, 1H), 8.06 (td, *J* = 8.3, 6.5 Hz, 1H), 7.29 (ddd, *J* = 18.5, 10.2, 4.5 Hz, 5H), 6.99 (tdd, *J* = 12.7, 8.4, 2.3 Hz, 2H), 4.47 (t, *J* = 7.0 Hz, 2H), 3.02 (t, *J* = 7.0 Hz, 2H). <sup>13</sup>C NMR (75 MHz, CDCl<sub>3</sub>) δ 168.6, 168.5, 165.2, 165.2, 165.1, 162.9, 162.8, 161.7, 161.5, 156.5, 137.3, 134.4, 134.4, 134.2, 134.2, 129.1, 128.7, 126.9, 112.5, 112.4, 112.2, 112.2, 112.0, 112.0, 106.1, 105.8, 105.5, 67.5, 35.3. **HRMS** (ESI, *m/z*) calcd for C<sub>16</sub>H<sub>13</sub>F<sub>2</sub>N<sub>1</sub>O<sub>4</sub>Na [M+Na]<sup>+</sup>: 344.0705, found: 344.0705.

#### Compound 9ag

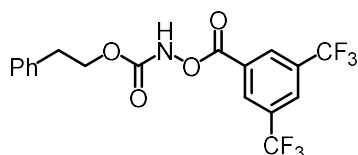


**9ag**: white solid. <sup>1</sup>H NMR (300 MHz, CDCl<sub>3</sub>) δ 8.32 (s, 1H), 7.74 (dd, *J* = 8.2, 1.6 Hz, 1H), 7.51 (d, *J* = 1.6 Hz, 1H), 7.36-7.19 (m, 5H), 6.90 (d, *J* = 8.2 Hz, 1H), 6.10 (s, 2H), 4.45 (t, *J* = 7.0 Hz, 2H), 3.01 (t, *J* = 7.0 Hz, 2H). <sup>13</sup>C NMR (75 MHz, CDCl<sub>3</sub>) δ 165.4, 156.7, 152.9, 148.2, 137.4, 129.1, 128.7,

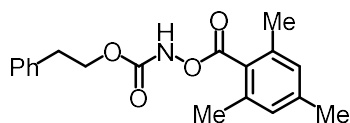
126.9, 126.5, 120.5, 109.8, 108.5, 102.3, 67.3, 35.3. **HRMS** (ESI,  $m/z$ ) calcd for  $C_{17}H_{15}N_1O_6Na$   $[M+Na]^+$ : 352.0792, found: 352.0792.

**Compound 9ah**

**9ah**: white solid.  $^1H$  NMR (300 MHz,  $CDCl_3$ )  $\delta$  8.29 (s, 1H), 7.91 (d,  $J = 8.5$  Hz, 1H), 7.57 (d,  $J = 1.8$  Hz, 1H), 7.42-7.20 (m, 7H), 4.49 (t,  $J = 7.0$  Hz, 2H), 3.03 (t,  $J = 7.0$  Hz, 2H).  $^{13}C$  NMR (75 MHz,  $CDCl_3$ )  $\delta$  164.0, 156.5, 140.1, 137.2, 136.0, 133.0, 131.5, 129.1, 128.8, 127.5, 126.9, 124.9, 67.5, 35.3. **HRMS** (ESI,  $m/z$ ) calcd for  $C_{16}H_{13}Cl_2N_1O_4Na$   $[M+Na]^+$ : 376.0114, found: 376.0114.

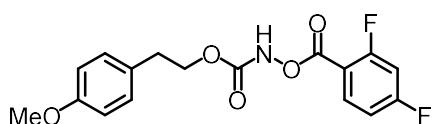
**Compound 9ai**

**9ai**: white solid.  $^1H$  NMR (300 MHz,  $CDCl_3$ )  $\delta$  8.54 (s, 2H), 8.35 (s, 1H), 8.18 (s, 1H), 7.42-7.06 (m, 5H), 4.50 (t,  $J = 6.9$  Hz, 2H), 3.03 (t,  $J = 6.9$  Hz, 2H).  $^{13}C$  NMR (75 MHz,  $CDCl_3$ )  $\delta$  163.5, 156.3, 137.1, 133.6, 133.1, 132.7, 132.2, 130.2, 129.2, 129.0, 128.7, 127.8, 127.8, 127.7, 127.0, 124.6, 121.0, 117.4, 67.7, 35.2. **HRMS** (ESI,  $m/z$ ) calcd for  $C_{18}H_{13}F_6N_1O_4Na$   $[M+Na]^+$ : 444.0641, found: 444.0641.

**Compound 9aj**

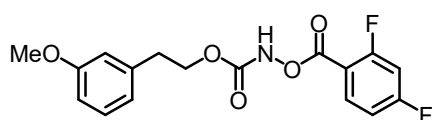
**9aj**: white solid.  $^1H$  NMR (300 MHz,  $CDCl_3$ )  $\delta$  8.30 (s, 1H), 7.39-7.21 (m, 5H), 6.92 (s, 2H), 4.49 (t,  $J = 7.1$  Hz, 2H), 3.05 (t,  $J = 7.1$  Hz, 2H), 2.36 (d,  $J = 15.2$  Hz, 9H).  $^{13}C$  NMR (75 MHz,  $CDCl_3$ )  $\delta$  169.1, 156.6, 141.1, 137.3, 136.9, 129.1, 128.8, 128.8, 126.9, 126.7, 67.3, 35.4, 21.4, 20.1. **HRMS** (ESI,  $m/z$ ) calcd for  $C_{18}H_{21}N_1O_4Na$   $[M+Na]^+$ : 350.1363, found: 350.1363.

## Compound 9b



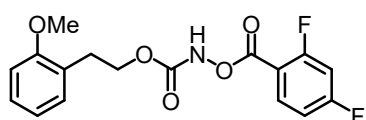
**9b:** white solid.  $^1\text{H NMR}$  (300 MHz,  $\text{CDCl}_3$ )  $\delta$  8.27 (s, 1H), 8.02 (td,  $J = 8.3, 6.4$  Hz, 1H), 7.18-7.06 (m, 2H), 7.05-6.90 (m, 2H), 6.86-6.73 (m, 2H), 4.40 (t,  $J = 7.0$  Hz, 2H), 3.78 (s, 3H), 2.93 (t,  $J = 7.0$  Hz, 2H).  $^{13}\text{C NMR}$  (75 MHz,  $\text{CDCl}_3$ )  $\delta$  168.5, 165.2, 165.0, 162.9, 162.8, 161.5, 158.6, 156.5, 134.4, 134.4, 134.2, 134.2, 130.0, 129.3, 114.2, 112.5, 112.4, 112.2, 112.2, 106.1, 105.8, 105.5, 67.7, 55.4, 34.4. **HRMS** (ESI,  $m/z$ ) calcd for  $\text{C}_{17}\text{H}_{15}\text{F}_2\text{NO}_5\text{Na}$   $[\text{M}+\text{Na}]^+$ : 374.0811, found: 374.0811.

## Compound 9c



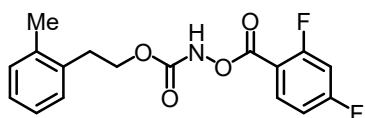
**9c:** white solid.  $^1\text{H NMR}$  (300 MHz,  $\text{CDCl}_3$ )  $\delta$  8.23 (s, 1H), 8.03 (dd,  $J = 14.8, 8.3$  Hz, 1H), 7.24-7.15 (m, 1H), 7.06-6.90 (m, 2H), 6.78 (dd,  $J = 9.7, 7.3$  Hz, 3H), 4.44 (t,  $J = 7.0$  Hz, 2H), 3.79 (s, 3H), 2.97 (t,  $J = 7.0$  Hz, 2H).  $^{13}\text{C NMR}$  (75 MHz,  $\text{CDCl}_3$ )  $\delta$  168.5, 162.9, 160.0, 156.5, 138.8, 134.4, 134.2, 129.7, 121.4, 114.9, 112.5, 112.3, 106.2, 105.8, 105.5, 67.4, 55.4, 35.4. **HRMS** (ESI,  $m/z$ ) calcd for  $\text{C}_{17}\text{H}_{15}\text{F}_2\text{NO}_5\text{Na}$   $[\text{M}+\text{Na}]^+$ : 374.0811, found: 374.0811.

## Compound 9d



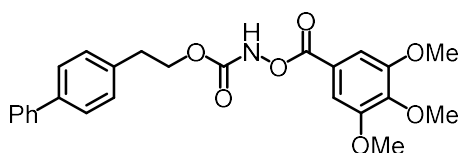
**9d:** white solid.  $^1\text{H NMR}$  (300 MHz,  $\text{CDCl}_3$ )  $\delta$  8.23 (s, 1H), 8.03 (dd,  $J = 14.8, 8.2$  Hz, 1H), 7.25-7.17 (m, 1H), 7.14 (d,  $J = 7.7$  Hz, 1H), 7.04-6.89 (m, 2H), 6.85 (dd,  $J = 7.6, 4.1$  Hz, 2H), 4.43 (t,  $J = 7.0$  Hz, 2H), 3.82 (s, 3H), 3.01 (t,  $J = 7.0$  Hz, 2H).  $^{13}\text{C NMR}$  (75 MHz,  $\text{CDCl}_3$ )  $\delta$  157.8, 156.6, 134.4, 134.2, 131.0, 128.3, 125.5, 120.6, 112.5, 112.4, 112.2, 112.1, 110.5, 106.1, 105.8, 105.5, 66.5, 55.4, 30.3. **HRMS** (ESI,  $m/z$ ) calcd for  $\text{C}_{17}\text{H}_{15}\text{F}_2\text{NO}_5\text{Na}$   $[\text{M}+\text{Na}]^+$ : 374.0811, found: 374.0812.

## Compound 9e



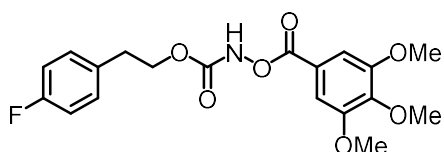
**9e:** white solid.  $^1\text{H NMR}$  (300 MHz,  $\text{CDCl}_3$ )  $\delta$  8.29 (s, 1H), 8.04 (td,  $J = 8.3, 6.5$  Hz, 1H), 7.21-7.08 (m, 4H), 7.06-6.88 (m, 2H), 4.41 (t,  $J = 7.4$  Hz, 2H), 3.01 (t,  $J = 7.3$  Hz, 2H), 2.34 (s, 3H).  $^{13}\text{C NMR}$  (75 MHz,  $\text{CDCl}_3$ )  $\delta$  168.6, 168.5, 165.2, 165.1, 162.9, 162.8, 161.7, 156.5, 136.6, 135.2, 134.4, 134.4, 134.2, 134.2, 130.6, 129.7, 127.1, 126.3, 112.5, 112.5, 112.2, 112.2, 106.2, 105.8, 105.5, 66.6, 32.6, 19.5. **HRMS** (ESI,  $m/z$ ) calcd for  $\text{C}_{17}\text{H}_{15}\text{F}_2\text{NO}_4\text{Na}$   $[\text{M}+\text{Na}]^+$ : 358.0861, found: 358.0861.

## Compound 9f



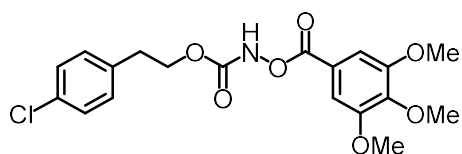
**9f:** white solid.  $^1\text{H NMR}$  (300 MHz,  $\text{CDCl}_3$ )  $\delta$  8.22 (s, 1H), 7.59-7.39 (m, 6H), 7.32 (q,  $J = 7.8$  Hz, 5H), 4.48 (t,  $J = 6.9$  Hz, 2H), 3.91 (d,  $J = 9.0$  Hz, 9H), 3.04 (t,  $J = 6.9$  Hz, 2H).  $^{13}\text{C NMR}$  (75 MHz,  $\text{CDCl}_3$ )  $\delta$  165.8, 156.8, 153.4, 143.7, 141.0, 139.9, 136.4, 129.5, 129.0, 127.5, 127.4, 127.2, 121.5, 107.5, 67.4, 61.2, 56.5, 35.0. **HRMS** (ESI,  $m/z$ ) calcd for  $\text{C}_{25}\text{H}_{25}\text{NO}_7\text{Na}$   $[\text{M}+\text{Na}]^+$ : 474.1523, found: 474.1523.

## Compound 9g



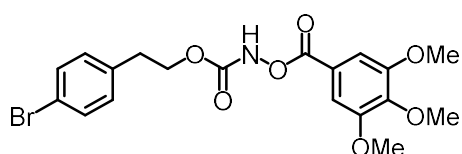
**9g:** white solid.  $^1\text{H NMR}$  (300 MHz,  $\text{CDCl}_3$ )  $\delta$  8.21 (d,  $J = 5.3$  Hz, 1H), 7.32 (s, 2H), 7.16 (dd,  $J = 8.3, 5.5$  Hz, 2H), 6.94 (t,  $J = 8.6$  Hz, 2H), 4.41 (t,  $J = 6.9$  Hz, 2H), 3.92 (d,  $J = 7.6$  Hz, 9H), 2.96 (t,  $J = 6.8$  Hz, 2H).  $^{13}\text{C NMR}$  (75 MHz,  $\text{CDCl}_3$ )  $\delta$  165.8, 163.6, 160.3, 156.7, 153.3, 143.7, 133.0, 133.0, 130.6, 130.5, 121.4, 115.7, 115.4, 107.5, 67.2, 61.2, 56.5, 34.5.  $^{19}\text{F NMR}$  (235 MHz,  $\text{CDCl}_3$ )  $\delta$  -116.30. **HRMS** (ESI,  $m/z$ ) calcd for  $\text{C}_{19}\text{H}_{20}\text{NO}_7\text{Na}$   $[\text{M}+\text{Na}]^+$ : 416.1116, found: 416.1116.

## Compound 9h



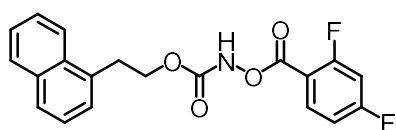
**9h**: white solid.  $^1\text{H NMR}$  (300 MHz,  $\text{CDCl}_3$ )  $\delta$  8.18 (s, 1H), 7.32 (s, 2H), 7.22 (d,  $J = 8.4$  Hz, 2H), 7.13 (d,  $J = 8.4$  Hz, 2H), 4.41 (t,  $J = 6.8$  Hz, 2H), 3.93 (d,  $J = 7.8$  Hz, 9H), 2.96 (t,  $J = 6.8$  Hz, 2H).  $^{13}\text{C NMR}$  (75 MHz,  $\text{CDCl}_3$ )  $\delta$  165.8, 156.7, 153.4, 143.7, 135.8, 132.8, 130.4, 128.9, 121.4, 107.5, 67.0, 61.2, 56.6, 34.7. **HRMS** (ESI,  $m/z$ ) calcd for  $\text{C}_{19}\text{H}_{20}\text{ClNO}_7\text{Na}$   $[\text{M}+\text{Na}]^+$ : 432.0821, found: 432.0820.

## Compound 9i



**9i**: white solid.  $^1\text{H NMR}$  (300 MHz,  $\text{CDCl}_3$ )  $\delta$  8.20 (s, 1H), 7.37 (d,  $J = 8.3$  Hz, 2H), 7.31 (s, 2H), 7.07 (d,  $J = 8.3$  Hz, 2H), 4.41 (t,  $J = 6.8$  Hz, 2H), 3.93 (d,  $J = 8.0$  Hz, 10H), 2.94 (t,  $J = 6.8$  Hz, 2H).  $^{13}\text{C NMR}$  (75 MHz,  $\text{CDCl}_3$ )  $\delta$  165.8, 156.7, 153.4, 143.7, 136.4, 131.8, 130.8, 121.4, 120.8, 107.5, 66.9, 61.2, 56.6, 34.7. **HRMS** (ESI,  $m/z$ ) calcd for  $\text{C}_{19}\text{H}_{20}\text{BrNO}_7\text{Na}$   $[\text{M}+\text{Na}]^+$ : 476.0315, 478.0298, found: 476.0316, 478.0296.

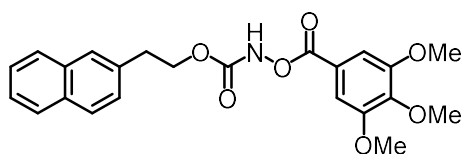
## Compound 9j



**9j**: white solid.  $^1\text{H NMR}$  (300 MHz,  $\text{CDCl}_3$ )  $\delta$  8.26 (s, 1H), 8.11-7.97 (m, 2H), 7.92-7.82 (m, 1H), 7.76 (dd,  $J = 7.0, 2.3$  Hz, 1H), 7.61-7.44 (m, 2H), 7.43-7.34 (m, 2H), 7.04-6.89 (m, 2H), 4.57 (t,  $J = 7.4$  Hz, 2H), 3.48 (t,  $J = 7.4$  Hz, 2H).  $^{13}\text{C NMR}$  (75 MHz,  $\text{CDCl}_3$ )  $\delta$  168.7, 168.5, 165.1, 162., 161.6, 156.6, 134.4, 134.2, 134.1, 133.1, 132.2, 129.1, 127.8, 127.3, 126.5, 125.9, 125.7, 123.6, 112.5, 112.5, 112.2, 112.2, 106.2, 105.8, 105.5, 100.2, 67.0, 32.4. **HRMS** (ESI,  $m/z$ ) calcd for  $\text{C}_{20}\text{H}_{15}\text{F}_2\text{NO}_4\text{Na}$   $[\text{M}+\text{Na}]^+$ : 394.0861, found: 394.0861.

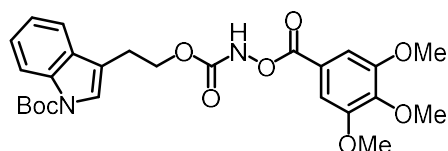


## Compound 9k



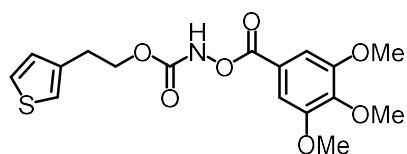
**9k:** white solid.  $^1\text{H NMR}$  (300 MHz,  $\text{CDCl}_3$ )  $\delta$  8.21 (s, 1H), 7.77 (dt,  $J = 11.7, 4.4$  Hz, 3H), 7.65 (s, 1H), 7.49-7.39 (m, 2H), 7.39-7.27 (m, 3H), 4.54 (t,  $J = 6.9$  Hz, 2H), 3.91 (d,  $J = 16.5$  Hz, 10H), 3.16 (t,  $J = 6.9$  Hz, 2H).  $^{13}\text{C NMR}$  (75 MHz,  $\text{CDCl}_3$ )  $\delta$  165.8, 156.8, 153.3, 143.6, 134.8, 133.7, 132.5, 128.4, 127.8, 127.7, 127.6, 127.4, 126.3, 125.8, 121.4, 107.5, 67.3, 61.2, 56.5, 35.5. **HRMS** (ESI,  $m/z$ ) calcd for  $\text{C}_{23}\text{H}_{23}\text{NO}_7\text{Na}$   $[\text{M}+\text{Na}]^+$ : 448.1367, found: 448.1366.

## Compound 9l



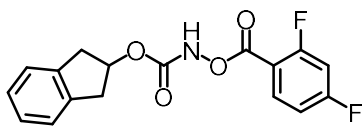
**9l:** white solid.  $^1\text{H NMR}$  (300 MHz,  $\text{CDCl}_3$ )  $\delta$  8.23 (s, 1H), 8.12 (d,  $J = 8.1$  Hz, 1H), 7.55 (d,  $J = 7.8$  Hz, 1H), 7.46 (s, 1H), 7.36-7.28 (m, 3H), 7.22 (d,  $J = 7.4$  Hz, 1H), 4.51 (t,  $J = 7.1$  Hz, 2H), 3.92 (d,  $J = 7.8$  Hz, 9H), 3.10 (t,  $J = 7.1$  Hz, 2H), 1.67 (s, 9H).  $^{13}\text{C NMR}$  (75 MHz,  $\text{CDCl}_3$ )  $\delta$  165.8, 156.8, 153.4, 143.7, 130.5, 124.7, 123.7, 122.7, 121.4, 119.0, 116.1, 115.5, 107.5, 83.8, 66.2, 61.2, 56.5, 28.4, 24.9. **HRMS** (ESI,  $m/z$ ) calcd for  $\text{C}_{26}\text{H}_{30}\text{N}_2\text{O}_9\text{Na}$   $[\text{M}+\text{Na}]^+$ : 537.1844, found: 537.1843.

## Compound 9m



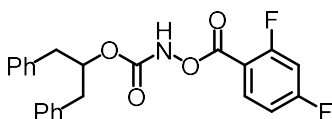
**9m:** white solid.  $^1\text{H NMR}$  (300 MHz,  $\text{CDCl}_3$ )  $\delta$  8.23 (s, 1H), 7.33 (s, 2H), 7.26-7.19 (m, 1H), 7.04 (s, 1H), 6.96 (d,  $J = 4.8$  Hz, 1H), 4.44 (t,  $J = 6.8$  Hz, 2H), 3.92 (d,  $J = 6.0$  Hz, 9H), 3.03 (t,  $J = 6.8$  Hz, 2H).  $^{13}\text{C NMR}$  (75 MHz,  $\text{CDCl}_3$ )  $\delta$  165.8, 156.7, 153.4, 143.7, 137.5, 128.3, 125.9, 122.0, 121.4, 107.5, 66.8, 61.2, 56.5, 29.8. **HRMS** (ESI,  $m/z$ ) calcd for  $\text{C}_{17}\text{H}_{19}\text{S}_1\text{N}_1\text{O}_7\text{Na}$   $[\text{M}+\text{Na}]^+$ : 404.0774, found: 404.0775.

## Compound 9n



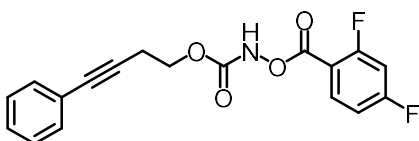
**9n**: white solid.  $^1\text{H NMR}$  (300 MHz,  $\text{CDCl}_3$ )  $\delta$  8.22 (s, 1H), 8.12-7.93 (m, 1H), 7.36-7.16 (m, 4H), 7.12-6.85 (m, 2H), 5.74-5.53 (m, 1H), 3.38 (dd,  $J = 17.2, 6.2$  Hz, 2H), 3.14 (dd,  $J = 17.1, 2.7$  Hz, 2H).  $^{13}\text{C NMR}$  (75 MHz,  $\text{CDCl}_3$ )  $\delta$  168.6, 168.4, 165.2, 165.0, 163.0, 162.9, 161.5, 156.4, 140.1, 134.3, 134.2, 127.1, 124.9, 112.5, 112.4, 112.2, 112.1, 106.1, 105.8, 105.5, 78.6, 39.7. **HRMS** (ESI,  $m/z$ ) calcd for  $\text{C}_{17}\text{H}_{13}\text{F}_2\text{N}_1\text{O}_4\text{Na}$   $[\text{M}+\text{Na}]^+$ : 356.0705, found: 356.0707.

## Compound 9o



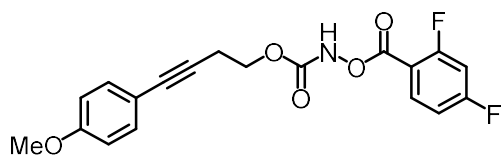
**9o**: white solid.  $^1\text{H NMR}$  (300 MHz,  $\text{CDCl}_3$ )  $\delta$  8.30 (s, 1H), 8.13-7.97 (m, 1H), 7.41-7.15 (m, 11H), 7.12-6.89 (m, 2H), 5.45-5.23 (m, 1H), 3.11-2.82 (m, 4H).  $^{13}\text{C NMR}$  (75 MHz,  $\text{CDCl}_3$ )  $\delta$  168.6, 168.4, 165.2, 165.0, 162.7, 162.7, 161.5, 156.1, 136.9, 134.4, 134.3, 134.2, 134.2, 129.6, 128.6, 126.9, 112.5, 112.4, 112.2, 112.1, 112.0, 106.1, 105.8, 105.5, 78.7, 39.7. **HRMS** (ESI,  $m/z$ ) calcd for  $\text{C}_{23}\text{H}_{19}\text{F}_2\text{N}_1\text{O}_4\text{Na}$   $[\text{M}+\text{Na}]^+$ : 434.1174, found: 434.1175.

## Compound 9p



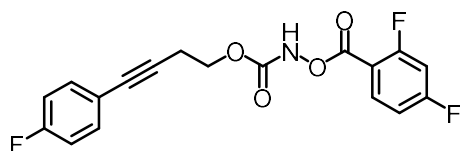
**9p**: white solid.  $^1\text{H NMR}$  (300 MHz,  $\text{CDCl}_3$ )  $\delta$  8.32 (s, 1H), 8.17-7.98 (m, 1H), 7.41 (dd,  $J = 6.7, 3.0$  Hz, 2H), 7.34-7.25 (m, 4H), 7.07-6.86 (m, 2H), 4.44 (t,  $J = 6.8$  Hz, 2H), 2.85 (t,  $J = 6.8$  Hz, 2H).  $^{13}\text{C NMR}$  (75 MHz,  $\text{CDCl}_3$ )  $\delta$  168.5, 162.8, 156.3, 134.4, 134.2, 131.8, 128.4, 128.2, 123.4, 112.5, 112.2, 106.2, 105.8, 105.5, 84.8, 82.5, 64.8, 20.3. **HRMS** (ESI,  $m/z$ ) calcd for  $\text{C}_{18}\text{H}_{13}\text{F}_2\text{N}_1\text{O}_4\text{Na}$   $[\text{M}+\text{Na}]^+$ : 368.0705, found: 368.0721.

## Compound 9q



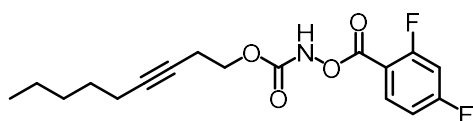
**9q:** white solid.  $^1\text{H NMR}$  (300 MHz,  $\text{CDCl}_3$ )  $\delta$  8.33 (s, 1H), 8.17-7.96 (m, 1H), 7.43-7.22 (m, 3H), 7.08-6.91 (m, 2H), 6.83 (d,  $J = 8.8$  Hz, 2H), 4.43 (t,  $J = 6.8$  Hz, 2H), 3.83 (s, 3H), 2.82 (t,  $J = 6.8$  Hz, 2H).  $^{13}\text{C NMR}$  (75 MHz,  $\text{CDCl}_3$ )  $\delta$  173.0, 168.6, 165.2, 165.0, 162.8, 159.6, 156.3, 134.4, 134.2, 133.2, 115.5, 114.0, 112.5, 112.2, 106.2, 105.8, 105.5, 83.3, 82.3, 65.0, 55.5, 20.3. **HRMS** (ESI,  $m/z$ ) calcd for  $\text{C}_{19}\text{H}_{15}\text{F}_2\text{N}_1\text{O}_5\text{Na}$   $[\text{M}+\text{Na}]^+$ : 398.0811, found: 398.0826.

## Compound 9r



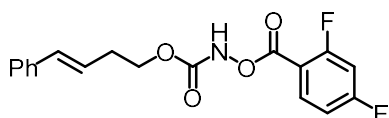
**9r:** white solid.  $^1\text{H NMR}$  (300 MHz,  $\text{CDCl}_3$ )  $\delta$  8.29 (s, 1H), 8.12-7.97 (m, 1H), 7.40-7.30 (m, 2H), 7.05-6.82 (m, 4H), 4.40 (t,  $J = 6.8$  Hz, 2H), 2.80 (t,  $J = 6.8$  Hz, 2H).  $^{13}\text{C NMR}$  (75 MHz,  $\text{CDCl}_3$ )  $\delta$  165.1, 164.2, 162.9, 162.8, 160.9, 134.4, 134.2, 133.7, 133.6, 119.4, 115.8, 115.5, 112.5, 112.2, 106.2, 105.8, 105.5, 84.6, 81.5, 64.8, 20.2.  $^{19}\text{F NMR}$  (235 MHz,  $\text{CDCl}_3$ )  $\delta$  -98.58, -98.64, -101.39, -101.45, -111.47. **HRMS** (ESI,  $m/z$ ) calcd for  $\text{C}_{18}\text{H}_{12}\text{F}_3\text{N}_1\text{O}_4\text{Na}$   $[\text{M}+\text{Na}]^+$ : 386.0626, found: 386.0626.

## Compound 9s



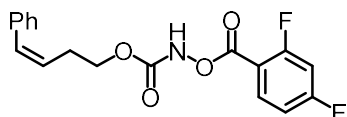
**9s:** white solid.  $^1\text{H NMR}$  (300 MHz,  $\text{CDCl}_3$ )  $\delta$  8.32 (s, 1H), 8.06 (td,  $J = 8.3, 6.5$  Hz, 1H), 7.09-6.84 (m, 2H), 4.39-4.20 (m, 2H), 2.54 (tt,  $J = 7.0, 2.3$  Hz, 2H), 2.11 (tt,  $J = 7.1, 2.2$  Hz, 2H), 1.59-1.40 (m, 2H), 1.39-1.22 (m, 4H), 0.89 (t,  $J = 7.0$  Hz, 3H).  $^{13}\text{C NMR}$  (75 MHz,  $\text{CDCl}_3$ )  $\delta$  168.7, 165.2, 165.1, 162.8, 162.8, 161.7, 156.3, 134.4, 134.2, 112.5, 112.5, 112.2, 112.2, 106.2, 105.8, 105.5, 82.8, 74.9, 65.4, 31.2, 28.7, 22.4, 19.6, 18.8, 14.2. **HRMS** (ESI,  $m/z$ ) calcd for  $\text{C}_{17}\text{H}_{19}\text{F}_2\text{N}_1\text{O}_4\text{Na}$   $[\text{M}+\text{Na}]^+$ : 362.1174, found: 362.1190.

## Compound (E)-9t



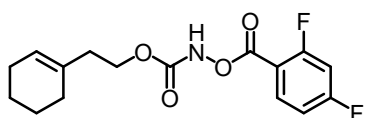
(E)-9t: white solid.  $^1\text{H NMR}$  (300 MHz,  $\text{CDCl}_3$ )  $\delta$  8.28 (s, 1H), 8.13-7.97 (m, 1H), 7.38-7.14 (m, 5H), 7.04-6.86 (m, 2H), 6.49 (d,  $J = 15.9$  Hz, 1H), 6.17 (dt,  $J = 15.8, 7.0$  Hz, 1H), 4.38 (t,  $J = 6.6$  Hz, 2H), 2.63 (q,  $J = 6.7$  Hz, 2H).  $^{13}\text{C NMR}$  (75 MHz,  $\text{CDCl}_3$ )  $\delta$  168.6, 168.4, 165.2, 165.0, 163.0, 162.9, 161.7, 161.5, 156.6, 137.3, 134.3, 134.2, 133.1, 128.7, 128.5, 127.5, 126.3, 125.0, 112.5, 112.4, 112.2, 112.1, 106.1, 105.8, 105.4, 66.3, 32.6. **HRMS** (ESI,  $m/z$ ) calcd for  $\text{C}_{18}\text{H}_{15}\text{F}_2\text{N}_1\text{O}_4\text{Na}$   $[\text{M}+\text{Na}]^+$ : 370.0861, found: 370.0875.

## Compound (Z)-9t



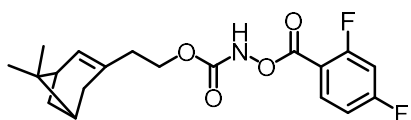
(Z)-9t: white solid.  $^1\text{H NMR}$  (300 MHz,  $\text{CDCl}_3$ )  $\delta$  8.29 (s, 1H), 8.14-7.98 (m, 1H), 7.42-7.16 (m, 5H), 7.06-6.91 (m, 2H), 6.59 (d,  $J = 11.7$  Hz, 1H), 5.68 (dt,  $J = 11.7, 7.2$  Hz, 1H), 4.35 (t,  $J = 6.7$  Hz, 2H), 2.75 (qd,  $J = 6.9, 1.6$  Hz, 2H).  $^{13}\text{C NMR}$  (75 MHz,  $\text{CDCl}_3$ )  $\delta$  168.5, 165.2, 162.8, 156.5, 137.1, 134.4, 134.2, 132.1, 128.8, 128.6, 128.5, 127.1, 126.7, 112.5, 112.5, 112.2, 112.2, 106.2, 105.8, 105.5, 66.5, 28.3. **HRMS** (ESI,  $m/z$ ) calcd for  $\text{C}_{18}\text{H}_{15}\text{F}_2\text{N}_1\text{O}_4\text{Na}$   $[\text{M}+\text{Na}]^+$ : 370.0861, found: 370.0875.

## Compound 9u



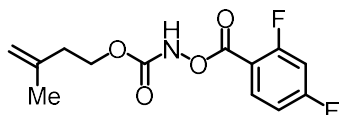
9u: white solid.  $^1\text{H NMR}$  (300 MHz,  $\text{CDCl}_3$ )  $\delta$  8.23 (s, 1H), 8.06 (td,  $J = 8.3, 6.5$  Hz, 1H), 7.06-6.84 (m, 2H), 5.46 (s, 1H), 4.29 (t,  $J = 6.9$  Hz, 2H), 2.30 (t,  $J = 6.8$  Hz, 2H), 1.94 (d,  $J = 3.9$  Hz, 4H), 1.78-1.33 (m, 5H).  $^{13}\text{C NMR}$  (75 MHz,  $\text{CDCl}_3$ )  $\delta$  168.5, 165.2, 165.1, 162.9, 162.9, 161.6, 156.7, 134.3, 134.2, 133.2, 124.2, 112.5, 112.5, 112.2, 112.2, 106.2, 105.8, 105.5, 77.6, 77.2, 76.8, 65.7, 37.2, 28.5, 25.4, 23.0, 22.4. **HRMS** (ESI,  $m/z$ ) calcd for  $\text{C}_{16}\text{H}_{17}\text{F}_2\text{N}_1\text{O}_4\text{Na}$   $[\text{M}+\text{Na}]^+$ : 348.1018, found: 348.1033.

## Compound 9v



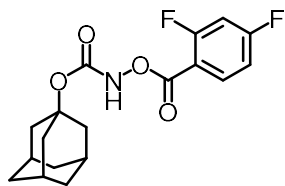
**9v**: colorless oil.  $^1\text{H NMR}$  (300 MHz,  $\text{CDCl}_3$ )  $\delta$  8.23 (s, 1H), 8.06 (dd,  $J = 14.8, 8.3$  Hz, 1H), 6.97 (ddd,  $J = 18.8, 10.8, 2.3$  Hz, 2H), 5.30 (s, 1H), 4.33-4.14 (m, 2H), 2.47-1.99 (m, 7H), 1.26 (s, 3H), 1.13 (d,  $J = 8.6$  Hz, 1H), 0.81 (s, 3H).  $^{13}\text{C NMR}$  (75 MHz,  $\text{CDCl}_3$ )  $\delta$  168.6, 165.2, 165.0, 162.9, 162.9, 161.7, 156.6, 143.6, 134.4, 134.2, 119.5, 112.5, 112.5, 112.2, 112.2, 106.2, 105.8, 105.5, 65.4, 45.8, 40.9, 38.2, 36.1, 31.8, 31.5, 26.4, 21.3. **HRMS** (ESI,  $m/z$ ) calcd for  $\text{C}_{19}\text{H}_{21}\text{F}_2\text{N}_1\text{O}_4\text{Na}$   $[\text{M}+\text{Na}]^+$ : 388.1331, found: 388.1341.

## Compound 9w



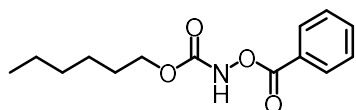
**9w**: white solid.  $^1\text{H NMR}$  (300 MHz,  $\text{CDCl}_3$ )  $\delta$  8.23 (s, 1H), 8.11-8.01 (m, 1H), 7.08-6.87 (m, 2H), 4.78 (d,  $J = 18.1$  Hz, 2H), 4.34 (t,  $J = 6.8$  Hz, 2H), 2.39 (t,  $J = 6.8$  Hz, 2H), 1.75 (s, 3H).  $^{13}\text{C NMR}$  (75 MHz,  $\text{CDCl}_3$ )  $\delta$  168.7, 165.3, 165.1, 162.9, 156.6, 141.1, 134.4, 134.2, 112.9, 112.5, 112.2, 106.2, 105.8, 105.5, 65.3, 36.9, 22.6. **HRMS** (ESI,  $m/z$ ) calcd for  $\text{C}_{13}\text{H}_{12}\text{F}_2\text{N}_1\text{O}_4\text{Na}$   $[\text{M}+\text{Na}]^+$ : 308.0705, found: 308.0720.

## Compound 9x



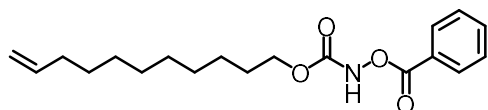
**9x**: white solid.  $^1\text{H NMR}$  (300 MHz,  $\text{CDCl}_3$ )  $\delta$  8.11 (s, 1H), 8.06 (td,  $J = 8.3, 6.6$  Hz, 1H), 7.04 – 6.86 (m, 2H), 2.17 (d,  $J = 13.1$  Hz, 9H), 1.66 (s, 6H).  $^{13}\text{C NMR}$  (75 MHz,  $\text{CDCl}_3$ )  $\delta$  168.4, 165.0, 163.2, 163.1, 155.1, 134.3, 134.2, 112.5, 112.4, 112.2, 112.1, 106.1, 105.8, 105.4, 83.7, 41.5, 36.2, 31.2. **HRMS** (ESI,  $m/z$ ) calcd for  $\text{C}_{18}\text{H}_{19}\text{F}_2\text{N}_1\text{O}_4\text{Na}$   $[\text{M}+\text{Na}]^+$ : 374.1174, found: 374.1192.

## Compound 9y



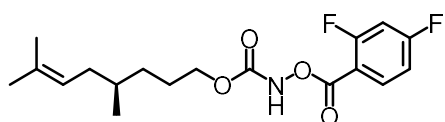
**9y:** colorless oil.  $^1\text{H NMR}$  (300 MHz,  $\text{CDCl}_3$ )  $\delta$  8.28 (s, 1H), 8.10 (d,  $J = 7.5$  Hz, 2H), 7.63 (d,  $J = 7.6$  Hz, 1H), 7.49 (t,  $J = 7.8$  Hz, 2H), 4.22 (t,  $J = 6.7$  Hz, 2H), 1.74-1.61 (m, 2H), 1.41-1.22 (m, 7H), 0.88 (t,  $J = 6.7$  Hz, 3H).  $^{13}\text{C NMR}$  (75 MHz,  $\text{CDCl}_3$ )  $\delta$  166.1, 156.9, 134.4, 130.2, 128.9, 127.0, 67.3, 31.5, 28.8, 25.5, 22.7, 14.1. **HRMS** (ESI,  $m/z$ ) calcd for  $\text{C}_{14}\text{H}_{19}\text{N}_1\text{O}_4\text{Na}$   $[\text{M}+\text{Na}]^+$ : 288.1206, found: 288.1213.

## Compound 9z

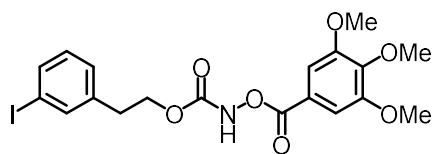


**9z:** white solid.  $^1\text{H NMR}$  (300 MHz,  $\text{CDCl}_3$ )  $\delta$  8.3 (s, 1H), 8.16-8.06 (m, 2H), 7.64 (dd,  $J = 10.6, 4.3$  Hz, 1H), 7.49 (t,  $J = 7.7$  Hz, 2H), 5.81 (ddt,  $J = 16.9, 10.2, 6.7$  Hz, 1H), 5.11-4.89 (m, 2H), 2.04 (q,  $J = 6.8$  Hz, 2H), 1.74-1.61 (m, 2H), 1.32 (dd,  $J = 20.6, 9.0$  Hz, 13H).  $^{13}\text{C NMR}$  (75 MHz,  $\text{CDCl}_3$ )  $\delta$  166.1, 156.9, 139.4, 134.4, 130.2, 128.9, 127.0, 114.3, 67.3, 34.0, 29.6, 29.5, 29.3, 29.3, 29.1, 28.9, 25.8. **HRMS** (ESI,  $m/z$ ) calcd for  $\text{C}_{19}\text{H}_{27}\text{N}_1\text{O}_4\text{Na}$   $[\text{M}+\text{Na}]^+$ : 356.1832, found: 356.1849.

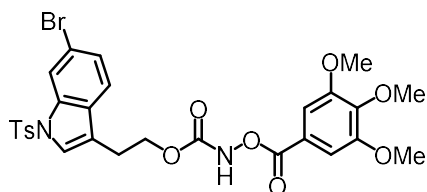
## Compound 9za



**9za:** colorless oil.  $^1\text{H NMR}$  (300 MHz,  $\text{CDCl}_3$ )  $\delta$  8.27 (s, 1H), 8.16-7.92 (m, 1H), 7.10-6.78 (m, 2H), 5.07 (t,  $J = 7.0$  Hz, 1H), 4.34-4.16 (m, 2H), 1.95 (dq,  $J = 15.4, 7.6$  Hz, 2H), 1.72 (dd,  $J = 12.6, 4.9$  Hz, 1H), 1.67 (s, 3H), 1.59 (s, 3H), 1.50 (ddd,  $J = 20.7, 12.5, 6.7$  Hz, 2H), 1.40-1.26 (m, 1H), 1.26-1.10 (m, 1H), 0.91 (d,  $J = 6.3$  Hz, 3H).  $^{13}\text{C NMR}$  (75 MHz,  $\text{CDCl}_3$ )  $\delta$  168.6, 168.5, 165.2, 165.0, 163.0, 162.9, 161.7, 161.5, 156.7, 154.0, 134.4, 134.3, 134.2, 134.2, 131.6, 124.6, 112.5, 112.5, 112.2, 112.2, 106.2, 105.8, 105.5, 65.9, 37.1, 35.7, 29.5, 25.9, 25.6, 19.5, 17.8. **HRMS** (ESI,  $m/z$ ) calcd for  $\text{C}_{18}\text{H}_{23}\text{F}_2\text{N}_1\text{O}_4\text{Na}$   $[\text{M}+\text{Na}]^+$ : 378.1487, found: 378.1502.

**Compound 9zb**

**9zb**: white solid.  $^1\text{H NMR}$  (300 MHz,  $\text{CDCl}_3$ )  $\delta$  8.32 (s, 1H), 7.65-7.49 (m, 2H), 7.31 (t,  $J = 1.9$  Hz, 2H), 7.16 (d,  $J = 7.7$  Hz, 1H), 6.98 (td,  $J = 7.7, 2.0$  Hz, 1H), 4.40 (ddd,  $J = 6.8, 4.4, 1.7$  Hz, 2H), 3.91 (dt,  $J = 4.3, 1.8$  Hz, 9H), 2.92 (t,  $J = 6.8$  Hz, 2H).  $^{13}\text{C NMR}$  (75 MHz,  $\text{CDCl}_3$ )  $\delta$  165.7, 156.6, 153.3, 143.7, 139.8, 138.0, 136.0, 130.4, 128.4, 121.4, 121.4, 107.5, 94.7, 66.8, 61.2, 56.6, 34.8. **HRMS** (ESI,  $m/z$ ) calcd for  $\text{C}_{19}\text{H}_{20}\text{I}_1\text{N}_1\text{O}_7\text{Na}$   $[\text{M}+\text{Na}]^+$ : 524.0177, found: 524.0177.

**Compound 9zc**

**9zc**: white solid.  $^1\text{H NMR}$  (300 MHz,  $\text{CDCl}_3$ )  $\delta$  8.16 (d,  $J = 11.5$  Hz, 2H), 7.74 (d,  $J = 8.3$  Hz, 2H), 7.42-7.30 (m, 5H), 7.23 (s, 1H), 4.45 (t,  $J = 6.8$  Hz, 2H), 3.92 (d,  $J = 9.5$  Hz, 10H), 3.03 (t,  $J = 6.7$  Hz, 2H), 2.35 (s, 3H).  $^{13}\text{C NMR}$  (75 MHz,  $\text{CDCl}_3$ )  $\delta$  165.8, 156.7, 153.4, 145.4, 136.0, 135.2, 130.3, 129.6, 127.0, 126.8, 124.5, 121.3, 120.6, 118.8, 118.1, 117.0, 107.5, 65.7, 61.2, 56.5, 24.8, 21.8. **HRMS** (ESI,  $m/z$ ) calcd for  $\text{C}_{28}\text{H}_{27}\text{Br}_1\text{N}_2\text{O}_9\text{S}_1\text{Na}$   $[\text{M}+\text{Na}]^+$ : 669.0513 & 671.0496, found: 669.0536 & 671.0514.

**4.5.3 Ruthenium Catalyzed Asymmetric Intramolecular C–H Amidation**

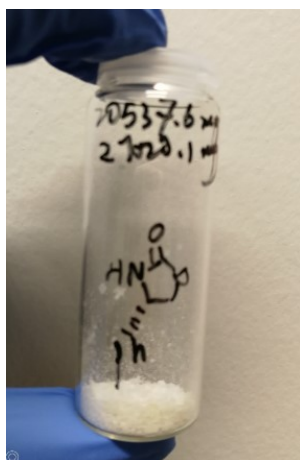
**General procedure:** A pre-dried Schlenk tube (10 mL) was charged with substrates (0.2 mmol), chiral ruthenium catalyst  $\Lambda$ -**Ru13** (0.004 mmol, 2.0 mol%) and  $\text{K}_2\text{CO}_3$  (82.8 mg, 0.6 mmol) under an atmosphere of  $\text{N}_2$ . Solvent 1,2-dichlorobenzene (4.0 mL) was added via syringe. The reaction mixture was stirred at 30 °C for 20 h under an atmosphere of  $\text{N}_2$ . Afterwards, the mixture was transferred to a column and purified by flash chromatography on silica gel (EtOAc/*n*-Hexane = 1:3 to 1:1) to afford the analytical pure product.

*Additional experimental information:*

**a) Execution of the reactions.** All catalytic reactions were carried out in 10 mL Schlenk tubes from “Synthware” under  $\text{N}_2$  atmosphere (see image below).



**b) Isolation of the final product.** The C-H amination products can be isolated by flash chromatography without any trace contaminations from the ruthenium catalyst as evident by the white color of the products (see image below).



**c) TLC monitor** (*n*-Hexane:EtOAc = 2:1), See image below.

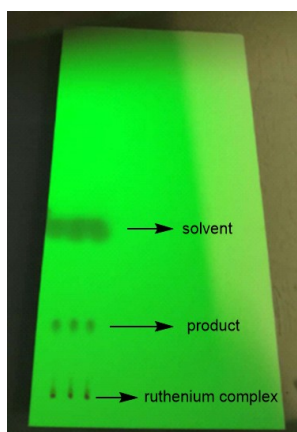
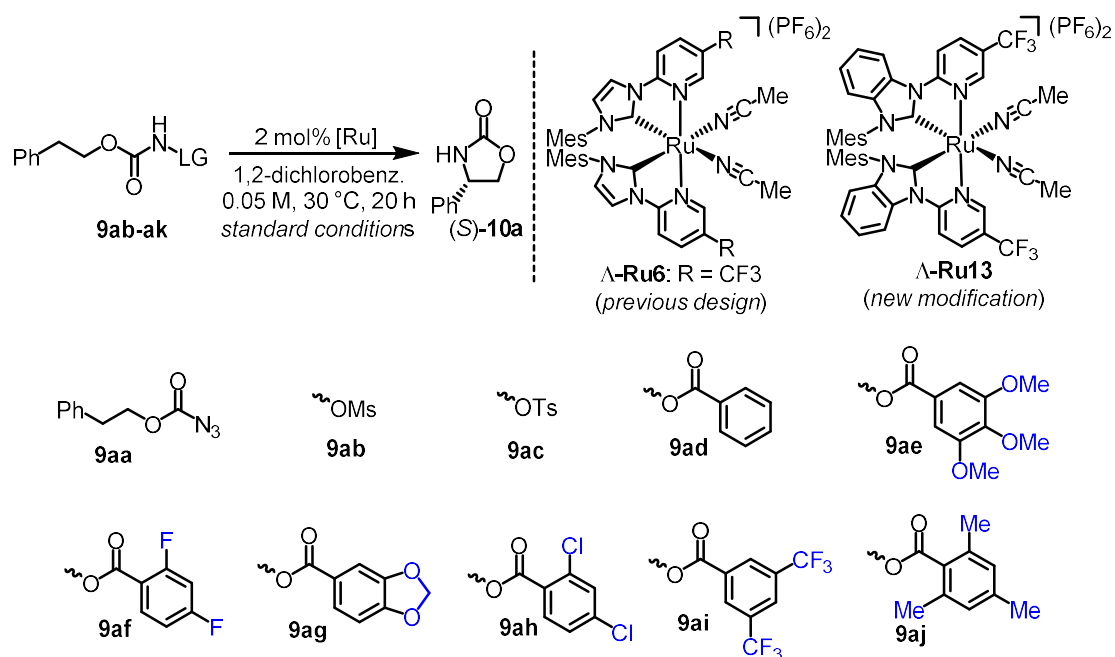


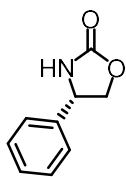


Table 9. Additional screening of different leaving groups<sup>a</sup>

Entry	Substrate	Catalyst	Conditions <sup>b</sup>	NMR yield (%) <sup>d</sup>	ee (%) <sup>e</sup>
1	<b>9aa</b>	$\Delta$ - <b>Ru6</b>	CH <sub>2</sub> Cl <sub>2</sub> at 25 °C without base	0	-
2	<b>9ab</b>	$\Delta$ - <b>Ru6</b>	CH <sub>2</sub> Cl <sub>2</sub> at 25 °C	69	68
3	<b>9ac</b>	$\Delta$ - <b>Ru6</b>	CH <sub>2</sub> Cl <sub>2</sub> at 25 °C	94	62
4	<b>9ad</b>	$\Delta$ - <b>Ru6</b>	CH <sub>2</sub> Cl <sub>2</sub> at 25 °C	97	78
5	<b>9ad</b>	$\Delta$ - <b>Ru6</b>	standard	98	82
6	<b>9ad</b>	$\Delta$ - <b>Ru13</b>	standard	95	86
7	<b>9ae</b>	$\Delta$ - <b>Ru13</b>	40 °C instead	97	90
8	<b>9af</b>	$\Delta$ - <b>Ru13</b>	standard	quant. (99) <sup>f</sup>	90
9	<b>9af</b>	$\Delta$ - <b>Ru13</b>	no base	< 5	n.d. <sup>g</sup>
10	<b>9af</b>	$\Delta$ - <b>Ru13</b>	under air	92	90
11	<b>9ag</b>	$\Delta$ - <b>Ru13</b>	standard	98	84
12	<b>9ah</b>	$\Delta$ - <b>Ru13</b>	standard	96	83
13	<b>9ai</b>	$\Delta$ - <b>Ru13</b>	standard	18	n.d. <sup>g</sup>
14	<b>9aj</b>	$\Delta$ - <b>Ru13</b>	standard	52	75

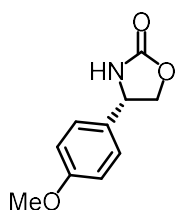
[a] Standard conditions: **9a** (0.2 mmol), K<sub>2</sub>CO<sub>3</sub> (0.6 mmol), Ru catalyst (0.002 mmol) in 1,2-dichlorobenzene (4 mL) stirred at the 30 °C for 20 h under N<sub>2</sub> unless noted otherwise. [b] Deviations from standard conditions are shown. [c] Conversion. [d] Determined by <sup>1</sup>H NMR of the crude products using Cl<sub>2</sub>CHCHCl<sub>2</sub> as internal standard. [e] Enantiomeric excess determined by HPLC analysis of the crude main product on a chiral stationary phase. [f] Isolated yield in brackets. [g] Not determined.

## Compound 10a

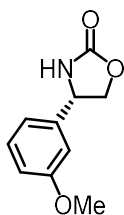


Starting from **9af** (62.2 mg, 0.20 mmol) according to the general procedure to provide **10a** as a white solid (32.3 mg, 99% yield). Enantiomeric excess was established by HPLC analysis as 90% ee (column: Daicel Chiralpak ODH 250 x 4.6 mm, absorption:  $\lambda = 210$  nm, mobile phase: *n*-Hexane/isopropanol = 80:20, flow rate: 1.0 mL/min, column temperature: 25 °C, retention times:  $t_r$  (major) = 15.0 min,  $t_r$  (minor) = 13.9 min).  $[\alpha]_D^{22} = +25.6^\circ$  ( $c = 1.0$ ,  $\text{CH}_2\text{Cl}_2$ ).  $^1\text{H NMR}$  (300 MHz,  $\text{CDCl}_3$ )  $\delta$  7.53-7.31 (m, 5H), 5.61 (s, 1H), 5.05 – 4.89 (m, 1H), 4.74 (t,  $J = 8.6$  Hz, 1H), 4.20 (dd,  $J = 8.5, 6.9$  Hz, 1H).  $^{13}\text{C NMR}$  (75 MHz,  $\text{CDCl}_3$ )  $\delta$  159.6, 139.6, 129.5, 129.1, 126.2, 72.7, 56.6. **HRMS** (ESI,  $m/z$ ) calcd for  $\text{C}_9\text{H}_9\text{NO}_2\text{Na}$   $[\text{M}+\text{Na}]^+$ : 186.0525, found: 186.0531.

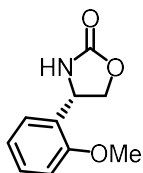
## Compound 10b



Starting from **9b** (70.2 mg, 0.20 mmol) according to the general procedure to provide **10b** as a white solid (38.2 mg, 99% yield). Enantiomeric excess was established by HPLC analysis as 90% ee (column: Daicel Chiralpak IG 250 x 4.6 mm, absorption:  $\lambda = 210$  nm, mobile phase: *n*-Hexane/isopropanol = 80:20, flow rate: 1.0 mL/min, column temperature: 25 °C, retention times:  $t_r$  (major) = 17.3 min,  $t_r$  (minor) = 16.1 min).  $[\alpha]_D^{22} = +20.2^\circ$  ( $c = 1.0$ ,  $\text{CH}_2\text{Cl}_2$ ).  $^1\text{H NMR}$  (300 MHz,  $\text{CDCl}_3$ )  $\delta$  7.34-7.09 (m, 2H), 6.95-6.76 (m, 2H), 5.53 (s, 1H), 4.91-4.76 (m, 1H), 4.63 (t,  $J = 8.6$  Hz, 1H), 4.09 (dd,  $J = 8.5, 7.0$  Hz, 1H), 3.74 (s, 3H).  $^{13}\text{C NMR}$  (75 MHz,  $\text{CDCl}_3$ )  $\delta$  160.2, 159.6, 131.5, 127.6, 114.8, 72.9, 56.2, 55.6. **HRMS** (ESI,  $m/z$ ) calcd for  $\text{C}_{10}\text{H}_{11}\text{NO}_3\text{Na}$   $[\text{M}+\text{Na}]^+$ : 216.0631, found: 216.0636.

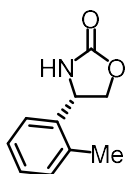
**Compound 10c**

Starting from **9c** (70.2 mg, 0.20 mmol) according to the general procedure to provide **10c** as a white solid (38.3 mg, 99% yield). Enantiomeric excess was established by HPLC analysis as 92% ee (column: Daicel Chiralpak ODH 250 x 4.6 mm, absorption:  $\lambda = 210$  nm, mobile phase: *n*-Hexane/isopropanol = 80:20, flow rate: 1.0 mL/min, column temperature: 25 °C, retention times:  $t_r$  (major) = 20.0 min,  $t_r$  (minor) = 22.2 min).  $[\alpha]_D^{22} = +18.8^\circ$  ( $c = 1.0$ ,  $\text{CH}_2\text{Cl}_2$ ).  $^1\text{H NMR}$  (300 MHz,  $\text{CDCl}_3$ )  $\delta$  7.30 (dd,  $J = 8.7, 7.6$  Hz, 1H), 7.02-6.80 (m, 3H), 5.98 (s, 1H), 4.98-4.84 (m, 1H), 4.71 (t,  $J = 8.7$  Hz, 1H), 4.17 (dd,  $J = 8.5, 7.0$  Hz, 1H), 3.81 (s, 3H).  $^{13}\text{C NMR}$  (75 MHz,  $\text{CDCl}_3$ )  $\delta$  160.5, 159.8, 141.3, 130.5, 118.3, 114.4, 111.7, 72.6, 56.5, 55.5. **HRMS** (ESI,  $m/z$ ) calcd for  $\text{C}_{10}\text{H}_{11}\text{NO}_3\text{Na}$   $[\text{M}+\text{Na}]^+$ : 216.0631, found: 216.0636.

**Compound 10d**

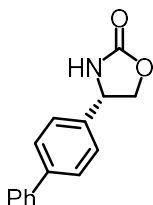
Starting from **9d** (70.2 mg, 0.20 mmol) according to the general procedure to provide **10d** as a white solid (38.1 mg, 99% yield). Enantiomeric excess was established by HPLC analysis as 93% ee (column: Daicel Chiralpak IG 250 x 4.6 mm, absorption:  $\lambda = 210$  nm, mobile phase: *n*-Hexane/isopropanol = 80:20, flow rate: 1.0 mL/min, column temperature: 25 °C, retention times:  $t_r$  (major) = 15.7 min,  $t_r$  (minor) = 13.4 min).  $[\alpha]_D^{22} = +83.1^\circ$  ( $c = 1.0$ ,  $\text{CH}_2\text{Cl}_2$ ).  $^1\text{H NMR}$  (300 MHz,  $\text{CDCl}_3$ )  $\delta$  7.32 (dd,  $J = 9.7, 7.7$  Hz, 2H), 7.00 (t,  $J = 7.5$  Hz, 1H), 6.90 (d,  $J = 8.1$  Hz, 1H), 5.83 (s, 1H), 5.24 (dd,  $J = 8.5, 6.7$  Hz, 1H), 4.80 (t,  $J = 8.7$  Hz, 1H), 4.17 (dd,  $J = 8.4, 6.4$  Hz, 1H), 3.86 (d,  $J = 12.0$  Hz, 3H).  $^{13}\text{C NMR}$  (75 MHz,  $\text{CDCl}_3$ )  $\delta$  160.2, 156.7, 129.6, 128.0, 125.7, 121.1, 110.7, 71.7, 55.6, 51.5. **HRMS** (ESI,  $m/z$ ) calcd for  $\text{C}_{10}\text{H}_{11}\text{NO}_3\text{Na}$   $[\text{M}+\text{Na}]^+$ : 216.0631, found: 216.0636.

## Compound 10e

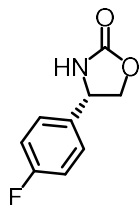


Starting from **9e** (67.0 mg, 0.20 mmol) according to the general procedure to provide **10e** as a white solid (35.1 mg, 99% yield). Enantiomeric excess was established by HPLC analysis as 92% ee (column: Daicel Chiralpak ODH 250 x 4.6 mm, absorption:  $\lambda = 210$  nm, mobile phase: *n*-Hexane/isopropanol = 80:20, flow rate: 1.0 mL/min, column temperature: 25 °C, retention times:  $t_r$  (major) = 24.1 min,  $t_r$  (minor) = 13.3 min).  $[\alpha]_D^{22} = +179.4^\circ$  ( $c = 1.0$ ,  $\text{CH}_2\text{Cl}_2$ ).  $^1\text{H NMR}$  (300 MHz,  $\text{CDCl}_3$ )  $\delta$  7.47-7.31 (m, 1H), 7.27-7.06 (m, 3H), 5.85 (s, 1H), 5.22-5.09 (m, 1H), 4.72 (t,  $J = 8.6$  Hz, 1H), 4.03 (dd,  $J = 8.3, 7.0$  Hz, 1H), 2.23 (s, 3H).  $^{13}\text{C NMR}$  (75 MHz,  $\text{CDCl}_3$ )  $\delta$  160.1, 137.7, 134.8, 131.1, 128.5, 127.1, 124.9, 71.8, 53.3, 19.2. **HRMS** (ESI,  $m/z$ ) calcd for  $\text{C}_{10}\text{H}_{11}\text{NO}_2\text{Na}$   $[\text{M}+\text{Na}]^+$ : 200.0682, found: 200.0687.

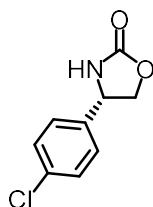
## Compound 10f



Starting from **9f** (90.2 mg, 0.20 mmol) according to the general procedure to provide **10f** as a white solid (47.3 mg, 99% yield). Enantiomeric excess was established by HPLC analysis as 98% ee (column: Daicel Chiralpak ODH 250 x 4.6 mm, absorption:  $\lambda = 254$  nm, mobile phase: *n*-Hexane/isopropanol = 80:20, flow rate: 1.0 mL/min, column temperature: 25 °C, retention times:  $t_r$  (major) = 26.5 min,  $t_r$  (minor) = 24.4 min).  $[\alpha]_D^{22} = +3.8^\circ$  ( $c = 1.0$ ,  $\text{CH}_2\text{Cl}_2$ ).  $^1\text{H NMR}$  (300 MHz,  $\text{CDCl}_3$ )  $\delta$  7.71-7.55 (m, 4H), 7.41 (dtd,  $J = 9.6, 7.2, 3.2$  Hz, 5H), 5.58 (s, 1H), 5.07-4.93 (m, 1H), 4.77 (t,  $J = 8.7$  Hz, 1H), 4.24 (dd,  $J = 8.6, 6.9$  Hz, 1H).  $^{13}\text{C NMR}$  (75 MHz,  $\text{CDCl}_3$ )  $\delta$  159.5, 142.2, 140.4, 138.5, 129.1, 128.2, 127.9, 127.3, 126.7, 72.7, 56.3. **HRMS** (ESI,  $m/z$ ) calcd for  $\text{C}_{15}\text{H}_{13}\text{NO}_2\text{H}$   $[\text{M}+\text{H}]^+$ : 240.1019, found: 240.1025.

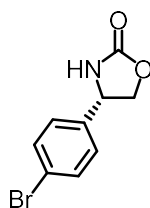
**Compound 10g**

Starting from **9g** (78.6 mg, 0.20 mmol) according to the general procedure to provide **10g** as a white solid (35.7 mg, 99% yield). Enantiomeric excess was established by HPLC analysis as 90% ee (column: Daicel Chiralpak ODH 250 x 4.6 mm, absorption:  $\lambda = 210$  nm, mobile phase: *n*-Hexane/isopropanol = 90:10, flow rate: 1.0 mL/min, column temperature: 25 °C, retention times:  $t_r$  (major) = 23.6 min,  $t_r$  (minor) = 26.8 min).  $[\alpha]_D^{22} = +26.2^\circ$  ( $c = 1.0$ ,  $\text{CH}_2\text{Cl}_2$ ).  **$^1\text{H NMR}$**  (300 MHz,  $\text{CDCl}_3$ )  $\delta$  7.38-7.28 (m, 2H), 7.08 (t,  $J = 8.6$  Hz, 2H), 6.44 (s, 1H), 5.09-4.82 (m, 1H), 4.71 (t,  $J = 8.7$  Hz, 1H), 4.13 (dd,  $J = 8.6, 6.9$  Hz, 1H).  **$^{13}\text{C NMR}$**  (75 MHz,  $\text{CDCl}_3$ )  $\delta$  164.7, 161.4, 160.0, 135.5, 135.5, 128.0, 127.9, 116.5, 116.2, 72.7, 72.7, 56.0.  **$^{19}\text{F NMR}$**  (235 MHz,  $\text{CDCl}_3$ )  $\delta$  -112.89. **HRMS** (ESI,  $m/z$ ) calcd for  $\text{C}_9\text{H}_8\text{FNO}_2\text{Na}$   $[\text{M}+\text{Na}]^+$ : 204.0431, found: 204.0437.

**Compound 10h**

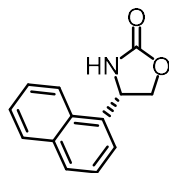
Starting from **9h** (81.8 mg, 0.20 mmol) according to the general procedure to provide **10h** as a white solid (36.2 mg, 92% yield). Enantiomeric excess was established by HPLC analysis as 88% ee (column: Daicel Chiralpak IC 250 x 4.6 mm, absorption:  $\lambda = 210$  nm, mobile phase: *n*-Hexane/isopropanol = 60:40, flow rate: 1.0 mL/min, column temperature: 25 °C, retention times:  $t_r$  (major) = 11.5 min,  $t_r$  (minor) = 18.1 min).  $[\alpha]_D^{22} = +16.8^\circ$  ( $c = 1.0$ ,  $\text{CH}_2\text{Cl}_2$ ).  **$^1\text{H NMR}$**  (300 MHz,  $\text{CDCl}_3$ )  $\delta$  7.37 (d,  $J = 8.5$  Hz, 2H), 7.27 (d,  $J = 8.3$  Hz, 2H), 6.29 (s, 1H), 5.03-4.85 (m, 1H), 4.13 (dd,  $J = 8.6, 6.8$  Hz, 1H).  **$^{13}\text{C NMR}$**  (75 MHz,  $\text{CDCl}_3$ )  $\delta$  159.9, 138.2, 134.9, 129.6, 127.6, 72.5, 56.0. **HRMS** (ESI,  $m/z$ ) calcd for  $\text{C}_9\text{H}_8\text{ClNO}_2\text{Na}$   $[\text{M}+\text{Na}]^+$ : 220.0136, found: 220.0141.

## Compound 10i



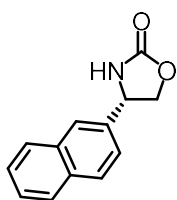
Starting from **9i** (90.6 mg, 0.20 mmol) according to the general procedure to provide **10i** as a white solid (47.5 mg, 99% yield). Enantiomeric excess was established by HPLC analysis as 90% ee (column: Daicel Chiralpak IG 250 x 4.6 mm, absorption:  $\lambda = 210$  nm, mobile phase: *n*-Hexane/isopropanol = 80:20, flow rate: 1.0 mL/min, column temperature: 25 °C, retention times:  $t_r$  (major) = 16.9 min,  $t_r$  (minor) = 11.7 min).  $[\alpha]_D^{22} = +13.7^\circ$  ( $c = 1.0$ ,  $\text{CH}_2\text{Cl}_2$ ).  $^1\text{H NMR}$  (300 MHz,  $\text{CDCl}_3$ )  $\delta$  7.54 (d,  $J = 8.4$  Hz, 2H), 7.34-7.10 (m, 2H), 6.02 (s, 1H), 5.09-4.82 (m, 1H), 4.73 (t,  $J = 8.7$  Hz, 1H), 4.14 (dd,  $J = 8.4, 7.0$  Hz, 1H).  $^{13}\text{C NMR}$  (75 MHz,  $\text{CDCl}_3$ )  $\delta$  160.2, 138.8, 138.7, 132.6, 132.5, 127.9, 122.9, 72.4, 56.0. **HRMS** (ESI,  $m/z$ ) calcd for  $\text{C}_9\text{H}_8\text{BrNO}_2\text{Na}$   $[\text{M}+\text{Na}]^+$ : 263.9631, found: 263.9638.

## Compound 10j



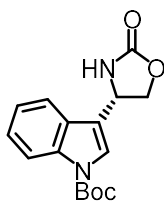
Starting from **9j** (74.2 mg, 0.20 mmol) according to the general procedure to provide **10j** as a white solid (42.2 mg, 99% yield). Enantiomeric excess was established by HPLC analysis as 93% ee (column: Daicel Chiralpak IA 250 x 4.6 mm, absorption:  $\lambda = 210$  nm, mobile phase: *n*-Hexane/isopropanol = 90:10, flow rate: 1.0 mL/min, column temperature: 25 °C, retention times:  $t_r$  (major) = 15.8 min,  $t_r$  (minor) = 14.1 min).  $[\alpha]_D^{22} = +186.4^\circ$  ( $c = 1.0$ ,  $\text{CH}_2\text{Cl}_2$ ).  $^1\text{H NMR}$  (300 MHz,  $\text{CDCl}_3$ )  $\delta$  7.99-7.90 (m, 1H), 7.86 (d,  $J = 8.2$  Hz, 1H), 7.77 (dd,  $J = 5.8, 3.3$  Hz, 1H), 7.66 (d,  $J = 7.1$  Hz, 1H), 7.62-7.46 (m, 3H), 6.21 (s, 1H), 5.83-5.64 (m, 1H), 5.00 (t,  $J = 8.7$  Hz, 1H), 4.22 (dd,  $J = 8.5, 6.5$  Hz, 1H).  $^{13}\text{C NMR}$  (75 MHz,  $\text{CDCl}_3$ )  $\delta$  160.0, 135.2, 134.2, 130.2, 129.5, 129.2, 127.1, 126.4, 125.8, 122.4, 121.9, 72.0, 53.3. **HRMS** (ESI,  $m/z$ ) calcd for  $\text{C}_{13}\text{H}_{11}\text{NO}_2\text{Na}$   $[\text{M}+\text{Na}]^+$ : 236.0682, found: 236.0688.

## Compound 10k



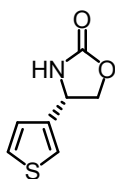
Starting from **9k** (85.0 mg, 0.20 mmol) according to the general procedure to provide **10k** as a white solid (41.3 mg, 97% yield). Enantiomeric excess was established by HPLC analysis as 92% ee (column: Daicel Chiralpak ODH 250 x 4.6 mm, absorption:  $\lambda = 210$  nm, mobile phase: *n*-Hexane/isopropanol = 60:40, flow rate: 1.0 mL/min, column temperature: 25 °C, retention times:  $t_r$  (major) = 14.1 min,  $t_r$  (minor) = 17.1 min).  $[\alpha]_D^{22} = +11.2^\circ$  ( $c = 1.0$ , CH<sub>2</sub>Cl<sub>2</sub>). <sup>1</sup>H NMR (300 MHz, CDCl<sub>3</sub>)  $\delta$  8.03-7.72 (m, 4H), 7.50 (ddt,  $J = 10.2, 8.5, 3.0$  Hz, 3H), 5.59 (s, 1H), 5.20-5.04 (m, 1H), 4.81 (t,  $J = 8.7$  Hz, 1H), 4.29 (dd,  $J = 8.6, 6.8$  Hz, 1H). <sup>13</sup>C NMR (75 MHz, CDCl<sub>3</sub>)  $\delta$  159.53, 136.80, 133.63, 133.38, 129.73, 128.10, 128.02, 127.05, 126.89, 125.65, 123.36, 72.57, 56.70. HRMS (ESI,  $m/z$ ) calcd for C<sub>13</sub>H<sub>11</sub>NO<sub>2</sub>Na [M+Na]<sup>+</sup>: 236.0682, found: 236.0688.

## Compound 10l



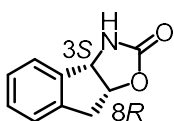
Starting from **9l** (102.8 mg, 0.20 mmol) according to the general procedure to provide **10l** as a white solid (39.8 mg, 66% yield). Enantiomeric excess was established by HPLC analysis as 85% ee (column: Daicel Chiralpak ODH 250 x 4.6 mm, absorption:  $\lambda = 210$  nm, mobile phase: *n*-Hexane/isopropanol = 80:20, flow rate: 1.0 mL/min, column temperature: 25 °C, retention times:  $t_r$  (major) = 10.4 min,  $t_r$  (minor) = 12.1 min).  $[\alpha]_D^{22} = +8.5^\circ$  ( $c = 1.0$ , CH<sub>2</sub>Cl<sub>2</sub>). <sup>1</sup>H NMR (300 MHz, CDCl<sub>3</sub>)  $\delta$  8.18 (d,  $J = 8.3$  Hz, 1H), 7.61 (s, 1H), 7.54 (d,  $J = 7.7$  Hz, 1H), 7.41-7.32 (m, 1H), 7.31-7.20 (m, 1H), 6.00 (s, 1H), 5.20 (dd,  $J = 8.7, 6.7$  Hz, 1H), 4.76 (t,  $J = 8.7$  Hz, 1H), 4.41 (dd,  $J = 8.6, 6.6$  Hz, 1H), 1.67 (s, 10H). <sup>13</sup>C NMR (75 MHz, CDCl<sub>3</sub>)  $\delta$  159.6, 149.5, 136.4, 127.4, 125.4, 123.9, 123.3, 119.0, 118.8, 115.9, 84.5, 70.6, 49.8, 28.3. HRMS (ESI,  $m/z$ ) calcd for C<sub>16</sub>H<sub>18</sub>N<sub>2</sub>O<sub>4</sub>Na [M+Na]<sup>+</sup>: 325.1159, found: 325.1166.

## Compound 10m



Starting from **9m** (76.2 mg, 0.20 mmol) according to the general procedure to provide **10m** as a white solid (26.0 mg, 77% yield). Enantiomeric excess was established by HPLC analysis by using a Daicel Chiralpak ADH column, ee = 93% (HPLC: 210 nm, *n*-Hexane/isopropanol = 85:15, flow rate 0.8 mL/min, 40 °C,  $t_r$  (major) = 11.2 min,  $t_r$  (minor) = 10.3 min).  $[\alpha]_D^{22} = +9.0^\circ$  ( $c = 1.0$ , CH<sub>2</sub>Cl<sub>2</sub>). **<sup>1</sup>H NMR** (300 MHz, CDCl<sub>3</sub>)  $\delta$  7.39 (dd,  $J = 5.0, 3.0$  Hz, 1H), 7.08 (dd,  $J = 5.0, 1.2$  Hz, 1H), 6.03 (s, 1H), 5.11-4.99 (m, 1H), 4.69 (t,  $J = 8.6$  Hz, 1H), 4.23 (dd,  $J = 8.5, 6.6$  Hz, 1H). **<sup>13</sup>C NMR** (75 MHz, CDCl<sub>3</sub>)  $\delta$  159.6, 140.9, 128.0, 125.2, 122.6, 72.0, 52.4. **HRMS** (ESI,  $m/z$ ) calcd for C<sub>7</sub>H<sub>7</sub>N<sub>1</sub>O<sub>2</sub>S<sub>1</sub>Na [M+Na]<sup>+</sup>: 192.0090, found: 192.0092.

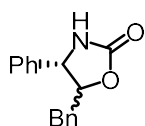
## Compound 10n



Starting from **9n** (66.6 mg, 0.20 mmol) according to the general procedure to provide **10n** as a white solid (34.8 mg, 99% yield). Enantiomeric excess was established by HPLC analysis as 95% ee (column: Daicel Chiralpak ODH 250 x 4.6 mm, absorption:  $\lambda = 210$  nm, mobile phase: *n*-Hexane/isopropanol = 90:10, flow rate: 1.0 mL/min, column temperature: 25 °C, retention times:  $t_r$  (major) = 21.0 min,  $t_r$  (minor) = 24.9 min).  $[\alpha]_D^{22} = -58.1^\circ$  ( $c = 1.0$ , CH<sub>2</sub>Cl<sub>2</sub>). **<sup>1</sup>H NMR** (300 MHz, CDCl<sub>3</sub>)  $\delta$  7.39-7.14 (m, 4H), 6.70 (s, 1H), 5.41 (ddd,  $J = 8.1, 6.0, 2.3$  Hz, 1H), 5.17 (d,  $J = 7.3$  Hz, 1H), 3.50-3.24 (m, 2H). **<sup>13</sup>C NMR** (75 MHz, CDCl<sub>3</sub>)  $\delta$  159.9, 140.5, 139.9, 129.5, 128.1, 125.7, 125.0, 80.8, 61.4, 39.0. **HRMS** (ESI,  $m/z$ ) calcd for C<sub>10</sub>H<sub>9</sub>NO<sub>2</sub>Na [M+Na]<sup>+</sup>: 198.0525, found: 198.0530.

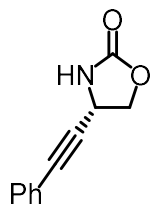


## Compound 10o



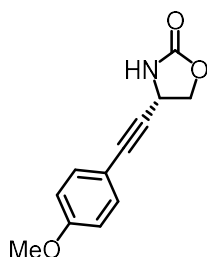
Starting from **9o** (82.2 mg, 0.20 mmol) according to the general procedure to provide **10o** as a white solid (42.0 mg, 83% yield). Diastereomeric ratio and enantiomeric excess was established by HPLC analysis as 1.8:1 d.r., 92%/97% ee (column: Daicel Chiralpak ODH 250 x 4.6 mm, absorption:  $\lambda = 210$  nm, mobile phase: *n*-Hexane/isopropanol = 80:20, flow rate: 0.8 mL/min, column temperature: 30 °C, retention times: for major diastereomer,  $t_r$  (major) = 15.6 min,  $t_r$  (minor) = 14.1 min), for minor diastereomer,  $t_r$  (major) = 18.5 min,  $t_r$  (minor) = 17.3 min).  $[\alpha]_D^{22} = +2.4^\circ$  ( $c = 1.0$ ,  $\text{CH}_2\text{Cl}_2$ ). For major diastereomer,  $^1\text{H NMR}$  (300 MHz,  $\text{CDCl}_3$ )  $\delta$  7.39-7.22 (m, 11H), 5.53 (s, 1H), 4.73 -4.54 (m, 2H), 3.15 (qd,  $J = 14.4, 5.7$  Hz, 2H).  $^{13}\text{C NMR}$  (75 MHz,  $\text{CDCl}_3$ )  $\delta$  158.7, 139.4, 135.3, 129.9, 129.3, 129.2, 128.9, 126.3, 85.3, 60.8, 39.9. **HRMS** (ESI,  $m/z$ ) calcd for  $\text{C}_{16}\text{H}_{15}\text{NO}_2\text{Na}$   $[\text{M}+\text{Na}]^+$ : 276.0995, found: 276.1004.

## Compound 10p



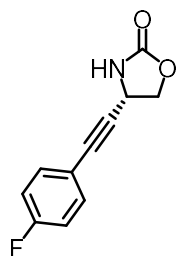
Starting from **9p** (69.0 mg, 0.20 mmol) according to the general procedure to provide **10p** as a white solid (34.0 mg, 91% yield). Enantiomeric excess was established by HPLC analysis as 91% ee (column: Daicel Chiralpak ODH 250 x 4.6 mm, absorption:  $\lambda = 210$  nm, mobile phase: *n*-Hexane/isopropanol = 90:10, flow rate: 1.0 mL/min, column temperature: 25 °C, retention times:  $t_r$  (major) = 18.2 min,  $t_r$  (minor) = 24.6 min).  $[\alpha]_D^{22} = -40.6^\circ$  ( $c = 1.0$ ,  $\text{CH}_2\text{Cl}_2$ ).  $^1\text{H NMR}$  (300 MHz,  $\text{CDCl}_3$ )  $\delta$  7.53-7.30 (m, 5H), 5.53 (s, 1H), 4.83 (dd,  $J = 8.4, 5.7$  Hz, 1H), 4.65 (t,  $J = 8.4$  Hz, 1H), 4.46 (dd,  $J = 8.3, 5.6$  Hz, 1H).  $^{13}\text{C NMR}$  (75 MHz,  $\text{CDCl}_3$ )  $\delta$  158.8, 132.0, 129.3, 128.6, 121.7, 85.9, 85.3, 70.5, 44.4. **HRMS** (ESI,  $m/z$ ) calcd for  $\text{C}_{11}\text{H}_9\text{NO}_2\text{Na}$   $[\text{M}+\text{Na}]^+$ : 210.0525, found: 210.0530.

## Compound 10q



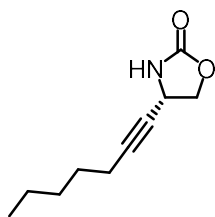
Starting from **9q** (75.0 mg, 0.20 mmol) according to the general procedure to provide **10q** as a white solid (39.5 mg, 91% yield). Enantiomeric excess was established by HPLC analysis by using a Daicel Chiralpak ODH column, ee = 94% (HPLC: 220 nm, *n*-Hexane/isopropanol = 80:20, flow rate 1.0 mL/min, 25 °C,  $t_r$  (major) = 15.0 min,  $t_r$  (minor) = 16.6 min).  $[\alpha]_D^{22} = -79.8^\circ$  ( $c = 1.0$ , CH<sub>2</sub>Cl<sub>2</sub>). **<sup>1</sup>H NMR** (300 MHz, CDCl<sub>3</sub>)  $\delta$  7.41-7.29 (m, 2H), 6.92-6.76 (m, 2H), 5.80 (s, 1H), 4.81 (dd,  $J = 8.4$ , 5.7 Hz, 1H), 4.62 (t,  $J = 8.3$  Hz, 1H), 4.43 (dd,  $J = 8.3$ , 5.7 Hz, 1H), 3.81 (s, 3H). **<sup>13</sup>C NMR** (75 MHz, CDCl<sub>3</sub>)  $\delta$  160.4, 159.0, 133.5, 114.3, 113.7, 85.8, 84.0, 70.6, 55.5, 44.5. **HRMS** (ESI,  $m/z$ ) calcd for C<sub>12</sub>H<sub>11</sub>N<sub>1</sub>O<sub>3</sub>Na [M+Na]<sup>+</sup>: 240.0631, found: 240.0631.

## Compound 10r

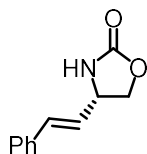


Starting from **9r** (72.6 mg, 0.20 mmol) according to the general procedure to provide **10r** as a white solid (34.9 mg, 85% yield). Enantiomeric excess was established by HPLC analysis by using a Daicel Chiralpak ODH column, ee = 90% (HPLC: 220 nm, *n*-Hexane/isopropanol = 80:20, flow rate 1.0 mL/min, 25 °C,  $t_r$  (major) = 8.3 min,  $t_r$  (minor) = 10.8 min).  $[\alpha]_D^{22} = -52.4^\circ$  ( $c = 1.0$ , CH<sub>2</sub>Cl<sub>2</sub>). **<sup>1</sup>H NMR** (300 MHz, CDCl<sub>3</sub>)  $\delta$  7.56-7.33 (m, 2H), 7.10-6.95 (m, 2H), 5.77 (s, 1H), 4.82 (dd,  $J = 8.4$ , 5.6 Hz, 1H), 4.64 (t,  $J = 8.4$  Hz, 1H), 4.44 (dd,  $J = 8.3$ , 5.6 Hz, 1H). **<sup>13</sup>C NMR** (75 MHz, CDCl<sub>3</sub>)  $\delta$  164.8, 161.5, 159.0, 134.0, 133.9, 117.8, 117.7, 116.1, 115.8, 85.1, 84.8, 70.4, 44.4. **<sup>19</sup>F NMR** (235 MHz, CDCl<sub>3</sub>)  $\delta$  -109.44. **HRMS** (ESI,  $m/z$ ) calcd for C<sub>11</sub>H<sub>8</sub>F<sub>1</sub>N<sub>1</sub>O<sub>2</sub>Na [M+Na]<sup>+</sup>: 228.04319, found: 228.0435.

## Compound 10s

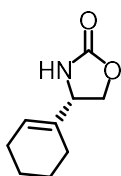


Starting from **9s** (67.8 mg, 0.20 mmol) according to the general procedure to provide **10s** as a white solid (30.4mg, 84% yield). Enantiomeric excess was established by HPLC analysis by using a Daicel Chiralpak ODH column, ee = 90% (HPLC: 205 nm, *n*-Hexane/isopropanol = 80:20, flow rate 1.0 mL/min, 25 °C,  $t_r$  (major) = 5.2 min,  $t_r$  (minor) = 6.3 min).  $[\alpha]_D^{22} = +3.6^\circ$  ( $c = 1.0$ , CH<sub>2</sub>Cl<sub>2</sub>). **<sup>1</sup>H NMR** (300 MHz, CDCl<sub>3</sub>)  $\delta$  5.86 (s, 1H), 4.64-4.46 (m, 2H), 4.27 (dd,  $J = 7.3, 5.0$  Hz, 1H), 2.17 (td,  $J = 7.1, 1.7$  Hz, 2H), 1.58-1.42 (m, 2H), 1.38-1.22 (m, 4H), 0.89 (dd,  $J = 8.2, 5.8$  Hz, 3H). **<sup>13</sup>C NMR** (75 MHz, CDCl<sub>3</sub>)  $\delta$  159.2, 867.0, 76.7, 70.8, 44.1, 31.2, 28.2, 22.3, 18.7, 14.1. **HRMS** (ESI,  $m/z$ ) calcd for C<sub>10</sub>H<sub>15</sub>N<sub>1</sub>O<sub>2</sub>Na [M+Na]<sup>+</sup>: 204.0995, found: 204.1000.

Compound (*E*)-10t

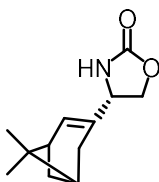
Starting from (*E*)-**9t** (69.4 mg, 0.20 mmol) according to the general procedure to provide **10t** as a white solid (33.3 mg, 88% yield). Enantiomeric excess was established by HPLC analysis by using a Daicel Chiralpak IC column, ee = 63% (HPLC: 210 nm, *n*-Hexane/isopropanol = 30:70, flow rate 1.0 mL/min, 25 °C,  $t_r$  (major) = 7.7 min,  $t_r$  (minor) = 15.2 min).  $[\alpha]_D^{22} = +91.6^\circ$  ( $c = 1.0$ , CH<sub>2</sub>Cl<sub>2</sub>). **<sup>1</sup>H NMR** (300 MHz, CDCl<sub>3</sub>)  $\delta$  7.43-7.27 (m, 5H), 6.61 (d,  $J = 15.8$  Hz, 1H), 6.13 (dd,  $J = 15.8, 7.6$  Hz, 1H), 5.75 (s, 1H), 4.67-4.49 (m, 2H), 4.22-4.05 (m, 1H). **<sup>13</sup>C NMR** (75 MHz, CDCl<sub>3</sub>)  $\delta$  159.6, 135.6, 134.1, 128.9, 128.7, 126.9, 126.6, 70.4, 55.3. **HRMS** (ESI,  $m/z$ ) calcd for C<sub>11</sub>H<sub>11</sub>NO<sub>2</sub>Na [M+Na]<sup>+</sup>: 212.0682, found: 212.0687.

## Compound 10u



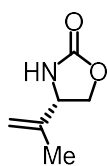
Starting from **9u** (65.0 mg, 0.20 mmol) according to the general procedure to provide **10u** as a white solid (32.0 mg, 96% yield). Enantiomeric excess was established by HPLC analysis as 92% ee (column: Daicel Chiralpak ODH 250 x 4.6 mm, absorption:  $\lambda = 220$  nm, mobile phase: *n*-Hexane/isopropanol = 80:20, flow rate: 1.0 mL/min, column temperature: 25 °C, retention times:  $t_r$  (major) = 6.0 min,  $t_r$  (minor) = 7.0 min).  $[\alpha]_D^{22} = +14.6^\circ$  ( $c = 1.0$ ,  $\text{CH}_2\text{Cl}_2$ ).  $^1\text{H NMR}$  (300 MHz,  $\text{CDCl}_3$ )  $\delta$  5.77 (s, 1H), 5.71 (s, 1H), 4.47 (t,  $J = 8.6$  Hz, 1H), 4.35-4.24 (m, 1H), 4.08 (dd,  $J = 8.4, 6.1$  Hz, 1H), 2.11-1.82 (m, 4H), 1.76-1.48 (m, 4H).  $^{13}\text{C NMR}$  (75 MHz,  $\text{CDCl}_3$ )  $\delta$  160.1, 135.2, 125.8, 69.5, 58.3, 25.1, 23.3, 22.4, 22.4. **HRMS** (ESI,  $m/z$ ) calcd for  $\text{C}_9\text{H}_{13}\text{N}_1\text{O}_2\text{Na}$   $[\text{M}+\text{Na}]^+$ : 190.0838, found: 190.0844.

## Compound 10v



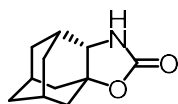
Starting from **9v** (73.0 mg, 0.20 mmol) according to the general procedure to provide **10v** as a white solid (35.9 mg, 87% yield). Enantiomeric excess was established by HPLC analysis as 96:4 d.r. (HPLC: column: Daicel Chiralpak ODH 250 x 4.6 mm, absorption:  $\lambda = 210$  nm, mobile phase: *n*-Hexane/isopropanol = 90:10, flow rate: 1.0 mL/min, column temperature: 25 °C, retention times:  $t_r$  (major) = 8.7 min,  $t_r$  (minor) = 10.1 min).  $[\alpha]_D^{22} = -48.8^\circ$  ( $c = 1.0$ ,  $\text{CH}_2\text{Cl}_2$ ).  $^1\text{H NMR}$  (300 MHz,  $\text{CDCl}_3$ )  $\delta$  5.54 (s, 2H), 4.39 (dt,  $J = 14.4, 8.8$  Hz, 2H), 3.95 (dd,  $J = 7.8, 5.6$  Hz, 1H), 2.53-2.00 (m, 5H), 1.31 (s, 3H), 1.15 (d,  $J = 8.7$  Hz, 1H), 0.80 (s, 3H).  $^{13}\text{C NMR}$  (75 MHz,  $\text{CDCl}_3$ )  $\delta$  159.9, 145.0, 122.1, 68.3, 56.8, 41.2, 40.9, 38.1, 31.8, 31.3, 26.2, 21.4. **HRMS** (ESI,  $m/z$ ) calcd for  $\text{C}_{12}\text{H}_{17}\text{N}_1\text{O}_2\text{Na}$   $[\text{M}+\text{Na}]^+$ : 230.1152, found: 230.1161.

## Compound 10w



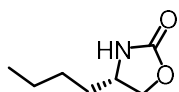
Starting from **9w** (57.0 mg, 0.20 mmol) according to the general procedure to provide **10w** as a white solid (20.1 mg, 79% yield). Enantiomeric excess was established by HPLC analysis as 61% ee (column: Daicel Chiralpak ODH 250 x 4.6 mm, absorption:  $\lambda = 210$  nm, mobile phase: *n*-Hexane/isopropanol = 90:10, flow rate: 1.0 mL/min, column temperature: 25 °C, retention times:  $t_r$  (major) = 10.8 min,  $t_r$  (minor) = 13.2 min).  $[\alpha]_D^{22} = +38.0^\circ$  ( $c = 1.0$ ,  $\text{CH}_2\text{Cl}_2$ ).  $^1\text{H NMR}$  (300 MHz,  $\text{CDCl}_3$ )  $\delta$  5.99 (s, 1H), 4.98 (d,  $J = 22.4$  Hz, 2H), 4.52 (t,  $J = 8.6$  Hz, 1H), 4.37 (dd,  $J = 8.8, 6.1$  Hz, 1H), 4.08 (dd,  $J = 8.4, 6.0$  Hz, 1H), 1.75 (s, 3H).  $^{13}\text{C NMR}$  (75 MHz,  $\text{CDCl}_3$ )  $\delta$  160.0, 142.5, 113.8, 77.6, 77.2, 76.8, 69.4, 57.8, 17.3. **HRMS** (ESI,  $m/z$ ) calcd for  $\text{C}_6\text{H}_9\text{N}_1\text{O}_2\text{Na}$   $[\text{M}+\text{Na}]^+$ : 150.0525, found: 150.0527.

## Compound 10x



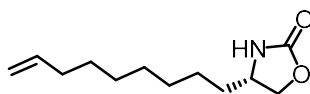
Starting from **9x** (70.2 mg, 0.20 mmol) according to the general procedure to provide **10x** as a white solid (38.2 mg, 99% yield). Enantiomeric excess was established by HPLC analysis using a Bz-protected product for the testament as 99% ee (HPLC: column: Daicel Chiralpak ODH 250 x 4.6 mm, absorption:  $\lambda = 210$  nm, mobile phase: *n*-Hexane/isopropanol = 80:20, flow rate: 1.0 mL/min, column temperature: 25 °C, retention times:  $t_r$  (major) = 8.1 min,  $t_r$  (minor) = 9.9 min).  $[\alpha]_D^{22} = +14.6^\circ$  ( $c = 1.0$ ,  $\text{CH}_2\text{Cl}_2$ ).  $^1\text{H NMR}$  (300 MHz,  $\text{CDCl}_3$ )  $\delta$  5.30 (d,  $J = 3.5$  Hz, 1H), 3.66 (d,  $J = 1.6$  Hz, 1H), 2.28 (s, 2H), 2.22-1.95 (m, 4H), 1.93-1.54 (m, 7H).  $^{13}\text{C NMR}$  (75 MHz,  $\text{CDCl}_3$ )  $\delta$  161.1, 80.7, 64.2, 40.2, 37.3, 36.5, 36.4, 31.4, 31.2, 29.4, 29.2. **HRMS** (ESI,  $m/z$ ) calcd for  $\text{C}_{11}\text{H}_{15}\text{NO}_2\text{Na}$   $[\text{M}+\text{Na}]^+$ : 216.0995, found: 216.1000.

## Compound 10y



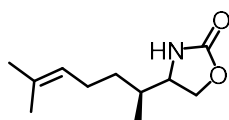
Starting from **9y** (53.0 mg, 0.20 mmol) according to the general procedure to provide **10y** as a colorless oil (15.0 mg, 53% yield). Enantiomeric excess was established by HPLC analysis using a Bz-protected product for the testament as 80% ee (HPLC: column: Daicel Chiralpak ODH 250 x 4.6 mm, absorption:  $\lambda = 210$  nm, mobile phase: *n*-Hexane/isopropanol = 80:20, flow rate: 1.0 mL/min, column temperature: 25 °C, retention times:  $t_r$  (major) = 11.5 min,  $t_r$  (minor) = 18.7 min).  $[\alpha]_D^{22} = -9.6^\circ$  ( $c = 1.0$ ,  $\text{CH}_2\text{Cl}_2$ ).  $^1\text{H NMR}$  (300 MHz,  $\text{CDCl}_3$ )  $\delta$  5.83 (s, 1H), 4.48 (t,  $J = 8.4$  Hz, 1H), 4.02 (dd,  $J = 8.4, 6.2$  Hz, 1H), 3.93-3.73 (m, 1H), 1.58 (dt,  $J = 12.4, 6.5$  Hz, 2H), 1.34 (tdd,  $J = 13.9, 9.4, 4.3$  Hz, 4H), 0.91 (t,  $J = 6.9$  Hz, 4H).  $^{13}\text{C NMR}$  (75 MHz,  $\text{CDCl}_3$ )  $\delta$  159.9, 70.5, 52.8, 35.2, 27.5, 22.6, 14.0. All other datas were in agreement with literature report.<sup>4</sup>

## Compound 10z



Starting from **9z** (53.0 mg, 0.20 mmol) according to the general procedure to provide **10z** as a colorless oil (17.3 mg, 41% yield). Enantiomeric excess was established by HPLC analysis using a Bz-protected product for the testament as 79% ee (column: Daicel Chiralpak ODH 250 x 4.6 mm, absorption:  $\lambda = 210$  nm, mobile phase: *n*-Hexane/isopropanol = 80:20, flow rate: 1.0 mL/min, column temperature: 25 °C, retention times:  $t_r$  (major) = 14.3 min,  $t_r$  (minor) = 19.9 min).  $[\alpha]_D^{22} = -11.2^\circ$  ( $c = 1.0$ ,  $\text{CH}_2\text{Cl}_2$ ).  $^1\text{H NMR}$  (300 MHz,  $\text{CDCl}_3$ )  $\delta$  5.92-5.62 (m, 2H), 5.07-4.85 (m, 2H), 4.48 (t,  $J = 8.4$  Hz, 1H), 4.01 (dd,  $J = 8.5, 6.2$  Hz, 1H), 3.90-3.77 (m, 1H), 2.04 (q,  $J = 6.8$  Hz, 2H), 1.59 (d,  $J = 14.7$  Hz, 2H), 1.44-1.17 (m, 12H).  $^{13}\text{C NMR}$  (75 MHz,  $\text{CDCl}_3$ )  $\delta$  159.9, 139.2, 114.5, 70.5, 52.8, 35.5, 33.9, 29.5, 29.4, 29.1, 29.0, 25.4. **HRMS** (ESI,  $m/z$ ) calcd for  $\text{C}_{12}\text{H}_{21}\text{N}_1\text{O}_2\text{Na}$   $[\text{M}+\text{Na}]^+$ : 234.1465, found: 234.1471.

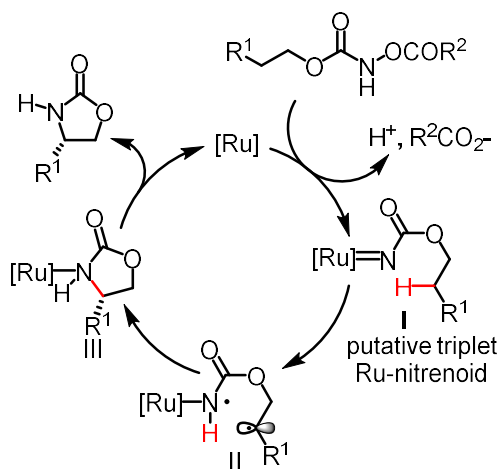
## Compound 10za



Starting from **9za** (71.0 mg, 0.20 mmol) according to the general procedure to provide **10za** as a colorless oil (7.1 mg, 18% yield). Diastereomeric ratio was determined by  $^1\text{H}$  NMR spectrum as > 20:1 d.r.  $^1\text{H}$  NMR (300 MHz,  $\text{CDCl}_3$ )  $\delta$  5.55 (s, 1H), 5.18-4.96 (m, 1H), 4.43 (t,  $J = 8.7$  Hz, 1H), 4.11 (dd,  $J = 8.7, 6.3$  Hz, 1H), 3.70 (dd,  $J = 14.9, 7.1$  Hz, 1H), 2.19-1.85 (m, 2H), 1.69 (s, 3H), 1.60 (s, 3H), 1.46-1.35 (m, 1H), 1.16 (dd,  $J = 8.9, 4.7$  Hz, 1H), 0.90 (d,  $J = 6.8$  Hz, 4H).  $^{13}\text{C}$  NMR (75 MHz,  $\text{CDCl}_3$ )  $\delta$  159.87, 132.58, 123.74, 68.31, 57.31, 37.00, 32.62, 25.88, 25.14, 17.89, 14.28. All other data were in agreement with literature report.

## 4.5.4 Mechanistic Experiments

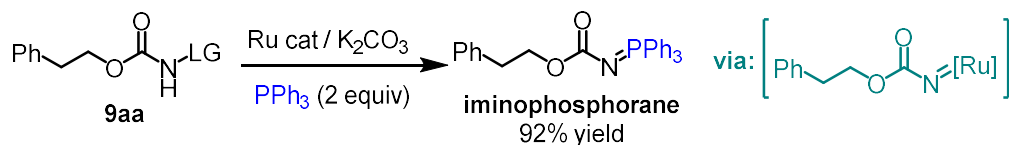
## 1) Proposed mechanism



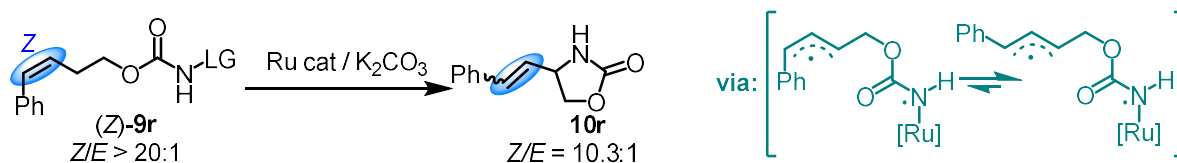
**Figure 92.** Proposed reaction pathway.

**Proposed mechanism:** Upon release of benzoic acid from the *N*-benzyloxycarbamate, the ruthenium catalyst forms a ruthenium nitrenoid intermediate (**I**). The ruthenium nitrenoid from its triplet state subsequently performs a 1,5-hydrogen atom transfer (HAT) to provide the radical intermediate **II**. This is followed by C-N bond formation through radical-radical recombination to provide the ruthenium-coordinated product (**III**), which is released to regenerate the active catalyst for a new catalytic cycle.

## 2) Mechanistic experiments

a) Nitrene trapping with PPh<sub>3</sub>

## b) Olefin isomerization



**Nitrene trapping with PPh<sub>3</sub>:** A dry Schlenk tube (10 mL) was charged with substrates (64.2 mg, 0.2 mmol), chiral ruthenium catalyst  $\Lambda$ -**Ru13** (0.004 mmol, 2.0 mol%), PPh<sub>3</sub> (105 mg, 0.4 mmol) and K<sub>2</sub>CO<sub>3</sub> (82.8 mg, 0.6 mmol) under an atmosphere of N<sub>2</sub>. Solvent 1,2-dichlorobenzene (4.0 mL) was added via syringe. The reaction mixture was stirred at 30 °C for 20 h under an atmosphere of N<sub>2</sub>. Afterwards, the mixture was transferred to a column and purified by flash chromatography on silica gel (EtOAc/*n*-Hexane = 1:3 to 1:1) to afford the analytical pure product **iminophosphorane** in 92% yield.

**Iminophosphorane:** colorless oil. <sup>1</sup>H NMR (300 MHz, CD<sub>3</sub>CN)  $\delta$  7.75-7.59 (m, 9H), 7.56-7.46 (m, 6H), 7.30-7.15 (m, 5H), 4.15 (t, *J* = 6.8 Hz, 2H), 2.84 (t, *J* = 6.8 Hz, 2H). <sup>13</sup>C NMR (75 MHz, CD<sub>3</sub>CN)  $\delta$  162.5, 140.2, 133.9, 133.7, 133.6, 133.5, 130.1, 129.89, 129.87, 129.7, 129.3, 128.7, 127.1, 66.6, 66.6, 36.4. HRMS (ESI, *m/z*) calcd for C<sub>27</sub>H<sub>24</sub>N<sub>1</sub>O<sub>2</sub>P<sub>1</sub>H<sub>1</sub> [M+H]<sup>+</sup>: 426.1617, found: 426.1628.

**Olefin isomerization:** A dry Schlenk tube (10 mL) was charged with substrates **(Z)-9b** (0.2 mmol),  $\Lambda$ -**Ru13** (0.002 mmol, 1 mol%) and K<sub>2</sub>CO<sub>3</sub> (82.8 mg, 0.6 mmol) under an atmosphere of N<sub>2</sub>. Solvent 1,2-dichlorobenzene (4.0 mL) was added via syringe. The reaction mixture was stirred at 30 °C for 20 h under an atmosphere of N<sub>2</sub>. Afterwards, the crude reaction solution was filtered through a thin layer of celite and washed with 5 mL EtOAc. Filtrate was collected and organic solvent was removed under vacuo. The ratio of **(Z)-10r** and **(E)-10r** was analyzed by <sup>1</sup>H NMR of crude reaction solutions (see attached spectrum). The ratio of **(Z)-10r**:(**E)-10r** are 10.3:1.



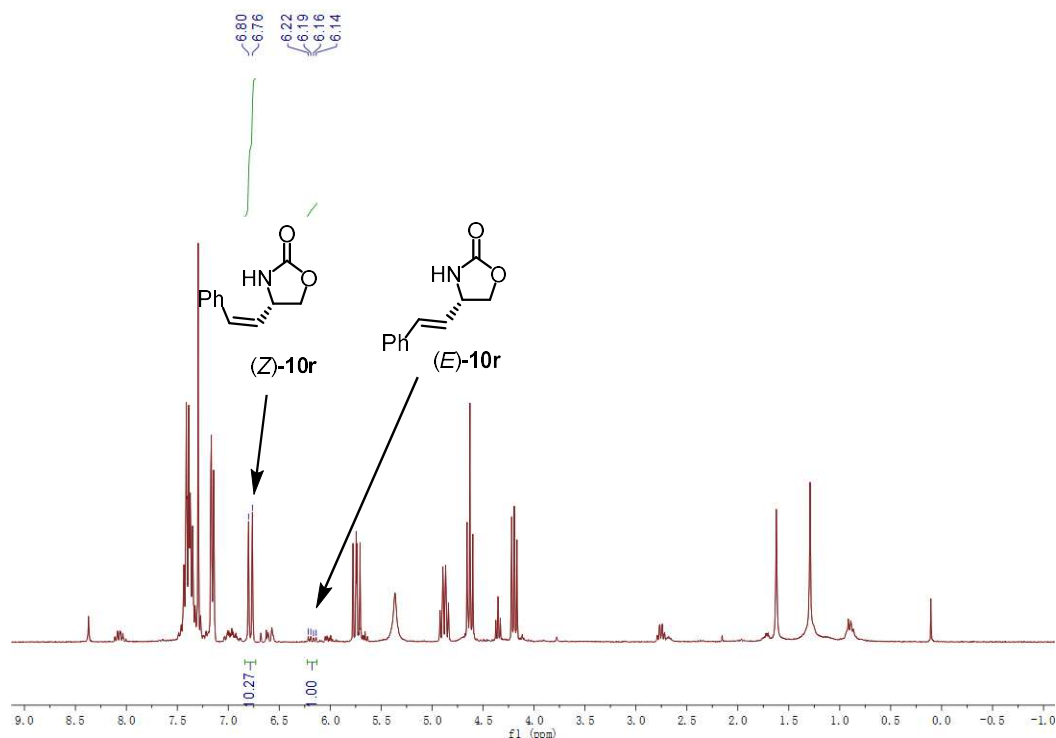
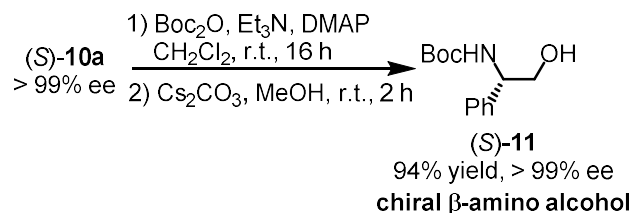


Figure 93. <sup>1</sup>H NMR of crude reaction solutions for analysis of *Z/E* ratio.

#### 4.5.5 Synthetic Applications

##### 1) Synthesis of chiral β-amino alcohols

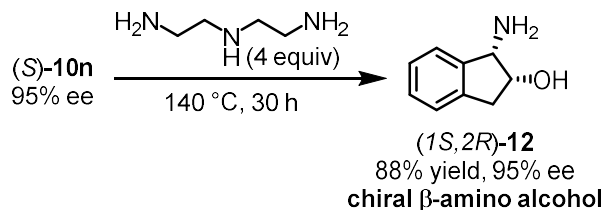
Method A:



**Procedure:** To a solution of (S)-10a (101 mg, 0.62 mmol) and Boc<sub>2</sub>O (214 mg, 0.98 mmol) in 16 mL THF was added Et<sub>3</sub>N (120 μL, 0.88 mmol). After stirring at room temperature for 10 min, DMAP (7.6 mg, 10 mol%) was added in one portion. The resulting solution was stirred at room temperature for 16 h. Solvent was removed in *vacuo*. The resulting solid dissolved in 6 mL MeOH was added Cs<sub>2</sub>CO<sub>3</sub> (20 mol%). The resulting solution was stirred at room temperature for 2 h. After that, citric acid was added until pH = 7. Solvent was removed in *vacuo*. The residue was subjected to a flash silica gel chromatography (*n*-Hexane/EtOAc = 5:1 to 2:1) to provide analytical pure (S)-11 in 94% yield. Enantiomeric excess was established by HPLC analysis by using a Daicel Chiralpak IG column, > 99% ee (HPLC: 210 nm, *n*-Hexane/isopropanol = 90:10, flow rate 1.0 mL/min, 25 °C, *t<sub>r</sub>* (major) = 12.1 min). <sup>1</sup>H NMR (300 MHz, CDCl<sub>3</sub>) δ 7.42-7.26 (m, 5H), 5.22 (d, *J* = 6.5 Hz, 1H), 4.77 (s, 1H),

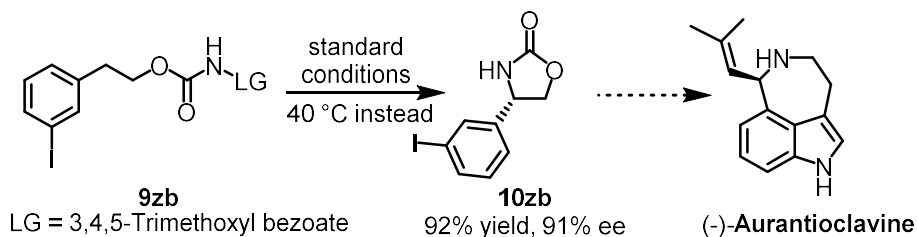
3.96-3.74 (m, 2H), 2.29 (s, 1H), 1.43 (s, 9H).  $^{13}\text{C}$  NMR (75 MHz,  $\text{CDCl}_3$ )  $\delta$  156.3, 139.7, 129.0, 128.0, 126.8, 80.2, 67.2, 57.2, 28.5.

Method B:



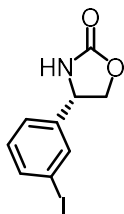
**Procedure:**  $(3S,8R)\text{-10n}$  (35 mg) in diethylenetriamine (86.4  $\mu\text{L}$ , 4 equiv) was heated at 140  $^\circ\text{C}$  for 30 h. Afterwards, it was directly subjected to a flash silica gel chromatography ( $\text{CH}_2\text{Cl}_2/\text{MeOH}/\text{Et}_3\text{N}=100:10:1$ ) to provide analytical pure  $(1S,2R)\text{-13}$  as light pink solid in 88% yield. Enantiomeric excess was determined by transforming back to corresponding carbamate as 95% ee.  $^1\text{H}$  NMR (300 MHz,  $\text{CDCl}_3$ )  $\delta$  7.42-7.18 (m, 4H), 4.52-4.23 (m, 2H), 3.12 (dd,  $J = 16.4, 5.4$  Hz, 1H), 2.97 (dd,  $J = 16.4, 2.7$  Hz, 1H), 2.81 (s, 3H).  $^{13}\text{C}$  NMR (75 MHz,  $\text{CDCl}_3$ )  $\delta$  144.1, 141.1, 128.2, 127.1, 125.6, 124.1, 72.9, 58.7, 39.6.

## 2) Synthesis of Natural Products



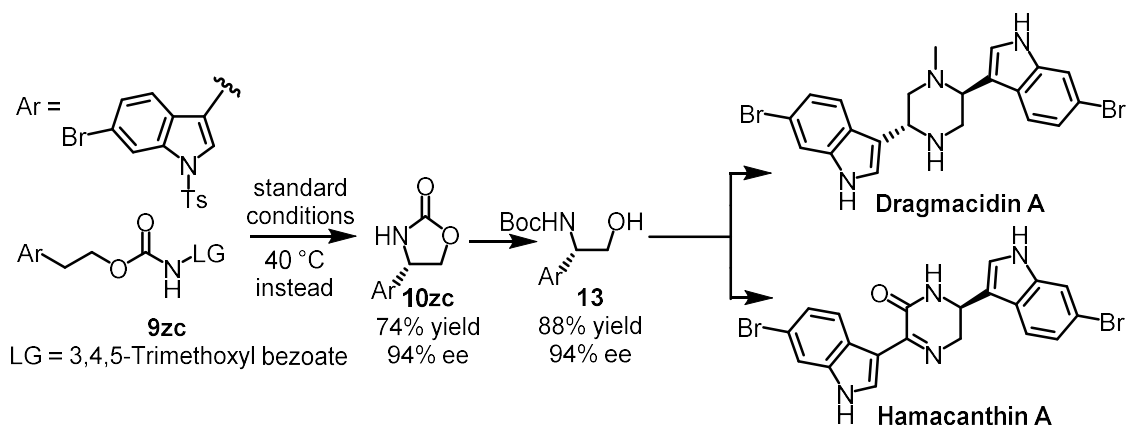
$(S)\text{-10zb}$  was synthesized according to the general procedure shown before.

### Compound 10zb



Starting from **9zb** (100.2 mg, 0.20 mmol) according to the general procedure to provide **10zb** as a white solid (53.0 mg, 92% yield). Enantiomeric excess was established by HPLC analysis by using a Daicel Chiralpak ODH column, 91% ee (HPLC: 220 nm,  $n$ -Hexane/isopropanol = 60:40, flow rate 1.0

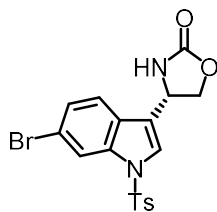
mL/min, 25 °C,  $t_r$  (major) = 13.7 min,  $t_r$  (minor) = 9.1 min).  $[\alpha]_D^{22} = +39.2^\circ$  ( $c = 1.0$ ,  $\text{CH}_2\text{Cl}_2$ ).  $^1\text{H NMR}$  (300 MHz,  $\text{CDCl}_3$ )  $\delta$  7.74-7.65 (m, 2H), 7.31 (d,  $J = 7.8$  Hz, 1H), 7.14 (t,  $J = 8.0$  Hz, 1H), 6.15 (s, 1H), 4.99-4.80 (m, 1H), 4.72 (t,  $J = 8.7$  Hz, 1H), 4.15 (dd,  $J = 8.6, 6.7$  Hz, 1H).  $^{13}\text{C NMR}$  (75 MHz,  $\text{CDCl}_3$ )  $\delta$  159.6, 142.0, 138.2, 135.3, 131.1, 125.4, 95.1, 72.4, 55.8. **HRMS** (ESI,  $m/z$ ) calcd for  $\text{C}_9\text{H}_8\text{I}_1\text{N}_1\text{O}_2\text{Na}$   $[\text{M}+\text{Na}]^+$ : 311.9492, found: 311.9503.



(*S*)-**10zc** was synthesized according to the general procedure shown before.

(*S*)-**13** was synthesized according to the general procedure shown before (Method A).

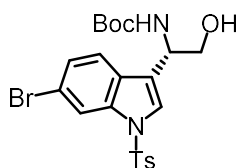
### Compound **10zc**



Starting from **9zc** (64.6 mg, 0.10 mmol) according to the general procedure to provide **10zc** as a white solid (32.1 mg, 74% yield). Enantiomeric excess was established by HPLC analysis by using a Daicel Chiralpak IA column, 94% ee (HPLC: 254 nm, *n*-Hexane/isopropanol = 85:15, flow rate 1.0 mL/min, 25 °C,  $t_r$  (major) = 17.4 min,  $t_r$  (minor) = 20.8 min).  $[\alpha]_D^{22} = +18.6^\circ$  ( $c = 1.0$ ,  $\text{CH}_2\text{Cl}_2$ ).  $^1\text{H NMR}$  (300 MHz,  $\text{CDCl}_3$ )  $\delta$  8.18 (s, 1H), 7.79 (d,  $J = 8.3$  Hz, 2H), 7.55 (s, 1H), 7.38 (s, 2H), 7.29 (d,  $J = 8.2$  Hz, 2H), 5.76 (s, 1H), 5.15 (dd,  $J = 8.6, 6.6$  Hz, 1H), 4.74 (t,  $J = 8.8$  Hz, 1H), 4.31 (dd,  $J = 8.6, 6.4$  Hz, 1H), 2.38 (s, 3H).  $^{13}\text{C NMR}$  (75 MHz,  $\text{CDCl}_3$ )  $\delta$  159.1, 146.0, 136.5, 134.9, 130.5, 127.3, 127.2, 126.4, 124.5, 120.7, 120.4, 119.6, 117.3, 70.4, 49.5, 21.8. **HRMS** (ESI,  $m/z$ ) calcd for  $\text{C}_{18}\text{H}_{16}\text{Br}_1\text{N}_2\text{O}_4\text{S}_1\text{H}_1$

[M+H]<sup>+</sup>: 435.0009 & 436.9989, found: 435.0017 & 436.9997.

### Compound 13



Starting from **10zc** (30.4 mg, 0.07 mmol) according to the general procedure to provide **13** as a white solid (31.2 mg, 88% yield). Enantiomeric excess was established by HPLC analysis by using a Daicel Chiralpak IA column, 94% ee (HPLC: 210 nm, *n*-Hexane/isopropanol = 85:15, flow rate 1.0 mL/min, 25 °C, *t<sub>r</sub>* (major) = 9.7 min, *t<sub>r</sub>* (minor) = 13.7 min).  $[\alpha]_D^{22} = +20.9^\circ$  (*c* = 1.0, CH<sub>2</sub>Cl<sub>2</sub>). <sup>1</sup>H NMR (300 MHz, CDCl<sub>3</sub>) δ 8.15 (d, *J* = 1.1 Hz, 1H), 7.75 (d, *J* = 8.3 Hz, 2H), 7.54 (s, 1H), 7.43 (d, *J* = 8.5 Hz, 1H), 7.35 (dd, *J* = 8.5, 1.6 Hz, 1H), 7.26 (t, *J* = 4.0 Hz, 3H), 5.07 (t, *J* = 14.2 Hz, 2H), 3.95 (s, 2H), 2.36 (s, 3H), 2.20 (s, 1H), 1.44 (s, 9H). <sup>13</sup>C NMR (75 MHz, CDCl<sub>3</sub>) δ 155.9, 145.6, 136.1, 135.1, 130.3, 128.2, 127.1, 127.0, 124.3, 121.2, 119.0, 117.0, 80.45, 65.1, 28.5, 21.8. HRMS (ESI, *m/z*) calcd for C<sub>22</sub>H<sub>25</sub>BrN<sub>2</sub>O<sub>5</sub>SiNa<sub>1</sub> [M+Na]<sup>+</sup>: 531.0560 & 533.0541, found: 531.0571 & 533.0550.

#### 4.5.6 Single Crystal X-Ray Diffraction Studies

Crystallography of compound (*S*)-**10i**: Single crystals of (*S*)-**10i** were obtained by slow diffusion from the solution in EtOAc layered with *n*-Hexane at room temperature. A suitable crystal of C<sub>9</sub>H<sub>8</sub>BrNO<sub>2</sub> was selected under inert oil and mounted using a MiTeGen loop. Intensity data of the crystal were recorded with a D8 Quest diffractometer (Bruker AXS). The instrument was operated with Mo-Kα radiation (0.71073 Å, microfocus source) and equipped with a PHOTON 100 detector. Evaluation, integration and reduction of the diffraction data was carried out using the Bruker APEX 3 software suite.<sup>1</sup> Multi-scan and numerical absorption corrections were applied using the SADABS program.<sup>2,3</sup> The structure was solved using dual-space methods (SHELXT-2014/5) and refined against *F*<sup>2</sup> (SHELXL-2018/3 using ShelXle interface).<sup>4-6</sup> All non-Hydrogen atoms were refined with anisotropic displacement parameters. The hydrogen atoms attached to carbon atoms were refined using the “riding model” approach with isotropic displacement parameters 1.2 times of that of the preceding carbon atom. The hydrogen atom at the nitrogen atom was refined using a restraint on the bond length to prevent too strong underestimation of the atom distance. CCDC 2012187 contains the supplementary crystallographic data for this paper. These data can be obtained free of charge from The Cambridge

Crystallographic Data Centre via [www.ccdc.cam.ac.uk/structures](http://www.ccdc.cam.ac.uk/structures).

**Table 10.** Selected crystallographic data and details of the structure determination for C<sub>9</sub>H<sub>8</sub>BrNO<sub>2</sub>.

Identification code	( <i>S</i> )- <b>10i</b>
Empirical formula	C <sub>9</sub> H <sub>8</sub> BrNO <sub>2</sub>
Molar mass / g·mol <sup>-1</sup>	242.07
Space group (No.)	<i>P</i> 2 <sub>1</sub> 2 <sub>1</sub> 2 <sub>1</sub> (19)
<i>a</i> / Å	5.6166(3)
<i>b</i> / Å	7.7164(4)
<i>c</i> / Å	21.6106(11)
<i>V</i> / Å <sup>3</sup>	936.60(8)
<i>Z</i>	4
$\rho_{calc.}$ / g·cm <sup>-3</sup>	1.717
$\mu$ / mm <sup>-1</sup>	4.353
Color	colorless
Crystal habitus	block
Crystal size / mm <sup>3</sup>	0.265 x 0.239 x 0.168
<i>T</i> / K	100
$\lambda$ / Å	0.71073 (Mo-K $\alpha$ )
$\theta$ range / °	2.803 to 31.638
Range of Miller indices	-8 ≤ <i>h</i> ≤ 8 -11 ≤ <i>k</i> ≤ 11 -31 ≤ <i>l</i> ≤ 31
Absorption correction	multi-scan and numerical
<i>T</i> <sub>min</sub> , <i>T</i> <sub>max</sub>	0.4622, 0.5826
<i>R</i> <sub>int</sub> , <i>R</i> <sub><math>\sigma</math></sub>	0.0210, 0.0160
Completeness of the data set	0.999
No. of measured reflections	17155
No. of independent reflections	3139
No. of parameters	123
No. of restraints	1
<i>S</i> (all data)	1.091
<i>R</i> ( <i>F</i> ) ( <i>I</i> ≥ 2σ( <i>I</i> ), all data)	0.0171, 0.0188
<i>wR</i> ( <i>F</i> <sup>2</sup> ) ( <i>I</i> ≥ 2σ( <i>I</i> ), all data)	0.0405, 0.0412
Extinction coefficient	0.0127(10)
Flack parameter <i>x</i>	-0.006(3)
$\Delta\rho_{max}$ , $\Delta\rho_{min}$ / e·Å <sup>-3</sup>	0.336, -0.238

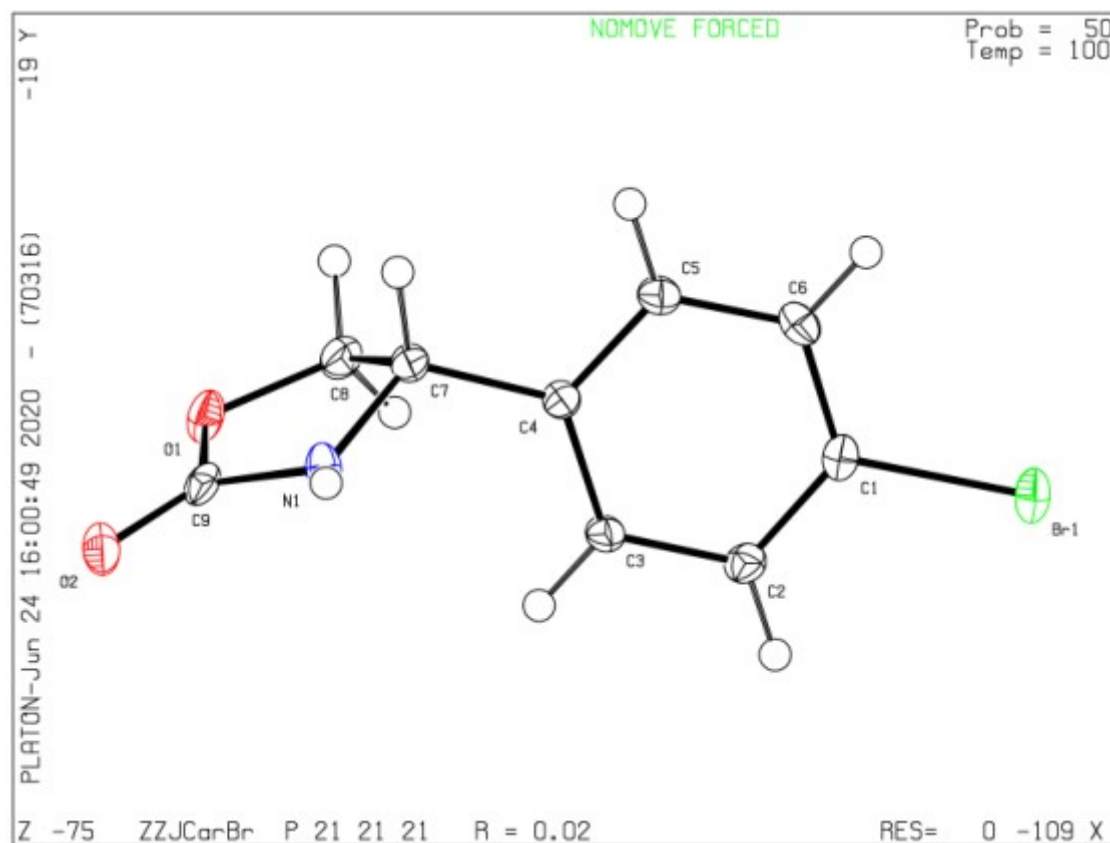


Figure 94. Crystal structure of compound (S)-10i.

## References

1. APEX3, Bruker AXS Inc., Madison, Wisconsin, USA, 2018.
2. SADABS, Bruker AXS Inc., Madison, Wisconsin, USA, 2016.
3. L. Krause, R. Herbst-Irmer, G. M. Sheldrick, D. Stalke, *J. Appl. Crystallogr.* **2015**, *48*, 3.
4. G. M. Sheldrick, *Acta Crystallogr., Sect. A: Found. Adv.* **2015**, *71*, 3.
5. G. M. Sheldrick, *Acta Crystallogr., Sect. C: Struct. Chem.* **2015**, *71*, 3.
6. C. B. Hübschle, G. M. Sheldrick, B. Dittrich, *J. Appl. Crystallogr.* **2011**, *44*, 1281.
7. A. L. Spek, *PLATON - A Multipurpose Crystallographic Tool*, Utrecht University, Utrecht, The Netherlands, 2019.

## Chapter 5: Appendices

### 5.1 List of Abbreviations

$^1\text{H}$ NMR	proton nuclear magnetic resonance spectroscopy
$^{13}\text{C}$ NMR	carbon nuclear magnetic resonance spectroscopy
$^9\text{F}$ NMR	fluorine nuclear magnetic resonance spectroscopy
$\delta$	chemical shift
J	coupling constant
br	broad
s	singlet
d	doublet
t	triplet
q	quartet
m	multiplet
ppm	parts per million
AcOH	acetic acid
aq	aqueous
Ar	Aryl-group
bpy	2,2'-bipyridine
CD	circular dichroism
$\text{CH}_2\text{Cl}_2/\text{DCM}$	dichloromethane
$\text{CD}_2\text{Cl}_2$	dideuteromethylenechloride
$\text{CHCl}_3$	chloroform
$\text{CDCl}_3$	deuteriochloroform
$\text{CH}_3\text{CN}/\text{MeCN}$	acetonitrile
conc	concentrated
DMAP	4-dimethylaminopyridine
DMF	dimethylformamide
DMSO	dimethyl sulfoxide
dr	diastereomeric ratio

## Chapter 5. Appendices

---

ee	enantiomeric excesses
et al.	et alii (lat.: and others)
EtOH	ethanol
Et <sub>2</sub> O	diethyl ether
Et <sub>3</sub> N	triethyl amine
EtOAc	ethyl acetate
EDG	electron donating group
EWG	electron withdrawing group
HAT	hydrogen atom transfer
h	hour(s)
HPLC	high performance liquid chromatography
HRMS	high resolution mass spectrometry
IR spectra	infrared spectra
Ir	iridium
Rh	rhodium
Ru	ruthenium
Fe	iron
Ag	silver
Mn	manganese
L	liter(s)
M	mol/liter
<i>m</i>	meta-
min	minute(s)
mL	milliliter(s)
mmol	millimole
MS	mass spectroscopy
N <sub>2</sub>	nitrogen
Ph	phenyl
PPh <sub>3</sub>	triphenylphosphine
ppm	parts per million



## Chapter 5. Appendices

---

<i>rac</i>	racemate
rt	room temperature
TFA	trifluoroacetic acid
THF	tetrahydrofuran
TLC	thin layer chromatography

## 5.2 List of Figures

<b>Figure 1.</b> General concept of asymmetric C–H amination via nitrene insertion. ....	1
<b>Figure 2.</b> Mechanism of intramolecular C–H amination via metal-nitrenoid intermediate.....	2
<b>Figure 3.</b> Ring-open of chiral cyclic sulfamidates.....	2
<b>Figure 4.</b> Research from the Chi-Ming Che group on the synthesis of chiral cyclic sulfamidates. ....	3
<b>Figure 5.</b> Research from the Simon Blakey group on the synthesis of chiral cyclic sulfamidates.....	3
<b>Figure 6.</b> Research from the Du Bois group on the synthesis of chiral cyclic sulfamidates. ....	4
<b>Figure 7.</b> Ring-open of chiral cyclic sulfamidates.....	4
<b>Figure 8.</b> Research from the Katsuki group on the synthesis of chiral cyclic sulfamides. ....	5
<b>Figure 9.</b> Research from the X. Peter Zhang group on the synthesis of 6-membered chiral cyclic sulfamides.....	6
<b>Figure 10.</b> Research from the X. Peter Zhang group on the synthesis of 5-membered chiral cyclic sulfamides.....	6
<b>Figure 11.</b> Research from the F. H. Arnold group on the synthesis of 5- and 6-membered chiral cyclic sulfamides.....	7
<b>Figure 12.</b> Research from the Meggers group on the synthesis of 5- and 6-membered chiral cyclic sulfamides.....	7
<b>Figure 13.</b> Synthesis of chiral sulfonamides via nitrene insertion.....	8
<b>Figure 14.</b> Research from the Davies group on the synthesis of chiral cyclic carbamates.....	9
<b>Figure 15.</b> Synthesis of chiral lactams via nitrene insertion.....	10
<b>Figure 16.</b> Synthesis of cyclic ureas in a racemic version from the Bois group.....	11
<b>Figure 17.</b> Nitrenes with different substituents. ....	11
<b>Figure 18.</b> Research work on the synthesis of the chiral Boc-protected pyrrolidine.....	12
<b>Figure 19.</b> Comparison of intra- and intermolecular C-H amination for the synthesis of chiral amines. ....	12
<b>Figure 20.</b> Pioneering work on intermolecular C-H amination of indane substrate.....	13
<b>Figure 21.</b> Intermolecular C-H amination work from the Davies group. ....	14
<b>Figure 22.</b> Intermolecular C-H amination work from the Dauban group.....	14
<b>Figure 23.</b> Intermolecular C-H amination work from the Bach group.....	15

Figure 24. Intermolecular C-H amination work from the Matsunaga group.....	15
Figure 25. Intermolecular C-H amination work from the Blakey group.....	16
Figure 26. Intermolecular C-H amination work from the Chi-Ming Che group.....	16
Figure 27. Intermolecular C-H amination work from the Katsuki group.....	17
Figure 28. Other transition-metals catalyzed asymmetric intermolecular C-H aminations. ....	18
Figure 29. Chiral-at-metal ruthenium catalysts for asymmetric alkynylation reactions. ....	19
Figure 30. Pioneering work on ruthenium catalyzed intramolecular C-H amination using aliphatic organic azides as nitrene precursors by the former group member Jie Qin.....	22
Figure 31. Attempts on the synthesis of different racemic ruthenium catalysts based on modifications of the pyridine moiety. [a] Yu Zheng's reported results. [b] Jie Qin's reported results. ....	23
Figure 32. Chiral-auxiliary-mediated synthesis of enantiomerically pure $\Lambda$ - <b>RuAux1-7</b> . [a] Yu Zheng's reported results. [b] Jie Qin's reported results.....	24
Figure 33. CD spectra of $\Lambda$ - <b>Ru7</b> recorded in CH <sub>3</sub> OH (0.2 mM). ....	24
Figure 34. Substrate scope. <sup>[a]</sup> $\Lambda$ -Ru5 as the catalyst instead. <sup>[b]</sup> Reaction temperature of 95 °C instead. ....	27
Figure 35. Synthesis of tri- and tetracyclic structures. <sup>[a]</sup> Reaction temperature of 105 °C for 60 h instead. ....	27
Figure 36. Proposed mechanism and DFT free energies (in kcal/mol) calculated with R <sup>1</sup> = R <sup>2</sup> = Ph at the M06-D3/6-311++G(d,p)-SDD, SMD (1,2-dichlorobenzene)//B3LYP-D3/6-31G(d)-LANL2DZ level of theory. These DFT calculations were performed by Dr. Shuming Chen (Houk group, UCLA).. ....	28
Figure 37. Mechanistic experiments. ....	30
Figure 38. Calculated transition state structures for the C–H insertion step at the M06-D3/6-311++G(d,p)-SDD, SMD (1,2-dichlorobenzene)//B3LYP-D3/6-31G(d)-LANL2DZ level of theory. Energies are shown in kcal/mol. Interatomic distances are denoted in Ångströms. Calculations performed by Dr. Shuming Chen (Houk group, UCLA).....	31
Figure 39. Yubiao Hong's pioneering exploration of new ruthenium complexes. ....	33
Figure 39. Main difference between previous ruthenium scaffold and the new one.....	34
Figure 40. Intramolecular C-H amidation catalyzed by electron rich iridium complex from Chang's group.....	34
Figure 41. Idea of applying our new ruthenium catalysts scaffold in asymmetric intramolecular C-H	

amidation reactions.....	34
Figure 42. My modified synthetic routes of the ruthenium complexes.....	35
Figure 43. Comparison of catalytic results by using different ruthenium catalysts. ....	36
Figure 44. New results by performing the reaction using NH <sub>4</sub> PF <sub>6</sub> as source of acid in 100 °C.....	37
Figure 45. New results by performing the reaction using NH <sub>4</sub> BF <sub>4</sub> as source of acid in different conditions. X = PF <sub>6</sub> or BF <sub>4</sub> .....	37
Figure 46. New results by performing the reaction using NH <sub>4</sub> BF <sub>4</sub> as source of acid in different conditions. X = PF <sub>6</sub> or BF <sub>4</sub> . water acetonitrile solvent mixture and further modification of catalyst...	38
Figure 47. Substrate scope.....	40
Figure 48. Gram-scale reaction with low catalyst loading and further transformations. (a) Gram-scale synthesis of ( <i>S</i> )- <b>4e</b> and ( <i>S</i> )- <b>4i</b> . (b) Synthetic applications of ( <i>S</i> )- <b>4i</b> .....	42
Figure 49. Proposed mechanism. Dr. Shuming Chen from the Houk group at UCLA performed the DFT calculations.....	43
Figure 50. Control experiments for elucidating the mechanism. ....	44
Figure 51. Calculated structures of ruthenium nitrene complexes at the B3LYP-D3/6-31G(d)–LANL2DZ (Ru) level of theory. Interatomic distances are in Ångströms (Å). Bolded numbers in orange indicate hirshfeld charges on individual atoms. Calculations performed by Dr. Shuming Chen (Houk group, UCLA). ....	45
Figure 52. Calculated C–H amidation and Curtius rearrangement transition states at the M06-D3/6-311++G(d,p)–SDD (Ru), SMD (1,2-dichlorobenzene) // B3LYP-D3/6-31G(d)–LANL2DZ (Ru) level of theory. Interatomic distances are in ångströms (Å). Energies are in kcal/mol. Activation barriers are calculated with respect to the lowest-energy conformers of Ru nitrene intermediate <b>III</b> . Calculations performed by Dr. Shuming Chen (Houk group, UCLA).....	46
Figure 53. Calculated C–H amidation transition states leading to major and minor lactam enantiomers. at the M06-D3/6-311++G(d,p)–SDD (Ru), SMD (1,2-dichlorobenzene) // B3LYP-D3/6-31G(d)–LANL2DZ (Ru) level of theory. Interatomic distances are in ångströms (Å). Energies are in kcal/mol. Activation barriers are calculated with respect to the lowest-energy conformer of Ru nitrene intermediate <b>III</b> . Calculations performed by Dr. Shuming Chen (Houk group, UCLA).	47
Figure 54 . Enantioselective intramolecular amination of prochiral C(sp <sup>3</sup> )-H bonds. (a) Chiral heterocycles accessible by this strategy. (b) Reaction design. ....	49

Figure 55. (a) Initial try for the synthesis of cyclic ureas via intramolecular C-H amination. (b) Yuqi Tan's pioneering exploration of using <i>N</i> -benzyloxycarbamate as nitrene precursor for intramolecular nitrene transfer reactions. (c) My idea of reaction design for the synthesis of chiral cyclic ureas.....	50
Figure 56. Scope with respect to synthesis of <i>N</i> -methyl cyclic ureas. <sup>a</sup> $\Lambda$ - <b>Ru6</b> was used as the catalyst instead.....	53
Figure 57. Substrate scope. Products <b>7p-r</b> formed with regioisomeric ratios of more than 20:1. <sup>a</sup> 40 h reaction time. <sup>b</sup> 16 hour reaction time. ....	53
Figure 58. Proposed mechanism through an intermediate triplet ruthenium nitrenoid. ....	55
Figure 59. Control experiments to probe the proposed radical mechanism. ....	55
Figure 60. Applications to the synthesis of medicinal agents, natural products, and a chiral organocatalyst. <sup>a</sup> Standard conditions followed by recrystallization in EtOAc/ <i>n</i> -hexane. MW = microwave. ....	57
Figure 61. (a) Overview of representative methods for the synthesis of chiral $\beta$ -amino alcohol; (b) Strategy to chiral $\beta$ -amino alcohols via transition-metal nitrenoid intermediates; (c) Preliminary result obtained by the previous group member Y. Tan; (d) My improved results. ....	61
Figure 62. Attempts on the synthesis of <i>rac</i> - <b>Ru13</b> based on modification of the NHC moiety.....	62
Figure 63. Chiral-auxiliary-mediated synthesis of enantiomerically pure $\Lambda$ - <b>Ru13</b> . ....	62
Figure 64. Substrate scope with respect to benzylic C-H aminations. Ar = 2,4-difluorophenyl unless noted otherwise. <sup>a</sup> Modified substrate and reaction conditions: Ar = 3,4,5-trimethoxyphenyl and reacted at 40 °C for 20 h. ....	65
Figure 65. Substrate scope with respect to non-benzylic C-H aminations. Ar = 2,4-difluorophenyl unless noted otherwise. <sup>a</sup> Ar = Ph.....	67
Figure 66. Gram-scale reaction and ring opening of chiral cyclic carbamates. ....	68
Figure 67. Synthetic application to natural products.....	69
Figure 68. An overview for this thesis. ....	71
Figure 69. Catalytic enantioselective intramolecular C-H amination of 2-azidoacetamides. ....	72
Figure 70. Enantioselective synthesis of $\gamma$ -lactams by intramolecular C-H amidation.....	73
Figure 71. Enantioselective synthesis of cyclic ureas by intramolecular C-H amidation. ....	73
Figure 72. Enantioselective synthesis of cyclic carbamates by intramolecular C-H amidation.....	74
Figure 73. Synthesis of new chiral <i>N</i> -heterocycles via asymmetric intramolecular C-H amiations. ..	75

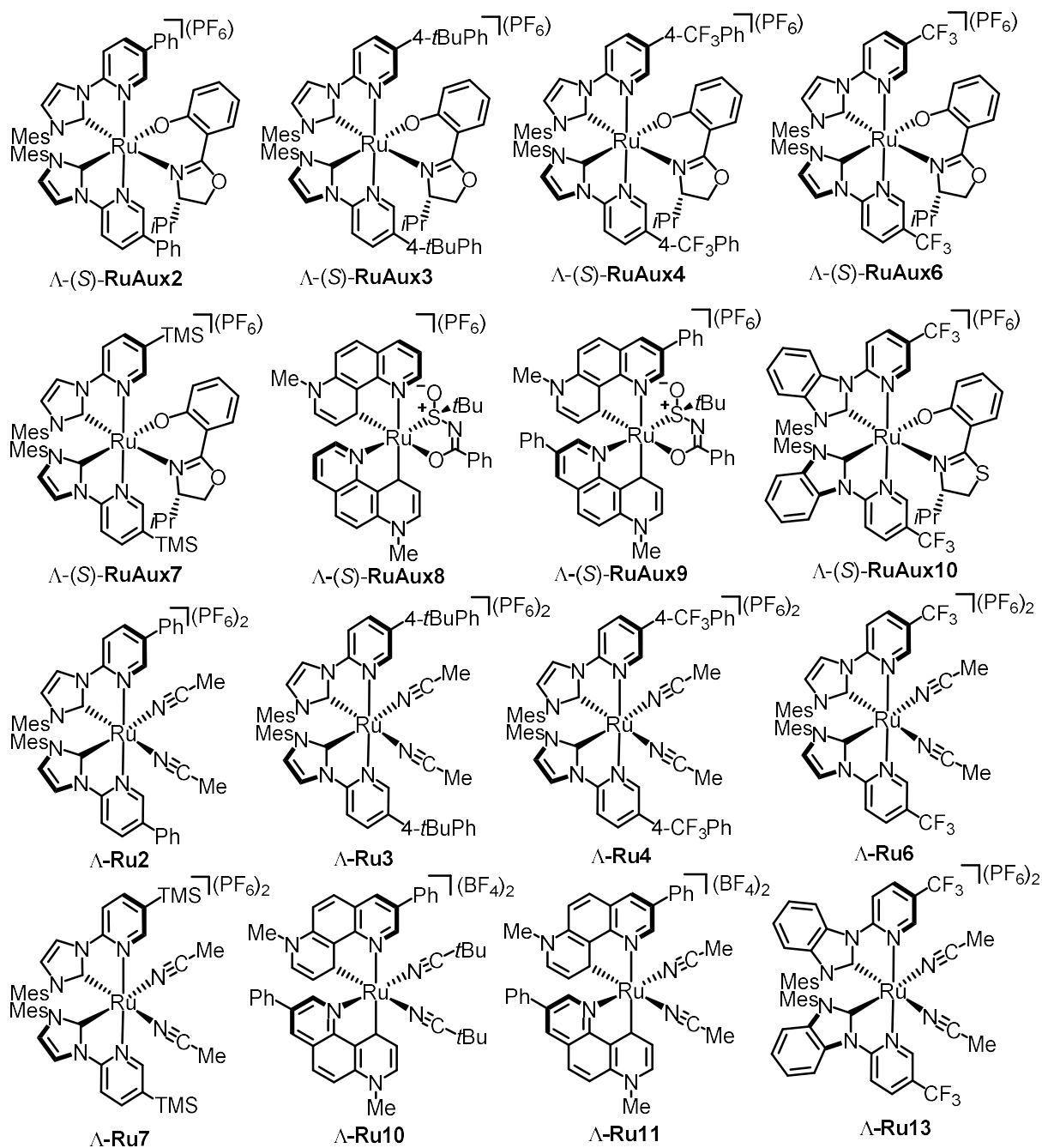
Figure 74. <sup>1</sup> H NMR of <b>2a-d2-1</b> reaction analysis.....	108
Figure 75. <sup>1</sup> H NMR of <b>2a-d2-2</b> reaction analysis.....	109
Figure 76. <sup>1</sup> H NMR of <b>1a</b> and <b>1a-d4</b> reaction analysis. ....	110
Figure 77. <sup>1</sup> H NMR of competition experiment analysis. ....	111
Figure 78. Crystal structure of compound ( <i>S</i> )- <b>2e</b> . ....	113
Figure 79. Crystal structure of compound <i>rac</i> - <b>Ruimine</b> .....	113
Figure 80. Initial rate of <b>4a</b> and <b>4a-d<sub>2</sub>-1</b> formation under the above reaction conditions. ....	141
Figure 81. <sup>1</sup> H NMR spectra for the analysis of KIE value. ....	142
Figure 82. <sup>1</sup> H NMR spectra for the analysis of KIE value.....	143
Figure 83. HPLC spectrums of <i>rac</i> - <b>4a-Me</b> and ( <i>S</i> )- <b>4a-Me</b> obtained by using $\Lambda$ - <b>Ru10</b> .....	144
Figure 84. HPLC spectrum of ( <i>S</i> )- <b>4a-Me</b> obtained by using $\Delta$ - <b>Ru10</b> .....	145
Figure 85. Crystal structure of ( <i>S</i> )- <b>10e</b> . ....	147
Figure 86. <sup>1</sup> H NMR spectrum analysis of the kinetic isotope experiment. ....	173
Figure 87. <sup>1</sup> H NMR spectrum analysis of crude reaction solution (at room temperature).....	174
Figure 88. <sup>1</sup> H NMR spectrum analysis of crude reaction solution (at 4 °C). ....	175
Figure 89. <sup>1</sup> H NMR spectrum analysis of crude reaction solution (at 40 °C). ....	175
Figure 90. Reaction set up in the microwave reactor. ....	180
Figure 91. X-ray structure analysis of compound ( <i>S</i> )- <b>7h</b> . ....	182
Figure 92. Proposed reaction pathway.....	213
Figure 93. <sup>1</sup> H NMR of crude reaction solutions for analysis of <i>Z/E</i> ratio. ....	215
Figure 94. Crystal structure of compound ( <i>S</i> )- <b>16i</b> .....	220

## 5.3 List of Tables

<b>Table 1.</b> Reaction Conditions Optimization <sup>a</sup> .....	25
<b>Table 2.</b> Comparison of different ruthenium catalysts <sup>a</sup> .....	39
<b>Table 3.</b> Evaluation of the C–H amination reaction <sup>a</sup> .....	51
<b>Table 4.</b> Initial experiments and optimization <sup>a</sup> .....	64
<b>Table 5.</b> Crystal data and structure refinement for ( <i>S</i> )- <b>7e</b> . .....	114
<b>Table 6.</b> Crystal data and structure refinement for <i>rac</i> - <b>Ruimine</b> . .....	116
<b>Table 7.</b> Crystal data and structure refinement for ( <i>S</i> )- <b>10e</b> . .....	147
<b>Table 8.</b> Selected crystallographic data and details of the structure determination for ( <i>S</i> )- <b>13h</b> . .....	182
<b>Table 9.</b> Additional screening of different leaving groups <sup>a</sup> . .....	199
<b>Table 10.</b> Selected crystallographic data and details of the structure determination for C <sub>9</sub> H <sub>8</sub> BrNO <sub>2</sub> . .....	219

## 5.4 List of New Compounds

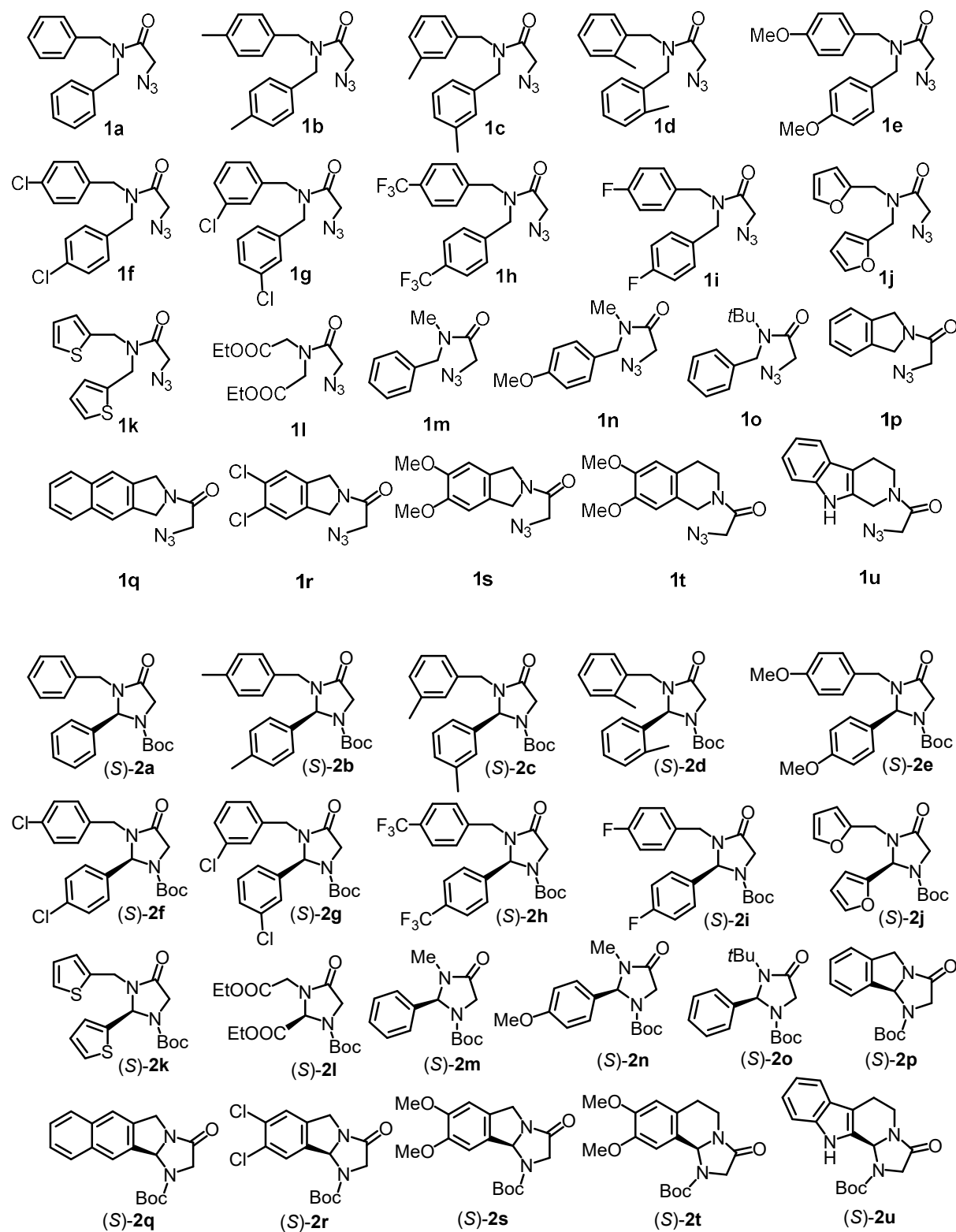
## 1) New Ruthenium Complexes:



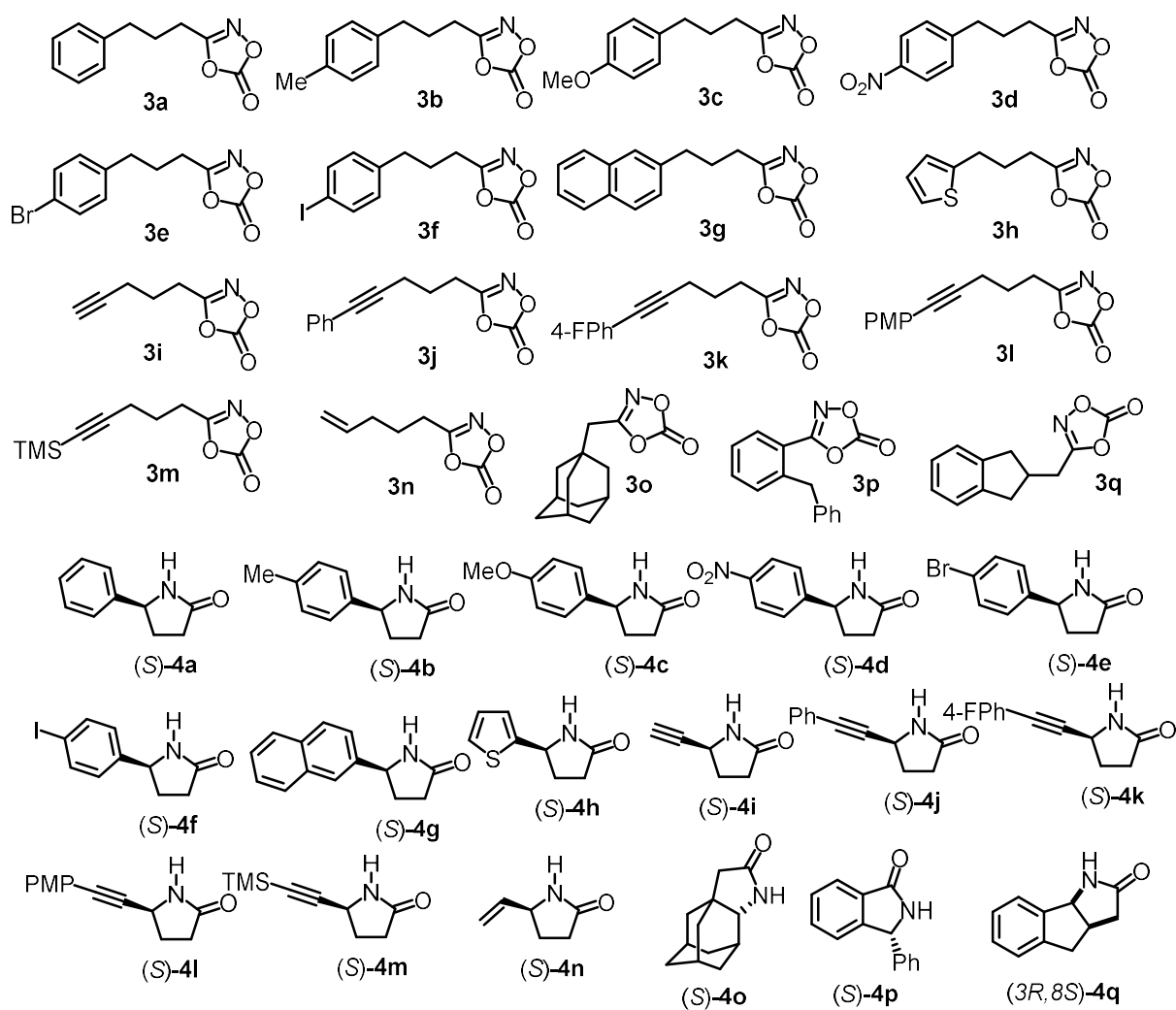


## 2) New Organic Compounds

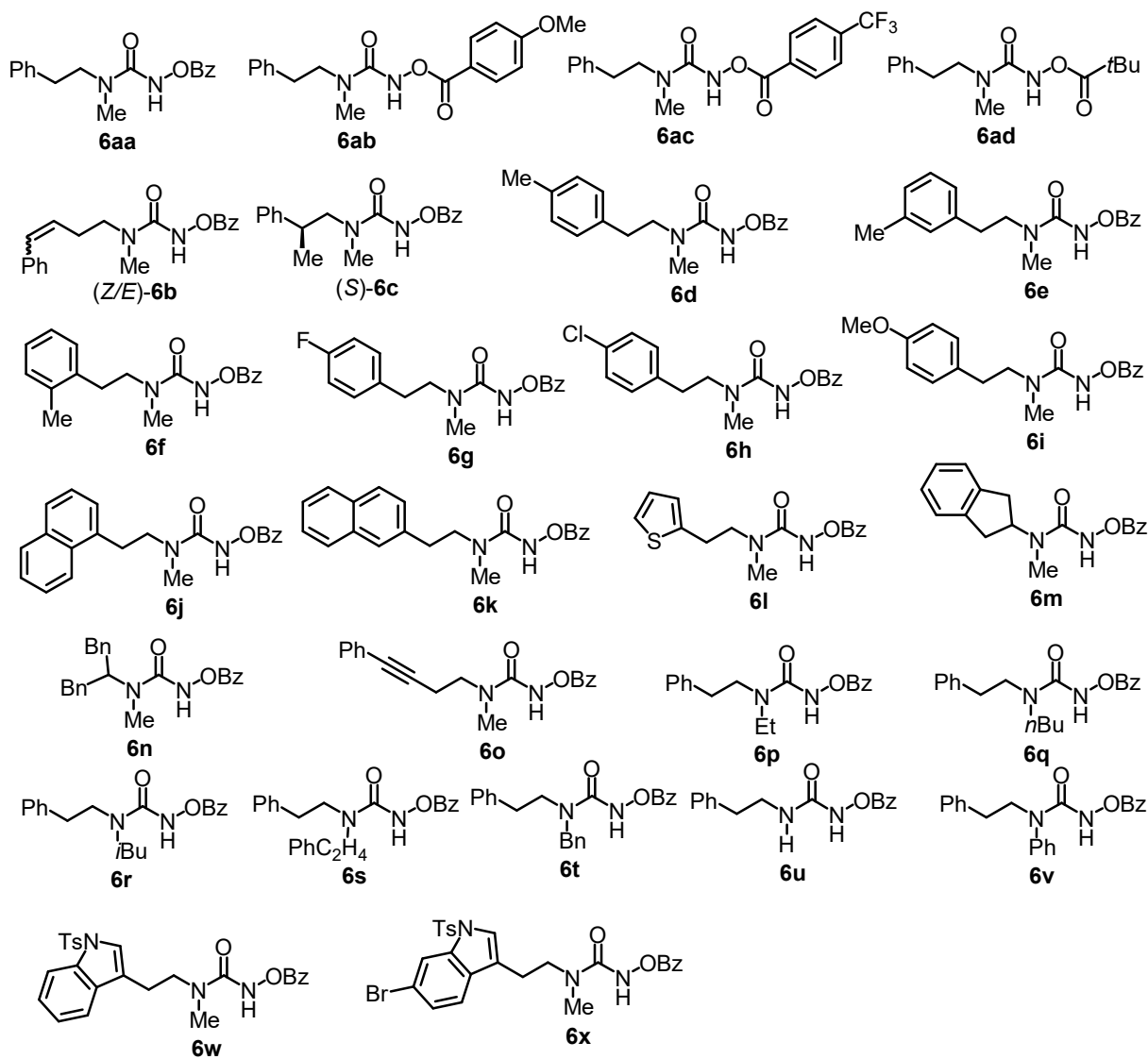
## Chapter 2.1 and its Experimental Part

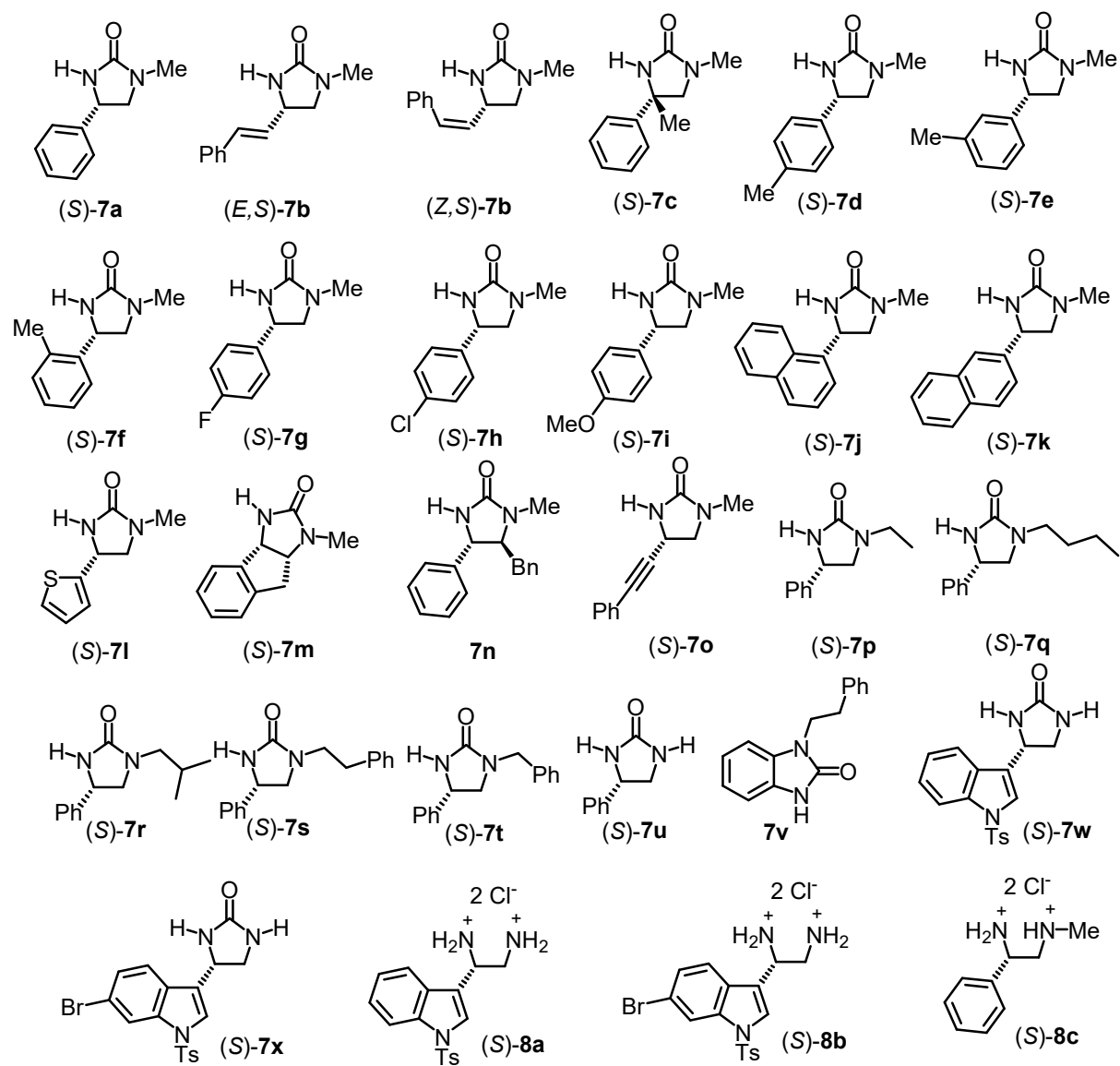


## Chapter 2.2 and its Experimental Part

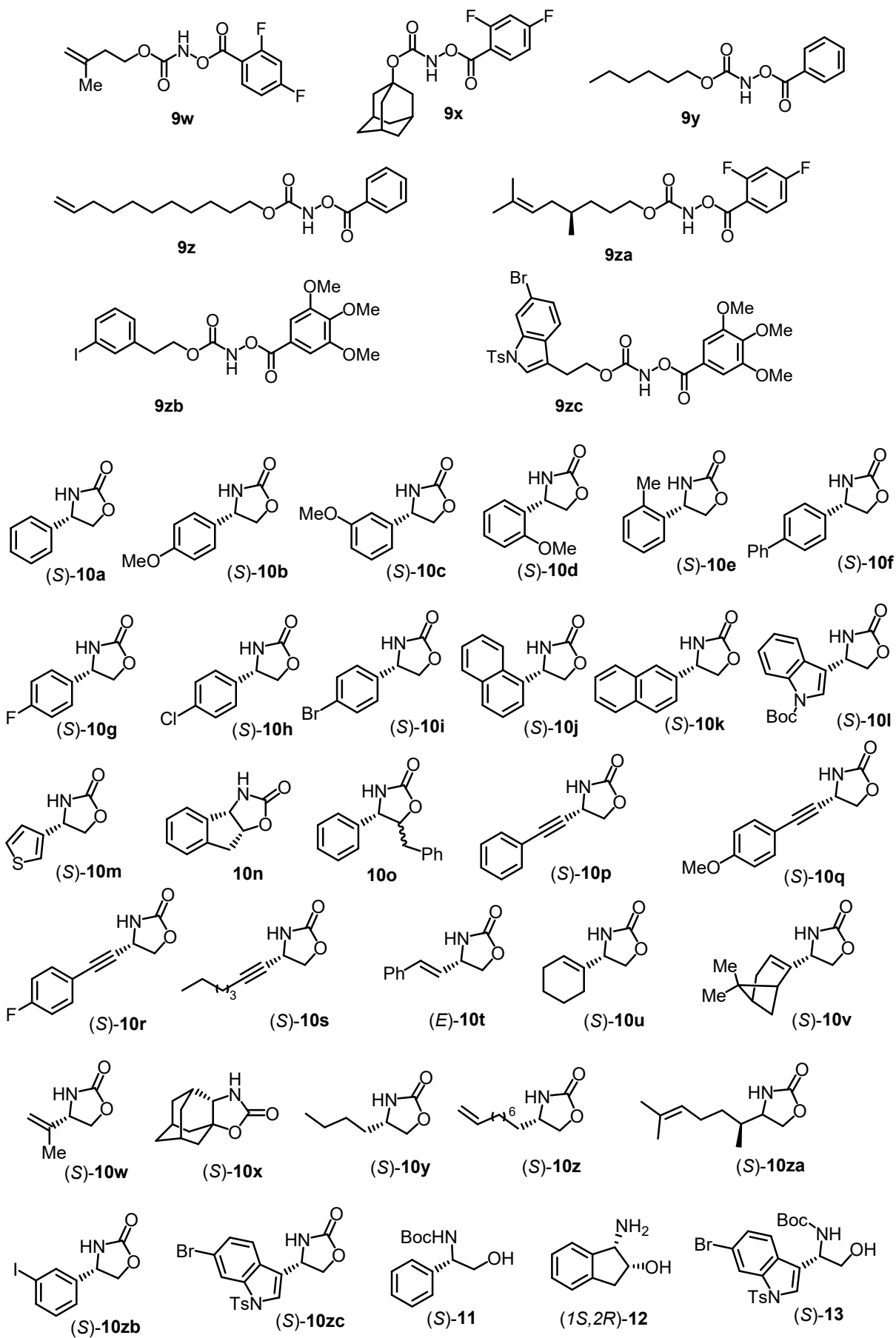


## Chapter 2.3 and its Experimental Part









## **Statement**

gemäß § 10, Abs. 1 der Promotionsordnung der mathematisch-naturwissenschaftlichen Fachbereiche und des Medizinischen Fachbereichs für seine mathematisch-naturwissenschaftlichen Fächer der Philipps-Universität Marburg vom 15.Oct.2020

Ich erkläre, dass eine Promotion noch an keiner anderen Hochschule als der Philipps-Universität Marburg, Fachbereich Chemie, versucht wurde und versichere, dass ich meine vorgelegte Dissertation

### **Asymmetric Intramolecular C–H Aminations with Chiral-at-Ruthenium Complexes**

selbst und ohne fremde Hilfe verfasst, nicht andere als die in ihr angegebenen Quellen oder Hilfsmittel benutz, alle vollständig oder sinngemäß übernommenen Zitate als solche gekennzeichnet sowie die Dissertation in der vorliegenden oder ähnlichen Form noch bei keiner anderen in- oder ausländischen Hochschule anlässlich eines Promotionsgesuchs oder zu anderen Prüfungszwecken eingereicht habe.

Zijun Zhou

Marburg, den 15.Oct.2020

## Curriculum Vitae

### Zijun Zhou

Male, born Aug 14, 1992 in Anhui, P. R. China

Email: [534809741@qq.com](mailto:534809741@qq.com)

### Education

- 08/2017–present      *Ph.D.* Organic Chemistry, University of Marburg, Germany  
*Supervisor:* Prof. Dr. Eric Meggers
- 2014/09–2017/06      *M.Sc.* Organic Chemistry, Xiamen University, China  
*Supervisor:* Prof. Dr. Eric Meggers and Prof. Dr. Lei Gong
- 2010/09–2014/07      *B.S.* Applied Chemistry, Hubei University, China  
*Supervisor:* Prof. Dr. Yan Li

### Research Experiences

**Ph.D. study: Asymmetric Intramolecular C–H Aminations with Chiral-at-Ruthenium Complexes**

Publications:

1. **Z. Zhou**, Y. Tan, X. Shen, S. Ivlev, E. Meggers, *manuscript submitted*.
2. **Z. Zhou**, Y. Tan, T. Yamahira, S. Ivlev, X. Xie, R. Riedel, M. Hemming, M. Kimura, E. Meggers, *Chem* **2020**, *6*, 2024.
3. **Z. Zhou**, S. Chen, Y. Hong, E. Winterling, Y. Tan, K. Harms, K. N. Houk, E. Meggers, *J. Am. Chem. Soc.* **2019**, *141*, 19048.
4. **Z. Zhou**, S. Chen, J. Qin, X. Nie, X. Zheng, K. Harms, R. Riedel, K. N. Houk, E. Meggers, *Angew. Chem. Int. Ed.* **2019**, *58*, 1088.
5. **Z. Zhou**, X. Nie, K. Harms, R. Riedel, L. Zhang, E. Meggers, *Sci. China Chem.* **2019**, *62*, 1512.

**M.Sc. study: Study on Bifunctional Catalysis & Lewis Acid / Visible Light Cooperative Catalysis Based on Metal-Centered Chirality**

Publications:

1. **Z. Zhou**, Y. Li, B. Han, L. Gong, E. Meggers, *Chem. Sci.* **2017**, *8*, 5757.
2. **Z. Zhou**, Y. Li, L. Gong, E. Meggers, *Org. Lett.* **2017**, *19*, 222.